FUNDAMENTAL ASPECTS OF TIMBER SEASONING

by

RICHARD DENIS SCHAFFNER

B.E. (hons.)

Submitted in fulfilment of the requirements

for the degree of

MASTER OF ENGINEERING SCIENCE

in the

Faculty of Engineering

UNIVERSITY OF TASMANIA

AUSTRALIA

November 1981

ABSTRACT

The aim of this investigation was to develop an economically viable method of seasoning back-sawn native Tasmanian eucalypts and to reduce the seasoning time required for these timbers.

The theory of unsteady state mass transfer based upon Fick's law of diffusion was used to study the drying process. The diffusion coefficients were measured directly by the diffusion cell method or deduced from a comparison of measured and calculated drying curves. The relationship between shrinkage of wood fibre and moisture concentration was obtained by slowly drying thin strips of wood and regularly measuring deformations. The effects of falling diffusivity and shrinkage with reducing moisture concentration were found to effectively cancel one-another in the case of the timbers tested during this investigation.

Drying stresses in wood were studied using the theory of elasticity in anisotropic bodies. Airy stress functions were used when solving for stresses. For simplicity, sawn boards were approximated to orthotropic bodies and only boards cut with face-planes parallel/perpendicular to the principle material property directions were studied. Some elastic properties of native Tasmanian eucalypt timbers were measured on small sample populations and found to be similar to those of various North American hardwoods (with similar densities) reported by other authors. The approximate elastic properties of Tasmanian eucalypts were deduced from this comparison.

The theories of mass transfer and stress analysis were combined to form a model describing the development of drying stresses. The wood was assumed to be linearly elastic and to be free of the effects of hysteresis and creep. The governing differential equations were solved by numerical methods.

The model was used to assess the effectiveness of semi-permeable surface coatings in reducing drying stresses in timber. Tests on timber coated with animal glue (cologen) showed that checking (cracking) in Tasmanian eucalypts brought about by high drying stresses was reduced in severity or completely eliminated, depending upon the thickness of the coating.

The seasoning (drying) of timber has been the subject of research for many years, most of it based on experimentation. Furthermore, the theories of mass transfer and stress analysis have been studied and criticised at great length. Therefore, many of the mathematical and experimental techniques described in this thesis have been published elsewhere. However, the work reported in this document is, to the best of my knowledge and belief, original in that it brings together philosophies and techniques which have not previously been directly associated.

I hereby declare that this thesis does not contain any material which has been accepted for the award of any other degree or diploma at any University, and that to the best of my knowledge and belief, this thesis does not contain a copy or paraphrase of material previously written or published by any other person, except when due reference is made in the text of this thesis.

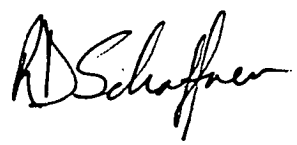

R. D. Schaffner.

CONTENTS

Contents ctd.

PREFACE

A mathematical model describing the drying of sawn boards was constructed. This model was based on Fick's Law of diffusion using either constant or variable mass diffusion co-efficients which included the lumped effects of the various moisture transfer regimes present in timber, changing permeability with moisture concentration and shrinkage. The diffusion co-efficients of "Tasmanian Oak" were estimated by fitting calculated drying curves and moisture distributions to those measured on small samples. This was affected by adjusting the values of the diffusion co-efficients used in the theoretical model until suitable agreement between theory and measurement was achieved over the extent of the test. Drying curves and moisture distributions were calculated by approximating the partial differential equations describing Fickian diffusion in

orthotropic materials with finite difference schemes and solving the resulting system of equations with the aid of a high-speed digital computer. The diffusion co-efficients of "Tasmanian Oak" in the radial direction (based on a constant diffusion co-efficient model) ranged from $1_{10}{}^{-7}$ m^2/hr to $2_{10}{}^{-7}$ m^2/hr over the sample population tested. The most common value of the radial diffusion co-efficient or "diffusivity" encountered was $1.7_{10}{}^{-7}$ m^2/hr. The agreement between measured and calculated drying curves and moisture distributions is remarkable considering the variability of the properties of wood.

The principles behing the use of "pre-surfacing" (coating) treatments on timber used as a means of controlling surface checking during drying were thoroughly investigated. The basic requirement of this process is that high surface-fibre moisture concentrations greater than fibre saturation be maintained for a sufficiently long period of time early in drying to limit differential shrinkage in the timber, and hence the drying stresses to levels at which checking is not promoted. This method of controlling checking has been investigated by a number of researchers (for example, Rietz and Jenson (1966) and Harrison (1968) and unsuccessfully applied to the seasoning of back-sawn "Tasmanian Oak" by MacKay (1972) and Campbell (1975)).

An approximate method of estimating the necessary combination of coating thickness and permeability (diffusivity) was developed. In this method,

it was assumed that no discontinuity in moisture concentration existed at the wood/coating interface and that the drying of sawn boards, particularly in the early stages, could be approximated to the drying of a semi-infinite slab. According to this simple model, the thickness of coating, d, required to hold the surface fibres of a board above the fibre saturation point for a time, t, is

$$d = \sqrt{D_c^2 t / D_w a}$$

where a = constant, dependant upon the initial moisture concentration of the timber and the drying conditions (typically, a = 8 for "Tasmanian Oak").

D_c = coating diffusivity

and D_w = diffusivity of wood (in the appropriate direction).

It was estimated that surface tensile stresses generated during drying would be limited to a sufficiently low maximum by maintaining the surface fibres of back-sawn boards at a moisture concentration for a period of 5 days.

A mixture of animal glue (collogen), talcum powder and water in the proportions

3.5 water : 1 dry animal glue crystals : 1.9 talcum powder

(by weight) was found to have a mass diffusivity of approximately

0.7_{10}^{-7} m^2/hr. According to the approximate method of determination of coating requirements, the necessary thickness of this mixture was between 0.60mm (radial diffusivity of wood = $2_{10}^{-7}m^2/hr$) and 0.85 mm (radial diffusivity of wood = $1_{10}^{-7}m^2/hr$). The most commonly encountered value for the radial diffusivity of wood was $1.7_{10}^{-7}m^2/hr$, required a coating thickness of 0.65mm.

Tests on stacks of timber built up of approximately 80 25mm (nominal thickness) back-sawn "Tasmanian Oak" boards, each 2.1m long (40 coated and 40 uncoated) showed that the animal glue - talcum powder coating applied to a thickness of 0.7mm (±10%) was effective in reducing face-checking to an acceptable level (or completely eliminating it) from about 80% of coated material. The relationship between surface fibre moisture concentration and time was measured on a typical back-sawn "Tasmanian Oak" board (radial diffusivity = 2.1_{10}^{-7} m^2/hr) coated with the animal glue - talcum powder mix to a thickness of 0.7mm. The surface fibres were found to remain above the fibre saturation point for about 10 days.

The measured (and predicted) drying rates for back-sawn boards were less than those of the uncoated back-sawn material although a direct comparison of the rates is not strictly valid due to checking of the uncoated material. Checks expose a greater surface area of timber to the atmosphere and hence accelerate drying.

A mathematical model describing the state of stress in anisotropic elastic bodies under conditions of plane strain and subjected to differential thermal or shrinkage strains was established. When this model was simplified for the isotropic case, the governing equation reduced to that derived for such materials by Timoshenko and Goodier (1970). The general relationship describing the state of stress in timber (an anisotropic material) was simplified by firstly approximating sawn boards to orthotropic bodies (principle material property axes orthogonal). The non-linear "elastic" behaviour of "Tasmanian Oak" was approximated by a linear model and the effects of creep, hysteresis and the development of checks were ignored.

To simplify the mathematics, the analysis of drying stresses was restricted to either purely back-sawn or purely quarter-sawn material. Furthermore, the boards were assumed to be very wide compared to their thickness. Under this assumption, the stresses acting in the direction perpendicular to the board faces are small at every point on the cross-section (away from the edges) and may be neglected; thus, drying stresses may be analysed using a one-dimensional model.

The relationship between moisture concentration and shrinkage, the permeability and the elastic constants of wood as well as the drying (boundry) conditions are the

major factors affecting drying stress levels in wood. A typical measured value of diffusivity and the measured mean shrinkage-moisture concentration relationships of "Tasmanian Oak" were used in the calculation of drying stresses in the simple linear model. The approximate elastic parameters of "Tasmanian Oak" used were deduced from a comparison of some (measured) properties of "Tasmanian Oak" with those published for various North American hardwoods. The simplified stress and moisture transfer equations were approximated by finite difference schemes and solved by digital computer.

From the calculated drying stress distributions in 25mm (nominal thickness) back-sawn "Tasmanian Oak" boards it was found that the maximum tensile stress in the surface fibres of boards coated to a thickness of 0.7mm with the animal glue - talcum powder mix were only one third of the maximum surface stress in matched uncoated boards dried under the same atmospheric conditions.

ADDITIONAL PUBLICATION

The following paper is to be presented to the 20th (Australian) Forest Products Research Conference (Melbourne, Australia) in November, 1981:

An Application of an Orthotropic Fickian Diffusion Model to Timber Drying:

by R.D. Schaffner and P.E. Doe*.

*Senior lecturer in Mechanical Engineering,
University of Tasmania.

ACKNOWLEDGEMENTS

Many people have assisted the author during the course of the research described in this document. To all of those people , no matter how small their contribution, the author extends his gratitude and appreciation. Special acknowledgement is recorded for the following people:

Dr.P.E.Doe ,my supervisor, for his advice, assistance and enthusiasm.

Dr.M.S.Gregory, joint supervisor, for his efforts in setting up the research program.

Professor A.R.Oliver for his advice and support.

Messrs. J.Hammond, J.Clark, the members of the Tasmanian Timber Promotion Board and the Board's staff for their initiative and support.

Mr.S.Goodwin for his patience and dedication in the fabrication and maintainance of equipment.

Lastly, my family for their patience and understanding, and for the typing.

CHAPTER 1

CHAPTER 1

INTRODUCTION

Seasoning techniques have long been the subject of timber research, much of it inconclusive. Nevertheless, seasoning remains the major problem confronting millers of Tasmanian hardwood as more than 50% of their product is used in a dried and dressed condition. In other Australian states, hardwoods are used mainly in the unseasoned state for structural purposes (domestic, agricultural).

The hardwoods milled in Australia are predominantly of the genus Eucalyptus and range in density (at a moisture content of 12%, dry basis) from 630 kg/m^3 to 1140 kg/m^3. The species milled on a large scale in Tasmania are of low density, being

Eucalyptus regnans - average density = 630 kg/m^3,

Eucalytpus delegatensis - average density = 650 kg/m^3,

Eucalyptus obliqua - average density = 710 kg/m^3.

These species together form what is commonly known as the "Tasmanian Oak" group of species; most of the sawn hardwood produced in Tasmania is marketed under this name.

In general, boards may be sawn from logs in two distinctly different ways. Quarter-sawn boards are cut with their wide faces essentially perpendicular to the seasonal or growth rings; that is, the wide faces are cut radially with respect to a log cross-section (see figure 1.1).

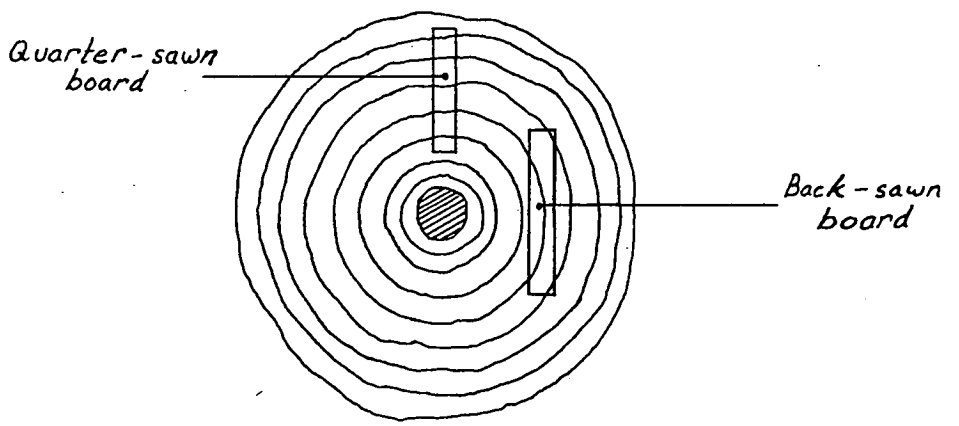

Figure 1.1

Cross-section of a log showing quarter-sawn and back-sawn boards.

On the other hand, back-sawn boards are cut with their wide faces tangential to the growth rings. The growth

rings appear as linear markings on the faces of quarter-sawn boards which run in the longitudinal direction and are between 1.5 & 3 mm apart in close-grained timbers such as those making up the "Tasmanian Oak" group. However, the faces of back-sawn boards are heavily figured. The difference in appearance is demonstrated in figure (1.2).

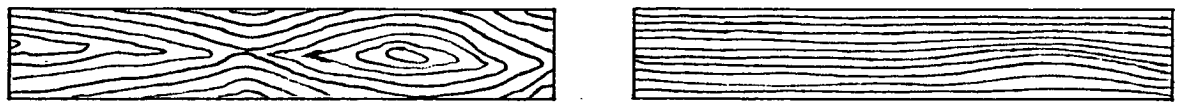

Back-sawn board *Quarter-sawn board*

Figure 1.2

Figuring on the faces of back-sawn and quarter-sawn boards.

The faces of back-sawn boards are more visually appealing than those of quarter-sawn boards and consequently back-sawn material is in great demand for decorative applications including furniture, feature panelling and flooring.

Unfortunately, severe cracks or "checks" * are formed on the faces of a large percentage (70 to 80%) of back-sawn "Tasmanian Oak" boards as they are dried from the "green" condition to equilibrium with the atmosphere. Badly-checked material is unsuitable for decorative applications and it is therefore uneconomic to produce back-sawn "Tasmanian Oak" using the methods currently

* "Checks" are defined as cracks or fissures in wood fibre running in the longitudinal direction but not extending through the piece from one surface to another.

employed in the Tasmanian timber industry. Checking during drying is uncommon on the faces of quarter-sawn boards; however, edge-checking in quarter-sawn material is a problem with degrade ranging from 3 to 5% in 25 mm boards to up to 50% in 50 mm boards. "Tasmanian Oak" is therefore quarter-sawn in order to minimise degradation of sawn material during drying. As previously indicated, a major disadvantage of quarter-sawing is the lack of visual appeal of the end product. Consequently, "Tasmanian Oak" cannot compete on equal terms with other hardwoods in the decorative timber market.

The quarter-sawing process is slow and costly. Logs are generally quartered (figure 1.3) and each board is sawn individually from the large billetts or "flitches" resulting.

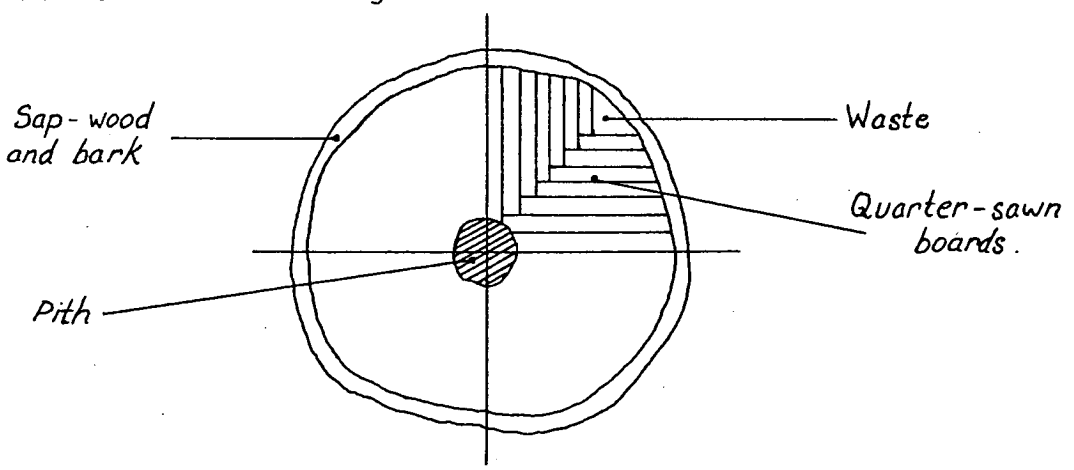

Figure 1.3

Quarter-sawing

The maximum width of board that may be cut from a given log is less than 50% of the diameter and the wastage of

timber, in terms of both saw-dust and unmillable remainders, is high. In fact, the typical volumetric recovery of dry, rough-sawn boards from a given log intake ranges from 30 to 40% depending on log diameter and the amount of shrinkage during drying.

"Bark to bark" sawing (figure 1.4) produces a large percentage of wide back-sawn boards and recovery of dry, sawn material ranges from 50 to 65%.

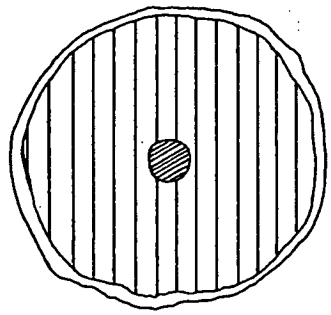

Figure 1.4

"Bark to bark" sawing.

This process involves less handling and is much faster than the quarter-sawing process. Gangs of parallel saw-blades are often used. Millers of "Tasmanian Oak" (and other Australian-grown eucalypt species) are at present unable to use the "bark to bark" sawing technique, primarily because of the excessive rate of degradation of back-sawn material during drying. To further complicate matters, hardwood millers in Tasmania face a reduction in the size and quantity of available sawlogs.

The future of the Tasmanian hardwood milling

industry therefore rests heavily upon the development of a method of reducing the level of degradation due to face-checking during the seasoning of back-sawn "Tasmanian Oak". In Australia, research on this particular problem has been pursued at various levels since the mid 1940's without an economic solution being reached. The research project described in this document was initiated by the Tasmanian Timber Promotion Board (T.T.P.B.) on behalf of the Tasmanian timber industry and backed financially by the T.T.P.B. and the Government of the State of Tasmania. The T.T.P.B. determined that a fresh attack should be made upon the problem at an institution with no previous connection with timber seasoning research, thus avoiding any preconceptions or prejudices. However, great value was attached to the work of other researchers (both published and privately communicated) without reference to which this project would surely not have progressed at a satisfactory pace.

CHAPTER 2

CHAPTER 2

THE STRUCTURE OF HARDWOODS AND SITES OF CHECK FORMATION.

Checking in sawn boards of "Tasmanian Oak" takes place primarily on back-sawn faces (or edges) and checks propogate into the boards in the radial direction with respect to the (seasonal) growth rings. Checks in small specimens of "Tasmanian Oak" were examined using optical and scanning electron microscopes and the cellular structure of the wood fibre related to the formation of checks. The reasons for concentration of stress at or near the surfaces of sawn boards are discussed and observations are compared with those of MacKay (1972).

The discussion of the structure of wood tissue given in this chapter briefly summarises information given in various texts (for example, U.S. F.P.L. (1974)).

2.1 The Formation of Mature Wood.

When first formed, wood cells consist of thin-walled tubes of cellulose. They contain living matter and grow rapidly. The walls become thicker and stronger as material containing lignin is deposited on the inner surfaces. After a time, the living matter in the cells dies and tannins and other substances are deposited in the cell cavities and on the cell walls. Occasionally, the cells become blocked by outgrowths from the walls or by resinous matter. The length, diameter and wall-thickness of wood-cells increase with age, reaching a maximum in eucalypts in 10 to 30 years (Hillis and Brown, 1978).

Hence, the dead cells in the inner layers of the sapwood are gradually converted into denser, darker-coloured true-wood. The materials deposited in the wood-cells increase the resistance of the fibre to attack by insects and fungi. All the cells in the heart-wood are dead and although they contain water, they do not play an active role in the growth process. The growth of the tree continues on the outside of the sapwood and the dead cells of the heart-wood merely provide support.

The growth-rate of a tree depends largely on seasonal (climatic) factors. During spring, growth is rapid and wood-cells produced in this period are generally of a larger diameter and are more numerous than those produced

during the autumn and winter. The cells making up the spring-wood ("early-wood") usually have thinner, lighter-coloured walls than those of the winter-wood ("late-wood"). This gives rise to the banded or ringed appearance of sections cut through the trunk of a tree, perpendicular to its length.

2.2 The cellular structure of hardwoods (specifically eucalypts).

The outstanding feature of hardwoods is the presence of large, tubular vessels (running longitudinally in the tree) distributed throughout a matrix of smaller cells, commonly called fibres or tracheids. (see figures 2.1 and 2.2).

The elements of a tree providing the bulk of the mechanical strength are the narrow, spindle-shaped fibres which contain a cavity or lumen. The fibres vary from about 0.5 mm to 3 mm in length and 0.015 mm to 0.025 mm in breadth (CSIRO, 1975) and are laid down longitudinally in the tree. The fibres overlap longitudinally and the lumina of adjacent fibres are often connected (in the radial direction with respect to the tree) by pores (pits, openings) in the cell walls. The fibres are cemented together by a material rich in lignin called the middle lamella.

The vessels are distributed amongst the fibres and, in their early life, conduct water (also minerals etc.) from the roots to the leaves. The vessels initially form as

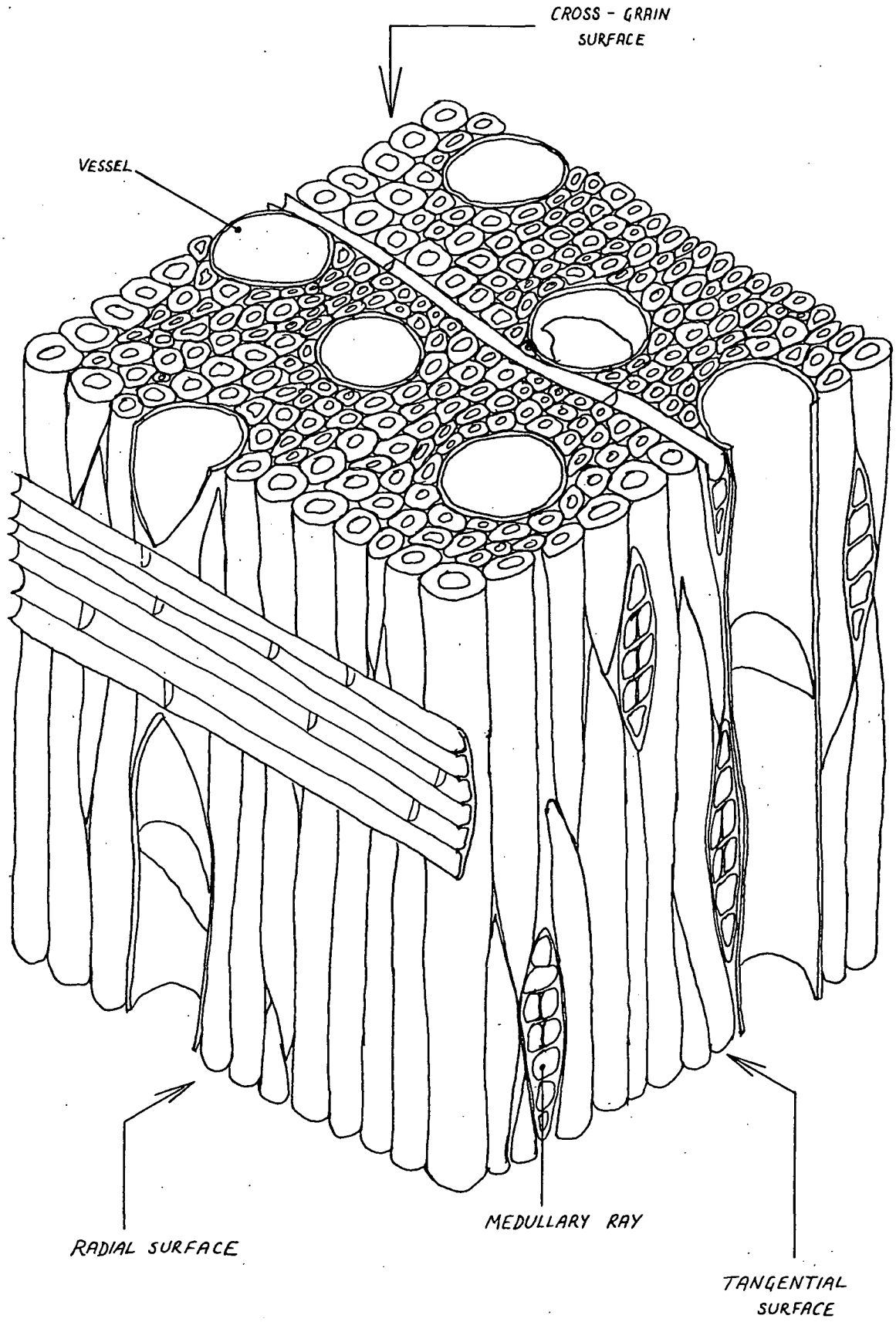

FIGURE 2.1

HARDWOOD

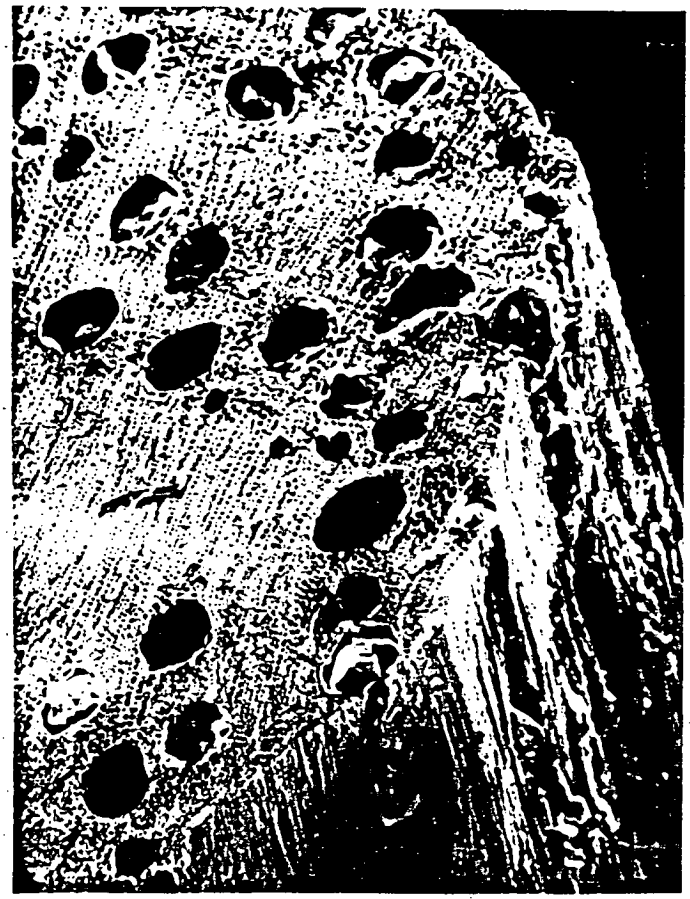

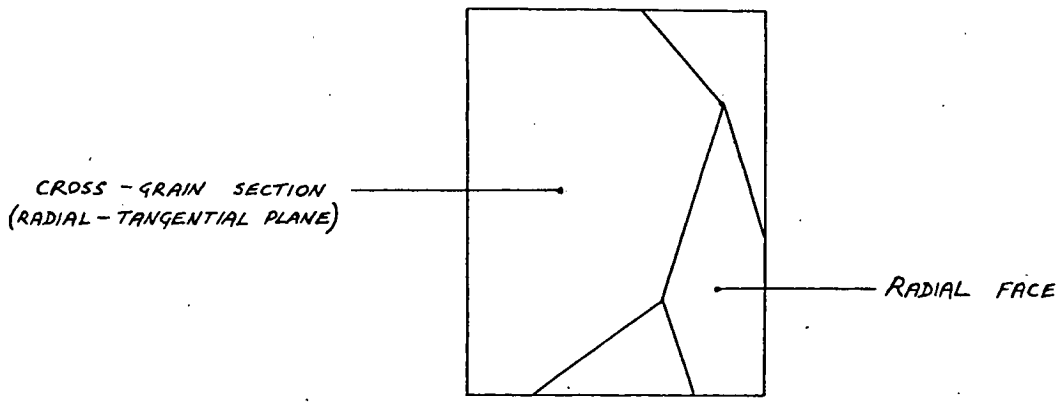

FIGURE 2·2

E. delegatensis – Magnification ≈ 60 X

closed cells, 0.04 mm to 0.25 mm in breadth and 0.5 mm to 2 mm in length, joined end to end. Eventually, the end-walls split forming long, continuous tubes. Vessels are not necessarily distributed evenly throughout the early-wood and late-wood. Those in the heart-wood do not conduct water and often become blocked by membranes (tyloses) and resinous deposits.

Medullary rays are groups of thin-walled cells running radially into the tree (at right-angles to its length) and exist for the purpose of distribution and storage of nutrients.

During the preceeding discussion, it has been stated that wood cells are laid down in preferred directions. It is evident, therefore, that the physical and mechanical properties of wood will be directionally dependent and that the principal directions are radial, tangential and longitudinal with respect to a tree. There are many excellent texts describing the anisotropic nature of wood, most of which quote the results of material property tests on selected species (for example, the United States Forest Products Laboratory "Wood Handbook").

2.3 The fine structure of the wood-cell wall.

The walls of wood-cells are composed of several layers which differ chemically or in the arrangement of

cellulose strands. The strands or "fibrils" are generally arranged in an ordered fashion. The fibrils consist of micro-fibrils which are built up from chains of cellulose molecules. The micro-fibrils are surrounded by hemi-cellulose molecules. The bulk of the cellulose is crystalline but amorphous regions exist along the length of each micro-fibril. Hydrogen bonds link the cellulose chains and therefore the mechanical properties are affected greatly by the uptake or loss of water in the amorphous regions of the structure (CSIRO, 1975). Hillis and Brown (1978) state that the micro-fibrils do not pack down completely, leaving spaces to which water has access. The size of these free spaces is not definite but it is known that various compounds of low molecular weight infiltrate these regions.

The primary (outer) wall of the wood-cell is laid down during extension growth and the fibrils making up the wall are randomly arranged. The secondary wall forms inside the primary wall after extension growth is complete and is much thicker than the primary wall. The secondary wall consists of several concentric lamellae in which the fibrils are arranged in a helical form at a small angle to the axis of the cell.

Lignin accounts for only 20% of the chemical constituents of the secondary wall but the major proportion of lignin found in wood occurs in the secondary wall due to its large volume. The concentration of lignin in the middle

lamella (bonding zone between cells) is greater than 50% (Hillis and Brown, 1978).

2.4 Chemical Composition (of eucalypts; approximately).

Wood, in general, is made up of five different groups of materials, those being cellulose, lignin, hemicellulose, extractives and ash-forming compounds. The following is a summary of information presented by Hillis and Brown (1978) and that contained in the U.S. F.P.L. "Wood Handbook" (1974).

a) Cellulose - accounts for between 40 and 62% of the dry weight of eucalypt fibre. Cellulose is a high molecular weight, linear polymer that yields the simple sugar, glucose, as the sole product of chemical action of mineral acids. The cellulose molecules in wood are arranged in an ordered fashion to form strands or fibrils.

b) Lignin - between 15 and 22% of the weight of dry eucalypt fibre. Lignin makes up a large proportion of the inter-cellular bonding material and is an intractable, insoluble material, probably bonded loosely to cellulose.

c) Hemicelluloses - between 12 and 22% by weight. Hemicellulose is a polymeric substance built up of simple sugars but yielding more than

one type of sugar on acid cleavage.

d) Extractives - 7.4 to 8.4% by weight. These are non-structural constituents contributing to colour, odour, taste, durability, workability, strength, density, hygroscopicity and flammability. The extractives include such materials as tannins, poly-phenolic substances, colouring matter, essential oils, fats, resins, waxes, kino (gum), starch and so on. The amount of phenolic extractives (those contributing largely to the durability of timbers) in eucalypts increase from the pith to the outer heart-wood with a lower amount in the sap-wood.

e) Ash-forming materials - 0.1 to 0.9% by weight, consisting primarily of Calcium, Potassium, Phosphate and Silica.

2.5 The formation of drying checks in eucalypt timbers.

A scanning electron microscope was used to examine drying checks existing in small samples of E. delegatensis. Samples (cubes with edges of approximately 10 mm) were cut from near the surfaces and back-sawn boards dried in the experiments described in Chapter 5. Checks present in the samples were carefully examined and the sites

of checking noted. The results of the examination of checks in E. delegatensis agree well with observations made by MacKay (1972) on E. obliqua.

In both E. delegatensis and E. obliqua, checks appear to start at vessels (figure 2.3) and to propogate in the radial direction, parallel to rays but not necessarily along rays. The results of investigations on checking in non-eucalypt timbers (briefly summarised by MacKay, 1972) shows that checks start in ray groups rather than in vessels and run along the rays. MacKay hypothesised that this difference in behaviour resulted from factors such as the relative sizes of vessels, rays and ordinary wood cells, the frequency and distribution of vessels and rays within the matrix tissue and the shrinkage behaviour of the timber as a whole (for example, propensity to collapse etc.). Eucalypts are characterised by large vessels and relatively small ray groups (see figure 2.2).

A vessel or group of vessels constitutes a large notch in the wood around which drying stresses concentrate. After forming at vessel sites, checks propogate radially (with respect to a log). The medullary ray groups reinforce the structure of wood against check propogation in the tangential direction; hence, the radial-longitudinal plane is the weakest plane.

MacKay reported that:

"After breaking through a vessel wall, checks

E. delegatensis – cross-section magnified 130 X. Check, initiated at vessel and running radially through the wood fibre. (Tip of check shown below)

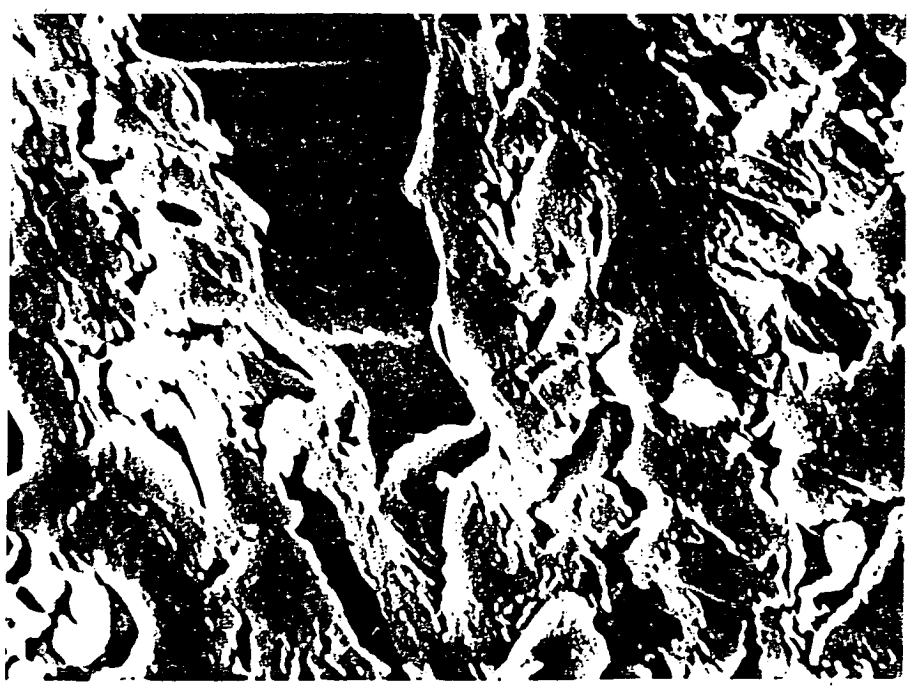

Tip of check – magnified 1240 X. Check runs through middle lamella (bonding zone) rather than through individual cells.

FIGURE 2·3

CHECKING IN *E. delegatensis*

FIGURE 2·4

Longitudinal cross-section through a vessel (magnification ≈ 120X) showing check running along vessel and into the wood fibre.

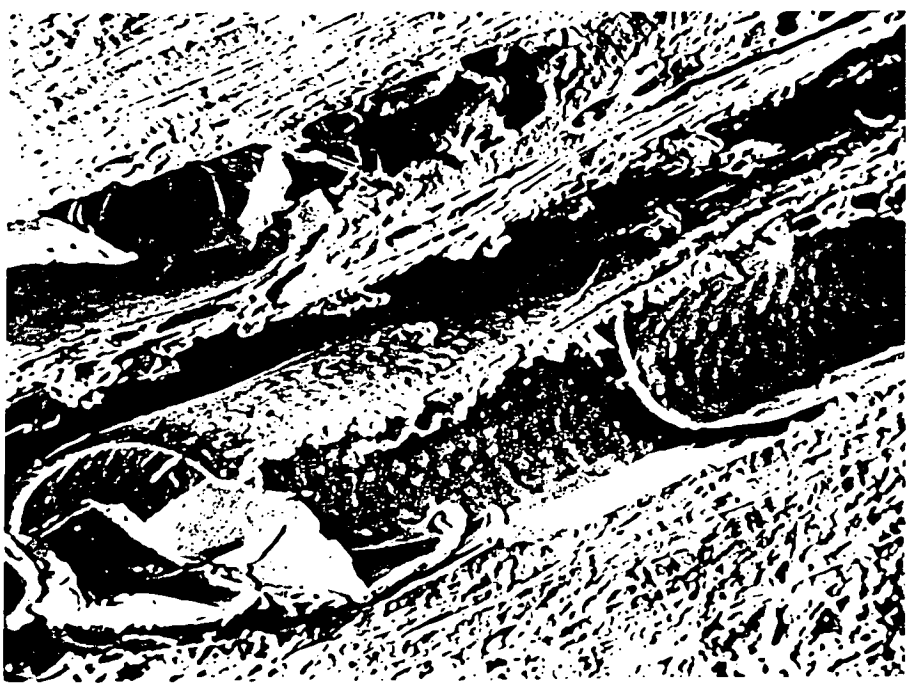

FIGURE 2·5

Longitudinal section (magnification ≈ 150X) showing two vessels with a check running between them.

> appeared to spread between fibres causing a separation of adjacent cells rather than a fracture of cell walls. That is, the zone of failure was in the middle lamella."

Observations made during this investigation support these statements. (Figures (2.3), (2.4) and (2.5) show various aspects of checks in E. delegatensis).

Further weakening or "notching" of the wood tissue at the surfaces of boards occurs as a result of sawing green wood. MacKay (1972) summarises the results obtained by various research workers by stating that:

> "....sawing, whether circular or band, resulted in crushing and tearing of up to 8 layers of wood cells."

Further work has shown that the intensity of surface checking can be correlated with saw-damage.

REFERENCES

C.S.I.R.O. (1975): Fundamentals of Timber Engineering Lectures (publ.) by Leicester, Armstrong and Kloot.
Division of Building Research, CSIRO, Melbourne, Australia.

MacKay, J.F.G., (1972): The Occurrence, Development and Control of Checking in Tasmanian Eucalyptus Obliqua.
CSIRO Forest Products Laboratory, Reprint No. 913.
Division of Forest Products, CSIRO, Australia.

U.S. F.P.L. (1974): Wood Handbook: Wood as an Engineering Material.
Agriculture Handbook No. 72.
Forest Products Laboratory,
Forest Service,
U.S. Dept. of Agric.
U.S. Govt. Printing Office,
Washington, D.C.

CHAPTER 3

CHAPTER 3

THE THEORY OF MASS TRANSFER IN WOOD

3.1.1 Factors affecting moisture transfer through wood fibre

The rate of moisture transfer through the cellular matrix of wood varies markedly with direction. The longitudinal transfer rate is approximately a factor of 10 faster than the rates in the transverse directions. The radial transfer rate is approximately one third greater than the tangential. However, sawn boards are typically 200 times as long as they are thick and, for the purpose of analysis, longitudinal moisture transfer may be ignored. The directions of major interest are therefore radial and tangential with respect to a log.

The difference between the radial and tangential transfer rates is attributable to the presence

of medullary rays, those groups of cells which transport materials to and from the bark radially into the tree. Rays provide paths of low resistance to radial moisture movement during drying.

The second characteristic contributing to the resistance to moisture movement is the variation in seasonal growth rate, observable as "growth rings". Spring-wood cells are relatively large and thin-walled. Winter-wood cells are formed when the growth rate of the tree is comparatively slow. They are small and tend to be thick-walled and therefore appear as dark bands or rings on the cross-section of a log. The relative proportions of winter-wood and spring-wood have a large bearing on the overall moisture transfer rate through the fibre during drying.

It should be noted that faster-grown trees have relatively open or coarse cellular structure with a high volume ratio of lumen to cell fibre. Timber grown on low-lying, gently sloping, fertile land grows quickly and will be less dense and more permeable overall than that grown on rocky, thin-soiled mountain slopes. Slow-grown trees have dense cell structure with low lumen to cell fibre volume ratio, are less permeable and therefore dry slowly with steep moisture gradients. Thus, they are more prone to seasoning faults such as checking.

The age of a tree also affects the drying rate. As a tree grows older, wood in the centre of the trunk

changes in character and no longer serves to conduct materials. Young wood (sapwood) takes an active part in the growth of a tree whereas old wood (heartwood) performs only the function of mechanical support. Sapwood is gradually transformed into heartwood as various substances are deposited in the cell cavities or infiltrate into the cell walls. These substances include both organic and inorganic compounds and are listed in Chapter 2. These deposits result in an increase in weight, hardness and durability of the heartwood and also a decrease in its permeability.

3.1.2 Transport Mechanisms.

Wood fibre belongs to a class of highly hydrophyllic substances; that is, those materials that exhibit energetic retention of water. The moisture present in wood does not exist only as free water. Much is bound in various ways to the fibrous matrix. The bonds must be broken before moisture movement can take place. Particularly at lower moisture concentrations, water exists within the cell lumen in layers of a few hundred molecules. Physical models for the behaviour of bulk fluids cannot, therefore, be used. Salts present within the matrix promote ionic bonding of water. Both hydrogen bonds and Van der Waal's forces exist. Therefore, the retention of water by wood fibre is a highly complex phenomenon.

Jason (1965) lists some of the transport mechanisms likely to operate on cellular materials.

These are:

1. Capillary flow of liquid water
2. Viscous flow of water vapour
3. Thermal diffusion
4. Surface diffusion in a porous medium
5. Gaseous diffusion
6. Molecular diffusion on a solid medium

An additon to this list is the flow of liquid water under the action of direct stresses generated in the material during drying. As water exists within timber in the gaseous, liquid and absorbed states, all transfer mechanisms probably exist.

Keey (1972) describes generally the drying of vegetable matter. In summary, he says that moisture in the larger capillaries evaporates, allowing moisture held within the finer capillaries to be removed. The cell walls act as semi-permeable membranes for the effusion of moisture which is mainly held osmotically. Some moisture is adsorbed on the skeletal frame in multi-molecular layers and water may be chemically combined either in the form of hydroxyl ions or more loosely in crystalline hydrates.

Keey shows that as drying progresses, the removal of moisture becomes progressively more difficult, requiring increasing amounts of energy to remove a given quantity of water.

From this discussion, it is clear that the movement of moisture through wood cannot be described fully by a simple model.

3.1.3 Recent discussion regarding classical mass transfer theory.

In 1855, Fick proposed that transfer of water by means other than convection was analogous to the conduction of heat as mathematically described by Fourier in 1822. Thus, the Fickian theory of diffusion in isotropic substances is based on the hypothesis that the rate of transfer of diffusing substance through a unit area of a section is proportional to the concentration gradient measured normal to the section.

i.e. $$F = -\mathcal{D} \frac{\partial c}{\partial x} \qquad \ldots (3.1)$$

where F = flux of diffusing substance,

c = concentration of diffusing substance,

$\mathcal{D}$ = diffusion coefficient,

and x = space co-ordinate perpenicular to section.

Diffusion as described by Crank (1956) is "the process by which matter is transported from one part of a system to another as a result of random molecular motion".
Bramhall (1979,a) defines two principal types of diffusion as:

1. Molecular (Fickian) diffusion: "the transport of a material by the continous random free movement of the total population of its molecules".
2. Sorption diffusion: "the random movement of only a

very small part of the population of the "diffusant" at any time."

Both Babbit (1977) and Bramhall (1979,a) point out that, as diffusion is the movement of mass, the driving force for diffusion must be a force (or pressure) to be consistent with Newtonian principles. Moisture concentration is not a force and therefore Ficks equation cannot rigorously apply in the general case. Bramhall (1979,a) shows that Ficks law is limited strictly to the description of mass transfer in "ideal" systems under isothermal conditions. He quotes a number of observations made by scientists in recent years which demonstrate that anomalies exist between measurement and theory when Ficks law is applied uncritically. He goes on to show that, where the partial pressure of a gas is used as the driving force, the actual physical behaviour of a gaseous system may be adequately explained.

Accepting that Ficks equation describes the case of isothermal gaseous diffusion, one finds that the equation has been assumed to adequately describe sorption or bound-water diffusion. In sorption diffusion, the movement of molecules occurs only when enough energy is received to break the bonds holding them to a sorption site. These molecules then move (due to the action of some driving force) until they are captured by another sorption site at which time they emit their activation energy. The migrating molecules are, in effect, in a separate

phase. Therefore, the use of total moisture concentration (being the sum of moving and bound water), as or directly related to the driving force, is not correct.

At first, Bramhall stated that the primary driving force for moisture diffusion through wood was the partial pressure of water vapour. Babbitt, while recognising that water vapour diffusion does exist in wood, proposed that this statement was not strictly true; rather, the "appropriate pressure is the two-dimensional pressure generated by the adsorbed molecules as they move from site to site on the internal surfaces of cellulose molecules". Bramhall (1977) later agreed. Babbitt explained that adsorbed molecules can move between adsorption sites on a surface without having sufficient energy to evaporate.

From the arguments put forward by Babbitt and Bramhall, one may deduce that the flow mechanisms listed by Jason (1965) probably all exist in the case of moisture diffusion through wood.

One very important omission from the above discussion has been the state of stress in the wood fibre. In later chapters, it will be shown that high stresses (of the order of 10^6Pa), both compressive and tensile, exist in sawn timbers due to differential shrinkage during drying. These stresses most certainly contribute to moisture movement, particularly in the early stages of drying when the stress gradients are steep and are changing rapidly

with time.

On the topic of the derivation of a simple equation describing moisture diffusion through wood, Babbitt (1977) identifies two major areas of difficulty. Firstly....

> "..the thermodynamical representation of the isotherm for the adsorption of water is far from exact, and the mechanism of the bonding of water molecules to cellulose appears to change as the moisture content increases..."

Secondly....

> "..because the moisture can exist simultaneously within the wood in various states (gas, liquid or adsorbed) and since the movement of the moisture obeys a different diffusion mechanism in each state and there will be a continous exchange of molecules between states, it is not possible to set up equations to study the flow without assuming a definite structural model for the system."

Babbitt goes on to say that experience has shown that the "...movement of moisture as adsorbed molecules dominates the system to a much greater extent than might be expected from superficial considerations." He states that by basing a physical model upon sorption diffusion and ignoring other modes of transfer, a good representation of results can be obtained.

On the same topic, Bramhall (1977) says:

"Data presently available to me fit consistently into this concept, which was expounded by Dr. Babbitt (1950)".

There is, therefore, strong evidence to support the argument that a force or pressure is the primary driving force for moisture diffusion, particularly in hygroscopic media.

A mathematical model which satisfactorily describes the transfer of moisture through wood fibre based upon the sorption or "bound-water" transfer model has been formulated. This model, as put forward by Bramhall (1977) is based upon the assumption that either "spreading" pressure or vapour pressure at any temperature are given by the Clausius-Clapeyron equation

$$P = Ke^{-E/RT} \qquad \ldots\ldots\ldots (3.2)$$

where K = constant,

E = activation energy,

R = gas constant,

and T = absolute temperature.

Bramhall states that the spreading pressure is..

"... found by multiplying the appropriate maximum value by the relative humidity of wood at that temperature and MC (moisture content), found in the RH - EMC tables".

That is, spreading pressure is dependent upon the sorption isotherm (the relationship between equilibrium moisture content and relative humidity at constant temperature) of wood which, according to Babbitt, is "far from exact".

Further, the activation energy associated with the determination of spreading pressure appears to be a variable quantity. Indeed, Bramhall hints at this and Babbitt (1977) states that:

> "... the mechanism of the bonding of the water molecules to cellulose appears to change as moisture content increases from low to high values".

The indication here is that the activation energy is dependent upon the amount of water present. Therefore, when the spreading pressure from equation (3.2) is substituted into the general rate equation

$$F = -\mathcal{D} \frac{\partial P}{\partial x} \qquad \text{.....(3.3)}$$

where F = rate of transport,

$\mathcal{D}$ = Diffusion coefficient,

and $\frac{\partial P}{\partial x}$ = gradient of driving force,

one finds that the right-hand side includes terms dependent upon moisture content.

Thus, we are pointed to the fact that, no matter which model we choose to accept, the limiting factor when stepping from the micro to the macro scale is the sorption isotherm which is itself a variable and imprecise relationship.

Whatever mode of transport is proposed as dominant, the diffusion model based on this mode must allow for the effects of the other transport regimes which are, no doubt, present. The total effect of these

regimes changes as the amount of water present in the material changes. The diffusion coefficient (which covers the effects of these "minor" transport phenomena) must, therefore, be a function of moisture concentration. Hence, it may be argued that a mathematical model based upon the assumption that moisture concentration is the driving force of mass diffusion in wood, while not being physically rigorous, may not be devoid of merit.

3.1.4 Fickian Diffusion

Bramhall (1979,a) found that the Fickian diffusion coefficients of wood (determined by the diffusion cell method) were dependent upon both moisture content and temperature. He states that the diffusion coefficient, D, is related to temperature (at constant moisture content) by the relationship

$$D = D_0 e^{-E/RT}$$

where D_0 = constant,

E = activation energy of diffusion,

R = universal gas constant,

and T = absolute temperature.

The effects of many different phenomena may be lumped together and handled very simply by determining the Fickian diffusion coefficients experimentally. In fact, many investigators have obtained satisfactory results from models based upon Fick's equation using variable diffusion coefficients.

Bui, Choong and Rudd (1980) studied the variation of the diffusion coefficients of certain woods with average moisture content in a series of drying experiments.

They assumed that the diffusion coefficient was constant over the sample cross-section but that it varied with average moisture content. They conclude that:

> "MC and RH were both valid driving forces for the Fickian equation in isothermal drying."

and

> "... the diffusion coefficient was found to be dynamically related to the moisture gradient, and was highest during the middle of a drying process."

Doe (1973) analyses moisture transfer through protein slabs. He suggests that:

> "Diffusivity must be inferred from measurements of a steady or unsteady diffusion process; thus values of diffusivity are dependent on the physical and mathematical models used to describe the diffusion process. A simple approach is to set the diffusivity constant throughout the drying process and to lump all factors which vary during drying into the description of shrinkage".

From this, it may be concluded that providing a given model is used consistently throughout an investigation

and that the factors which vary during drying are included in that model, satisfactory agreement between measurements and theory will result.

The aim of constructing a mathematical model for the drying of timber is to extend this model to investigations of the drying process itself. Thus a model which produces results to the degree of accuracy required in a particular investigation is all that is required.

The model used in this investigation is based upon Fick's equation with the diffusion coefficient, D, varying with both temperature and moisture content. Calculated results based on this model agree well with measurements.

3.2 Fickian diffusion in orthotropic media.

3.2.1 Diffusion equations

The mathematical theory of diffusion in isotropic substances as proposed by Fick is based upon the hypothesis that the rate of transfer of diffusing substance through a unit area of a section is proportional to the concentration gradient measured normal to the section. That is,

$$F = -D \frac{\partial c}{\partial x} \qquad \ldots\ldots\ (3.1)$$

where F = rate of transfer per unit area,

c = concentration of diffusing substance,

x = space co-ord. measured perpendicular to the section,

and D = diffusion coefficient.

It should be noted that equation (3.1) is applicable only for an isotropic medium. Because of the symmetry in such media, the flow of diffusing substance at any point is normal to the surface of constant concentration passing through the point. This need not be true in an anisotropic medium.

For the general orthotropic medium, the above equation is replaced by the following assumptions (Crank, 1975):

$$-F_x = \mathcal{D}_{xx}\frac{\partial c}{\partial x} + \mathcal{D}_{xy}\frac{\partial c}{\partial y} + \mathcal{D}_{xz}\frac{\partial c}{\partial z}$$
$$-F_y = \mathcal{D}_{yx}\frac{\partial c}{\partial x} + \mathcal{D}_{yy}\frac{\partial c}{\partial y} + \mathcal{D}_{yz}\frac{\partial c}{\partial z}$$
$$-F_z = \mathcal{D}_{zx}\frac{\partial c}{\partial x} + \mathcal{D}_{zy}\frac{\partial c}{\partial y} + \mathcal{D}_{zz}\frac{\partial c}{\partial z}$$

in three dimensions or, for the two-dimensional case,

$$-F_x = \mathcal{D}_{xx}\frac{\partial c}{\partial x} + \mathcal{D}_{xy}\frac{\partial c}{\partial y} \qquad \text{.....(3.4)}$$
$$-F_y = \mathcal{D}_{yx}\frac{\partial c}{\partial x} + \mathcal{D}_{yy}\frac{\partial c}{\partial y}$$

In these relations, terms such as $\mathcal{D}_{xy}\frac{\partial c}{\partial y}$ define the contribution to the transfer rate in the x-direction due to the concentration gradient in the y-direction, and so on.

Rohsenow and Choi (1961) discuss heat and mass transfer in an orthotropic plane and deduce equations (3.4) by considering an arbitrary plane cut in an orthotropic solid through which a substance is diffusing. Lines of constant concentration take the shape of ellipses, the

major and minor axis of which coincide with the principal directions of diffusion. The plane is assumed to be infinite (no boundary effects) and a source of diffusing substance is assumed to exist at the centre of the ellipses previously mentioned.

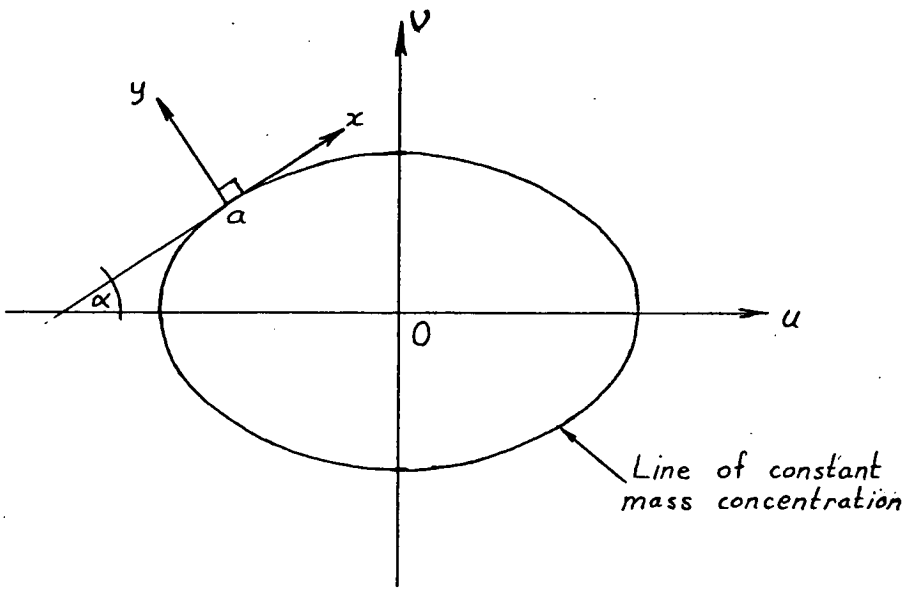

Figure 3.1
Semi-infinite anisotropic medium with source of diffusing substance at O

Let u and v be the principal directions of diffusion with corresponding diffusion coefficients $\mathcal{D}_u$ and $\mathcal{D}_v$.
The axes x/y are parallel/perpendicular to the elliptical mass concentration "contour" at a. The x-axis is rotated through the angle α with respect to the u-axis.
At a,

$$F_x = F_u \cos\alpha + F_v \sin\alpha .$$

From Fick's equation, $F_u = -\mathcal{D}_u \frac{\partial c}{\partial u}$ and so on.

Thus, $$F_x = -D_u \cos\alpha \frac{\partial c}{\partial u} - D_v \sin\alpha \frac{\partial c}{\partial v} \quad .$$

Similarly, $$F_y = D_u \sin\alpha \frac{\partial c}{\partial u} - D_v \cos\alpha \frac{\partial c}{\partial v} \qquad .....(3.5)$$

Also, $$\frac{\partial c}{\partial u} = \frac{\partial c}{\partial x}\frac{\partial x}{\partial u} + \frac{\partial c}{\partial y}\frac{\partial y}{\partial u} = \cos\alpha \frac{\partial c}{\partial x} - \sin\alpha \frac{\partial c}{\partial y}$$

and $$\frac{\partial c}{\partial v} = \frac{\partial c}{\partial x}\frac{\partial x}{\partial v} + \frac{\partial c}{\partial y}\frac{\partial y}{\partial v} = \sin\alpha \frac{\partial c}{\partial x} + \cos\alpha \frac{\partial c}{\partial y} \quad ..(3.6)$$

Substitution of equations (3.6) into (3.5) yields

$$F_x = -(D_u \cos^2\alpha + D_v \sin^2\alpha)\frac{\partial c}{\partial x} - (D_v - D_u)\sin\alpha\cos\alpha\frac{\partial c}{\partial y}$$

and $$F_y = -(D_v - D_u)\sin\alpha\cos\alpha \frac{\partial c}{\partial x} - (D_u \sin^2\alpha + D_v \cos^2\alpha)\frac{\partial c}{\partial y} \quad ...(3.7)$$

A similar analysis may be performed for the three-dimensional case. Note that equations (3.7) and (3.4) require

$$D_{xx} = D_u \cos^2\alpha + D_v \sin^2\alpha$$

$$D_{xy} = D_{yx} = (D_v - D_u)\sin\alpha\cos\alpha$$

$$D_{yy} = D_u \sin^2\alpha + D_v \cos^2\alpha$$

From equations (3.4) and (3.7), it is concluded that the mass fluxes F_x and F_y are coupled and that the coefficients responsible for the coupling, D_{xy} and D_{yx}, are equal.

The mass flux per unit area through any control surface in an orthotropic medium may therefore be calculated providing the principal diffusion coefficients and their directions are known.

Consider now an element of volume in an orthotropic material with sides dx, dy and dz parallel to the x, y and z axes respectively. Let the average

concentration of diffusant in the control volume be c.

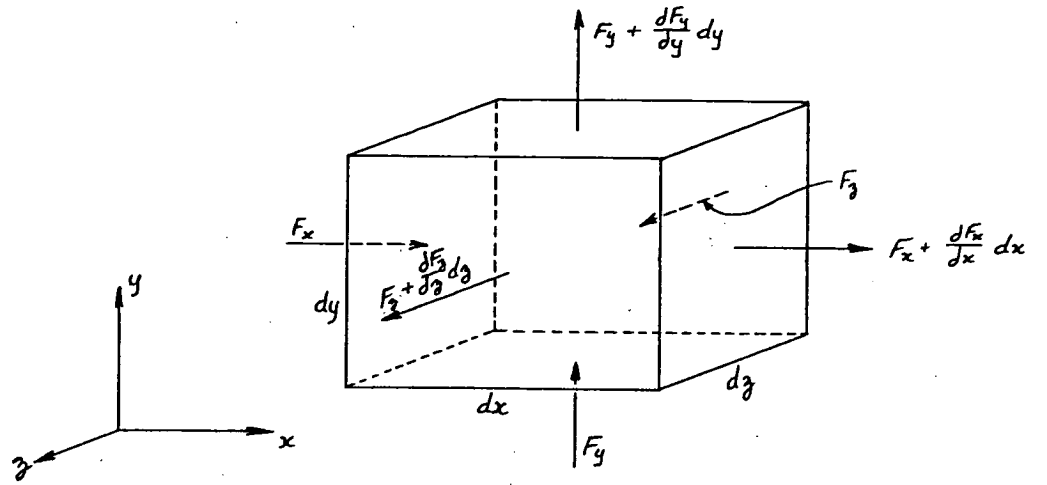

Figure 3.2
Mass diffusion through an element of orthotropic material.

Conservation of mass requires that

$$\left[\begin{array}{l}\text{The rate of change of}\\ \text{concentration in the}\\ \text{element.}\end{array}\right] = \left[\begin{array}{l}\text{The change in mass flux}\\ \text{through the element.}\end{array}\right]$$

In the x-direction, the change in mass flux through the element

$$= F_x\, dy\, dz - \left(F_x + \frac{\partial F_x}{\partial x} dx\right) dy\, dz$$

$$= -\frac{\partial F_x}{\partial x} dx\, dy\, dz .$$

Similar deductions can be made in the y and z directions. The rate of change of mass concentration in the element is given by

$$\frac{\partial c}{\partial t} dx\, dy\, dz .$$

Note that the units of mass flux, being kg/s/m^2 require that the mass concentration be given in units of kg/m^3.

Therefore, in three-dimensions,

$$\frac{\partial c}{\partial t}\, dx\, dy\, dz = -\left(\frac{\partial F_x}{\partial x} + \frac{\partial F_y}{\partial y} + \frac{\partial F_z}{\partial z} \right) dx\, dy\, dz$$

or

$$\frac{\partial c}{\partial t} = -\left(\frac{\partial F_x}{\partial x} + \frac{\partial F_y}{\partial y} + \frac{\partial F_z}{\partial z} \right) \qquad \ldots.(3.8).$$

For the two-dimensional case, we have

$$\frac{\partial c}{\partial t} = -\left(\frac{\partial F_x}{\partial x} + \frac{\partial F_y}{\partial y} \right) \qquad \ldots.(3.9).$$

Substituting for F_x and F_y from equations (3.4), we find

$$\frac{\partial c}{\partial t} = \frac{\partial}{\partial x}\left(D_{xx}\frac{\partial c}{\partial x} + D_{xy}\frac{\partial c}{\partial y} \right) + \frac{\partial}{\partial y}\left(D_{yx}\frac{\partial c}{\partial x} + D_{yy}\frac{\partial c}{\partial y} \right) . \quad \ldots(3.10)$$

Equation (3.10) is the general form of the unsteady state mass transfer equation in two dimensions based upon Fick's Law. This differential equation may be used to calculate the mass concentration distribution over a cross-section of orthotropic material subject to the condition that F_z = constant at all times, at all values of z .

Note that if the x and y axes coincide with the principle direction of diffusion, $D_{xy} = D_{yx} = 0$ and equation (3.10) reduces to

$$\frac{\partial c}{\partial t} = \frac{\partial}{\partial x}\left(D_{xx}\frac{\partial c}{\partial x} \right) + \frac{\partial}{\partial y}\left(D_{yy}\frac{\partial c}{\partial y} \right)$$

Furthermore, if D_{xx} is independent of x and D_{yy} is independent of y, we then find

$$\frac{\partial c}{\partial t} = D_{xx}\frac{\partial^2 c}{\partial x^2} + D_{yy}\frac{\partial^2 c}{\partial y^2} .$$

For the isotropic case $D_{xx} = D_{yy}$ and the common form of the equation results.

Providing that the diffusion coefficients in equation (3.10) are independent of concentration, c, a transformation to co-ordinates ξ, η may be found which reduces (3.10) to

$$\frac{\partial c}{\partial t} = D_\xi \frac{\partial^2 c}{\partial \xi^2} + D_\eta \frac{\partial^2 c}{\partial \eta^2} \quad . \qquad \text{.....(3.11)}$$

Crank (1956) states that this transformation may be made in a similar way to the transformation of the general ellipsoid

$$a_{11}x^2 + a_{22}y^2 + a_{33}z^2 + (a_{23}+a_{32})yz + (a_{31}+a_{13})zx + (a_{12}+a_{21})xy = const.$$

into the particular case where

$$a_1\xi^2 + a_2\eta^2 + a_3\zeta^2 = constant.$$

A further transformation putting

$$\xi_1 = \xi\sqrt{\frac{D}{D_\xi}} \qquad \text{and} \qquad \eta_1 = \eta\sqrt{\frac{D}{D_\eta}}$$

(where D may be chosen arbitrarily) yields

$$\frac{\partial c}{\partial t} = D\left(\frac{\partial^2 c}{\partial \xi_1^2} + \frac{\partial^2 c}{\partial \eta_1^2}\right) \qquad \text{.....(3.12)}$$

Thus, depending on boundary conditions and providing that the principle diffusion coefficients of a material are independent of concentration, c, problems in unsteady-state mass transfer in orthotropic materials may be reduced to problems in isotropic media.

3.2.2 Simultaneous heat and mass transfer

As stated earlier in this chapter, water is

energetically bound to the structural matrix of hydrophyllic materials. To remove moisture, we must supply enough energy to break the bonds holding the water molecules in place and thereby promote the process of diffusion. Bramhall (1979,a) shows that spreading pressure (when spreading pressure is used as the driving force of diffusion) and diffusion coefficient (when concentration is used as the driving force) both vary significantly with temperature. Therefore, mass and thermal diffusion must be studied simultaneously in the case of wood fibre.

Consider a small control volume of wood fibre through which moisture is diffusing.

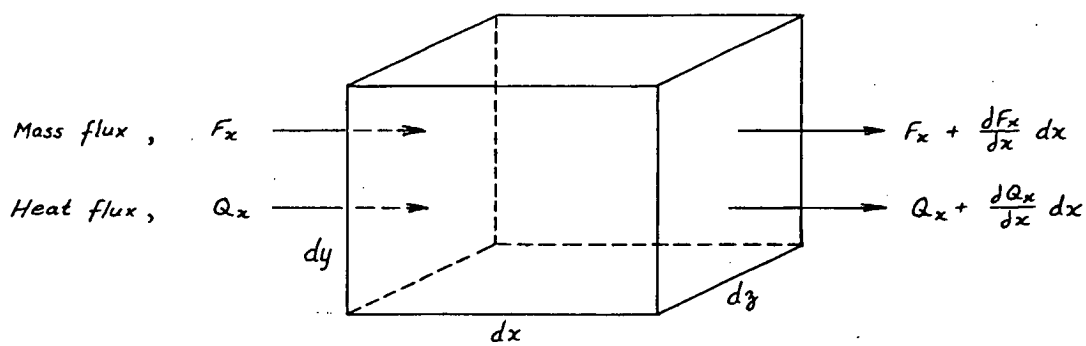

Figure 3.3
Simultaneous heat and mass transfer.

The rate equation for thermal diffusion as defined by Fourier states -

$$Q_x = -k \frac{\partial T}{\partial x}$$

where Q_x = thermal (heat) flux/unit area,

k = thermal conductivity,

and T = temperature.

As heat and mass transfer are analogous (according to Fick) and as the derivation of the mass transfer rate equations (3.7) and (3.2) are based on Fick's Law, we have, for heat transfer through orthotropic media:

$$-Q_x = k_{xx}\frac{\partial T}{\partial x} + k_{xy}\frac{\partial T}{\partial y} \quad ,$$

and $$-Q_y = k_{yx}\frac{\partial T}{\partial x} + k_{yy}\frac{\partial T}{\partial y} \quad . \qquad .....(3.13)$$

Conservation of energy requires that the energy used in the element to activate water molecules and promote mass diffusion must be equal to the change in heat flux across the element. That is,

$$\left[\begin{array}{c}\text{Change in mass}\\ \text{flux across the}\\ \text{element}\end{array}\right] \times \left[\begin{array}{c}\text{Activation}\\ \text{energy for}\\ \text{diffusion}\end{array}\right] + \left[\begin{array}{c}\text{Change in}\\ \text{heat flux across}\\ \text{the element}\end{array}\right] = 0$$

In the x - direction,

$$\left(\frac{\partial F}{\partial x}dx\ dy\ dz \times E\right) + \left(\frac{\partial Q_x}{\partial x}dx\ dy\ dz\right) = 0 \ .$$

Therefore, $$E\frac{\partial}{\partial x}\left(-D_{xx}\frac{\partial c}{\partial x} - D_{xy}\frac{\partial c}{\partial y}\right) + \frac{\partial}{\partial x}\left(-k_{xx}\frac{\partial T}{\partial x} - k_{xy}\frac{\partial T}{\partial y}\right) = 0$$

where E = activation energy of diffusion.

A similar expression may be derived for simultaneous heat and mass transfer in the y - direction. Thus, in two

dimensions, we find

$$\frac{\partial}{\partial x}\left[k_{xx}\frac{\partial T}{\partial x}+k_{xy}\frac{\partial T}{\partial y}\right]+\frac{\partial}{\partial y}\left[k_{yx}\frac{\partial T}{\partial x}+k_{yy}\frac{\partial T}{\partial y}\right]$$

$$=-E\left\{\frac{\partial}{\partial x}\left[\mathcal{D}_{xx}\frac{\partial c}{\partial x}+\mathcal{D}_{xy}\frac{\partial c}{\partial y}\right]+\frac{\partial}{\partial y}\left[\mathcal{D}_{yx}\frac{\partial c}{\partial x}+\mathcal{D}_{yy}\frac{\partial c}{\partial y}\right]\right\}. \qquad \ldots\ldots\ldots(3.14)$$

For the isotropic case, (3.14) reduces to

$$\frac{\partial^2 T}{\partial x^2}+\frac{\partial^2 T}{\partial y^2}=-\frac{\mathcal{D}E}{k}\left\{\frac{\partial^2 c}{\partial x^2}+\frac{\partial^2 c}{\partial y^2}\right\} \qquad \ldots\ldots(3.15)$$

and, providing $\mathcal{D}$, E and k are independent of temperature and assuming the moisture concentration distribution is known (from (3.10)), the temperature distribution may be calculated directly.

For wood, $\mathcal{D} = \mathcal{D}\ (c, T, \ldots.)$

$k = k\ (c, T, \ldots.)$

and therefore equations (3.10) and (3.14) should be solved simultaneously.

3.2.3 The independence of mass and thermal diffusion in "Tasmanian Oak" during drying.

Bramhall (1979,a) states that the relationship between the mass diffusion coefficient in timber and temperature (at constant moisture content) takes the form

$$\mathcal{D} = \mathcal{D}_0 e^{-E/RT}$$

where T = absolute temperature,

$\mathcal{D}_0$ = constant,

E = activation energy of diffusion,

and R = universal gas constant. (= 8.317 J/moleK)

Diffusion cell tests (see Chapter 5) were conducted on a number of samples of dry (moisture content =12%, dry basis) "Tasmanian Oak" cut in such a way that diffusion took place in the radial direction only. The apparatus described in section 5.2.6.2 was used and the relationship between mass diffusivity (diffusion coefficient) and moisture concentration determined at temperatures of 18, 28, 34 and 40°C (see Chapter 5). The results were rather inconsistent (primarily due to the effects described in section 3.6 and the occasional failure of the magnetic air-stirrers) but the general trend could be represented approximately by the relationship

$$D = D_0 e^{-\frac{3.8 \cdot 10^3}{T}} \qquad \ldots\ldots(3.16)$$

(see section 5.3.2)

According to Bramhall's model, the activation energy of diffusion indicated by equation (3.16) is approximately 1800 kJ/kg of water (compared with the "latent heat" of vapourisation of water at 20°C which is approximately 2500 kJ/kg). This agrees with the "spreading pressure" concept proposed by Babbitt (1977) and supported by Bramhall (1977) (see section 3.1.3).

The distribution of moisture and temperature within a drying material are linked by equation (3.15) which may be expressed in one dimension as follows:

$$\frac{\partial^2 T}{\partial x^2} = - \frac{ED}{k} \frac{\partial^2 c}{\partial x^2} \qquad \ldots\ldots(3.17)$$

where E = activation energy of diffusion ≃ 1800kJ/kg,

D = mass diffusivity ≃ $0.30_{10}{}^{-10}$ m^2/s for "Tasmanian Oak" in the tangential direction,

and k = thermal conductivity ≃ 0.6 $W/m^{o}C$ at high moisture concentrations.

Hence,

$$\frac{\partial^2 T}{\partial x^2} \simeq -9_{10}{}^{-5} \frac{\partial^2 c}{\partial x^2} \qquad \text{for "Tasmanian Oak".}$$

Assume that distributions of moisture of the form shown in figure (3.4) exist in "Tasmanian Oak" during drying and can be expressed as

$$c = c_o - (c_o - c_a)\left(\frac{x}{a}\right)^2$$

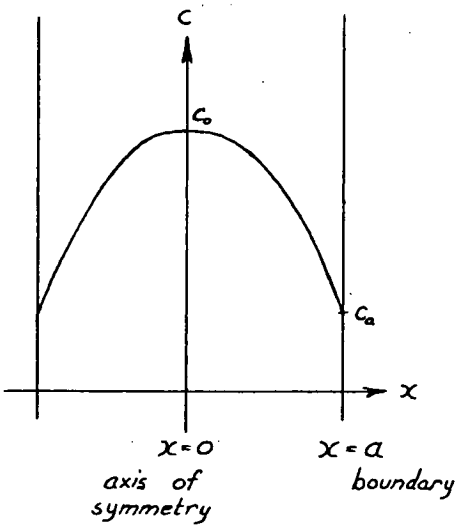

Figure 3.4

Parabolic moisture distribution in "Tasmanian Oak".

Hence,
$$\frac{\partial^2 c}{\partial x^2} = -\frac{2(c_o - c_a)}{a^2}$$

and therefore
$$\frac{\partial^2 T}{\partial x^2} = 9_{10}{}^{-5} \frac{2(c_o - c_a)}{a^2}$$

Intergration gives

$$T = T_a + 9_{10}\text{-}5\,(c_o - c_a)\left[\frac{x^2}{a^2} - 1\right]$$

where T_a = the temperature on the wood surface.

At the centre of the cross-section, $x = 0$ and

$$T = T_o = T_a - 9_{10}\text{-}5(c_o - c_a).$$

Typically, $T_a = 20^oC$, $c_o = 500$ kg/m^3, $c_a = 100$ kg/m^3 which gives the temperature in the centre of the material,

$$T_o = 19.96^oC$$

From data published by Barned (1970) and Young (1964), the following are typical properties of dry wood (M=12%):

Thermal conductivity, $k \simeq 0.16$ W/m^{o}C (across grain)

Specific heat, $C_p \simeq 1.9$ kJ/kg K.

Density, $\rho \simeq 750$ kg/m^3.

Thus, the thermal diffusivity,

$$\alpha_{dry} = \frac{k}{\rho C_p} \simeq 1.1_{10}\text{-}7 \text{ m}^2/\text{s}$$

According to the "Wood Handbook" published by the U.S. Forest Products Laboratory (1974), a typical value for the thermal diffusivity of dry wood (at a moisture content of 12%, dry basis) is $1.6_{10}\text{-}7$ m^2/s . It may be shown (U.S. F.P.L., 1974) that the thermal diffusivity of wood changes only marginally with moisture content.

The approximate mass diffusion coefficient of "Tasmanian Oak" in the tangential direction at moisture

concentrations above the fibre saturation point is $0.30_{10}{}^{-10}$ m^2/s at 30^oC (section 5.3.5). Therefore, the rate of thermal diffusion is very much greater than the rate of mass diffusion and hence heat and mass transfer may be studied independently in "Tasmanian Oak".

3.2.4 Initial and Boundary conditions

During this investigation, it has been assumed that the whole cross-section of the sample under consideration has initially uniform distributions of moisture concentration and temperature. Measurements in later chapters show these to be reasonable approximations.

At first, the boundary conditions during drying were handled by the assumption that the surface fibres of wood attain equilibrium moisture content with the atmosphere as soon as drying starts and remain at this value for all time thereafter. This is the usual approximation made when the mass/heat transfer through a material to its surface is very much slower than the transfer away from the surface into the surrounding medium. This does not strictly apply (Doe, 1981), particularly during the early stages of drying. Later in the investigation, surface fibre moisture concentration was measured as a function of time and typical relationships were used in the theoretical model. Such relationships were particularly important when analysing boards coated with semi-permeable materials.

3.3 Principal axes in sawn timber

Timber is an anisotropic material with the principal property directions shown in figure (3.5)

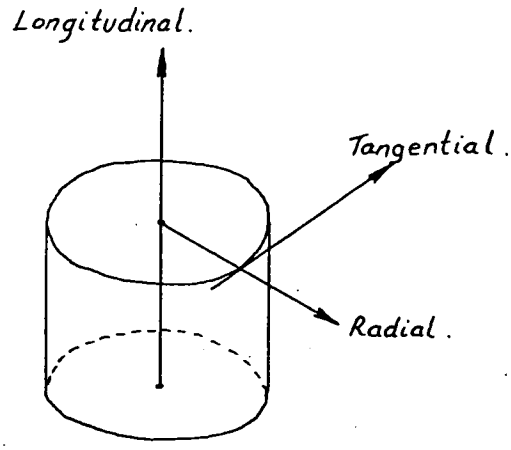

Figure 3.5

The principal axes of timber

Boards are sawn from a log so that their length coincides with the longitudinal direction and their cross-section is orientated somehow in the R-T plane. The two orientations of major interest are given in figure (3.6)

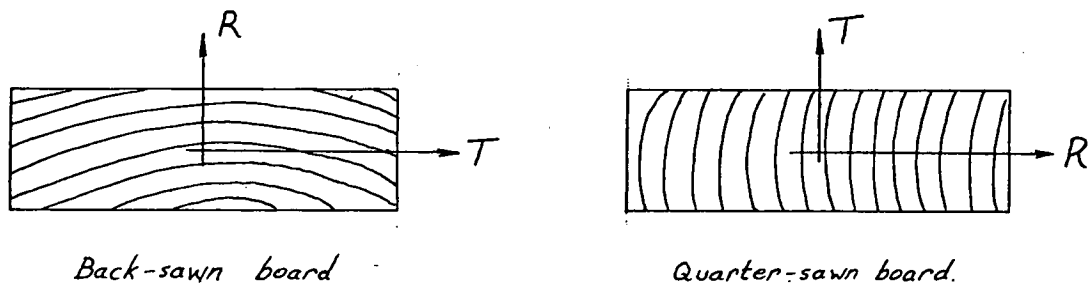

Figure 3.6

Cross-sections through back-sawn and quarter-sawn boards.

"T" and "R" correspond to the principal axes of diffusion during drying. If the radius from the centre of the tree is large with respect to the board dimensions, then the

growth-rings are essentially linear over the cross-section. That is, the directions of the principal axes of diffusion are invariant over the cross-section and are at right-angles to one-another. The equations (3.10) and (3.14) may therefore be used to describe simultaneous mass and heat transfer through wood. For perfectly backsawn and quartersawn boards, a further simplification may be made. In these cases, the x and y axes coincide with the principal directions of diffusion and therefore the angle $\alpha = 0$. Equations (3.10) and (3.14) become

$$\frac{\partial c}{\partial t} = D_x \frac{\partial^2 c}{\partial x^2} + D_y \frac{\partial^2 c}{\partial y^2} \qquad \ldots\ldots(3.18)$$

and

$$k_x \frac{\partial^2 T}{\partial x^2} + k_y \frac{\partial^2 T}{\partial y^2} = -E\left(D_x \frac{\partial^2 c}{\partial x^2} + D_y \frac{\partial^2 c}{\partial y^2} \right) \ldots.(3.19)$$

3.4.1 Mass transfer through composite slabs

A method of controlling the drying stresses in timber by coating each board with a semi-permeable substance is described in detail in Chapter 4. An understanding of mass transfer through composite slabs is therefore necessary.

Mass transfer through composite slabs where the interfaces between materials are sharply defined is not well documented. Such problems on heat transfer between isotropic substances with constant or quasi-constant material properties are discussed by Carslaw and Jaeger. They propose that the units of length in one material be scaled in such a way that either specific heat, C_p, or thermal conductivity, k

is constant throughout the modified slab. Note also that, at an interface, there can be no discontinuity in temperature although there may be a discontinuity in temperature gradient. In mass transfer, however, it is probable that a discontinuity at an interface exists in both the mass concentration distribution and the gradient of mass concentration.

If a pressure were used as the driving force for mass diffusion, a discontinuity at the interface seems most unlikely, providing that the flow mechanisms in the two materials are similar.

The discontinuity in mass concentration would depend on such factors as:

i) The densities, physical properties and chemical structures of the two materials.

ii) The ways in which diffusant is held in the materials.

iii) The transport regimes present on each side of the interface.

It is proposed that such phenomena be handled in a similar manner to the temperature changes which occur at a solid/gaseous interface in heat transfer: that is, by defining an "interface mass transfer coefficient" in much the same way as a surface heat transfer coefficient. This may be done in the following way:

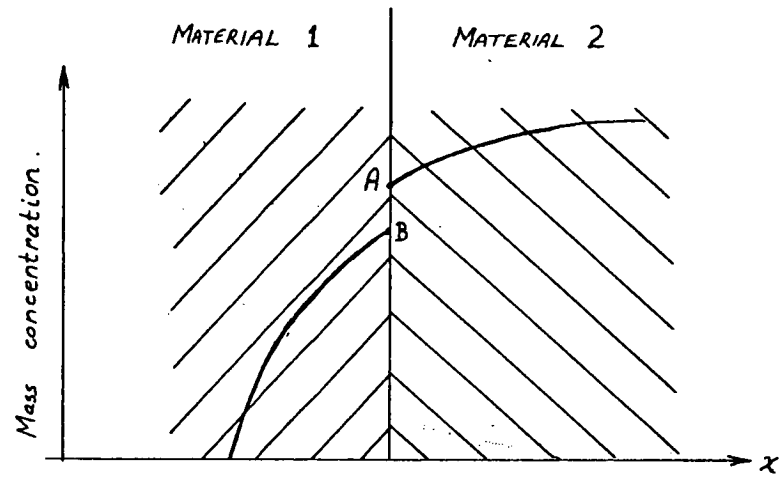

The mass flux through material 2 at A, δ^+, is given by

$$\delta = - D_2 \left.\frac{\partial c}{\partial x}\right|_{(A,2)} \qquad \ldots\ldots(3.20)$$

Assuming there is no storage or accumulation of mass at the interface, the mass flux through the interface, $\delta = \delta^+$. For continuity, the mass flux through material 1 at B, δ^-, is such that

$$\delta^- = \delta = \delta^+$$

The interface is considered to have no thickness, therefore the interface zone cannot possess physical properties, and the rate equation (see equations (3.1) and (3.20)) cannot be applied. However, the mass flux through the interface will depend upon the size of the concentration discontinuity. We therefore write

$$\delta = d\,(c_A - c_B) \qquad \ldots\ldots(3.21)$$

where d is the interface mass transfer coefficient and is dependent upon the two materials under consideration.

Providing the mass concentration distribution is known in one material, equation (3.21) enables us to establish boundary conditions for the purpose of calculating the concentration distribution in the other.

3.4.2 Estimation of required coating properties -approximate method

To effectively control the drying stresses in timber, a semi-permeable coating must hold the surface fibres of a board at or above the fibre saturation moisture concentration ($\simeq$ 170 kg/m^3, see section 4.1.5) for a period of time sufficient to allow the moisture gradients within the board to reduce to a suitably low level.

Consider a semi-infinite slab of wood drying through a water-permeable coating (figure 3.7). The coating has a mass diffusivity (diffusion coefficient) $\mathcal{D}_c$, and a thickness, d. Assume that the surface of the coating is in equilibrium with the atmosphere and that the temperature and humidity of the atmosphere are held constant. Assume also that there is no discontinuity in moisture concentration at the wood-coating interface. From results presented in section 5.3.3, it is reasonable to approximate the diffusivity of wood to a constant at moisture concentrations above the fibre saturation point.

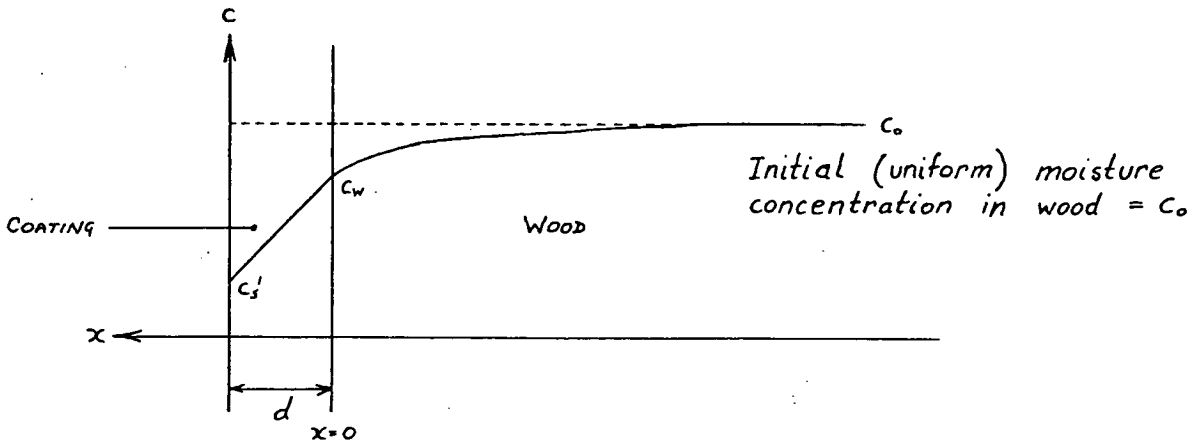

Figure 3.7
Moisture concentration distribution in wood and coating.

The mass flux per unit area through the coating, $\dot{e}_c$, is given approximately by

$$\dot{e}_c \simeq \frac{\mathcal{D}_c}{d} (c_w - c_s') \qquad .....(3.22)$$

In the wood, the mass flux per unit area in the x-direction at any point,

$$\dot{e}_w = - \mathcal{D}_w \frac{\partial c}{\partial x} \qquad .....(3.23)$$

The one-dimensional unsteady-state diffusion equation in the wood is

$$\frac{\partial c}{\partial t} = \mathcal{D}_w \frac{\partial^2 c}{\partial x^2} \qquad .....(3.24)$$

At the wood-coating interface $(x = 0)$, $\dot{e}_c = \dot{e}_w$.
That is,

$$- \left.\frac{\partial c}{\partial t}\right|_{x=0} + \frac{\mathcal{D}_c}{\mathcal{D}_w d} (c_w - c_s') = 0 \qquad .....(3.25)$$

By putting $v = c - c_s'$, the governing equation (equation 3.24) becomes

$$\frac{\partial v}{\partial t} = D_w \frac{\partial^2 v}{\partial x^2} \qquad \ldots.(3.26)$$

with the boundary (interface) condition

$$-\frac{\partial v}{\partial x} + \frac{D_c}{D_w d} v = 0 \qquad \ldots..(3.27)$$

at $x = 0$.

The required solution is that which describes the moisture concentration in the wood at the coating-wood interface as a function of time.

Carslaw and Jaeger (1959) give the required solution to equation (3.26) subject to the boundary condition (3.27) as

$$\frac{v_s}{V} = e^{At} \; erfc\sqrt{At}$$

where $erfc$ is the error function,

t = time,

$$A = \frac{D_c^2}{D_w d^2},$$

v_s = the value of v at the wood-coating interface,

and V = the initial value of v, $(c_o - c_s')$.

If $x \geqslant 2$, $\quad x\, e^{x^2}\, erfc\, x \simeq 0.5$.

Therefore,

$$\frac{v_s}{V}\sqrt{At} \simeq 0.5 \quad \text{if} \quad \sqrt{At} \geqslant 2.$$

Typically, c_o = 500 kg/m^3 for "Tasmanian Oak".

Assume that the moisture concentration in the coating at the coating/air interface, c_s' = 100 kg/m^3. Further, assume that the moisture concentration in the

wood at the wood/coating interface at time = t,

c_w = 200 kg/m^3 .

Therefore $$\frac{v_s}{V} = \frac{c_w - c_s'}{c_o - c_s'} = \frac{100}{400}$$

and hence $$\sqrt{At} \simeq 2 \quad .$$

Substituting for A and re-arranging yields

$$d \simeq \frac{D_c}{2}\sqrt{\frac{t}{D_w}} \qquad .....(3.28)$$

where d = thickness of coating with mass diffusivity, D_c, required to hold the surface fibres of a board (with a mass diffusivity D_w) above the fibre saturation moisture concentration for a time, t, after the commencement of drying.

3.5 Methods of solution of partial differential equations

3.5.1 Analytical methods

Analytical solutions to the Fourier heat transfer equation which, by Fick's assumption is analogous to the equation describing mass transfer, are available from many publications. One of the most thorough treatments of this topic is that given by Carslaw and Jaeger (1959). They show that the solution to the equation

$$\frac{\partial^2 T}{\partial x_1^2} + \frac{\partial^2 T}{\partial x_2^2} + \frac{\partial^2 T}{\partial x_3^2} = \frac{1}{k} \frac{\partial T}{\partial t} \quad , \qquad \ldots.(3.29)$$

when applied to a rectangular parallelepiped subject to certain initial and boundary conditions (Carslaw and Jaeger, 1959, p.33) is given by

$$T = T_1 (x_1, t).T_2 (x_2, t).T_3 (x_3, t) \ ,$$

where $T_1(x_1, t)$ is the solution to the simple equation

$$\frac{\partial^2 T_1}{\partial x_1^2} = \frac{1}{k} \frac{\partial T_1}{\partial t} \quad .$$

Constant temperature on the boundary and uniform initial temperature is a simple and important case in which the above simplification can be made. This is analogous to the simplest circumstances under which drying may take place.

Rephrasing Carslaw and Jaeger, the solution to the equation

$$\frac{\partial c}{\partial t} = D \frac{\partial^2 c}{\partial x^2} \qquad \ldots..(3.30)$$

in the semi infinite slab $-\ell < x < \ell$ (with uniform initial moisture concentration, c_o, and concentration on the boundaries kept at zero) is

$$c_x(x,\ell) = \frac{4c_o}{\pi} \sum_{n=0}^{\infty} \frac{(-1)^n}{(2n+1)} e^{-D(2n+1)^2\frac{\pi^2 t}{4\ell^2}} \cos\frac{(2n+1)\pi x}{2\ell} \quad \ldots.(3.31)$$

$$= c_o - c_o \sum_{n=0}^{\infty} (-1)^n \left\{ erfc\frac{(2n+1)\ell - x}{2\sqrt{Dt}} + erfc\frac{(2n+1)\ell + x}{2\sqrt{Dt}} \right\} \quad \ldots.(3.32)$$

providing the diffusion coefficient is a constant. The moisture concentration distribution as a function of time for a solid with uniform initial moisture concentration and moisture concentration held at zero on the boundaries and with the cross-section shown below

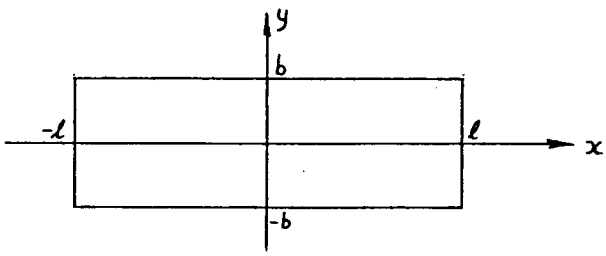

is given by

$$c = c_x(x, \ell).c_y(y, b)$$

where $c_x(c, \ell)$ is given in equations (3.31) and (3.32). For orthotropic materials where the directions of the principal axes of diffusion coincide with the x and y axes, the solution is obtained in a similar way.

Unfortunately, the orthotropic diffusion coefficients in wood are functions of moisture concentration and temperature and therefore the solutions given above cannot be used with a great degree of accuracy under most circumstances.

3.5.2 Numerical solutions to the governing equations

The finite difference approximation used in conjunction with digital computers is the simplest and most common method of solving partial differential equations with variable coefficients, variable boundary conditions or non-uniform initial conditions or any combination of these conditions. The method involves superimposing a grid with a finite number of intersections or points over the cross-section of a body. The unknowns are evaluated at each grid point. In the case of simultaneous moisture and heat transfer through wood the unknowns at each internal grid point are moisture concentration and temperature.

The initial conditions are given and the boundary conditions are assumed to be known for all time after drying starts.

Figure (3.8) shows a 9 x 7 = 63 point grid over a timber board of rectangular cross-section.

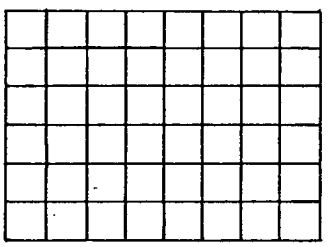

Figure 3.8
Finite difference grid over a body of rectangular cross-section

The number of unknowns at any time = (7 x 5) = 35.
Therefore, 35 equations must be solved at each point in time.

Finite difference approximations to derivatives are made in the following way -

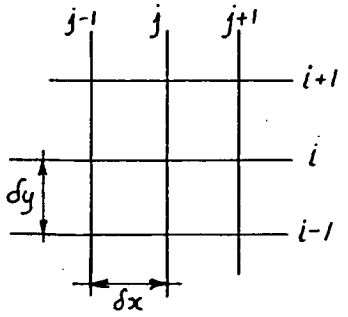

In forward differences, $\left.\frac{\partial c}{\partial x}\right|_f \simeq \frac{c(i,j+1) - c(i,j)}{\delta x}$

Similarly, backward differences give

$$\left.\frac{\partial c}{\partial x}\right|_b \simeq \frac{c(i,j) - c(i,j-1)}{\delta x}$$

and central differences $\left.\frac{\partial c}{\partial x}\right|_c \simeq \frac{c(i,j+1) - c(i,j-1)}{2\,\delta x}$.

Therefore $\frac{\partial^2 c}{\partial x^2} \simeq \frac{\left.\frac{\partial c}{\partial x}\right|_f - \left.\frac{\partial c}{\partial x}\right|_b}{\delta x} = \frac{c(i,j+1) - 2c(i,j) + c(i,j-1)}{\delta x^2}$

Higher order derivatives may be built up in a similar manner. The equation

$$\frac{\partial c}{\partial t} = \frac{\partial^2 c}{\partial x^2} \qquad \text{.....(3.33)}$$

may therefore be approximated to

$$\frac{c(i,t) - c(i,t-\delta t)}{\delta t} = \frac{c(i+1,t) - 2c(i,t) + c(i-1,t)}{\delta x^2}$$

where t = time and δt = time increment, δx = space increment. The LHS bas been evaluated by a backward difference. That is

$$\left(1 + \frac{2\delta t}{\delta x^2}\right)c(i,t) - \frac{\delta t}{\delta x^2}\left[c(i+1,t) + c(i-1,t)\right] = c(i,t-\delta t) \qquad \text{....(3.34)}$$

The left-hand side of this equation in unknown and the right-hand side known. This is called an implicit

approximation and requires that a set of simultaneous equations be solved in order to evaluate the unknowns. On the other hand, if the conditions at time = t are known and the left-hand side of equation (3.33) is approximated by forward differences, the finite difference approximation yields

$$c(i,t+\delta t) = c(i,t) + \frac{\delta t}{\delta x^2}\left[c(i+1,t) - 2c(i,t) + c(i-1,t)\right] \quad \ldots.(3.35)$$

where the left-hand side is unknown and the right-hand side is known. This is called the explicit method of solution. Although explicit methods require a minimum of computation, they require that the time increments, δt, be very small. This requirement arises from consideration of the convergence of the numerical solution to the exact solution of the partial differential equations. Implicit methods of solution are stable for far wider ranges of δt and δx and therefore are more often used. (The governing diffusion equation was approximated by the implicit method and used throughout this investigation - see Appendix B).

3.5.3 Convergence, stability and consistancy of finite difference systems

There are two different but related problems associated with the solution of partial differnetial equations by finite difference approximations. The first concerns the convergence of the exact solution of the approximating difference equations and the second concerns

the unbounded growth or controlled decay of any errors associated with the solution of the finite difference equations. G.D. Smith (1978) includes both qualitative and quantitative descriptions of convergence, stability and compatibility in his book on numerical solutions to partial differential equations. Discussion in this chapter is limited to qualitative definitions of the three topics mentioned.

3.5.3.1 Convergence

A finite difference equation is said to be convergent if the exact solution to the difference equation tends to the exact solution to the partial differential equation at a particular time as both the space and time intervals used in the approximation tend to zero. The difference between the two solutions is often called the discretization error, the size of which depends upon the finite sizes of the grid lengths (in space and time) and the difference approximation to the derivative. The discretization error can usually be reduced by decreasing the grid lengths but this leads to an increase in the number of equations to be solved. This method of improvement is limited by such factors as the cost and size of storage on available computing facilities and so on.

3.5.3.2 Stability

The exact solution to the difference equations would only be possible if all calculations were carried

out to an infinite number of decimal places. In practice, each calculation is carried out to a finite number of places which introduces a rounding error every time a given number is operated upon. The difference between the exact solution to the difference equations and the numerical solution is termed the global rounding error. The total error in the finite difference solution at any given mesh point is the sum of the discretization and global rounding errors. The global rounding error depends not only upon the finite difference equations but also upon the way in which the computer rounds off numbers. This error also differs from the discretization error in that it cannot be made to converge to zero as the mesh size tends to zero. In fact, the opposite would happen as smaller mesh sizes imply increased numbers of arithmetic operations. Fortunately, the rounding errors in modern computing machines are very small and the global rounding error is usually smaller than the discretization error.

3.5.3.3 Consistency (compatibility)

It is possible to approximate a partial differential equation by a finite difference scheme that is stable but which has a solution that converges to the solution of a different partial differential equation as the mesh size tends to zero. Such finite difference schemes are said to be inconsistent or incompatible with the partial differential equation. Smith quotes a theorem of Lax which states that:

"...if a linear finite difference equation is consistent with a properly posed linear initial-value problem then stability guarantees convergence."

He goes on to summarize by saying

"In general, a problem is properly posed if:

i) The solution is unique when it exists.

ii) The solution depends continuously on the initial data.

iii) A solution always exists for the initial data that is arbitrarily close to the initial data for which no solution exists."

3.6 Considerations regarding the determination of mass diffusion coefficients.

There are three major factors which must be considered when testing for the diffusion coefficients of wood, viz:

1) Sorption hysteresis
2) Sorption history
3) Moisture boundary layers in the air surrounding samples.

Christensen and Hergt (1969) reported:

"It has long been known that wood, wool and other swelling polymers do not behave reversibly during adsorption and desorption of vapours. One example of this is sorption hysteresis. It has also been shown that, even if sorption equilibrium at a given vapour pressure is approached in one direction only

> and from a reproducable starting point, the equilibrium moisture content may differ according to the number and size of the intermediate equilibrium steps by which it is reached".

Tests referred to by Bramhall (1979,a) indicate that at 75% relative humidity, the equilibrium moisture contents of various North American hardwoods differed in magnitude by 20% depending upon the direction (adsorbing, desorbing) from which equilibrium was approached.

Christensen and Hergt demonstrated that moisture transfer rates decrease as the time for which the sample is held in "equilibrium" increases. In summary, they state that:

> "....the rate of sorption of water vapour by wood and perhaps other swelling polymers depends strongly on the length of time for which they have been held at the preceeding "equilibrium" condition".

During this investigation, the aim of tests was to determine the diffusion coefficients applicable to the drying of "Tasmanian Oak" from the freshly sawn (green) condition to equilibrium with the atmosphere. The observations quoted point to the necessity of using samples that have no previous drying history. Only then will the diffusion coefficients determined be applicable to the initial drying process.

The third factor affecting the results of

diffusion tests was studied by McKay (1971). He noted that the results of diffusion cell experiments were greatly affected by the speed of "stirring" of the air inside diffusion cells. If the atmosphere at the surface of a piece of timber through which moisture transfer is taking place is stationary, significant moisture gradients are established in the air. Figure (3.9) demonstrates the effects of such boundary layers on the concentration gradients across samples in diffusion cells. The concentration difference across the sample in figure (3.9,a), $\Delta c'$, is very much lower than the maximum available concentration difference, Δc_{max}, between the two constant humidity atmospheres due to well-established boundary layers.

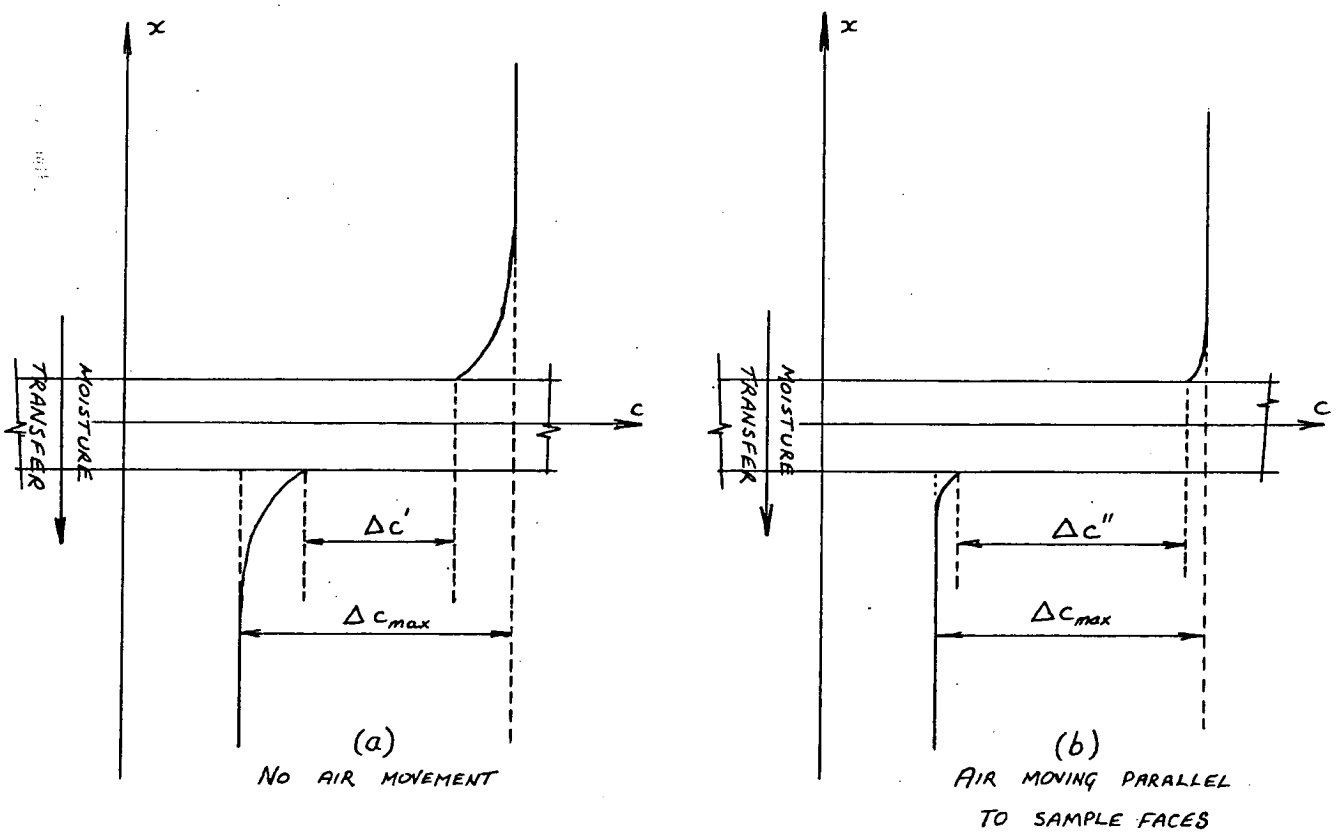

Figure 3.9

Varying conditions across wood samples in duffusion cells

The effects of boundary layers are reduced significantly by ensuring that there is sufficient air movement over the faces of the sample (figure 3.9,b). The usual assumption made when analysing moisture transfer through timber is that the surface fibres are in equilibrium with the atmosphere in which adsorption or desorption is taking place (based on the fact that diffusion of moisture through wood to its surface is much slower than the removal of moisture from the surface). This leads to the assumption that the concentration gradient across the sample of figure (3.9) is Δc_{max} which is reasonable in the case of figure (3.9,b). Care must therefore be taken to ensure that moisture boundary layers of significant magnitude do not exist at the surfaces of samples during diffusion tests.

McKay's tests on the stirring of air inside diffusion cells indicate that the flux of moisture through the sample changed by 50% over the range of stirring speeds available to him. He concluded that

> ".... one should be satisfied that while the pattern of results obtained is valid, the actual values themselves may be of little significance and meaning."

The boundary layer discussion is pertinent to the determination of diffusion coefficients by the method described in section 5.2.6.3 (method of inferring coefficients) although the effects may not be quite as marked.

Regardless of the procedure used to determine diffusion coefficients, great care must be taken to ensure that the assumptions made during analysis are consistent with the conditions of the experiment. Furthermore, if the diffusion coefficients determined are to be used in a mathematical model for the drying of boards from the freshly-sawn (green) condition to equilibrium with the atmosphere, the samples tested must themselves be freshly sawn. Only then will tests be free of historical effects (hysteresis, etc.).

REFERENCES

BABBITT, J.D. (1977): More on application of Fick's Laws. Wood Science 9(4): 149-151

BARNED, J.R. (1970): Thermal conductivity of building materials. Revised by L.F. O'Brien. Report R.2 Division of Building Research, C.S.I.R.O. Melbourne, Australia.

BRAMHALL, G. (1977): More on application of Fick's Laws. Wood Science 9(4): 152-153.

..... (1979,a): Sorption diffusion in wood. Wood Science 12(1): 3-13.

..... (1979,b): Mathematical model for lumber drying I. Principles Involved Wood Science 12(1): 14-21.

..... (1979,c): Mathematical model for lumber drying II. The model Wood Science 12(1): 22-26.

BUI, X., E.T. CHOONG, W.G. RUDD; (1980): Numerical methods for solving the equation for diffusion through wood during drying. Wood Science 13(2): 117-121.

CARSLAW, H.S., J.C. JAEGER, (1959): Conduction of heat in solids, 2nd Ed.
Oxford Univ. Press, London, England.

CHRISTENSEN, G.N., H.F.A. HERGT, (1969): Effects of previous history on kinetics of sorption by wood cell walls.
Journal of Polymer Science
Part A-1, Vol. 7 : 2427-2430.

CRANK, J. (1956): The mathematics of diffusion.
Oxford Univ. Press, London, England.

DOE, P.E. (1973): A mathematical model for shrinking solids during drying.
First Aust. Conf. on Heat and Mass Transfer.
Monash Univ. Melbourne, Australia.

.....(1981): On conditions at the boundary of hygroscopic materials during drying.
----- Under preparation -----
Univ. of Tasmania, Hobart, Australia.

JASON, A.C. (1965): A study of evaporation and diffusion processes in the drying of fish muscle.
J. of Sci., Food and Agric. 16:

KEEY, R.B. (1972): Drying principles and practice
Pergamon Press

McKAY, J.F.G. (1971): Moisture flux determinations infulenced by air circulation inside diffusion cells.
Wood Science 3(4): 220-222.

ROHSENOW, W.M., H.Y. CHOI (1961): Heat, mass and momentum transfer.
Prentice - Hall (Inc.).

SMITH, G.D. (1978): Numerical solution of partial differential equations: Finite difference methods. 2nd Ed.,
Oxford Univ. Press, London, England.

U.S. F.P.L. (1974): Wood handbook: Wood as an Engineering material.
Agricultural Handbook No. 72.
U.S. Government Printing Office
Washington, D.C.

YOUNG, H.D., (1964): Fundamentals of mechanics and heat.
McGraw - Hill Kogakusha, Tokyo, Japan.

CHAPTER 4

CHAPTER 4

THE SEASONING OF HARDWOODS.

4.1 Common Terms used in Timber Drying

Over the many years in which the seasoning of timber has been studied, names have been given to various phenomena commonly observed. Some of these terms are defined in this section.

4.1.1 "Set" is the term usually applied to semi-permanent or non-elastic deformation of wood fibre (in either tension or compression) as a result of the fibre being restrained in some way during drying (and hence while shrinking). It can be thought of as similar to creep.

4.1.2 "Case-hardening" is the term used to describe the state of timber which has been seasoned under severe

conditions (e.g. low humidity), resulting in extremely dry and tough surface zones. These zones form a "case" of material with low permeability around the central "core" of a board. Drying of the "core" becomes very difficult and is extremely slow.

As McMillen ( ) reports, this condition is brought about primarily as a result of high stresses early in drying causing a permanent deformation (set) of the wood cells at and near the surface. This causes disruption to the diffusion pathways and inhibits drying. The phenomenon of "collapse" (4.1.4) may also be a contributing factor. The apparent hardening of the case is probably brought about by stiffening of wood fibre as its moisture content decreases.

4.1.3 "Checking" is the formation of cracks or fissures in the wood fibre running along the grain but not extending through the piece from one surface to another. Checks generally result from stresses generated during seasoning and may be initiated at the surface (hence surface checking) or inside wood (internal checking or "honeycombing"). The term "checking" is generally used in connection with sawn or processed material.

4.1.4 "Collapse", as defined by Hillis and Brown (1978) is the

> "Flattening or buckling of the wood cells during drying, sometimes manifested in excessive and/or uneven (irregular) shrinkage."

The generally accepted theory regarding the cause of collapse is stated by Pankevicius (1960) in the following way:

> "... if the very small fibres of the wood are completely filled with water initially, and the free water in those fibres can dry out without air entering to take its place, then the resulting liquid tension forces become very large. When the magnitude of these forces exceeds the crushing strength of the fibre walls, these cave-in to cause collapse".

In the above context, "Liquid tension" is understood to mean "vapour pressure significantly below atmospheric pressure". Kauman (1966) summarises his experimental work on collapse by saying:

> "The accumulated experimental evidence is shown to support Tiemann's theory of hydrostatic tension as the main cause of collapse, with important additional contributions by drying stresses".

The term "hydrostatic tension" used by Kauman refers to liquid surface tension effects apparent in confined spaces. Collapse can only occur in wood fibre in which free water is present.

The large proportion of collapse may be removed by the process of "reconditioning". This requires that the timber be subjected to an atmosphere of saturated steam at

100°C for periods ranging from four to twelve hours and has the effect of returning most of the wood cells to their original unbuckled shape.

4.1.5 The "fibre saturation point" of wood fibre is the moisture content below which "free" water ceases to exist within the cell cavities. At this point, the wood-cell walls are still saturated. Many of the properties of wood change dramatically as the moisture content changes from above to below the fibre saturation point.

4.1.6 "Reaction Wood": From the glossary of terms in Hillis and Brown (1978), reaction wood is:

> "Wood with more or less distinctive anatomical characters formed typically in parts of leaning or crooked stems and in branches".

In eucalypts, this consists of "tension wood" or wood fibre laid down on the tension side of a leaning stem. Tension wood exhibits higher shrinkage than ordinary wood fibre and is characteristically difficult to season.

4.2 Geometric Considerations Related to Shrinkage.

Most timbers, including the "Tasmanian Oak" group, have the characteristic that the circumferential shrinkage is approximately twice the radial shrinkage. (These directions are defined with respect to a log). This difference in shrinkage leads to a geometric anomaly

during drying, brought about by the fact that the circumference of a circle is a linear function of the radius. If the radius varies by 10%, then the circumference must also vary by 10% for the sake of geometric consistency. Therefore, as logs dry, high circumferential stresses are generated and hence the tendancy for logs to develop radial splits. Such splits are initiated at the ends where drying is most rapid and may eventually run the full length of the log.

Similar behaviour is often observed in boards cut from near the heart of a tree, particularly where the radius of curvature of the seasonal or growth rings is small in relation to the dimensions of the board. If such material can be dried without excessive degradation, the residual stresses are usually high.

Approaching the drying of back-sawn material from a purely geometric viewpoint, it may be deduced that such material will inevitably distort in cross-section. This distortion takes the form of cupping (Fig. 4.1)

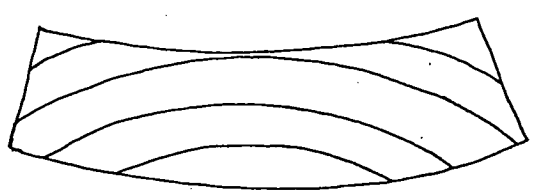

Figure 4.1

Distortion of a board cross-section by "cupping".

Campbell (1975,a) suggests that restraint of this cupping due to the weight of material stacked on top of a given board may contribute to checking.

4.3 Qualitative Description of the Drying of Hardwoods.

4.3.1 General

The drying of the "Tasmanian Oak" group of species when sawn into boards follows closely the pattern of drying of most hardwoods (McMillen,) with the additional complication that the characteristically large shrinkages observed in most eucalypt species increase the probability of seasoning degrade.

The surfaces of sawn boards tend to approach the equilibrium moisture content of wood fibre under the prevailing conditions very soon after the commencement of drying (see the sorption isotherm, Figure 4.2).

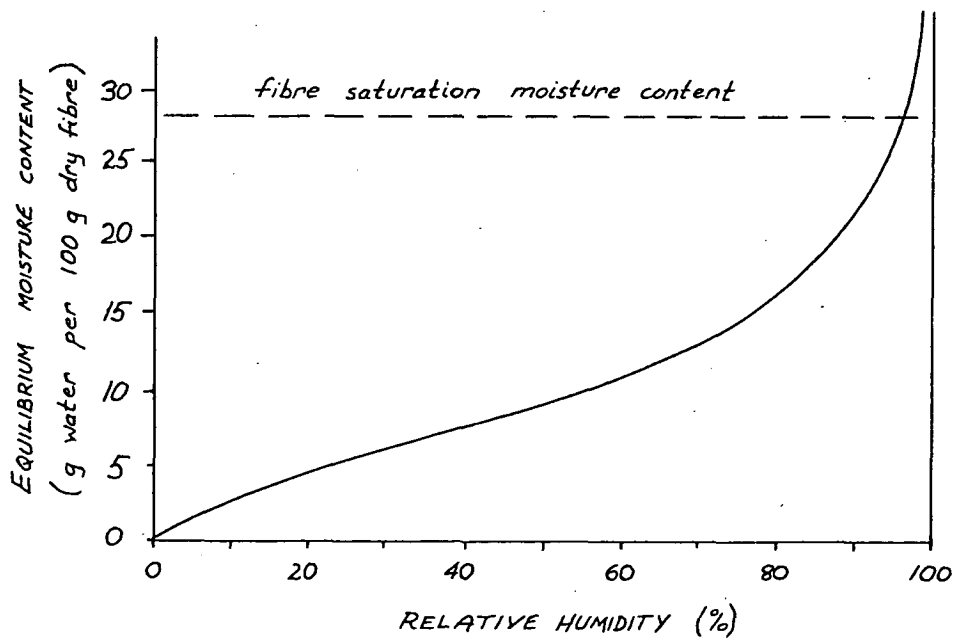

Figure 4.2

Approximate sorption isotherm for wood (Temp. approx. 20°C).

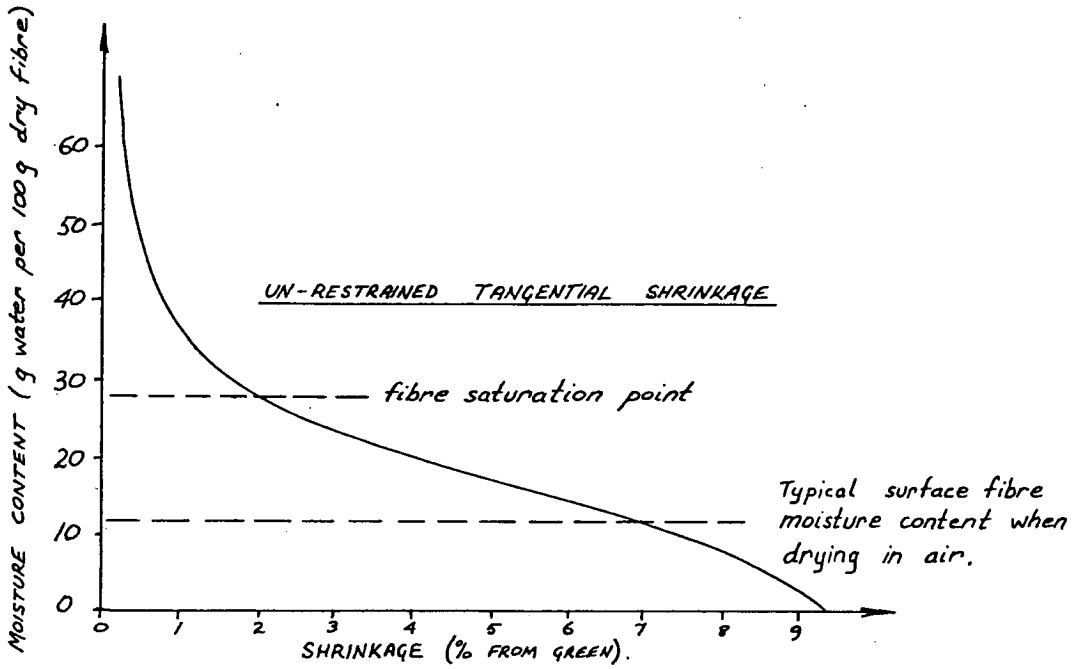

Figure 4.3

Typical moisture content-shrinkage relationship for eucalypt fibre.

The outer zones of the wood therefore dry below the fibre saturation point and tend to shrink (Figure 4.3) but are restrained by the inner zones which have not begun to shrink significantly. As a result, the outer zones are subjected to a tensile stress, and, as a reaction, the interior zones are subjected to a compressive stress. Because of tensile stresses increasing beyond the proportional limit and the action of prolonged stress (resulting in creep), tension set begins to take place in the outer zones almost immediately after drying starts. The tensile stresses increase to a maximum within 24 hours in the case of "Tasmanian Oak". It is at this stage that surface checking is most likely to develop due to the timber being stressed beyond its ultimate limit. Surface checking is simply a stress relief mechanism.

As drying proceeds, succeeding inner zones change from compression to tension and the tensile stress at the surface gradually reduces. Meanwhile, the compressive stress in the inner zones gradually builds to a maximum. As these compressive stresses increase beyond the proportional limit, creep takes place due to the prolonged action of stress and compression set develops. At this stage, the inner zones are still well above fibre saturation point.

Because tension set in the outer zones gives these zones a dimension larger than they would normally have at a given moisture content, the stress in the outer zones changes from tension to compression as the inner zones dry and shrink. To balance the compressive force in the outer zones, the inner zones go into tension and hence a complete stress reversal takes place. At such a time, surface checks close. However, if the surface checking has been severe and checks are deep, they may be propagated right through the central zones as tensile stresses there build up. At this stage, cupping due to drying stresses, particularly in back-sawn material, may become apparent.

After complete stress reversal, the outside layers rapidly proceed to a maximum compressive stress and a corresponding maximum tensile stress is generated in the central areas. The magnitude of this tensile stress depends upon the amount of set that has previously occurred and, if severe enough, will initiate internal checking or honeycombing. At this time, the center zones of the wood

are still near the fibre saturation point and therefore collapse may still be taking place.

When the inner zones fall below fibre saturation point, the average moisture content of the timber is typically 17 to 23% (dry basis) and the process of reconditioning may be used to remove collapse. Reconditioning results in collapsed sawn boards returning to approximately rectangular cross-sections. Residual drying stresses are also reduced during the process, and the moisture distribution becomes more uniform due to the uptake of moisture by the surface fibres. Surface checks may be re-opened during reconditioning, but internal checks usually close. Typically, the average moisture content of newly reconditioned boards is 20 to 25% (dry basis).

Drying from 20% to fibre equilibrium moisture content (12 to 14% in Tasmania) is very slow if affected in air. Kilns are usually employed at this stage. During kiln drying, drying stresses are usually not high and further degradation of the timber is uncommon providing suitable kiln schedules are observed.

4.3.2 Drying Eucalypt Timbers.

Eucalypt wood is relatively impermeable and difficult to season (Hillis and Brown, 1978). Therefore it dries slowly and with steep moisture gradients producing pronounced drying stresses and sets. Shrinkage is high and surface checking on back-sawn faces is typical. Nevertheless,

seasoned timber of high quality can be produced from a wide range of eucalypt species.

Campbell and Hartley (Hillis and Brown (1978), chapter 16) sum up the checking problem as follows:

> "Most of the eucalypts tend to check on back-sawn faces during seasoning, sometimes severely, but quarter-sawn faces usually remain comparatively free of checks. For this reason, and because of the greater dimensional stability of quarter-sawn material, it has been traditional practice in Victoria and Tasmania to quarter-saw Ash eucalypt timber for use as flooring, mouldings, joinery etc. Where checks do occur, they frequently close towards the end of drying and may be hard to detect on sawn faces".

Back-sawn timber exhibits more attractive grain patterns than quarter-sawn material. Premium quality back-sawn boards are in great demand in furniture manufacturing industries the world over with top prices being paid for such material. Furthermore, a miller can increase recovery of sawn timber from logs, reduce handling costs and increase drying rates slightly by back-sawing. However, excessive degradation of Eucalypt material, primarily due to face-checking, prevents him from taking advantage of these benefits.

Early drying tests conducted as part of this investigation demonstrated the difference in the drying rates of quarter-sawn and back-sawn material and also served to emphasise the variability of drying rates from tree to tree. Material being tested was predominantly mature growth from the south of Tasmania. Precise species identification was difficult at the sawmill, but it was thought that most samples were of Eucalyptus delegatensis. Typical drying curves are shown in Figure 4.4.

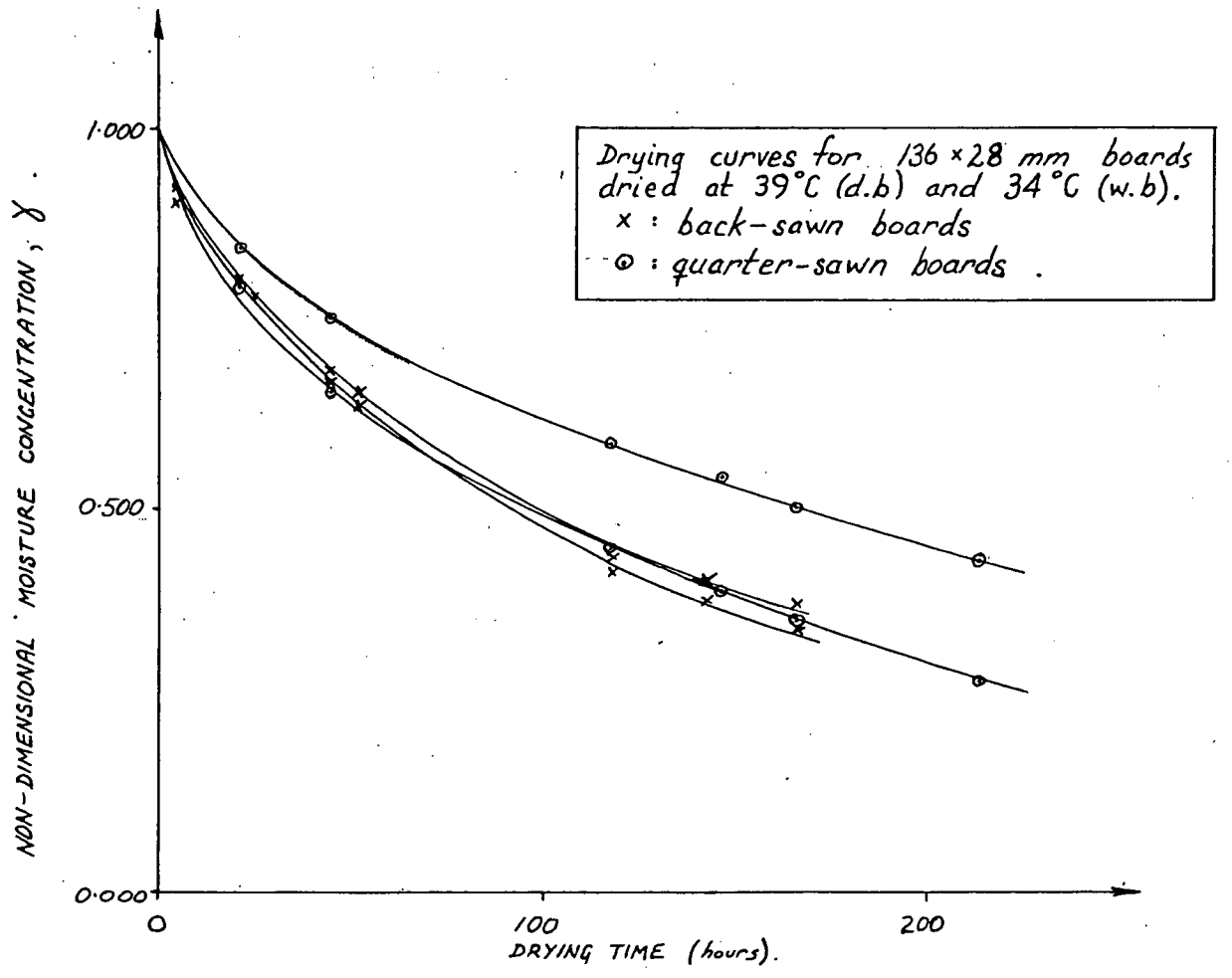

$$\gamma = \frac{(\text{moisture concentration at time, } t) - (\text{moisture concentration at time} = \infty)}{(\text{original moisture concentration}) - (\text{moisture concentration at time} = \infty)}$$

Figure 4.4

Typical Drying Curves for "Tasmanian Oak" (25mm nom. thickness)

The results of some drying tests on back-sawn material are not included in figure 4.4 as excessive checking causes drying rates to be accelerated significantly. Therefore, the drying curves associated with such material are not strictly comparable to those for unchecked quarter-sawn boards. In early tests, no back-sawn samples were dried check-free although a significant percentage (approximately 15%) were dried in later tests. Checks usually became apparent within four hours of the commencement of drying and were quite well developed within 24 hours.

4.4 Summary - The problem of face-checking in back-sawn "Tasmanian Oak".

Checking on the faces of back-sawn "Tasmanian Oak" is usually initiated within the first four hours of drying and is well developed within 24 hours. During this time, the surface fibres of the board rapidly approach the fibre equilibrium moisture content under the ambient conditions as defined in the sorption isotherm, figure 4.2. The surface fibres therefore attain moisture contents significantly below the fibre saturation moisture content. Figure 4.3 (unrestrained shrinkage - moisture content relationship) demonstrates that the tendancy for the surface fibres to shrink is far greater than that for the bulk of the material. That is, a state of differential shrinkage strain exists resulting in large tensile stresses in the surface layers. Permanent deformation or set occurs in the outer fibres as stresses pass the elastic limit. If these stresses exceed the

ultimate capacity of the wood fibre in tension across the grain, checks develop as a form of stress relief.

Drying of the newly-exposed wood fibre inside a check causes further localised shrinkage. Stresses developed by this shrinkage compound the already severe stress conditions associated with checks and help propogate them further into the material.

4.5 Summary of previous research into the seasoning of back-sawn "Tasmanian Oak".

During 1978, research into the seasoning of back-sawn "Tasmanian Oak" at C.S.I.R.O., D.B.R.* was being drawn to conclusion with no satisfactory solution to the checking problem having been found. The effects of numerous treatments had been evaluated experimentally over many years. While some ideas had shown promise during initial testing, none could be extended to commercial processes. Researchers were not prepared to state categorically that the seasoning of back-sawn ash-type eucalypts was impractical (Campbell, 1975,b) but on the other hand, they could recommend no method of consistently preventing surface checking.

* Commonwealth Scientific and Industrial Research Organisation, Division of Building Research, Melbourne, Australia.

The methods of controlling surface checking that have been extensively investigated at C.S.I.R.O. may be briefly summarised as follows (Campbell, 1975,a):

1) Control of drying conditions.

2) Physical treatments intended to modify the behaviour of the timber during drying
   a) Pre-steaming
   b) Ultrasonic or radio frequency heating.
   c) Pre-freezing.
   d) Transverse compression.

3) Chemical treatments designed to penetrate the wood in order to
   a) Control moisture gradients, or
   b) Produce "bulking" (anti-shrinkage) effects
   or a combination of both.

4) Surface treatment of the wood with the intention of either
   a) providing surface fibre reinforcement, or
   b) providing vapour barriers
   or combinations of these effects.

Many other methods of drying have been investigated, few of which have shown any promise in relation to back-sawn "Tasmanian Oak". For example, Cuevas (1974) produced fast drying times and good quality material when drying partly-dried quarter-sawn "Ash"-type eucalypts at temperatures greater than 100°C. However,

checks usually develop during the first day of drying. Drying green material at high temperatures was not at all successful.

Weeden (1980) and Neylon (1978) list a number of other drying methods which have not been successful. These include freeze-drying (sublimation), solvent soaking, "brusizing", Boultonising and impregnation with waxes and resins.

In summarising his investigations, Campbell (1975,b) suggests that cutting material from logs in such a way that the growth rings make an angle of more than 30^0 with the faces of the boards will, in general, avoid the need to use check-control methods. However, cutting the material in this way produces none of the advantages mentioned in section 4.3.2.

4.5.1 Control of drying conditions.

The basic principle of investigations in this field was to provide drying under carefully controlled conditions of temperature and humidity. Good results were obtained with a minor proportion of back-sawn samples when dried at low temperature and high humidity.

> Campbell (1975,a) sums up this work as follows: ".... it appears that there are no drying conditions available to a kiln operator within the scope of conventional kiln or

air-drying practice that would enable him to dry all fully back-sawn stock without the checking problems inherent in sawn material of this type".

4.5.2 Physical treatments.

Among timber researchers, it is commonly accepted that the pronounced moisture gradients present in "Ash"-type eucalypts during seasoning are a major contributing factor to the development of drying stresses and therefore checking. The primary objective of all physical treatments investigated was to reduce the steepness of moisture gradients.

4.5.2.1 Pre-steaming.

In 1957, it was recognised (Campbell, 1960) that the drying rate of quarter-sawn Eucalyptus Regnans could be increased by treating newly sawn material with steam at 100°C. No adverse effects were apparent following short treatments. Simpson (1975) reported an increase in the permeability of Red Oak after pre-steaming. When fully back-sawn "Tasmanian Oak" was pre-steamed, an increase in the tendency to check was observed (Campbell, 1975,a).

4.5.2.2 Ultrasonic and Radio frequency heating.

Methods of heating timber by ultrasonic and radio frequency waves were aimed primarily at controlling

collapse. As excessive collapse contributes to a tendency to check, it was thought that some improvement in the overall quality of back-sawn material might be apparent using these methods. Accepting the surface tension theory of collapse, the hypothesis put forward (Neylon, 1978) was that the formation of a high-pressure water vapour bubble in the cell lumen might offset the forces tending to collapse the cell. However, Neylon found that the high temperatures generated within the wood caused a significant weakening of the fibre structure and therefore helped promote checking.

4.5.2.3 Pre-freezing.

As early as 1959, researchers recognised that by freezing "difficult" timber before drying, a degree of control could be exercised over collapse. Wright (1967) noted that the pre-freezing treatment applied to quarter-sawn "Ash"-type eucalypts reduced the amount of collapse early in drying and proposed that checking associated with early collapse might be averted by such a treatment. Subsequent work reported by Campbell (1975,a) showed that, particularly in the case of back-sawn material, no reduction in checking was affected. Later, Christensen and Neylon (1979) proposed that freezing the water contained in cells might cause puncturing of the cell walls, thereby increasing the permeability of the wood and reducing moisture gradients. Neylon's tests (Neylon, 1978) clearly demonstrated that pre-freezing increased permeability but he, also, found no reduction in checking.

4.5.2.4 Transverse Compression.

In North America, much work has been done on the drying of hardwoods under applied lateral loads. Loads were applied using heated flat plates in direct contact with the board surfaces. Wang and Beall (1974) summarised this work. Campbell (1975,b) reported that extensive tests on back-sawn "Ash"-type eucalypts produced highly variable results. He indicated that further work was warranted, particularly on more refactory material.

4.5.3 Chemical Treatments.

There are two main areas of interest with regard to the chemical treatment of wood, particularly related to compounds (or solutions) that diffuse into the wood.

Firstly, a common method of changing the sorption behaviour of a material during drying is to soak it in a "salt" solution.

Secondly, some treatments reduce the amount of shrinkage of organic matter while drying. These are often referred to as "bulking" agents and produce their effect by replacing the bound or adsorbed water in the cell-wall structure. Sodium Chloride and Calcium Chloride were found to produce both sorption and bulking effects on wood following

soak treatments. Polyethyleneglycol (P.E.G.) and silicone hydrochloric acid primarily produce the "bulking" effect.

Campbell (1975,b) found that bulking usually produced by P.E.G. was ineffective on difficult back-sawn material. The cost of this chemical also proved prohibitive. Campbell did, however, report great success in eliminating checking in back-sawn material following soaking in saturated solutions of sodium chloride. Unfortunately, the salt penetrated quite deeply into the wood and not all of the affected material could be economically machined away. Residual salt was found to cause corrosion problems with regard to fasteners and to promote "sweating" of the timber at relative humidities greater than 75%. The use of such material would therefore be severely limited.

Calcium chloride produced similar results to sodium chloride in some instances but results were rather inconsistent and, on occasions, surface checking was observed during the soaking treatment.

The effects of many other chemicals have been studied but, as yet, none have produced a satisfactory solution to the problem of seasoning back-sawn "Tasmanian Oak".

4.5.4 Surface Treatments.

The two major principles evaluated in this field were:

Firstly - reinforcement or strengthening of the surface fibres, and

Secondly - provision of a vapour barrier to slow drying from the wood surface and hence relieve the moisture gradient conditions within the timber.

Harrison (1968) reported that a dip treatment in sodium alginate produced a film over the timber surface that helped reduce checking in quarter-sawn eucalypt stock. Campbell (1975,a) found that alginates failed to reduce checking in back-sawn "Tasmanian Oak".

A wide selection of surface coatings were tested by Campbell (1975,a and b). He summarised this work by saying:

"... in general, they failed to prevent checking from occurring, particularly in difficult material, and their use is not recommended".

4.6 Effective Control of Drying Stress.

In the past, researchers (Campbell (1959), Campbell (1975,a), Berni and Christensen (1979), Christensen and Neylon (1979)) have stated that the development of stress due to differential shrinkage is a direct effect of the moisture gradients in the timber. The theory of elasticity in orthotropic materials (developed in Chapter 7)

shows that it is the curvature of the shrinkage strain distribution that is directly responsible. It is therefore evident that careful control of shrinkage strain distribution, if it is possible, will result in control of drying stresses.

From figure 4.3, it may be deduced that maintainance of board surface fibre moisture contents above fibre saturation point will minimise the shrinkage strain at the surface while still allowing significant moisture gradients and therefore favourable drying conditions. In this way, stresses can be minimised early in drying.

In the long term, the moisture content of a board as a whole must be brought to equilibrium with the atmosphere. This requires that it be brought to well below the fibre saturation moisture content (see figure 4.2). If the surface fibres are lowered very slowly past the fibre saturation point at such a time when the moisture gradients within the timber are suitably low, it would be possible to dry any piece of wood without checking due to drying stresses. To accomplish this with the most "difficult" material, it would be necessary to maintain an almost uniform moisture distribution and therefore drying would be extremely slow.

The three major requirements of this "ideal" drying schedule are:

(a) Surface moisture content control must be established early (within four hours of sawing) to minimise the effects of surface shrinkage. The surface fibres must initially be held above fibre saturation point.

(b) The moisture distribution within the wood must be allowed to approach uniformity before the surface fibres are allowed to fall below the fibre saturation point, thereby limiting shrinkage strain differentials at this stage of drying. The degree of uniformity would depend upon the properties of individual boards.

(c) Drying must be carefully controlled, particularly during the period when the wood fibres fall below the fibre saturation point. Drying times would be, of necessity, slower than for uncoated material.

Difficult material would need to be dried more slowly (and therefore with more uniform moisture distributions) than mild material. It is therefore necessary to establish the optimum balance between the drying time and the percentage of material being dried check-free. It may not be economically feasible to dry all material.

4.7 Qualitative Performance of Water-permeable Coatings.

Early in the investigation, it became apparent to the author that the application of a water-permeable coating to the surface of timber could provide the ideal drying conditions described in section 4.6. The variable drying characteristics of the wood could be accommodated by adjusting the properties of the coating. The principle

of drying through permeable coatings may be demonstrated in the following way.

Consider moisture diffusion through a composite slab of two different materials, as shown in figure 4.5. Assume that the moisture content is initially uniform throughout the slab and that the two materials have the same permeability. Assume also that there is no discontinuity in the moisture distribution at the interface.

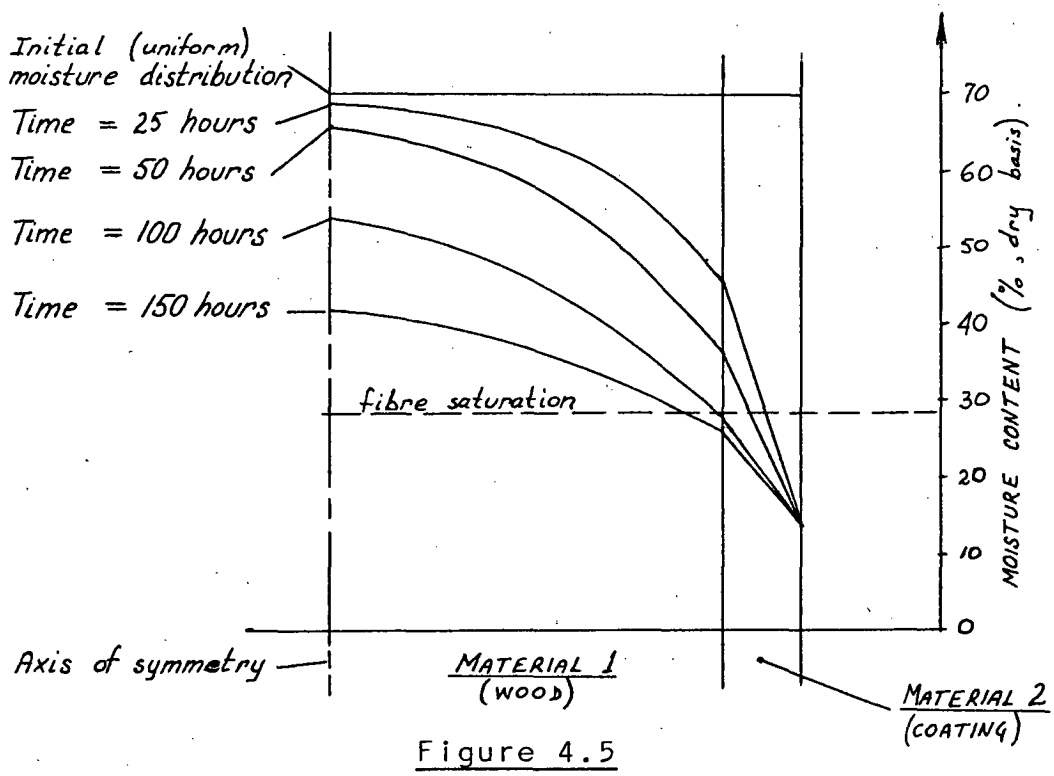

Figure 4.5

Typical moisture distributions in coated 25mm "Tasmanian Oak" boards.

The curves drawn in figure 4.5 represent typical moisture distributions that might exist within the slab as it dries from 70% moisture content to 13%. Figure 4.6 compares the moisture content at the interface between

the wood and the coating with the moisture content at the free surface of the coating as a function of time.

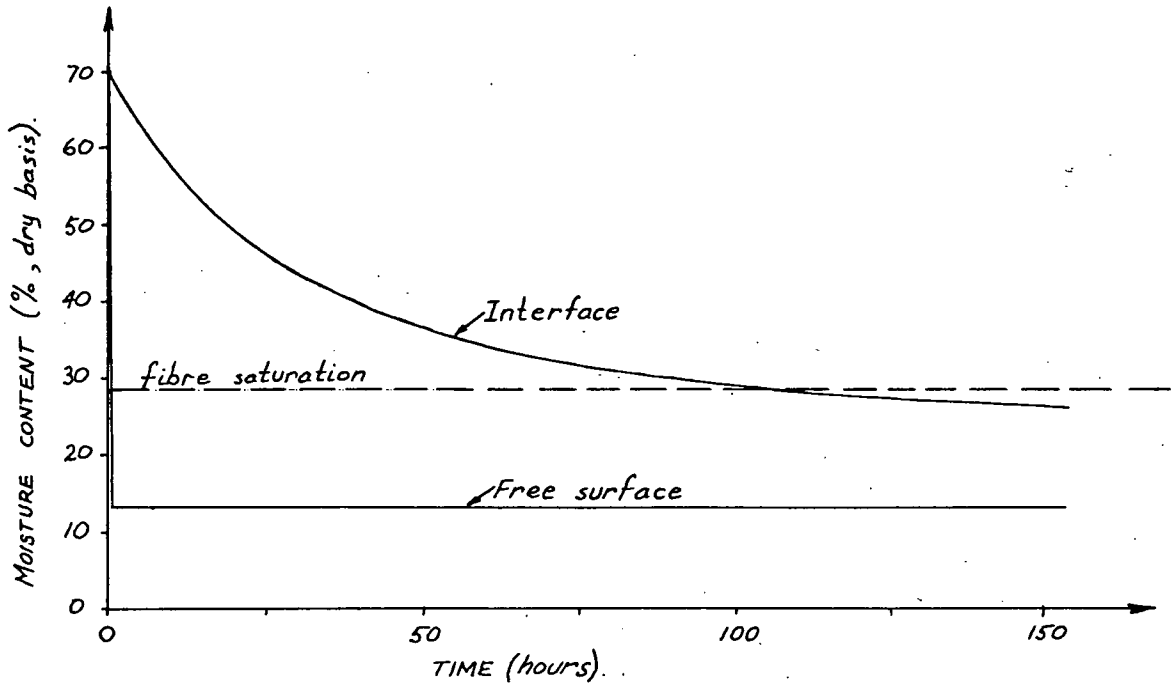

Figure 4.6

The variation of moisture content at the wood-coating interface.

Suppose material 1 of figure 4.5 to be wood with a fibre saturation moisture content of 28% (dry basis). Figures 4.5 and 4.6 then demonstrate that the surface fibres of the wood would remain above the fibre saturation point for a period of 100 hours. After 100 hours, the interface moisture content falls slowly towards the limiting value. The moisture content gradients at the wood surface after 100 hours are low. The conditions specified in section 4.6 are therefore satisfied.

Note that assuming the materials 1 and 2 of figure 4.5 have the same permeability, the interface moisture content - time relationship can be changed simply by changing

the thickness of material 2.

Thus, the only requirement of a coating (other than practical and economic requirements) is that it have the correct combination of thickness and permeability. These physical requirements are primarily dependent upon the relationship between the shrinkage strain and the moisture content of the wood fibre, and the relationship between stress and strain (and moisture content) in the wood. One objective of this investigation has therefore been to develop the mathematical tools and procedures necessary to enable effective "design" of suitable coatings and drying schedules based on physical requirements.

Drying tests on back-sawn "Tasmanian Oak" using suitable coatings(having the correct combination of thickness and permeability, Chapter 5) show that it is possible to achieve the required degree of control over drying stresses while drying coated material over an only slightly longer period than uncoated material.

REFERENCES.

BERNI, C.A., CHRISTENSEN, F.J.(1979): Influence of dynamic transverse compression and redrying conditions on internal checking in 45mm thick C.C.A. treated radiata pine.
19th Forest Products Research Conference.
C.S.I.R.O., Highett, Australia.

CAMPBELL, G.S. (1959): Can chemical seasoning help the timber industry?
C.S.I.R.O. Forest Products Newsletter No. 257.

..... (1960): Pre-steaming cuts drying time of "Ash" eucalypts.
C.S.I.R.O. Forest Products Newsletter No. 263.

..... (1975,a): Preliminary report on the control of surface checking in back-sawn Tasmanian "Ash" type eucalypts during seasoning.
C.S.I.R.O. internal report on project S15/3 (unpublished).

..... (1975,b): Control of checking in back-sawn E. delegatensis ex. Tasmania. (Second report).
C.S.I.R.O. internal report on project S15/3 (unpublished).

CHRISTENSEN, F.J., NEYLON, M. (1979): Effects of pre-freezing on the seasoning of back-sawn boards from Tasmanian-grown Eucalypts.
19th Forest Products Research Conference
C.S.I.R.O., Highett, Australia.

CUEVAS, L.E. (1974): High temperature drying - a new approach to increase efficiency in the Australian Hardwood Industry.
Aus. T.I.S. Conference, Wodonga.
C.S.I.R.O., D.B.R. reprint No. 724.

HARRISON, J. (1968): Reducing checking of timber by use of Alginates.
Australian Timber Journal 34(7).

HILLIS, W.E., BROWN, A.G. (1978)(Editors): Eucalypts for Wood Production.
Griffin Press, Adelaide, Australia.

KAUMAN, W.G. (1966): Cell Collapse in Wood.
C.S.I.R.O. D.F.P. reprint No. 566.

McMILLEN, J.M. ( ): Stresses in Wood during Drying.
F.P.L. Madison, Wisconsin, Canada.
Report No. 1652.

NEYLON, M. (1978): Investigations of ultrasonic and pre-freezing treatments for seasoning of Tasmanian E. Delegatensis.
Report to Tas. Timber Promotion Board.
(unpublished)

PANKEVICIUS, E.R. (1960): Recent Studies on Collapse.
C.S.I.R.O. Forest Products Newsletter No.

SIMPSON, W.T. (1976): Effect of Pre-steaming on Moisture Gradient of Northern Red Oak during Drying.
Wood Science 8(4): p.272 - 276.

WANG, J.H., BEALL, F.C. (1974): Laboratory Press-drying of Red Oak.
Wood Science 8(2): p.131 - 140.

WEEDEN, S.C. (1980): The Seasoning of Timber to reduce Checking.
Tas. Timber Promotion Board internal report.
(unpublished)

WRIGHT, G.W. (1967): Pre-freezing as a Drying Treatment.
C.S.I.R.O. Forest Products Newsletter
No. 377: 6-8.

CHAPTER 5

CHAPTER 5

DRYING TESTS

5.1 Introduction

Early drying tests conducted on the "Tasmanian Oak" group of species confirmed that their behaviour while seasoning is similar to that of hardwoods in general (see sections 4.3 and 4.4). During these tests, sufficient data were collected to enable an accurate mathematical model of the drying process to be developed, the basis for which appears in Chapter 3. This model predicted the distribution of moisture within a piece of sawn timber as a function of time and was used later (Chapter 8) in conjunction with the theory of elasticity of orthotropic materials (developed in Chapter 6) to demonstrate the reduction in drying stress levels in timber coated with water-permeable materials.

The effectiveness of using water-permeable coatings to control face-checking in back-sawn "Tasmanian Oak" was demonstrated in large scale tests, the timber being dried according to procedures similar to those currently used in the Tasmanian timber industry. The drying times required for the coated back-sawn material were comparable to those necessary for quarter-sawn boards of a similar thickness.

5.1.1 Test Objectives.

The samples of sawn "Tasmanian Oak" used in drying tests were selected randomly from mature logs available in sawmill yards. Accurate identification of species was not always possible, but it is believed that the majority of samples came from logs of E. delegatensis or E. regnans. It is also highly likely that material from hybrid trees was tested. All test samples were taken from mature trees (older than 100 years).

The pattern of behaviour of all samples was similar, but the variation in drying rates (and also the amounts of gross shrinkage, collapse and checking) was quite remarkable. A proper understanding of the drying process in the total population depends heavily upon the accurate modelling of the drying of individual samples. A large amount of information can therefore be gained from a relatively small number of tests.

The data collected during early tests were

used to refine a mathematical model of drying that could be used to predict the moisture distribution in any single piece of wood as a function of time, using the particular diffusion properties of that piece. The determination of the mass diffusion coefficients (and their variability) was therefore of primary importance.

In Chapter 4, it was proposed that permiable coatings be used to hold the surface fibres of boards above the fibre saturation point during the first few days of drying, thus limiting the amount of differential shrinkage between the surface fibres and the remainder of the board. The mean moisture transfer rates through "Tasmanian Oak" were used in the calculation of the necessary physical properties of these coatings. Further drying tests were conducted in order to investigate the performance of coatings with various combinations of thickness and permeability. In these tests, the behaviour of relatively large sample populations were studied.

5.1.2. Test samples.

Tasmanian hardwood mills cut boards with various nominal thicknesses depending upon log quality and size, end use, market conditions, and so on. 38 and 50mm material is sawn mainly during the Tasmanian winter when atmospheric relative humidity is high and therefore air-drying conditions are mildest. Boards with these thicknesses are produced mainly for structural purposes. 25mm boards are produced largely for decorative applications

and are sawn all year round at most mills. They are generally converted from the green condition to dry, marketable material in 5 to 12 months. On the other hand, 38mm boards generally take between 12 and 15 months to dry and 50mm material takes between 18 and 24 months.

Fluctuating market conditions, increasing interest charges and large amounts of degradation of thick material during seasoning have contributed to cut backs in the production of 38 and 50mm material and concentration on the production of 19 and 25mm stock.

25mm (nom. thickness) boards were used exclusively throughout this investigation. However, the models formulated for the analysis of this material and the stress-control methods developed may be applied to any timber of any thickness.

5.1.3 Experimental drying conditions.

Drying curves for hydrophyllic materials are usually obtained by weighing test samples periodically as they dry and recording their weight as a function of time. The total weight of the sample is related to its average moisture concentration. In many materials, the drying rate (in air) is governed by the diffusion of moisture through the body to its surface rather than by the rate of mass transfer from the surface to the atmosphere, providing the air is moving. Under these conditions, moisture gradients through the surface boundary

layers in the air are very small and the surface zones of the body rapidly approach equilibrium with the atmosphere.

The rate of moisture transfer through timber reduces as moisture concentration decreases (section 5.3), hence the conditions at the surface have an important influence on drying rates. Test results can only be directly compared if the drying conditions under which measurements are taken are accurately monitored and controlled. For the sake of simplifying the theoretical analysis of test results, it is usual to dry samples under constant conditions. Experimental drying chambers (kilns) must therefore have facilities for controlling air temperature and humidity as well as the air speed over the surfaces of the samples. Details of the kilns used during this investigation are given in section 5.2.

5.1.4 Measurement of the amount of moisture present in samples.

The most common term used in the timber industry to express the amount of moisture present in a piece of wood is "moisture content", defined by

$$\text{moisture content, } M = \frac{\text{mass of water}}{\text{mass of dry fibre}} \quad \text{(non-dimensional)}$$

Moisture content is usually quoted as a percentage.

In classical mass transfer theory (Chapter3), the amount of moisture present in a material is described

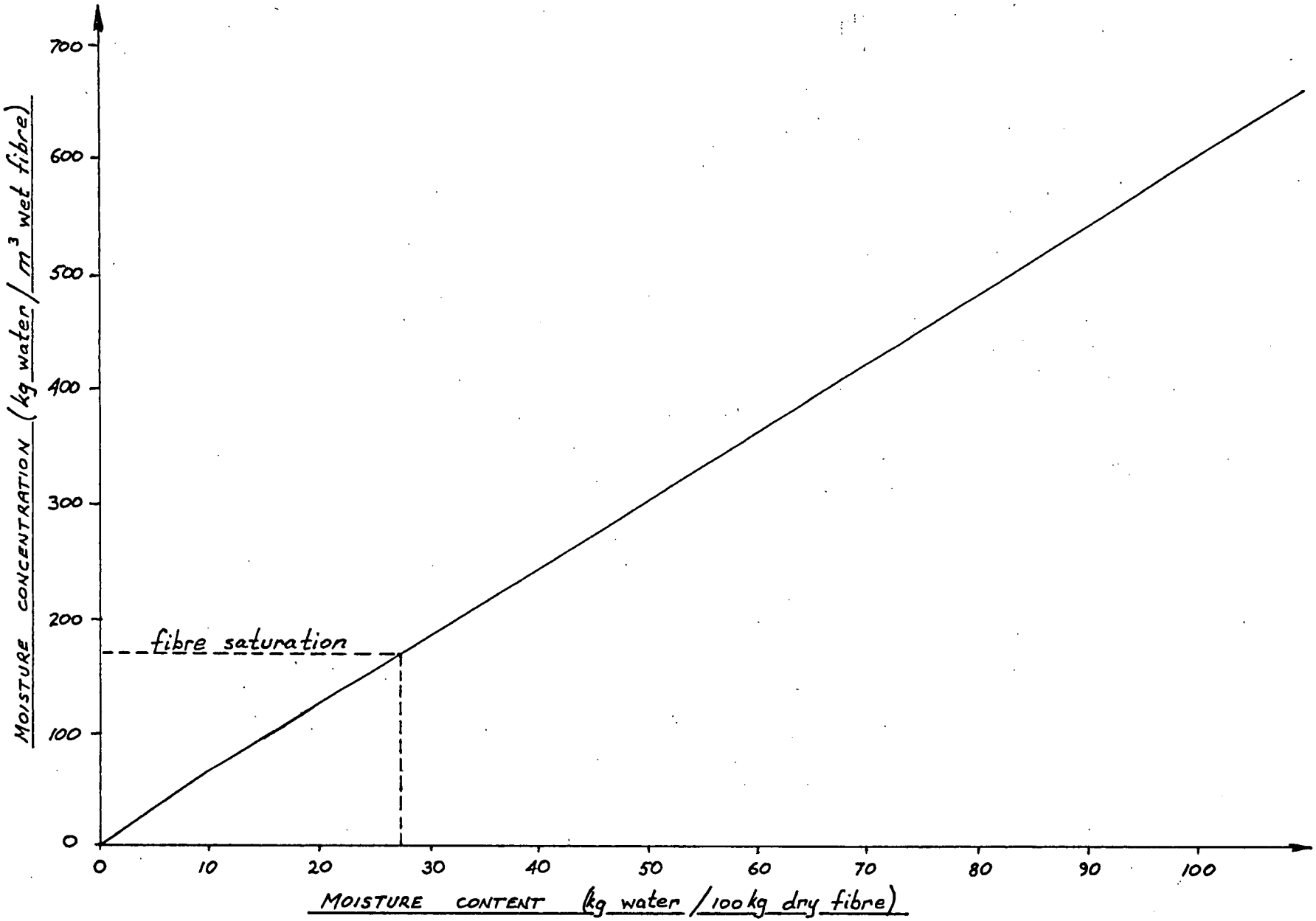

FIGURE 5·1

RELATIONSHIP BETWEEN MOISTURE CONTENT AND MOISTURE CONCENTRATION — FOR TIMBER WITH DRY DENSITY = 700 kg/m³

in terms of a concentration such that

$$\text{moisture concentration, } c = \frac{\text{mass of water}}{\text{volume of material}} \quad (kg/m^3)$$

"Moisture concentration" is independent of the density of the material through which diffusion is taking place; "moisture content" is not. Therefore, variations in density within a given piece of timber (for example, between spring wood and winter wood) can lead to apparent irregularities in the moisture content distribution even though the material may be in a condition of equilibrium (no moisture movement). The approximate relationship between moisture content and moisture concentration for "Tasmanian Oak" with a dry density of 700kg/m^3 is given in figure 5.1.

5.2 Materials and Methods

5.2.1 Introduction

Drying tests were conducted in three kilns of different capacity. During all tests, average moisture content was monitored either by recording the total weight of a sample or by conducting oven-drying tests (CSIRO, 1974). Average moisture concentration followed from volume measurements. The moisture concentration distribution over the cross-section of samples was measured using a microtoming (slicing) technique in conjunction with oven-drying tests.

The determination of the diffusion coefficients required for theoretical modelling was effected using a combination of the diffusion cell method (Fish, 1957; McKay, 1971; Rohsenow and Choi, 1961; Bramhall, 1979,a) and the method of fitting coefficients to measured drying behaviour (Fish,

1957; Doe, 1973,a; Bui, Choong and Rudd, 1980).

5.2.2 Kiln A: Small modified recirculating wind tunnel.

Capacity = 0.0068m^3 (3 superficial feet).

This kiln and its controls are described in detail by Doe (1973,b). During the course of tests, the temperature controller was changed from the Rototherm (which was found to be insensitive at low temperatures) to a Honeywell type R 7308 temperature controller. This gave control of dry-bulb temperature to within 0.5^{o}C at temperatures between 30 and 60^{o}C. The working section of the kiln is shown in figure 5.2 (a).

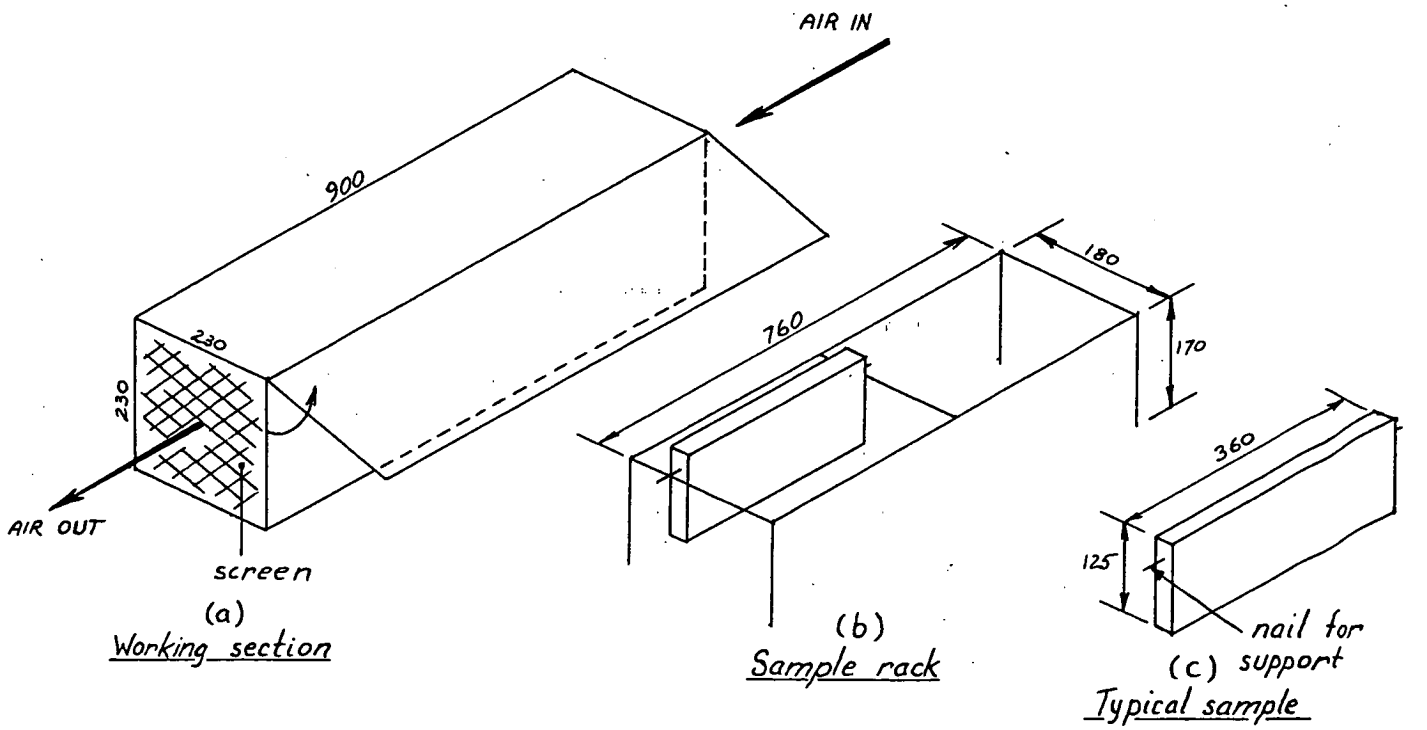

Figure 5.2

Working section of 0.007m^3 (3 sup. ft.) kiln

The typical dimensions of samples dried in the kiln are given in figure (5.2,c). The ends of each sample were coated with a bituminous water-proof sealant to prevent drying from the ends. Six samples could be placed in the removable sample rack (figure5.2,b). Samples were suspended from the rack on 50mm nails partly driven into the ends.

The air flow across the board faces was in the longitudinal direction (figure 5.2,a), the available range of air speeds being from 0 to 20(+) m/s with the working section empty.

The maximum temperature/humidity condition available was 85^{o}C at 90 ± 5% relative humidity.

5.2.3. Kiln B: Modified experimental hop kiln.

Capacity = 0.084m^{3} (38 superficial feet). This kiln was also of the re-circulating type. The general detail is given by Doe (1979). However, a number of modifications were necessary before conditions suitable for timber drying could be sustained.

The size of the inlet and outlet ventilation ports was reduced to 100mm square to increase the percentage of air recirculated. Humidity was controlled by injection of steam from a low pressure boiler via a 6mm (¼") ASCO steam solenoid valve. The open time of the solenoid valve was

controlled by an automatic decimal counter * linked to the existing system via micro-switches operated by the ventilation dampers. If the vents were fully open (conditions too humid), the amount of steam introduced every minute was reduced and vice versa. This gave control of wet-bulb temperatures to within 0.5°C at dry-bulb temperatures ranging from 20 to 50°C.

The working section of the kiln is shown in figure (5.3,a).

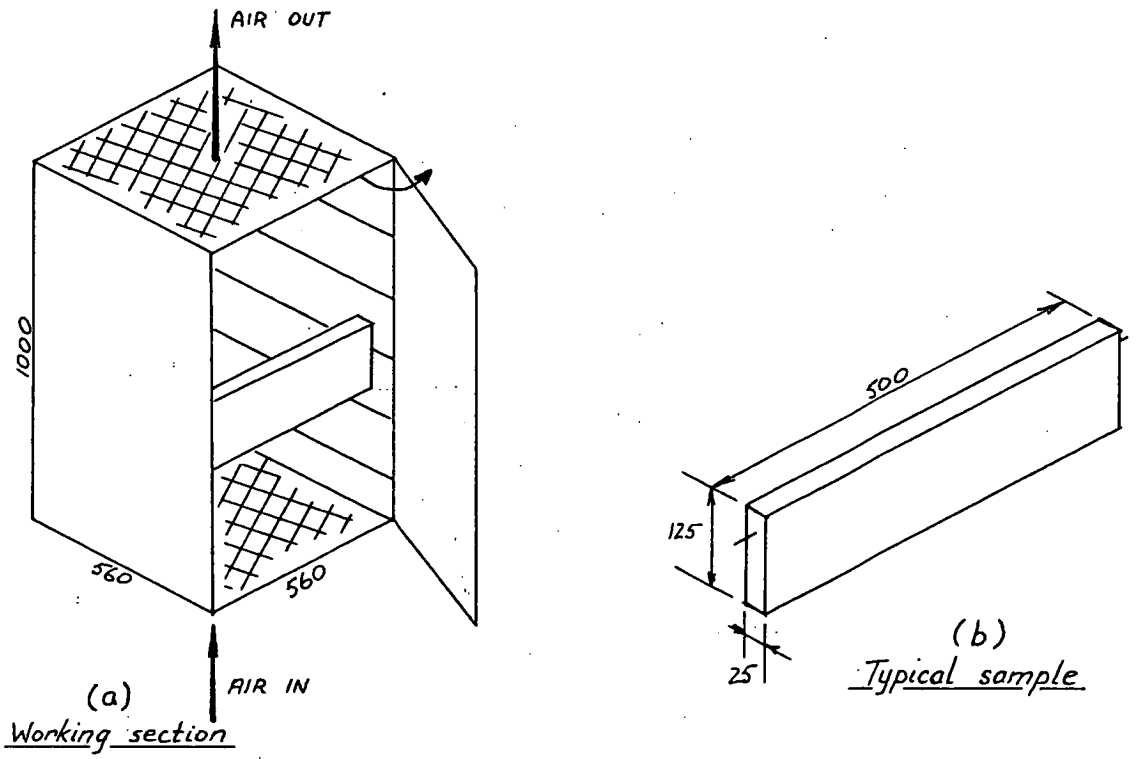

Figure 5.3

Working section of 0.08m³ (38 sup. ft.) kiln

* Automatic electronic decimal counter - designed and built at the University of Tasmania, Dpt. of Mechanical Engineering. Injects between 1 and 16 seconds of steam every minute, depending upon requirements.

A total of 54 samples (figure 5.3,b) could be placed in the kiln at any one time. Again, the ends of the samples were sealed with a waterproof coating and the samples were suspended from racks on 50mm nails partly driven into their ends.

The air flow across the board faces was in the transverse direction (figure 5.3,a). The maximum velocity of air through the unloaded working section was 2 m/s.

The maximum dry-bulb temperature available was 140^{o}C. At 100^{o}C, the maximum relative humidity attainable was less than 70%.

5.2.4. Kiln C: Experimental timber kiln.

Capacity = 0.50m^{3} (220 superficial feet).

Early tests on small timber samples coated with water-permeable materials proved that drying stresses (and therefore checking) in backsawn "Tasmanian Oak" could be controlled. Testing on a large scale became necessary and an experimental timber kiln (figure 5.4) was designed and constructed.

Care was taken during the design* to ensure

---

* The experimental timber kiln was designed in 1980 by C. Purdon, mechanical design engineer, Tasmanian Timber Promotion Board in conjunction with the Dpt. of Mechanical Engineering, University of Tasmania.

uniformity of conditions in the working section. Air was circulated by a reversible, 500mm diameter axial flow fan driven by a 750 watt variable speed D.C. motor. The maximum air flow rate through the working section (fully loaded) was 1.70m^3/s. The kiln was constructed solely of aluminium and was covered with 50mm rock wool insulation backed with reflective foil.

Dry-bulb temperature was sensed and controlled by electronic equipment designed and built in the Department of Mechanical Engineering at the University of Tasmania and gave control to $\pm$ 0.5^{o}C over the temperature range 10 to 60^{o}C. Heating was provided by two 1500 watt finned-tube electric heating elements.

Humidity was sensed by a SAUTER HBCC humidistat mounted in the working area and effective over the range 0 to 95% relative humidity (sensivity $\pm$2% r.h.). Control of humidity was effected by venting and steam injection in a similar way to that used in kiln B. The ventilation dampers were operated automatically by a Modutrol motor regulated by the humidistat.

Conditions necessary for the reconditioning of timber (dry-bulb temperatures of 95 to 100^{o}C, saturated humidity, sections 4.1.4 and 4.3) were provided by introducing "wet" steam (100^{o}C, atmospheric pressure) to the working section from a 15 kW boiler.

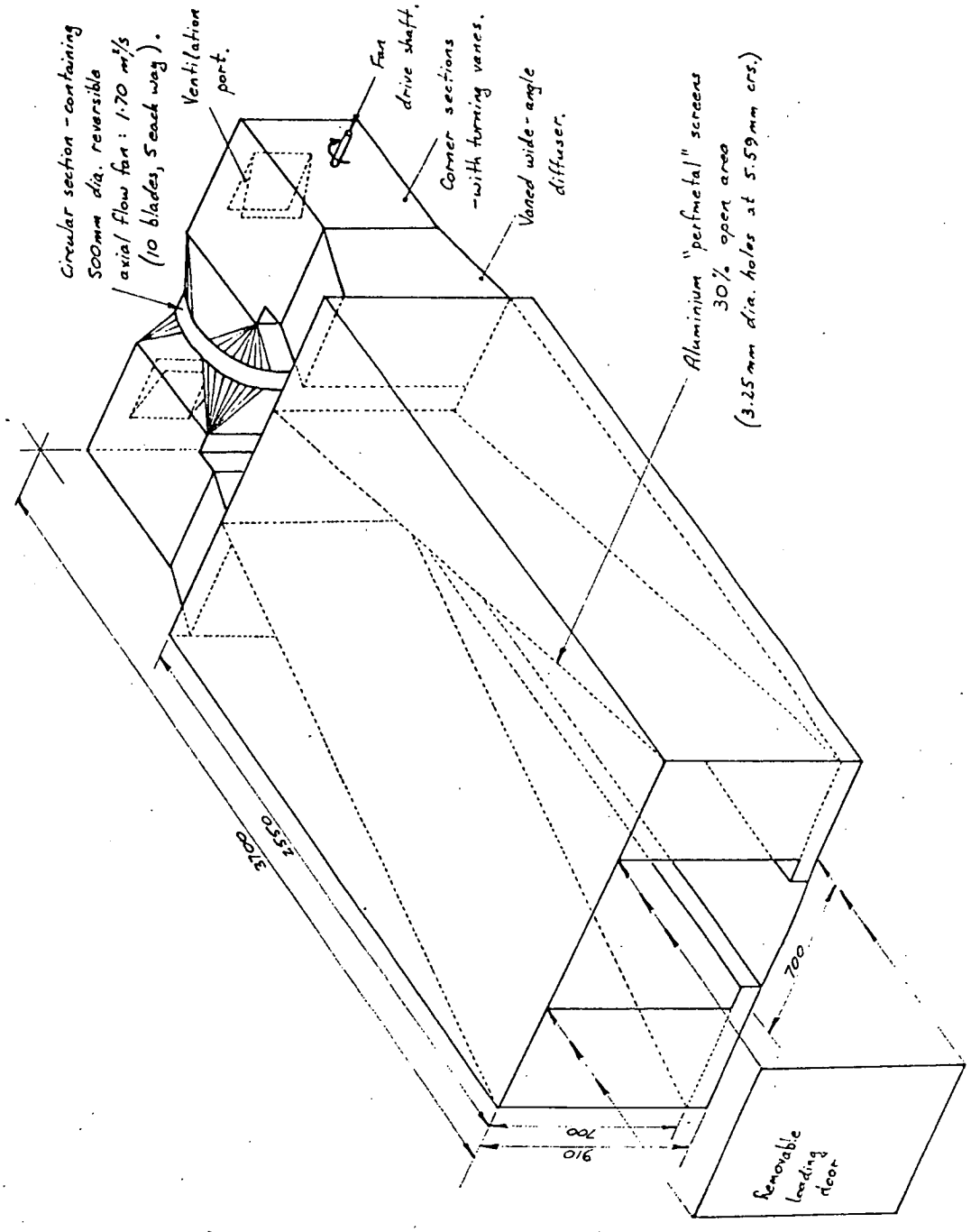

FIGURE 5·4

EXPERIMENTAL TIMBER KILN

Stacks of timber, built up of 125 x 25mm (nominal size) boards, having a cross-section of approximately 0.6m square and a length of 2.2m were constructed (figure 5.5 and 5.19) and wheeled into the kiln on a modified hydraulic pallet track.

Figure 5.5
Test stack being loaded into experimental timber kiln.

5.2.5 Microtome (for measurement of moisture distributions)

During drying, the lines joining points of equal moisture concentration in a wide board take the form shown in figure (5.6).

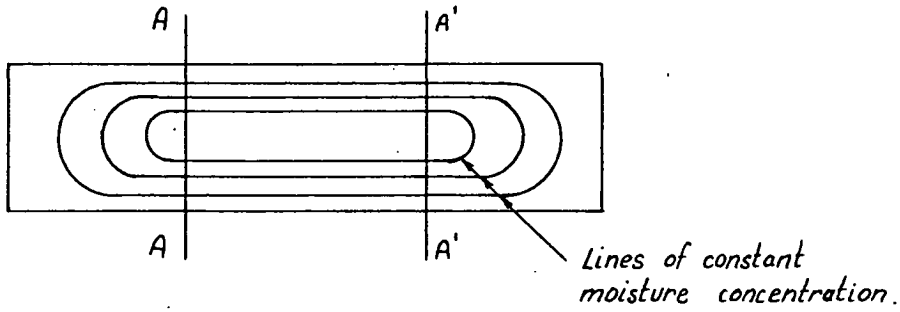

Figure 5.6

Cross section of a sawn timber board showing lines of constant moisture concentration during drying.

Slices from the region AA-A'A' cut parallel to the faces of the board will also be cut parallel to the moisture "contours" in that region. If the slices are cut thinly and their moisture concentrations determined (by oven drying), the distribution of moisture through the board may be plotted. Distributions measured in this way provide a means of assessing the moisture concentration at the wood/coating interface of a piece of coated timber.

The microtome shown in figure (5.7) was used to slice timber samples. The minimum practical slice thickness was found to be 0.2mm. Thinner slices could be cut but these became brittle and difficult to handle when oven dry.

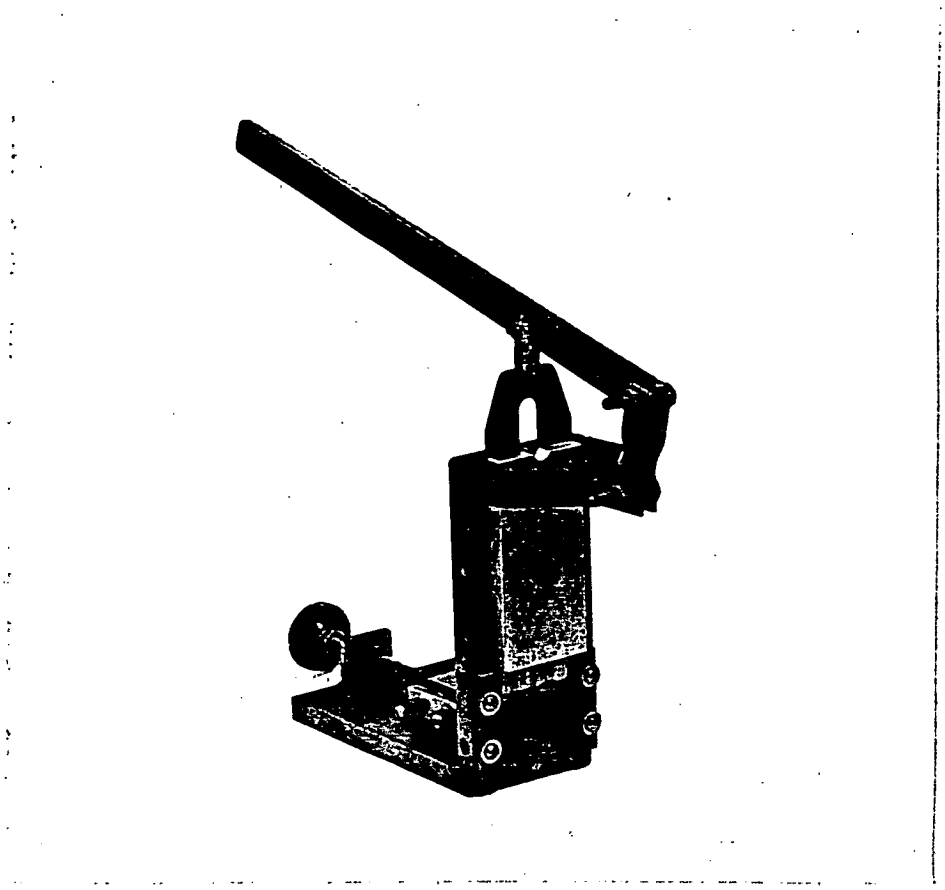

Figure 5.7

Microtome

5.2.6 Measurement of diffusion coefficients.

5.2.6.1 Introduction

The principal directions of diffusion in timber are longitudinal, radial and tangential with respect to a log (chapter 2). The drying of long boards takes place primarily through the board faces and therefore it is diffusion in the transverse plane that is of greatest interest.

The diffusion coefficients of timber vary with moisture concentration (Bramhall, 1979,a: Bui, Choong and Rudd, 1980). Therefore, to enable accurate modelling of the diffusion process, it is necessary to determine the relationship between moisture concentration and the diffusion

coefficients in the two principle transverse directions.

5.2.6.2 Direct measurement of mass diffusion coefficients - Diffusion cell method.

The mass diffusion coefficients of wood can be directly determined from measurements of steady-state moisture transfer rates through thin samples. During this investigation, timber samples with a thickness of approximately 1mm were mounted on perspex vials, as shown in figure (5.8).

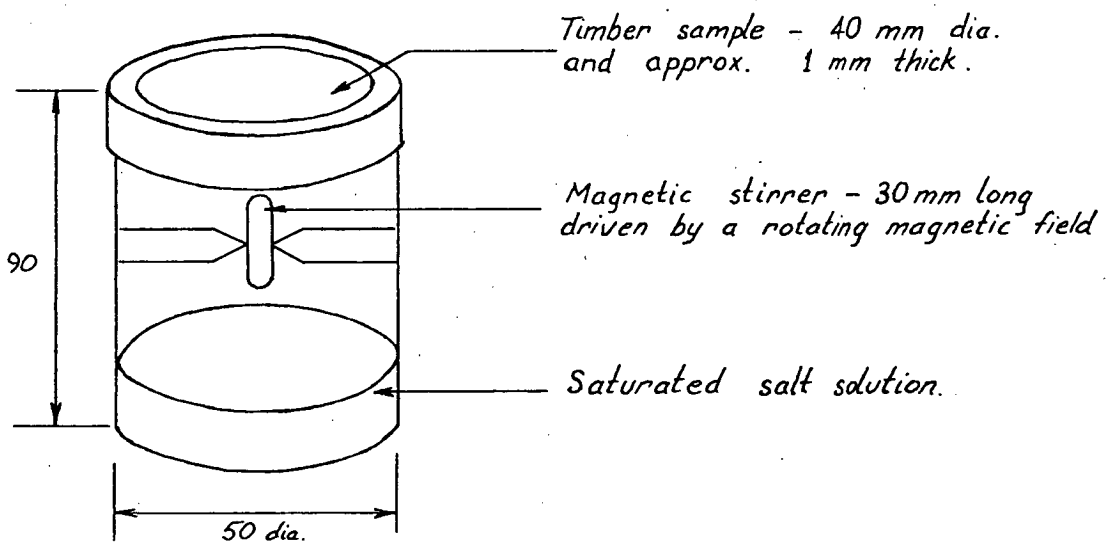

Figure 5.8
Thin wood sample mounted on diffusion cell

The humidity inside the vial was held at a constant value due to the presence of a saturated salt solution. The vial was placed inside a chamber which was held at a different but constant relative humidity and the system was held at a steady temperature. Moisture diffused through the timber sample due to the difference in relative humidities

on either side. Thus, moisture passed either into or out of the vial, the transfer reaching a steady state when the weight of the vial changed at a constant rate. The diffusion coefficient, $\mathcal{D}$, is calculated from the steady state mass flow rate using Fick's Law, viz:

$$\dot{e} = -\mathcal{D}A\frac{\partial c}{\partial x}$$

where $\dot{e}$ = mass flow rate (kg/s),

A = area through which diffusion takes place,

and $\frac{\partial c}{\partial x}$ = mass concentration gradient.

The mass concentration gradient may be obtained by conditioning small pieces of timber (from the same sample as that mounted on the vial) in atmospheres having the same relative humidity as those inside and outside the vial. The equilibrium moisture concentrations of these pieces give an estimate of the surface moisture concentrations of the diffusion sample. The difference between the two concentrations, Δc, divided by the sample thickness, Δx, is a reasonable estimate of the average concentration gradient through the sample providing the moisture boundary layers are insignificant (section 3.6). Thus, the diffusion coefficient,

$$\mathcal{D} \simeq \frac{\dot{e}}{A}\frac{\Delta x}{\Delta c} \qquad \text{--------} \quad (5.1)$$

If the concentration difference across the sample, Δc, is small, a moisture diffusion coefficient determined by the above method may be quoted as that

corresponding to the average moisture concentration of the sample. Thus, a graph of the relationship between diffusion coefficient and moisture concentration may be built up by running a number of tests under different conditions of humidity.

With this in mind, the equipment illustrated in figure (5.9) was constructed.

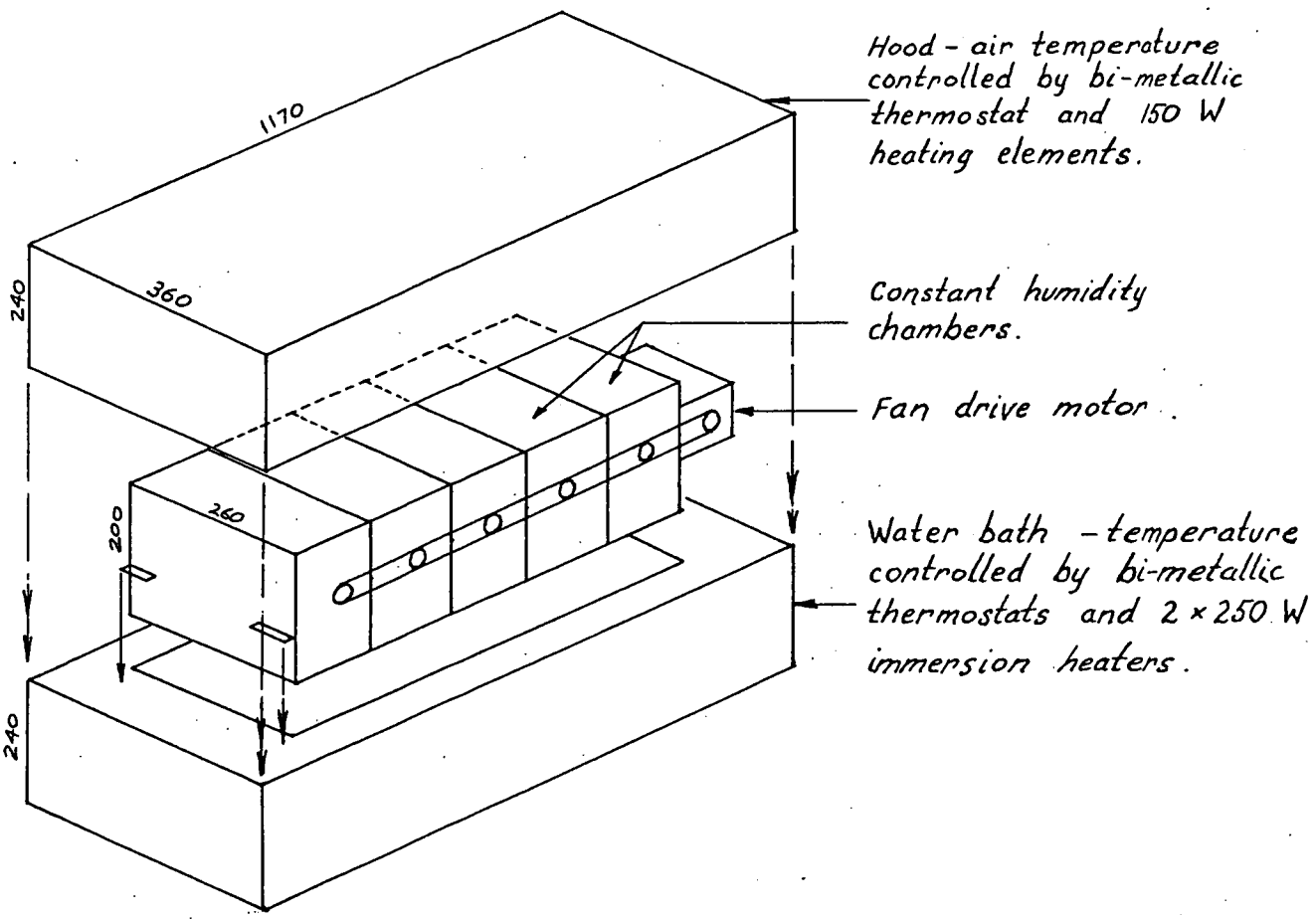

Figure 5.9a

Constant humidity chambers - general arrangement

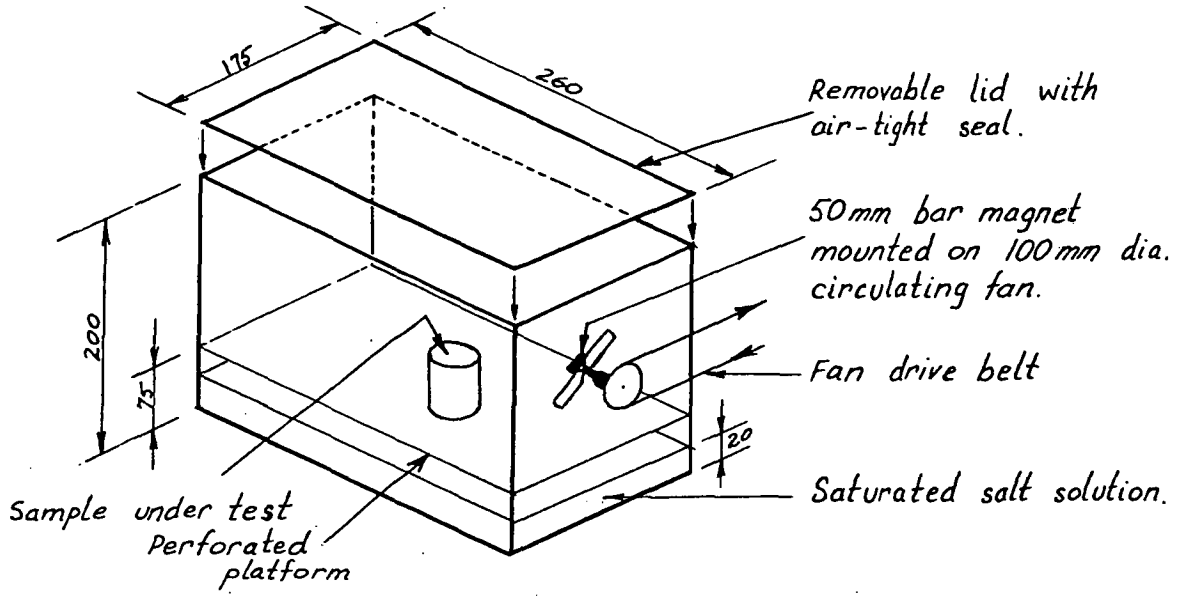

Figure 5.9b

Constant humidity chamber

The air inside each of the constant humidity chambers was circulated by a 100mm diameter belt driven fan. A powerful bar magnet attached to the hub of each fan provided the rotating magnetic field necessary to drive the stirrers inside the vials (figure 5.8). The vials holding the test specimens were placed on a perforated platform inside each chamber and the mass flow rate through the samples determined by periodically weighing each vial. The saturated salt solution required to give a particular constant humidity was placed in the bottom of the chamber. A different humidity was maintained in each chamber. The chambers were partly immersed in a constant temperature water bath and covered by a hood under which the air temperature could be regulated.

Five diffusion cell tests could be conducted simultaneously. If the samples being tested were cut from the same small piece of wood, five points on a graph of diffusion coefficient against moisture concentration could be obtained from one test run.

Examination of the sorption isotherm for wood (figure 4.2) reveals that the measurement of diffusion coefficients at moisture concentrations greater than the fibre saturation point is impractical by the diffusion cell method. A suitable method is that of fitting a mathematical model of the diffusion process to measured drying behaviour by adjusting the diffusion coefficients (section 5.2.6.3).

5.2.6.3 Mass diffusion coefficients inferred from drying tests

The method of inferring diffusion coefficients from drying tests is well established (Fish, 1957; Doe, 1973,a; Choong and Rudd, 1980). A mathematical model of the drying process is constructed and the diffusion coefficients are adjusted until the solutions to the model fit the measured behaviour.

The diffusion equation (equation 3.18) was approximated by an implicit finite difference scheme and the resulting equation system solved by digital computer (see Appendix B). Care was taken to ensure that the solutions were stable and convergent (Chapter 3).

The approximate relationship between the diffusion coefficients and moisture concentration may be determined by fitting the mathematical model to the results of drying tests conducted between equilibrium conditions associated with small changes in moisture concentration. This was achieved by taking small samples of timber (figure 5.10), sealing their edges and allowing them to come to equilibrium under conditions of constant temperature and humidity.

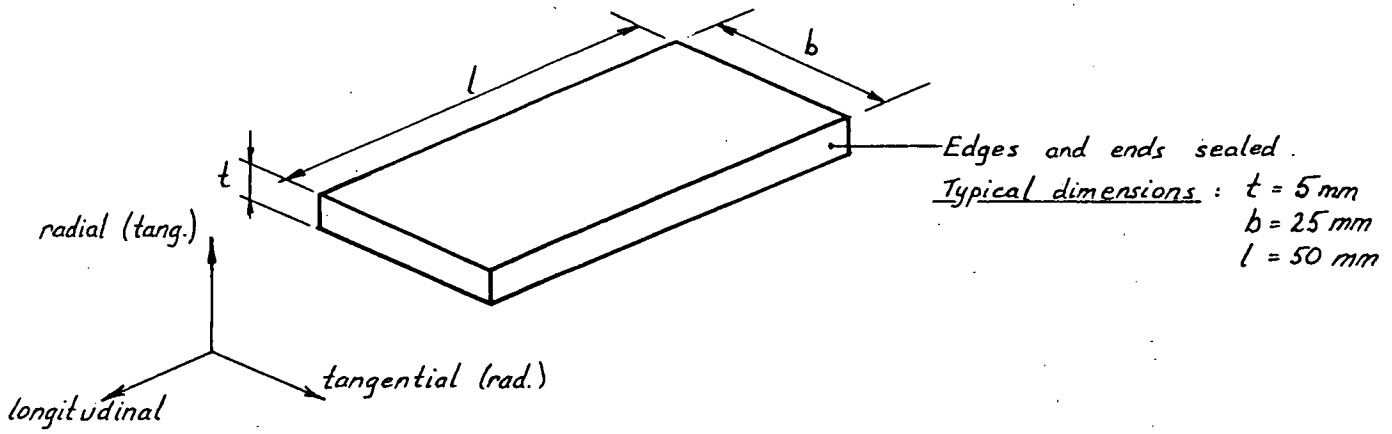

Figure 5.10

Wood samples used for the determination of diffusion coefficients by the method of inference

The samples were then transferred to an atmosphere of different (lower) humidity and their weights (and thicknesses) recorded as a function of time. When the samples approached equilibrium under the new conditions, they were oven-dried to enable calculation of moisture concentrations. If all edges of a sample have been sealed, moisture transfer takes place in one direction only, simplifying the theoretical analysis. Theoretical

desorption/adsorption curves were calculated assuming that the diffusion coefficient (in the relevant direction, eg: radial, tangential) was roughly constant through the range of moisture concentrations over which the test was being conducted. The diffusion coefficient resulting in the closest agreement between theory and measurement was approximately that corresponding to the average equilibrium moisture concentration for wood fibre over the test range. Care must be taken to avoid the problems described in section 3.6.

The equilibrium moisture concentration of "Tasmanian Oak" at 95% relative humidity is approximately 150kg/m^3. The determination of diffusion coefficients at higher moisture concentrations is possible by a similar method. Samples of green timber (figure 5.10) may be placed in an atmosphere having a high relative humidity (say 90%), the diffusion coefficients being inferred by the method previously described.

The relationships between the mass diffusion coefficients and moisture concentration determined by the methods outlined in section 5.2.6 are approximate. The model may be refined by fitting theoretical drying curves to those measured for sawn boards.

5.3 The diffusion coefficients of "Tasmanian Oak"

5.3.1 Introduction

It was demonstrated in section 3.2.3 that mass and thermal diffusion in "Tasmanian Oak" may be considered independently during drying at low temperatures (of the order of 40^{o}C). The relative magnitudes of the radial and tangential mass diffusion coefficients were determined from diffusion cell tests over a range of moisture concentrations. A relationship similar to that used by Bramhall (1979,b) to describe the dependence of mass diffusion coefficients upon moisture content (concentration) was adopted. The maximum value of the mass diffusion coefficient was adjusted (keeping the shape of the relationship unchanged) until measured and calculated drying curves matched well. The variability of the coefficients was studied by analysing the results of a number of tests.

During the course of analysis, good agreement was observed between measured drying curves and those calculated using constant diffusion coefficients (independent of moisture concentration). The mathematical model used made no allowance for shrinkage during drying. It may therefore be deduced that the effects of falling diffusivity and fibre shrinkage associated with the drying of "Tasmanian Oak" below the fibre saturation moisture concentration effectively cancel each other.

From the inferred values of the mass diffusion coefficients, the approximate properties of water-permeable coatings required to maintain moisture concentrations

greater than the fibre saturation point on the faces of back-sawn boards during the early stages of drying were estimated and a number of suitable materials identified. Tests using a mixture of animal glue (gelatine) and talcum powder (filler) proved experimentally that checking (and therefore drying stresses) in back-sawn "Tasmanian Oak" could be controlled.

5.3.2 Diffusion cell test results

Veneers approximately 2mm thick were cut from a 300mm long, clear, dry (M≃12%) piece of quarter-sawn "Tasmanian Oak" with 100 × 50mm cross-section. Exact species identification was not possible, but the sample was thought to be either E. delegatensis or E. regnans. The veneers were sliced both parallel and perpendicular to the growth rings in order that both the radial and tangential moisture diffusion coefficients could be measured.

Five specimens from one piece of veneer cut parrallel to the growth rings were fitted to vials and placed in the constant humidity chambers of the diffusion cell apparatus (section 5.2.6.2). The test is described diagramatically in figure (5.11).

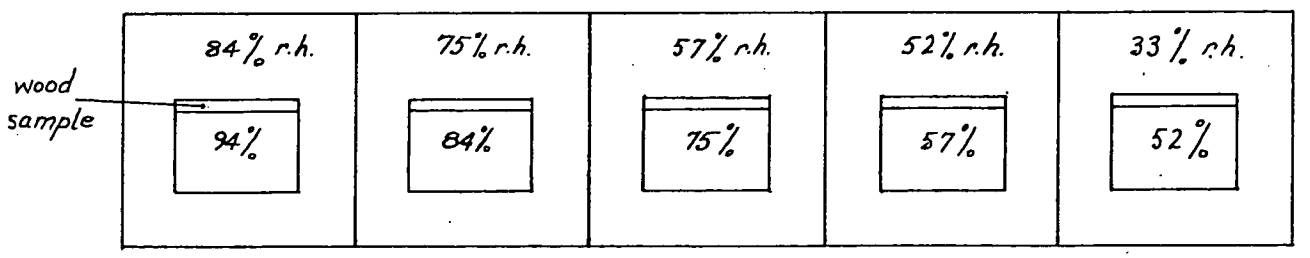

FIGURE 5.11
Test for diffusion co-efficients by diffusion cell method.

The temperature of the system was held at 30 ± 2°C. The air inside the vials was not stirred but that outside was. The vials were weighed every second or third day for approximately 28 days. Steady state prevailed in all cases after the 14th day. Samples cut from the original piece of veneer were placed in each of the constant humidity chambers in order to determine the equilibrium moisture concentrations of the wood under various conditions of humidity (i.e. to determine the appropriate sorption isotherm). The diffusion coefficients were determined from equation (5.1) using the measured steady-state mass transfer rates. At the end of the test, the samples were removed from the vials and oven-dried to determine their average moisture concentrations. The test was repeated using veneers cut perpendicular to the growth rings in order to measure the tangential diffusion coefficients. The results are shown in figure (5.12).

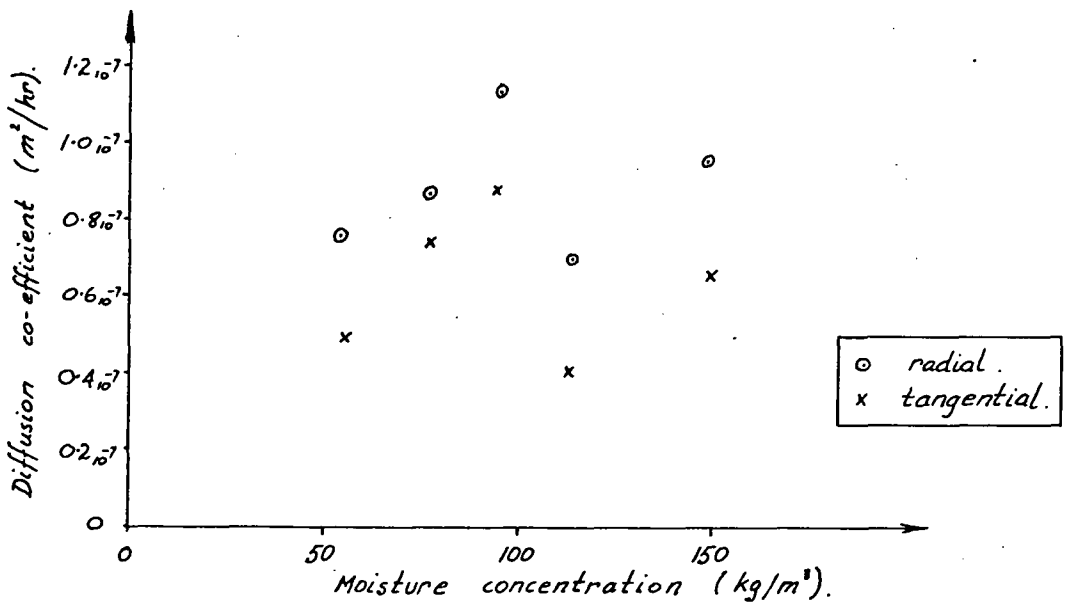

Figure 5.12

Diffusion cell test results

Diffusion cell tests were conducted on numerous samples of "Tasmanian Oak" with original moisture concentrations of between 70 and 90 kg/m^3. Regardless of whether the air inside the vials was or was not stirred, the results consistently took the form described in figure (5.12). Stirring did, however, increase the moisture transfer rates through the wood. The inconclusive nature of the diffusivity - moisture concentration relationship is probably due to the historical sorption effects described in section 3.6. Although the required relationship could not be deduced from these tests, two useful results were forthcoming.

Firstly, the ratio of the tangential to the radial mass diffusivities measured at the same temperature was approximately constant over the range of moisture concentrations covered by the test. From figure (5.12), it may be deduced that

$$\frac{\mathcal{D}(\text{tangential})}{\mathcal{D}(\text{radial})} \simeq 0.7$$

for "Tasmanian Oak".

Secondly, the radial diffusivity (measured as a function of temperature at approximately constant moisture concentration) displayed the trend shown in figure (5.13).

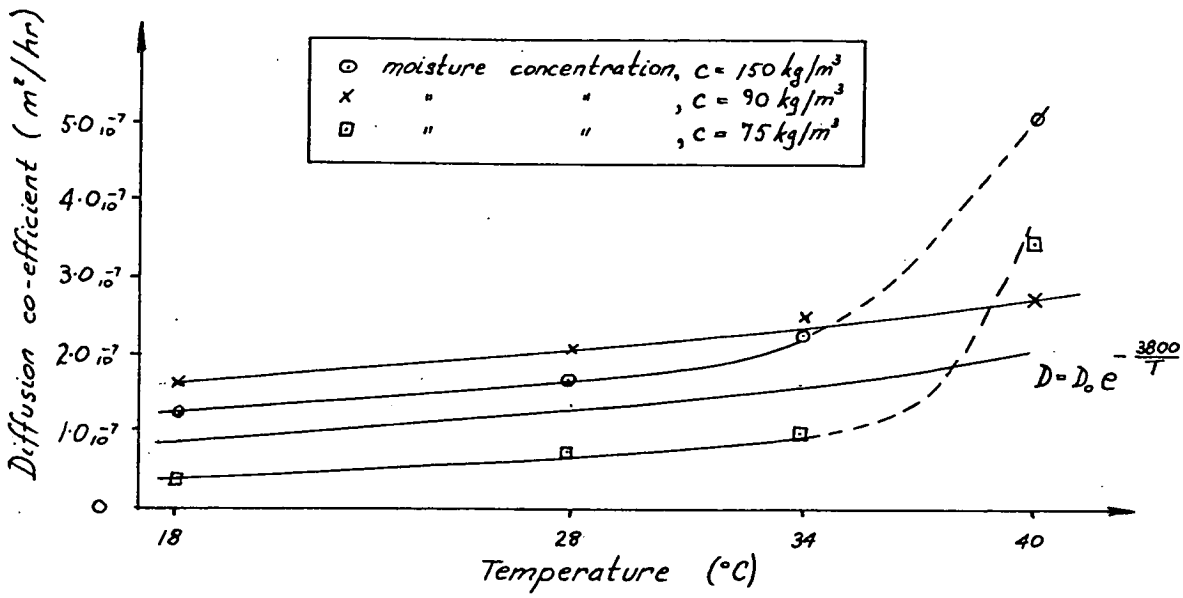

Figure 5.13

The variation of diffusion coefficients with temperature (for "Tasmanian Oak")

A relationship between diffusivity and absolute temperature similar to that proposed by Bramhall (1979,a) was fitted to the measurements in order to obtain an estimate of the activation energy of diffusion (section 3.2.3). The slope of the fitted curve is similar to those measured over the range 18 to 34°C. However, at temperatures greater than 34°C, the measured diffusion rates at moisture concentrations of 75 and 150 kg/m³ increased rapidly. These observations are due in part to difficulties experienced in humidity control in the diffusion cell apparatus. In some cells, the solutions used for humidity control became unsaturated due to the increase in the solubility of the salts at elevated temperatures resulting in loss of control over humidity. Further testing is necessary before results can be quoted with confidence.

Never the less, the relationship

$$D = D_0 e^{-\left(\frac{3800}{T}\right)}$$

where T = absolute temperature

does compare favourably with the results of other research workers as summarised by Bramhall (1977).

5.3.3 Diffusion coefficients inferred from drying tests.

Drying curves were obtained for 760mm long quarter-sawn "Tasmanian Oak" boards with original (green) cross-sections measuring 136 × 28mm. The drying tests were conducted in kiln A (section 5.2.2) under constant conditions of temperature and relative humidity. The test boards were periodically removed from the kiln and small sections cut from them for moisture concentration determination. Some test results are contained in Appendix C. The relationships between average moisture concentration and time were plotted (for example, figure 5.14).

The original moisture concentrations in the boards tested ranged from 400 to 700 kg/m^3 (moisture contents of 65% to 120%). Tests were generally conducted at 30^{o}C and 60 to 70% relative humidity. The drying rates, even over the relatively small sample population tested, varied markedly. The duration of early tests varied between 160 and 460 hours (that is, samples were not dried to equilibrium). A typical drying curve is shown in figure (5.14).

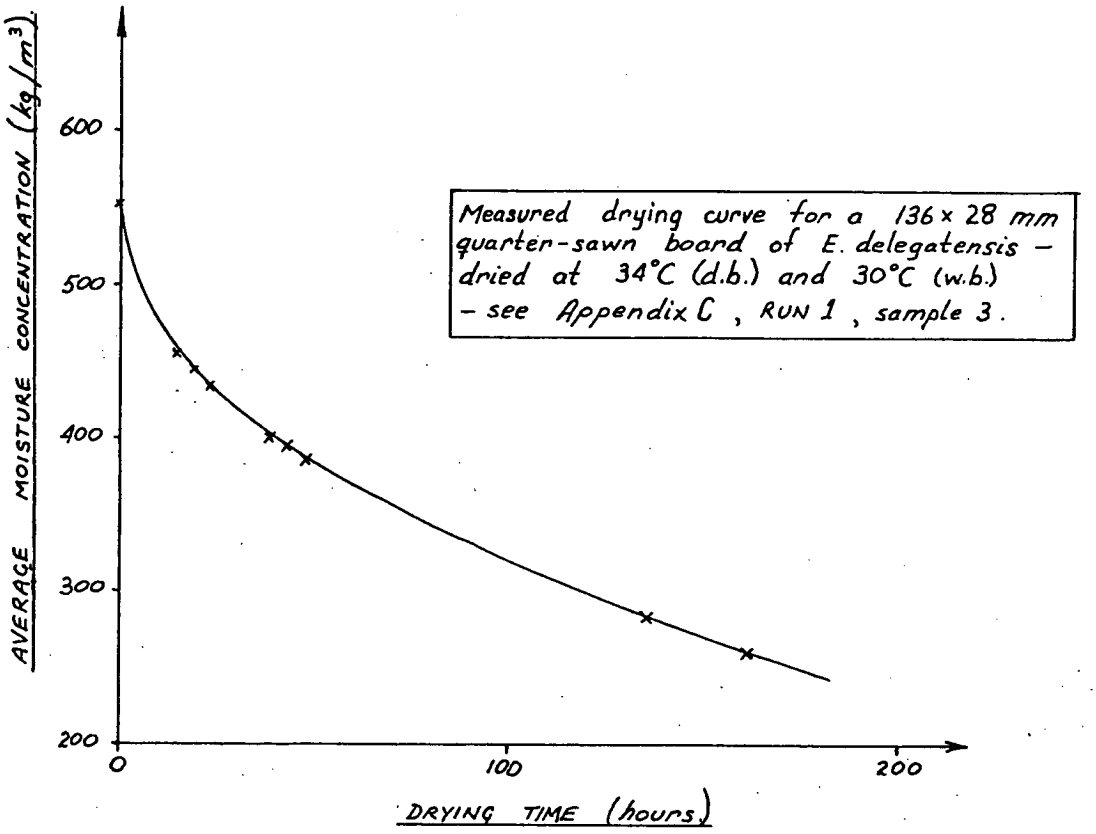

Figure 5.14

When describing moisture transfer through wood (using a pressure as the driving force for diffusion), Bramhall (1979,b) found that the mass diffusion coefficient (which, in his case, was independent of temperature) was best described by a function of the form

$$D = \exp\left(\frac{M}{A-BM} - E\right)$$

where A, B, E are constants

and M = moisture content.

This function became zero at about 7% (moisture content, dry basis). A parabola passing through the origin was used at moisture contents below 9%. During this investigarion, a similar function (equation 5.2) was used in conjunction

with an implicit finite difference approximation to the governing diffusion equation (equation 3.18) to calculate drying curves. The computer program described and listed in Appendix B was used for this purpose.

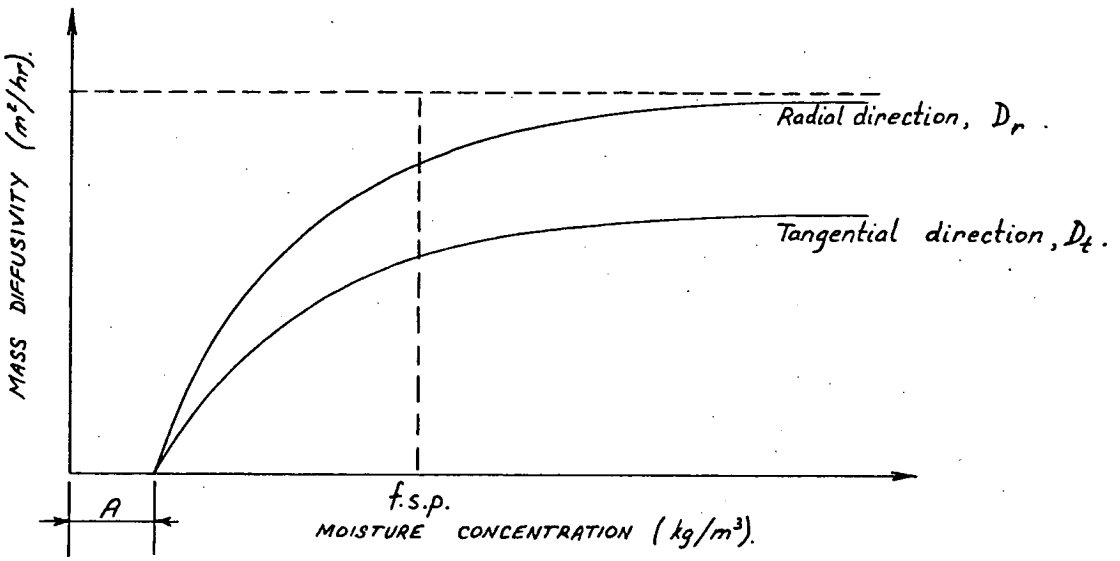

Figure 5.15
The approximate form of the Diffusivity-Moisture concentration relationship for "Tasmanian Oak".

The value of the diffusion coefficient in the radial direction, D_r, is given by

$$D_r = D_{max}\left[1 - \exp\left(\frac{A-c}{B}\right)\right] \qquad \text{-------} \quad (5.2)$$

where D_{max} = upper limit of diffusivity (m^2/hr)

A, B = constants,

and c = moisture concentration (kg/m^3).

The values of the constants D_{max}, A and B were adjusted until the calculated drying curves agreed closely with those

measured.

For simplicity, the ratio of

$$\frac{D_t}{D_r} = 0.7 \qquad \text{(section 5.3.2)}$$

was assumed to hold for all samples. Figure 5.16 shows the agreement between the measured and calculated drying curves for the example given in figure 5.14. A drying curve based on the assumption that the diffusion coefficients of "Tasmanian Oak" are independent of moisture concentration is also plotted in figure 5.16. The agreement between this curve and the measurements is better than that obtained from the falling diffusion coefficient model (equation 5.2). This was attributed to the combination of two effects.

Firstly, the mathematical model used (Appendix B) made no allowance for the shrinkage of the wood fibre during drying. The effect of shrinkage in the real situation is to shorten the diffusion pathways and therefore to accelerate drying.

Secondly, the diffusion coefficients of wood (using moisture concentration gradients as the driving "force" for diffusion) are known to decrease with decreasing moisture concentration (Bramhall, 1979,a; Christensen and Hergt, 1969; ...Also section 5.3.2). Decreasing diffusion coefficients tend to slow the drying process.

The fact that good agreement exists between measured drying curves and those calculated using constant diffusion coefficients leads to the deduction that the

effects of shrinkage and decreasing diffusion coefficient cancel one another.

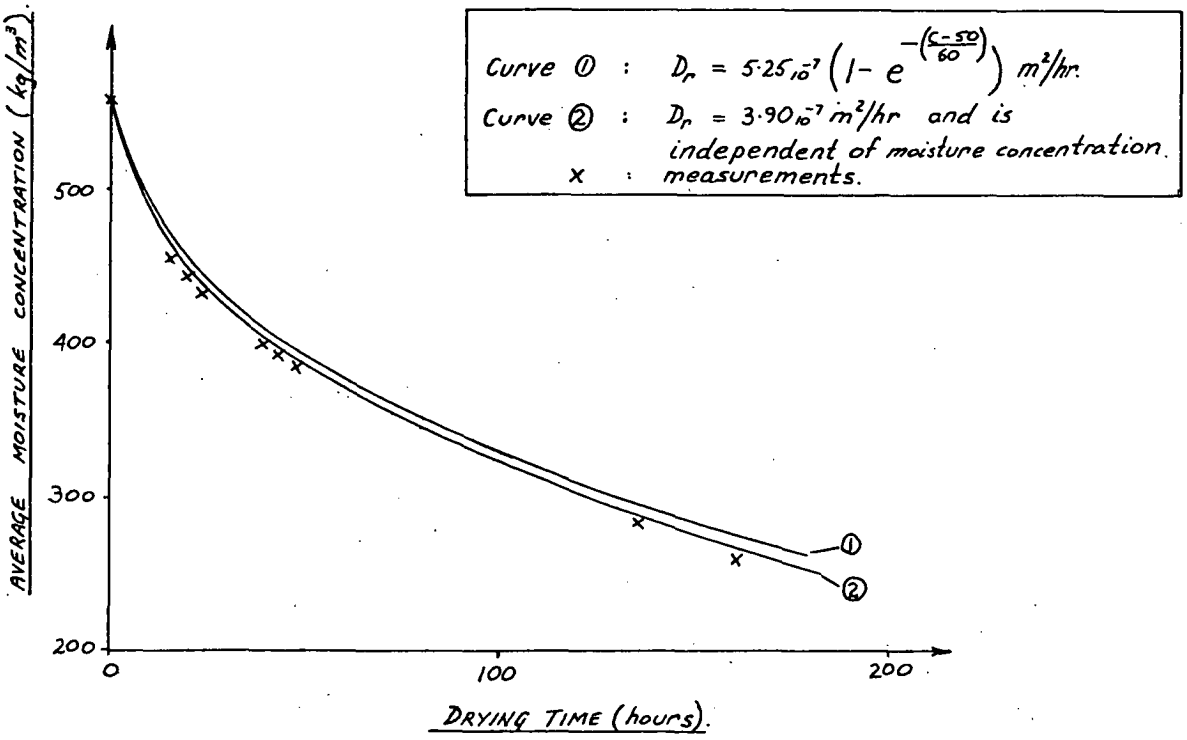

Figure 5.16

A comparison of measure and calculated drying curves for 136 x 28mm "Tasmanian Oak".

The diffusion coefficient of "Tasmanian Oak" in the radial direction (based on the simple constant coefficient model) was found to vary from $1.0_{10}{}^{-7}$ m²/hr to $2.0_{10}{}^{-7}$ m²/hr over the sample population tested. (See Appendix C for further details). The most commonly occuring value was found to be $1.7_{10}{}^{-7}$ m²/hr.

5.4 Initial trials on coated back-sawn "Tasmanian Oak"

5.4.1 Introduction

Freshly-sawn "Tasmanian Oak" boards have average moisture concentrations in the range of 400 to 700 kg/m³

and must be dried to an average moisture concentration of approximately 80 kg/m^3 (equilibrium with the atmosphere). As timber dries in air, its surface fibres rapidly approach the equilibrium moisture concentration of wood under the ambient conditions. In the early stages of drying, a large proportion of the cross-section of a board remains at a moisture concentration greater than the fibre saturation point (typically, fibre saturation point = 170 kg/m^3). The shrinkage rate of wood below the fibre saturation point is high compared with the rate above the f.s.p. (figure 4.3). Therefore, if the surface layers of a board could deform freely, they would shrink by a much greater amount than the inner zones of the board. However, the inner zones act as a restraint to the shrinkage of the surface fibres; thus, tensile stresses are generated at the surface. If these stresses become high enough, checks develop. By applying a semi-permeable coating to the surface of a board, the surface fibres can be held at moisture concentrations at or above the fibre saturation point for a period of time early in drying. In this way, differential shrinkage (and therefore drying stresses) can be controlled. (The principle is described in detail in section 4.6).

To be effective in controlling checking, a coating must have the correct combination of permeability and thickness. From known moisture diffusion rates through green wood, the approximate physical requirements of the coating were deduced and various potential coating materials selected on the basis of published or measured

moisture transfer properties. Qualitative tests were conducted on a small sample population to determine the relative performance of various coatings. A coating based on animal glue and talcum powder with a thickness of 0.7mm was found to consistently eliminate face-checks from approximately 80% of back-sawn 25mm (nominal thickness) "Tasmanian Oak" boards.

5.4.2 Estimation of required coating properties.

In section 3.4.2, an approximate method of determining the combination of coating thickness, d , and diffusivity (diffusion coefficient), D_c, required to hold the surface fibres of a back-sawn "Tasmanian Oak" board (having a radial diffusivity, D_w) above the fibre saturation moisture concentration for a time, t, is described. The relationship deduced (see equation 3.28) was

$$d \simeq \frac{D_c}{2}\sqrt{\frac{t}{D_w}}$$

where D_w lies between $1_{10}{}^{-7}$ m^2/hr and $2_{10}{}^{-7}$ m^2/hr for "Tasmanian Oak". Commonly, $D_w \simeq 1.7_{10}{}^{-7}$ m^2/hr.

It was estimated that if the surface fibres of back-sawn "Tasmanian Oak" boards were held above the fibre saturation moisture concentration for 120 hours (5 days), sufficient flattening of moisture gradients would occur. (At the time this estimation was made, detailed quantitative information on the development of drying stresses in timber was not available).

Subject to the various assumptions made in section 3.4.2, the required diffusivity of a coating, $\mathcal{D}_c$, having a thickness, d = 1mm, follows:

$$\mathcal{D}_c \simeq 0.58_{10}{}^{-7}\ m^2/hr \quad \text{if} \quad \mathcal{D}_w = 1_{10}{}^{-7} m^2/hr,$$

$$\text{or } \mathcal{D}_c \simeq 0.82_{10}{}^{-7}\ m^2/hr \quad \text{if} \quad \mathcal{D}_w = 2_{10}{}^{-7}\ m^2/hr.$$

Using the most commonly encountered value of the radial diffusivity of "Tasmanian Oak" ($\mathcal{D}_w \simeq 1.7_{10}{}^{-7}\ m^2/hr$) the required coating (with thickness, d=1mm) has a diffusivity, $\mathcal{D}_c \simeq 0.75_{10}{}^{-7}\ m^2/hr$.

5.4.3 Early tests on coated material

A coating based on animal glue (collagen) and mixed in the proportions

1 water : 0.4 dry animal glue crystals : 0.75 talcum powder

(by weight) was found to produce a tough material with a mass diffusivity of approximately $0.7_{10}{}^{-7}\ m^2/hr$ at a moisture content of approximately 5% (dry basis). The constituents of this coating were mixed at a temperature of about 50°C.

The mix was sprayed onto the surfaces of green boards at a temperature of about 40°C. At temperatures less than 30°C, the newly applied coating changed from a liquid to a jelly and adhered strongly to the wood. The coating was found to shrink by approximately 50% from its initial state to 5% moisture content (dry basis) and therefore the necessary "wet" thickness was about twice the required "dry" thickness. (The development of the coating

is detailed in Appendix D).

In order to examine the effectiveness of the animal glue/talcum powder coating, qualitative drying tests were conducted in kiln B on samples of back-sawn "Tasmanian Oak". Freshly back-sawn boards were obtained from logs selected at random. 125 x 25mm (nominal cross-section) boards, 4.2m long, were cut into 8 pieced (each 0.5m long), four of which were coated and four used as controls. The test samples were coated as soon after milling as possible (usually within 3 hours) to ensure that checking had not been initiated on the board faces prior to the application of the "moisture barrier". The test boards and their controls were dried in kiln B at approximately $30^{o}C$ and 70% relative humidity. In total, material from 15 different trees was tested.

Face checking was observed in the control boards from all but 2 trees. The effectiveness of animal glue/ talcum powder coatings with various thicknesses was studied on material ranging in initial moisture concentration from 400 to 700 kg/m^3. When checking occured in coated boards, it did so after a number (3 or 4) of days of drying and the checking was less extensive than that observed in the controls. Local variations in coating thickness contributed to the difficulty of assessing observations but coatings with a "dry" thickness of between 0.65 and 0.75mm were found to consistently eliminate checking in a large proportion (roughly 70%) of the material tested.

5.4.4 Measured moisture distributions.

Two samples, each 0.5m long, were cut from a board with 100 × 25mm (nominal) cross-section. One sample was coated with the animal glue/talcum powder mix to a thickness (at a moisture content of 10%, dry basis) of about 0.7mm and the other used as a control. Both samples were dried in kiln B at a temperature of 30°C and a relative humidity of 70%. Periodically, 50mm long sections were cut from each board and the microtome (section 5.2.5) was used to determine the distribution of moisture in the wood. The results appear in figure (5.17).

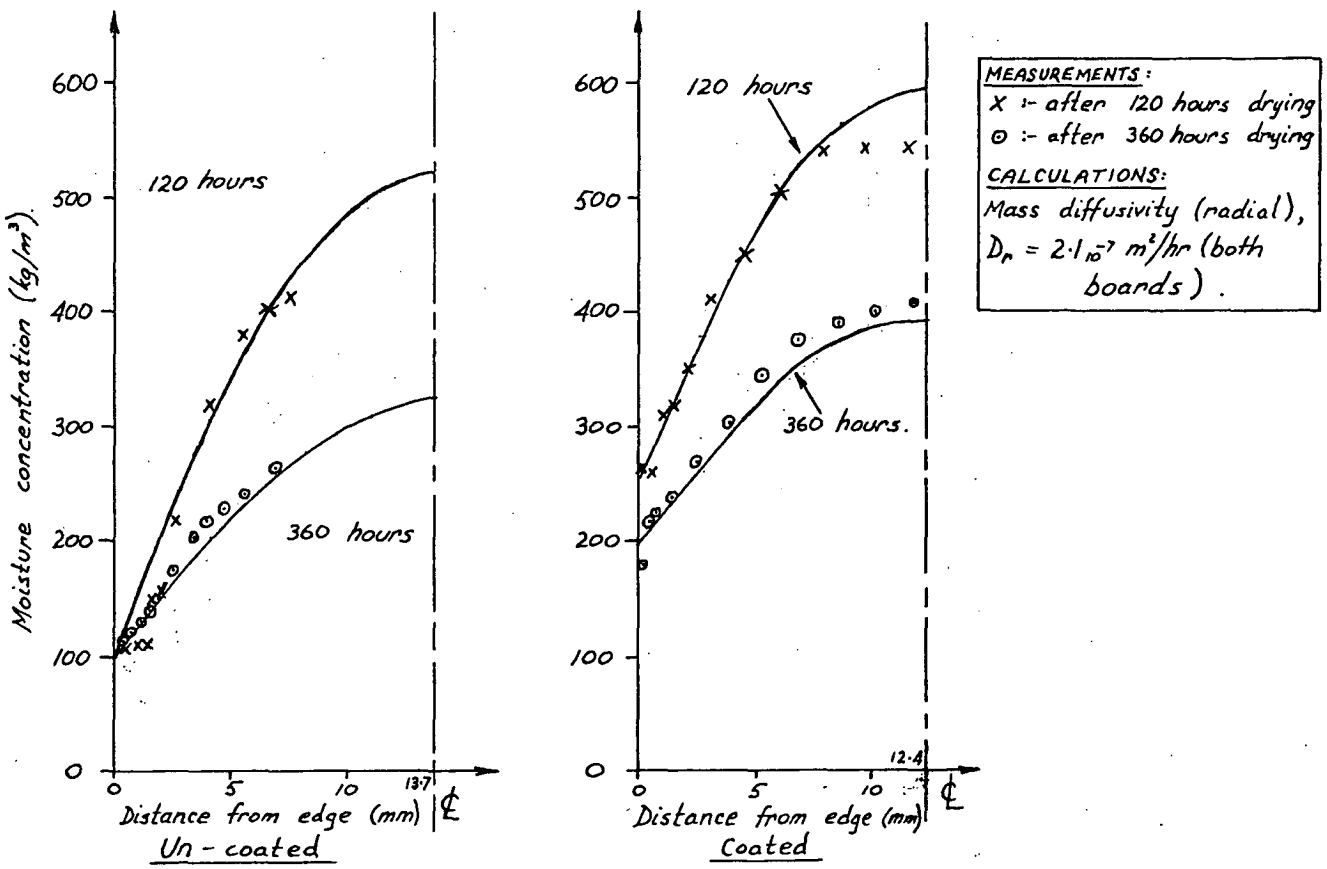

Figure 5.17

Measured and computed moisture distributions within coated and uncoated 25mm "Tasmanian Oak" boards.

The results presented in figure 5.17 clearly demonstrate

that the surface fibres of the coated board remain at moisture concentrations above the fibre saturation point for a considerable period of time following the commencement of drying.

5.5 Large-scale tests on coated timber.

5.5.1 Introduction

The results of drying tests conducted in kiln B (section 5.2.3) on a relatively small sample population (5.4.3) showed that a coating based on animal glue and talcum powder successfully eliminated face checking in a large proportion of back-sawn "Tasmanian Oak". The required "dry" thickness of coating was approximately 0.7mm (at a moisture content, M = 10%). The coating was mixed in the proportions

3.5kg water : 1kg dry animal glue crystals : 1.88kg talcum powder

(by weight) at a temperature of 50^{o}C and was sprayed onto the faces of freshly-cut (less than 4 hours old) back-sawn boards to a "wet" thickness of about 2mm. By spraying the coating onto the boards in thin layers, gradually building up to the required thickness, it was possible to obtain a reasonable uniform coverage (± 10% of the required thickness).

The effectiveness of the coating as a check-control method was examined using large sample populations of relatively long (2.2m) back-sawn boards. The timber

was dried under conditions similar to those found in industry.

5.5.2 Selection of material.

Four stacks (each of $0.5m^3$) of 25mm (nominal thickness) back-sawn E. delegatensis were dried from green to equilibrium with the atmosphere ($M \simeq 13\%$, $\rho \simeq 90$ kg/m^3). Three stacks were obtained from mills in southern Tasmania and one from northern Tasmania. 4.5m long boards were cut from randomly selected logs and, where possible, face-matched samples were obtained. All material tested was close to fully back-sawn. Each board was halved (to a length of 2.2m), tagged and stacked ready for transportation to the University of Tasmania (Hobart, southern Tasmania). Stacks were wrapped in damp hessian and covered with polythene during transportation and storage. Approximately half of the material in each stack was coated, the coating being applied a maximum of 24 hours after cutting.

The first stack was made up of material from twelve different logs, all grown in the central Tasmanian highlands. This material was reputedly amongst the most difficult ("refractory", prone to checking and collapse) milled in southern Tasmania. The material making up the second stack came from seven logs, all grown in south-western Tasmania. The third stack was cut from very poor quality logs, again from the central highlands. Nine logs were sampled. Only two logs were sampled in the fourth

stack, the material coming from the central north of Tasmania.

Prior to coating, the timber in all stacks was closely examined and the quality of the "raw material" noted. The boards making up the first, second and fourth stacks were considered to be a "run of the mill", average quality, there being no major or persistent natural defects. However, the majority of boards making up the third stack exhibited faults of some kind. There were many large deviations in grain direction (particularly around knots or other irregularities), and there was a higher than average amount of rotten pith and large numbers of gum veins and borer holes.

5.5.3 Method of applying the coating.

The animal glue/talcum powder mixture was sprayed onto the surfaces of green timber in a liquid form at a temperature of approximately 50^{o}C. Upon contact with the relatively cold board surfaces (usually 15^{o}C), the coating set to a rubbery jelly which adhered strongly to the boards. With a little care, freshly-sprayed boards could be handled without damaging the coating.

Hot coating mix was sprayed onto the faces of boards using the apparatus shown schematically in figure 5.18.

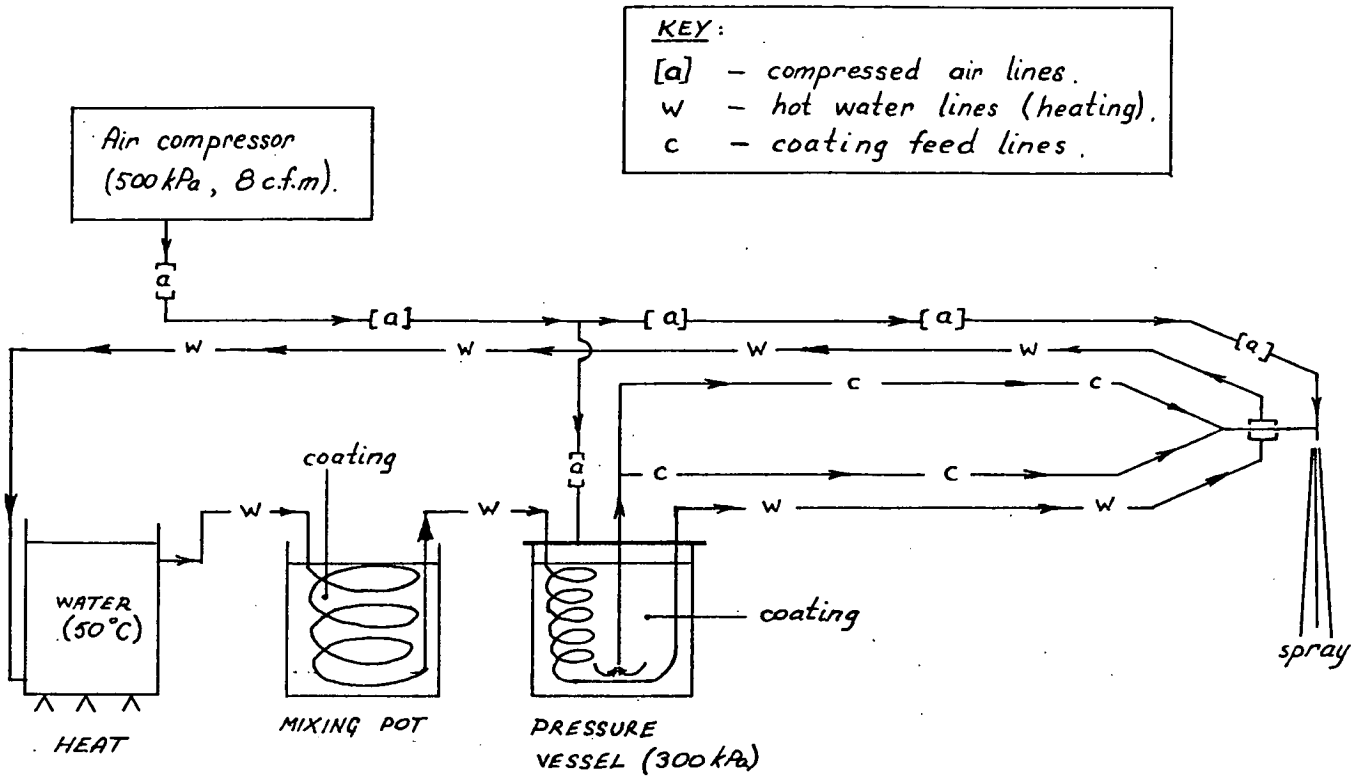

Figure 5.18

Schematic arrangement of animal glue spraying apparatus

Water at 60°C was circulated through the system in order to maintain temperatures at which the animal glue/ talcum powder mixture remained liquid. If the water was allowed to fall below 40°C, the viscosity of the mix increased markedly causing congestion in the feed lines to the spray nozzle. The mix "set" (jellified) at a temperature of approximately 30°C. The spray nozzle used was of the hand-held, compressed air operated type commonly found in the automotive repair industry and was fed by twin 6mm (¼") flexible jacketed hoses. The liquid coating mix was forced through the feed lines under an applied pressure

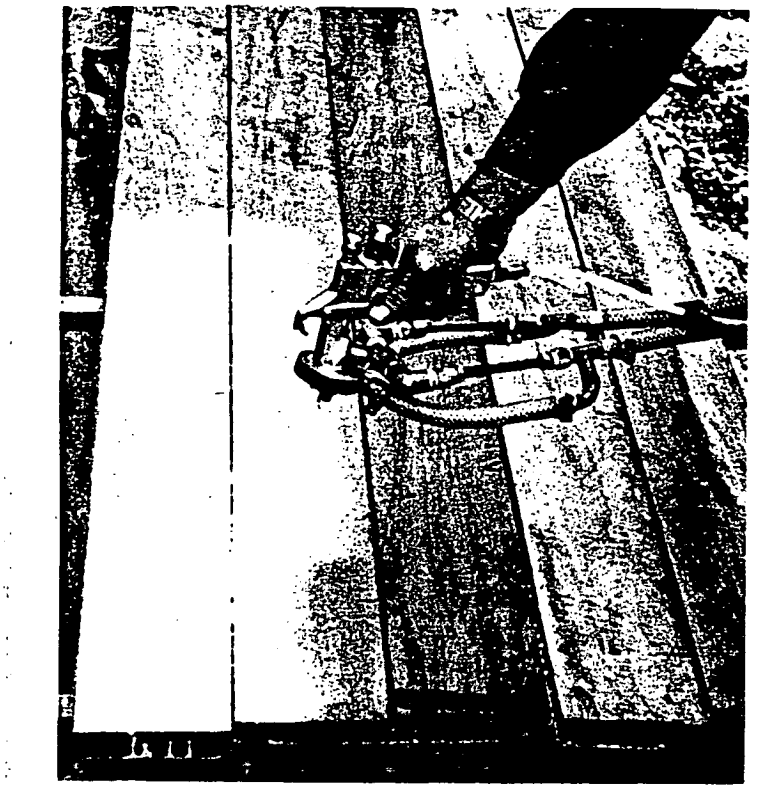

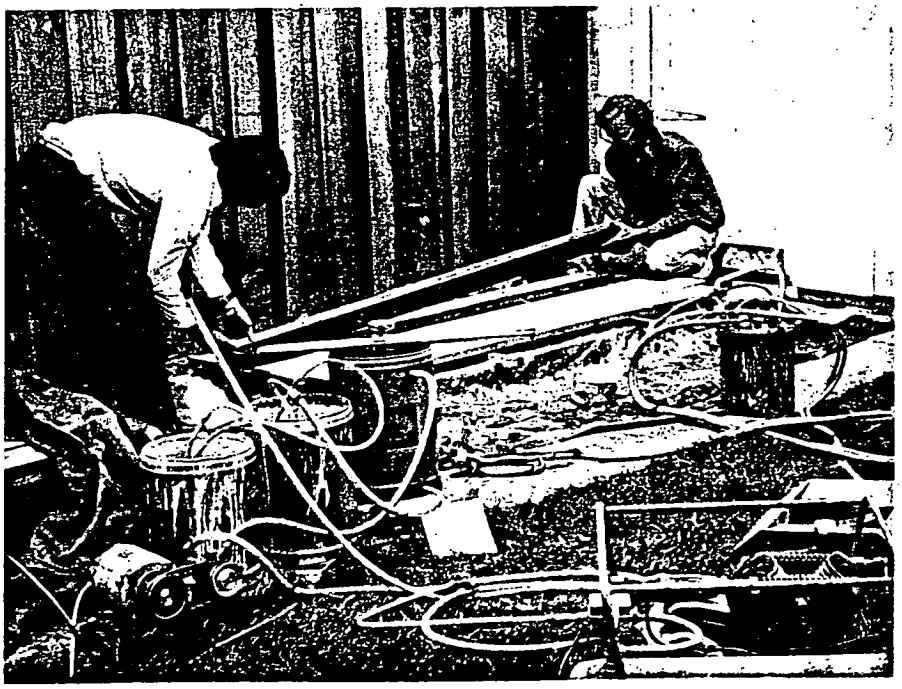

Figue 5.19

Application of the animal glue coating by spraying.

of 300kPa. The system was capable of coating both faces of a 3.5m long, 125 x 25mm (nominal) board in one minute.

Generally, the test boards were stacked in such a way that every alternate layer contained coated boards only. Matched pairs of coated and control boards were always placed vertically above one-another in adjacent layers. Figure (5.19) shows the apparatus in more detail.

5.5.4 Drying Schedules

The stacks were air-dried under shelter from the weather for approximately 8 weeks, followed by a period of approximately 2 weeks kiln-drying at 30°C and 50% relative humidity. They were then reconditioned (post-steamed) and allowed to air-dry for a further period of 7 to 10 days.

The drying schedules currently used in the Tasmanian hard-wood milling industry for quarter-sawn material vary greatly according to the geographical location of the seasoning yard and the properties of the species milled. An average drying schedule for 25mm (nominal) thick material might involve air-drying for 6 months (to an average moisture content of about 20%) followed by reconditioning for between 4 and 6 hours and kiln drying for a further 4 to 5 days, giving a total drying time of approximately 26 weeks. The use of pre-dryers (low temperature kilns) towards the end of air-drying shortens the total drying time to about 16 weeks.

Coated back-sawn material (with a nominal thickness of 25mm) was dried from green to a moisture content of 14% (dry basis) in 12 weeks.

5.5.5 Results

The quality of the timber dried after coating with a semi-permeable material was much higher than that dried without. About 10% of the control boards did not check, nor did the corresponding coated boards. Checks appeared in about 20% of the coated boards for which the controls checked. Coated boards did not, as a rule, exhibit as much collapse as the controls. However, the gross shrinkage of the coated material was marginally greater than the controls.

"Cupping" of the cross-section of coated boards was often more emphatic than that found in controls. The cupping of boards making up larger stacks would probably be reduced as greater restraint would be provided for most material due to increased dead-weight. However, the restraint of overall deformation would add to stresses over the cross-section and might increase the probability of formation of checks (see section 4.2).

Stack No. 1: The animal glue/talcum powder mix was sprayed onto the faces of the boards in a wet thickness of about 1.8mm, giving a dry thickness of 0.4 ± 0.05mm. This amount of shrinkage was not expected.

After drying in air for one day, face checking became apparent in the controls and after 6 days, checking was observed in about 30% of coated material. The test was

discontinued after 8 days when roughly 70% of the coated material had checked.

Stack No. 2: In this case, care was taken to ensure a "dry" coating thickness of 0.8 ± 0.1mm. Drying according to the schedule described in section 5.5.4 produced face checking in about 85% of control boards. Checking was eliminated in approximately 90% of coated material with matched control boards exhibiting checks.

Stack No 3: The coating had a "dry" thickness of between 0.7 and 0.8mm. All control boards checked and checking was eliminated in about 2/3 of coated material. This result was regarded as most satisfactory in view of the quality of the green material.

Stack No 4: Again, the coating had a dry thickness of between 0.7 and 0.8mm. 2/3 of the boards from each of the two logs were coated. The stack was made up of a total of 40 coated boards, each 2.2m long, and 20 controls of the same length. The total volume of timber in the stack was $0.39m^3$ (175 superficial feet). Only two of the control boards did not check, both of these coming from the same log. Checking was eliminated completely from 34 of the coated boards and the checking present in the remaining 6 was not severe.

Where present, checks in the coated boards were often associated with areas of damage to the coating or with an area in the coating where the required thickness

had not been attained. This re-emphasised the need for uniformity of coating thickness.

Drying curves for the three stacks dried to equilibrium with the atmosphere are given in figure (5.20). The moisture content of a number of boards in each stack was monitered. Oven drying tests were used exclusively.

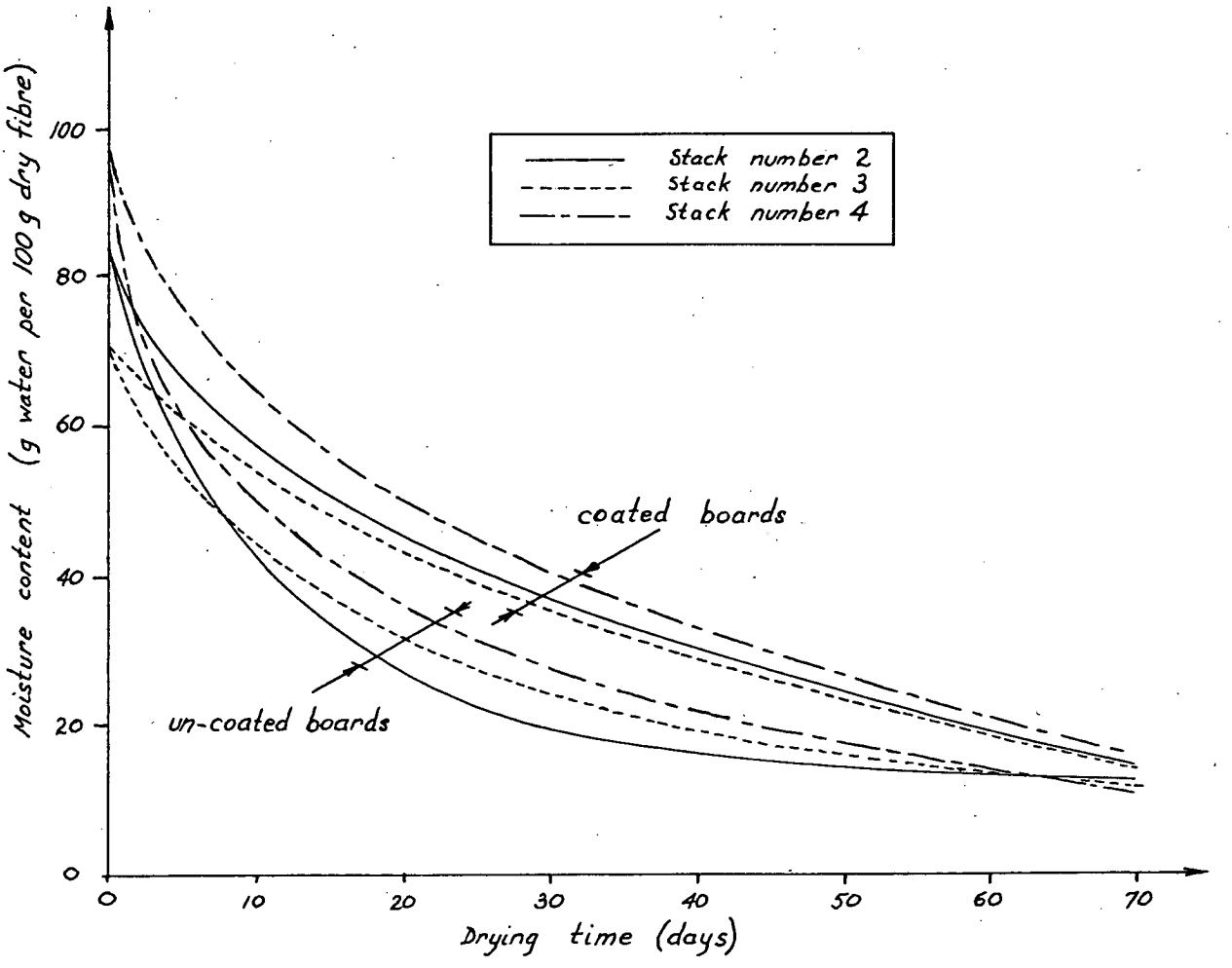

Figure 5.20

Typical drying curves for coated and uncoated 25mm "Tasmanian Oak" boards.

Note the pronounced period of constant rate drying of the coated boards brought about by the fact that the coating governs the moisture transfer rate from the wood surface.

The major economic advantages of back-sawing are to increase the recovery of dry sawn timber from each log,to reduce handling and to shorten drying times, thus lowering interest costs. Unfortunately, the cupping observed in a percentage of dry, coated back-sawn boards means that a larger percentage of wood than usual is lost during final machining (dressing). In a commercial situation, this would tend to off-set the increased recovery on initial sawing to some extent.

Although commercially uneconomic, large-scale tests using the animal glue/talcum powder coating proved the principle of drying through a semi-permeable material to be soundly based. The effect of coatings on the drying stresses in timber is more thoroughly examined in Chapter 8.

REFERENCES.

BRAMHALL, G. (1977): More on application of Fick's Laws.
Wood Science 9(4): 152-153.

..... (1979,a): Mathematical model for lumber drying. I. Principles involved.
Wood Science 12(1): 14-21.

..... (1979,b): Mathematical model for lumber drying. II. The model.
Wood Science 12(1): 22-26.

BUI, X., E.T. CHOONG, W.G. RUDD (1980): Numerical methods for solving the equation for diffusion through wood during drying.
Wood Science 13(2): 117-121.

CHRISTENSEN, G.N., H.F.A. HERGT, (1969): Effects of previous history on kinetics of sorption by wood cell walls.
Journal of Polymer Science
Part A-1, Vol.7 : 2427-2430.

C.S.I.R.O. (1974): Testing timber for moisture content
Division of Building Research, C.S.I.R.O.-
Special Report.
Melbourne, Australia.

DOE, P.E. (1973,a): A mathematical model for shrinking solids during drying.
First Aust. Conf. on Heat and Mass Transfer
Monash Univ. Melbourne, Australia.

DOE, P.E., D.G. JAMES, F. YOUNG (1973,b): Studies on the processing of abalone.
V. dried abalone : Techniques and Characteristics of drying.
Fd. Technol Aust. V25 No.4 : 189-195.

DOE, P.E., R.C. MENARY, (1979): Optimization of the Hop Drying Process with respect to Alpha Acid Content.
J. Agric. Engng Res. (1979) 24 : 233-248.

FISH, B.P. (1957): Diffusion and Equilibrium Properties of Water in Starch.
Dpt. Sci. and Industrial Res. - Food Investigation Technical Paper No.5.
H.M. Stationary Office, London, England.

MACKAY, J.F.G. (1971): Moisture flux Determinations Influenced by Air Circulation inside Diffusion Cells.
Wood Science 3(4) : 220-222.

ROHSENOW, W.M., H.Y. CHOI, (1961): Heat, Mass and Momentum Transfer. Prentice-Hall (Inc).

CHAPTER 6

CHAPTER 6

THE THEORY OF ELASTICITY OF ORTHOTROPIC MATERIALS

6.1 Introduction

The drying of timber gives rise to a state of differential shrinkage strain and therefore stress. These stresses are analogous to those resulting from thermal gradients. In order to fully describe the behaviour of timber while drying, it is necessary to develop a theoretical model which enables prediction of stresses and deformations. From such a model, rapid evaluation of the effectiveness of proposed stress control methods can be made and its use can be further extended to optimise the economic benefits of such processes. Before a study of the

state of stress in a material can be commenced, a number of assumptions must be made regarding its behaviour under load (stress).

In timber, as in most engineering materials, deformations result from the application of external forces. Provided these forces do not exceed certain limits, the deformation will disappear upon removal of the forces. Such behaviour is said to be perfectly elastic. Throughout the derivations in this chapter, it is assumed that the material under consideration is perfectly elastic and that a linear relationship exists between load and deformation. Further, it is assumed that the smallest element cut from the elastic body posesses the same properties as the body as a whole; that is, the material is assumed to be homogeneous. Although timber does not satisfy these conditions completely, solutions to theoretical models based on these assumptions give good approximations to the actual behaviour.

6.2 The Behaviour of Elastic Materials - the Basic Concepts.

6.2.1 Strain, displacement and deformation.

The deformations that commonly occur within elastic limits in engineering materials are small and vary continuously over the volume of the body under consideration.

Consider the element of an elastic body shown in figure 6.1. Let u, v and w represent the components of displacement in the x, y and z directions respectively. Assume that there are enough constraints on the elastic body to prevent it moving as a rigid body. Therefore, no part of the body may be displaced without the body being deformed.

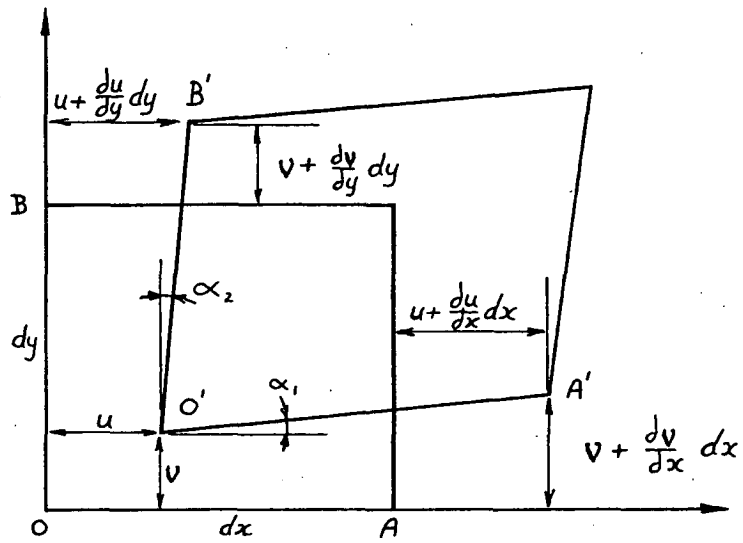

Figure 6.1

For small displacements, the elongation of OA is $\frac{\partial u}{\partial x}dx$

The unit elongation or "strain" at O in the x-direction is defined as $\varepsilon_x = \frac{\partial u}{\partial x}$; similarly, $\varepsilon_y = \frac{\partial v}{\partial y}$

Consider now the angle change at O produced by the deformation of the body. The total angle change is known as the shearing strain at O in the x-y plane and is made up of the two components α_1 and α_2 of figure 6.1.

That is, the shearing strain,

$$\gamma_{xy} = \alpha_1 + \alpha_2 = \frac{\partial v}{\partial x} + \frac{\partial u}{\partial y}.$$

The above discussion extended to three dimensions yields

$$\varepsilon_x = \frac{\partial u}{\partial x}, \quad \varepsilon_y = \frac{\partial v}{\partial y}, \quad \varepsilon_z = \frac{\partial w}{\partial z}$$

$$\gamma_{xy} = \frac{\partial u}{\partial y} + \frac{\partial v}{\partial x}; \quad \gamma_{yz} = \frac{\partial v}{\partial z} + \frac{\partial w}{\partial y}, \quad \gamma_{xz} = \frac{\partial u}{\partial z} + \frac{\partial w}{\partial x} \qquad \ldots(6.1)$$

Equations (6.1) fully define the state of strain at any point within a material.

6.2.2 Equation of compatibility.

The six strain components defined by equations (6.1) are completely dependent upon the three displacement components u, v and w. Therefore, the strain components are not independent.

From equations (6.1), we find that

$$\frac{\partial^2 \varepsilon_x}{\partial y^2} = \frac{\partial^3 u}{\partial x \partial y^2}; \quad \frac{\partial^2 \varepsilon_y}{\partial x^2} = \frac{\partial^3 v}{\partial x^2 \partial y}; \quad \frac{\partial^2 \gamma_{xy}}{\partial x \partial y} = \frac{\partial^3 u}{\partial x \partial y^2} + \frac{\partial^3 v}{\partial x^2 \partial y}$$

and therefore $$\frac{\partial^2 \varepsilon_x}{\partial y^2} + \frac{\partial^2 \varepsilon_y}{\partial x^2} = \frac{\partial^2 \gamma_{xy}}{\partial x \partial y} \qquad \ldots(6.2)$$

Also, $$\frac{\partial^2 \varepsilon_x}{\partial y \partial z} = \frac{\partial^3 u}{\partial x \partial y \partial z}; \quad \frac{\partial \gamma_{xy}}{\partial z} = \frac{\partial^2 u}{\partial y \partial z} + \frac{\partial^2 v}{\partial x \partial z};$$

$$\frac{\partial \gamma_{yz}}{\partial x} = \frac{\partial^2 v}{\partial x \partial z} + \frac{\partial^2 w}{\partial x \partial y}; \quad \frac{\partial \gamma_{xz}}{\partial y} = \frac{\partial^2 u}{\partial y \partial z} + \frac{\partial^2 w}{\partial x \partial y}$$

Therefore, $$2\frac{\partial^2 \varepsilon_x}{\partial y \partial z} = \frac{\partial}{\partial x}\left[\frac{\partial \gamma_{xy}}{\partial z} - \frac{\partial \gamma_{yz}}{\partial x} + \frac{\partial \gamma_{xz}}{\partial y}\right] \quad \ldots(6.3)$$

A total of four more equations (similar to 6.2 and 6.3) exist. Therefore, for the six strain components to be compatible, the following six relationships (known as the equations of compatibility) must hold.

$$\frac{\partial^2 \varepsilon_x}{\partial y^2} + \frac{\partial^2 \varepsilon_y}{\partial x^2} = \frac{\partial^2 \gamma_{xy}}{\partial x \partial y} \; ; \quad 2\frac{\partial^2 \varepsilon_x}{\partial y \partial z} = \frac{\partial}{\partial x}\left[\frac{\partial \gamma_{xy}}{\partial z} - \frac{\partial \gamma_{yz}}{\partial x} + \frac{\partial \gamma_{xz}}{\partial y}\right]$$

$$\frac{\partial^2 \varepsilon_y}{\partial z^2} + \frac{\partial^2 \varepsilon_z}{\partial y^2} = \frac{\partial^2 \gamma_{yz}}{\partial y \partial z} \; ; \quad 2\frac{\partial^2 \varepsilon_y}{\partial x \partial z} = \frac{\partial}{\partial y}\left[\frac{\partial \gamma_{xy}}{\partial z} + \frac{\partial \gamma_{yz}}{\partial x} - \frac{\partial \gamma_{xz}}{\partial y}\right]$$

$$\frac{\partial^2 \varepsilon_z}{\partial x^2} + \frac{\partial^2 \varepsilon_x}{\partial z^2} = \frac{\partial^2 \gamma_{xz}}{\partial x \partial z} \; ; \quad 2\frac{\partial^2 \varepsilon_z}{\partial x \partial y} = \frac{\partial}{\partial z}\left[-\frac{\partial \gamma_{xy}}{\partial z} + \frac{\partial \gamma_{yz}}{\partial x} + \frac{\partial \gamma_{xz}}{\partial y}\right]$$

$$\ldots(6.4)$$

6.2.3 Load - deformation relationships.

Consider a rectangular parallelepiped subjected to a uniform stress in the x- direction, σ_x, as shown in figure (6.2).

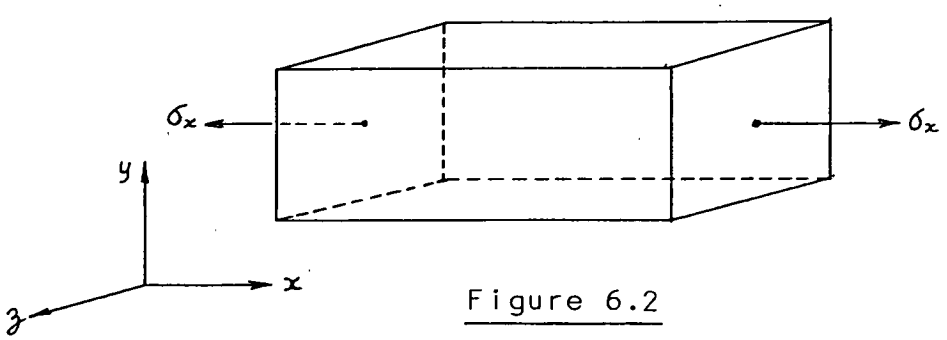

Figure 6.2

The unit elongation or strain in the x- direction associated with the applied stress is given by $\varepsilon_x = \frac{1}{E_x}\sigma_x$ where E_x is Young's modulus (constant) for linearly elastic materials.

The deformation in the x- direction is accompanied by unit lateral contractions,

$$\varepsilon_y = -\mu_{xy}\,\varepsilon_x \quad \text{and} \quad \varepsilon_z = -\mu_{xz}\,\varepsilon_x$$

where μ_{ij} = Poisson's ratio for determination of strains in the j- direction resulting from those in the i- direction.

Hence, strains resulting from a three-dimensional direct stress state may be expressed as

$$\varepsilon_x = \frac{\sigma_x}{E_x} - \mu_{yx}\frac{\sigma_y}{E_y} - \mu_{zx}\cdot\frac{\sigma_z}{E_z}$$

$$\varepsilon_y = -\mu_{xy}\cdot\frac{\sigma_x}{E_x} + \frac{\sigma_y}{E_y} - \mu_{zy}\cdot\frac{\sigma_z}{E_z}$$

$$\varepsilon_z = -\mu_{xz}\cdot\frac{\sigma_x}{E_x} - \mu_{yz}\frac{\sigma_y}{E_y} + \frac{\sigma_z}{E_z} \qquad \ldots(6.5)$$

Consider now the action of shear stresses only. Figure (6.3) shows an element of material in the x-y plane deformed due to the action of the shear stresses τ_{xy} and τ_{yx}.

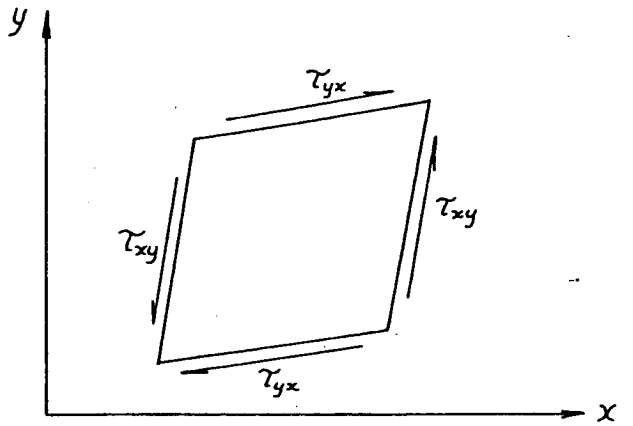

Figure 6.3

From static equilibrium requirements, it may be deduced that $\tau_{xy} = \tau_{yx}$. Shear strains are related to shear stresses by the simple relationships

$$\gamma_{xy} = \frac{1}{G_{xy}} . \tau_{xy} \; ; \; \gamma_{yz} = \frac{1}{G_{yz}} . \tau_{yz} \text{ and } \gamma_{zx} = \frac{1}{G_{zx}} . \tau_{zx} \; . \qquad \ldots(6.6)$$

where G_{ij} is the modulus of rigidity associated with shear deformation in the i-j plane and is a constant for a linearly elastic material.

Equations (6.5) and (6.6) together are known as the "generalised Hooke's Law equations".

6.2.4 Differential Equations of Static Equilibrium.

For a body, or any part of it, to be in static equilibrium, certain relationships between the six stress

components must exist. These relationships may be investigated by studying the conditions of equilibrium of a small element of an elastic body in the form of a rectangular parallelepiped, as shown in figure (6.4). The effects of small changes in the components of stress are of major importance and are due to the fact that, under most conditions, the stresses within a body vary continuously over its volume. The action of body forces (due, for example, to gravitational effects) must also be included.

Let the body forces per unit volume acting in the x, y and z directions be X, Y and Z respectively.

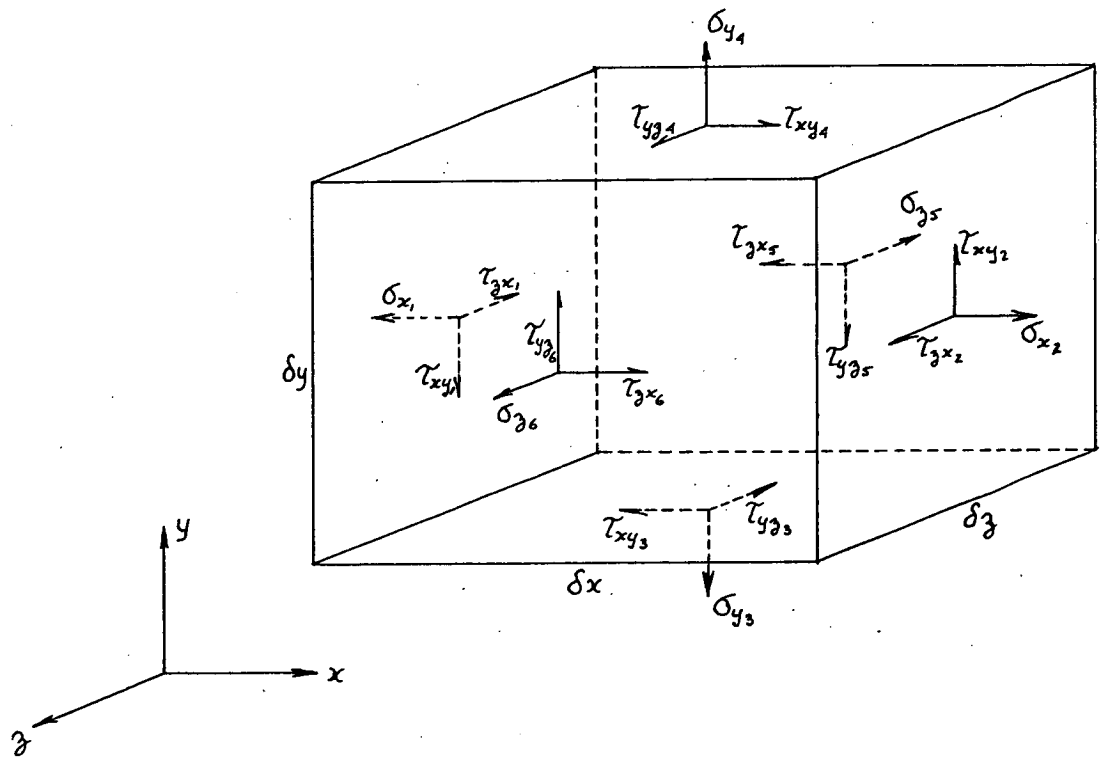

Figure 6.4

When calculating the forces acting on the faces of the element, it is assumed that the sides are very small and therefore that the force is given by multiplying the stress acting at the centroid of a side by the area of the side.

From figure (6.4), the equation of equilibrium in the x- direction is:

$$(\sigma_{x_2}-\sigma_{x_1})\delta y\delta z + (\tau_{xy_4}-\tau_{xy_3})\delta x\delta z + (\tau_{xz_6}-\tau_{xz_5})\delta x\delta y + X\delta x\delta y\delta z = 0$$

or $$\frac{(\sigma_{x_2}-\sigma_{x_1})}{\delta x} + \frac{(\tau_{xy_4}-\tau_{xy_3})}{\delta y} + \frac{(\tau_{xz_6}-\tau_{xz_5})}{\delta z} + X = 0$$

In the limit, as δx, δy and δz all tend to zero, the above equation becomes

$$\frac{\partial \sigma_x}{\partial x} + \frac{\partial \tau_{xy}}{\partial y} + \frac{\partial \tau_{xz}}{\partial z} + X = 0 .$$

Similarly, $$\frac{\partial \sigma_y}{\partial y} + \frac{\partial \tau_{xy}}{\partial x} + \frac{\partial \tau_{yz}}{\partial z} + Y = 0$$

and $$\frac{\partial \sigma_z}{\partial z} + \frac{\partial \tau_{xz}}{\partial x} + \frac{\partial \tau_{yz}}{\partial y} + Z = 0 \qquad \ldots(6.7)$$

Equation (6.7) must be satisfied at all points throughout the volume of the body. The stresses may vary throughout the body and, at the surface, they must be such that they are in equilibrium with the external forces acting on the surface of the body.

6.2.5 The Plane Strain Approximation.

When the dimension of a body in the z direction is large compared to the cross-sectional dimensions and the body is loaded by forces perpendicular to the longitudinal direction which are independent of z, it may be assumed that all cross-sections are in the same condition (Timoshenko and Goodier, 1970). Southwell (1941) deduced this from strain energy considerations and mentions a possible exception to the uniformity in the immediate neighbourhood of the ends. Such uniformity can be approximated by assuming that the ends of the body are restrained between two rigid, flat planes so that axial displacement, w, is prevented. By symmetry, $w = 0$ everywhere, plane cross-sections remain plane and conditions are therefore the same at every cross-section. The resultant axial forces and bending couples required at the ends can be removed by superposition of simple tension (or compression) and/or bending.

Under the above assumption, the components of displacement u and v are functions of x and y only. Also, the longitudinal displacement, w, is zero for all x, y and z, and therefore equations (6.1) give

$$\varepsilon_z = \frac{\partial w}{\partial z} = 0 \; ; \quad \gamma_{yz} = \frac{\partial v}{\partial z} + \frac{\partial w}{\partial y} = 0 \; ; \quad \gamma_{xz} = \frac{\partial u}{\partial z} + \frac{\partial w}{\partial x} = 0 \qquad \ldots(6.8)$$

Five of the six compatibility equations (equation 6.4) are identically satisfied, leaving only one compatibility requirement

$$\frac{\partial^2 \varepsilon_x}{\partial y^2} + \frac{\partial^2 \varepsilon_y}{\partial x^2} = \frac{\partial^2 \gamma_{xy}}{\partial x \partial y} \qquad \ldots (6.9)$$

From the load-deformation relations (equations 6.5 and 6.6),

$$\sigma_z = \mu_{xz} \frac{E_z}{E_x} \sigma_x + \mu_{yz} \frac{E_z}{E_y} \sigma_y$$

and $$\tau_{yz} = \tau_{xz} = 0 \qquad \ldots (6.10)$$

The equations of equilibrium (equations 6.7) therefore become

$$\frac{\partial \sigma_x}{\partial x} + \frac{\partial \tau_{xy}}{\partial y} + X = 0$$

and $$\frac{\partial \sigma_y}{\partial y} + \frac{\partial \tau_{xy}}{\partial x} + Y = 0 \qquad \ldots (6.11)$$

Thus, the plane strain problem reduces to the determination of σ_x, σ_y and τ_{xy} as functions of x and y only.

6.2.6 Rotation of Axes.

During the analysis of strain and stress in a body, it is often necessary to obtain the strain or stress components relative to a set of axes rotated through some angle with respect to the co-ordinate system in which strains or stresses are known. If the plane strain approximation of section 6.2.5 is adopted, analysis of stress and strain need be concerned only with the conditions over a cross-section perpendicular to the z- direction. Hence, rotation of axes within a single plane will be considered.

6.2.6.1 Strain at a point.

Providing the strain components relative to the x-y rectangular co-ordinate system ($\varepsilon_x, \varepsilon_y$ and γ_{xy}) are known, the strains relative to any other reference system in the same plane may be determined. Consider an element, TPQ, of an elastic body, as shown in figure (6.5).

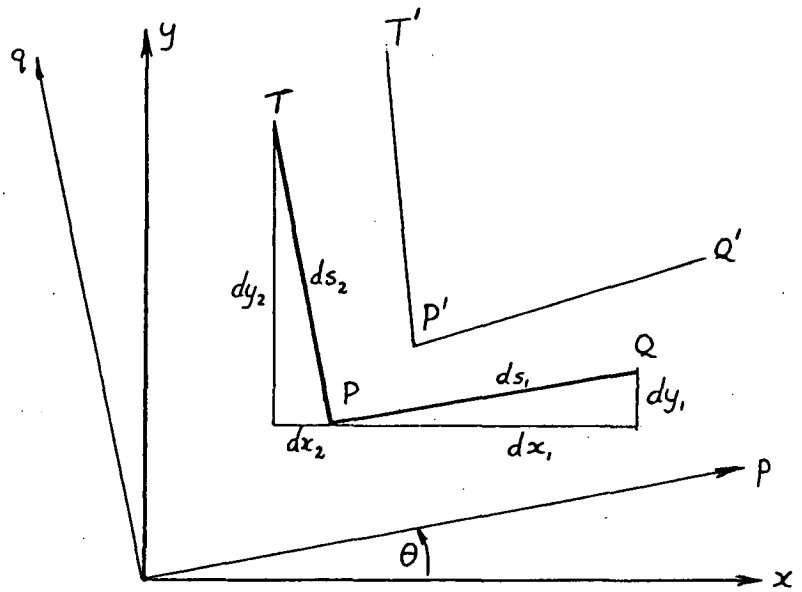

Figure 6.5

Sides PQ and PT of the element have lengths ds_1 and ds_2 respectively. PQ is paralled to the p-axis.

As in section 6.2.1, it is assumed that there are enough restraints on the elastic body to prevent it moving as a rigid body, and therefore no part of the body may be displaced without it being deformed. The deformed shape of the element under consideration is $T^1P^1Q^1$ where P^1 is

displaced from P by the amounts u and v in the x and y directions respectively. Q^1 is displaced from Q by the amounts

$$u + \frac{\partial u}{\partial x} dx_1 + \frac{\partial u}{\partial y} dy_1 \quad , \quad v + \frac{\partial v}{\partial x} dx_1 + \frac{\partial v}{\partial y} dy_1$$

Similarly, the displacements of T^1 from T are

$$u - \frac{\partial u}{\partial x} dx_2 + \frac{\partial u}{\partial y} dy_2 \quad , \quad v - \frac{\partial v}{\partial x} dx_2 + \frac{\partial v}{\partial y} dy_2$$

When working with strains, it is sufficient to consider relative displacements only, as described in figure (6.6).

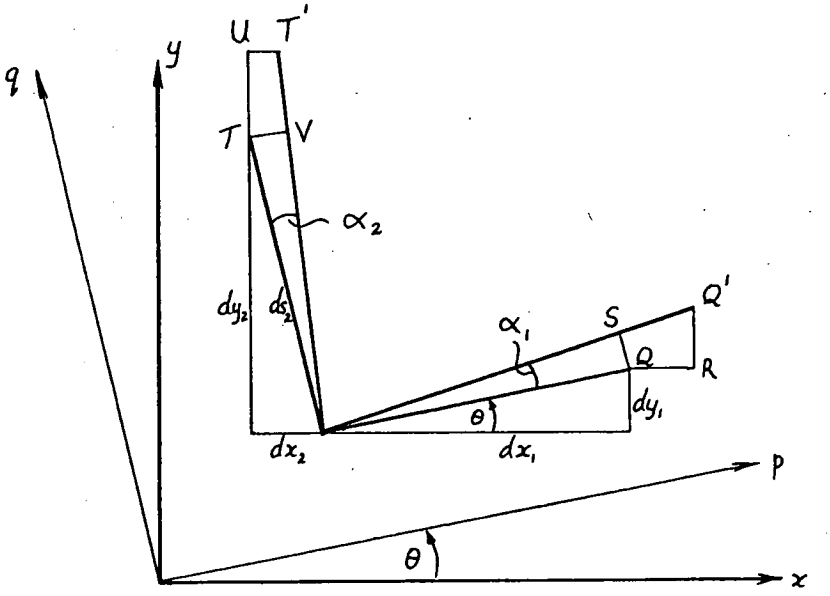

Figure 6.6

From figure (6.6), the components of relative displacement are

$$QR = \frac{\partial u}{\partial x} dx_1 + \frac{\partial u}{\partial y} dy_1 \; ; \quad UT^1 = - \frac{\partial u}{\partial x} dx_2 + \frac{\partial u}{\partial y} dy_2 \; ;$$

$$RQ^1 = \frac{\partial v}{\partial x} dx_1 + \frac{\partial v}{\partial y} dy_1 \; ; \quad TU = - \frac{\partial v}{\partial x} dx_2 + \frac{\partial v}{\partial y} dy_2$$

...(6.12)

Providing α_1 and α_2 are small, the direct strain in the p- direction is given by SQ^1/PQ and that in the q-direction is T^1V/TP. The components of relative displacement in the p and q directions at Q are

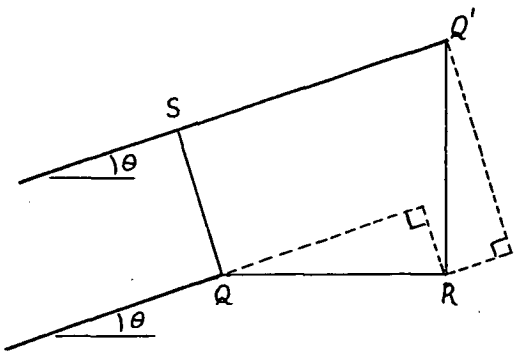

$$SQ = Q^1R \cos\theta - QR \sin\theta$$

and

$$SQ^1 = Q^1R \sin\theta + QR \cos\theta$$

...(6.13)

Similarly, the components at T are

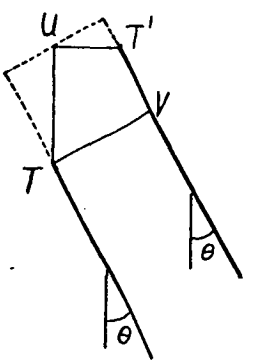

$$TV = TU \sin\theta + T^1U \cos\theta$$

and

$$T^1V = TU \cos\theta - T^1U \sin\theta$$

...(6.14)

The strains in the p and q directions are

$$\varepsilon_p = \frac{SQ^1}{ds_1} \; ; \quad \varepsilon_q = \frac{T^1V}{ds_2} \; ; \quad \gamma_{pq} = \frac{SQ}{ds_1} + \frac{TV}{ds_2}$$

From equations (6.12) and (6.13),

$$\varepsilon_p = \sin\theta \left[\frac{\partial v}{\partial x}\frac{dx_1}{ds_1} + \frac{\partial v}{\partial y}\frac{dy_1}{ds_1}\right] + \cos\theta \left[\frac{\partial u}{\partial x}\frac{dx_1}{ds_1} + \frac{\partial u}{\partial y}\frac{dy_1}{ds_1}\right]$$

$$= \sin\theta \left[\frac{\partial v}{\partial x}\cos\theta + \varepsilon_y \sin\theta\right] + \cos\theta \left[\varepsilon_x \cos\theta + \frac{\partial u}{\partial y}\sin\theta\right]$$

That is,

$$\varepsilon_p = \varepsilon_x \cos^2\theta + \varepsilon_y \sin^2\theta + \gamma_{xy} \sin\theta \cos\theta$$

Similarly,

$$\varepsilon_q = \varepsilon_x \sin^2\theta + \varepsilon_y \cos^2\theta - \gamma_{xy} \sin\theta \cos\theta,$$

and

$$\gamma_{pq} = -(\varepsilon_x - \varepsilon_y) \sin 2\theta + \gamma_{xy}(\cos^2\theta - \sin^2\theta) \quad \ldots(6.14)$$

Conversely, if the strains in the p-q reference frame are known, the strains in the x-y co-ordinate system are given by

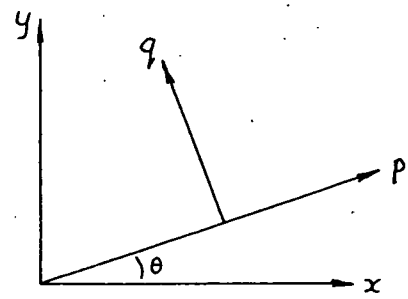

$$\varepsilon_x = \varepsilon_p \cos^2\theta + \varepsilon_q \sin^2\theta - \gamma_{pq} \sin\theta \cos\theta,$$

$$\varepsilon_y = \varepsilon_p \sin^2\theta + \varepsilon_q \cos^2\theta + \gamma_{pq} \sin\theta \cos\theta$$

and $$\gamma_{xy} = (\varepsilon_p - \varepsilon_q) \sin 2\theta + \gamma_{pq}(\cos^2\theta - \sin^2\theta).$$

$\ldots(6.15)$

6.2.6.2 Stress at a point.

If the stress components σ_x, σ_y and τ_{xy} are known at any point in a body in a condition of plane strain (or plane stress), then the stresses acting in any direction in the plane perpendicular to the z-direction (i.e., the x-y plane) can be calculated from the equations of statics.

Consider a very small element of material surrounding a point within a body at which σ_x, σ_y and τ_{xy} are known (figure 6.7,a). If the element is small enough, the forces acting on the side of the element may be calculated by assuming that the stresses are uniformly distributed over the sides (Timoshenko and Goodier, 1970). Body forces may be neglected as being small.

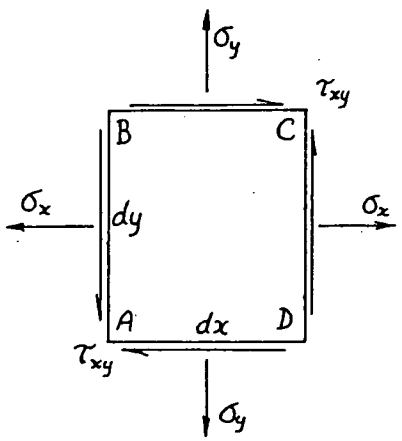

Figure 6.7,a

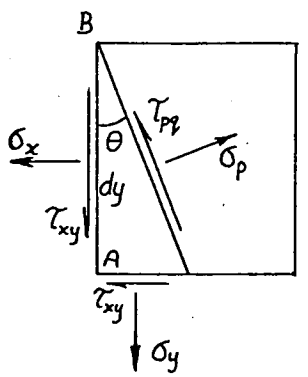

Figure 6.7,b

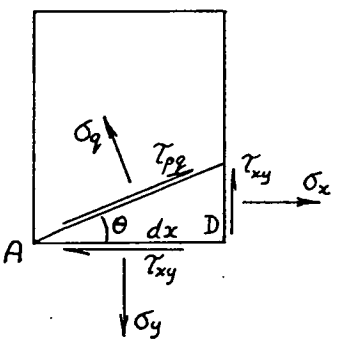

Figure 6.7,c

Assume the element to be of unit thickness. All stress components of figure (6.7,a) are known. We require the stress components σ_p, σ_q and τ_{pq} relative to the p-q reference frame which is rotated through an angle θ

with respect to the x-y co-ordinate system. Consider the state of equilibrium of the part of the element shown in figure (6.7,b). The equation of horizontal equilibrium is

$$\sigma_x dy + \tau_{xy}\, dy \tan\theta + \tau_{pq} \tan\theta\, dy = \sigma_p \frac{\cos\theta}{\cos\theta} dy$$

or $$\sigma_p = \sigma_x + \tau_{xy} \tan\theta + \tau_{pq} \tan\theta \qquad \ldots (6.16)$$

Similarly, the equation of vertical equilibrium gives

$$\tau_{pq} + \sigma_p \tan\theta = \tau_{xy} + \sigma_y \tan\theta. \qquad \ldots (6.17)$$

Horizontal and vertical equilibrium of the part of the element shown in figure (6.7,c) require that

$$\sigma_q \tan\theta + \tau_{xy} = \sigma_x \tan\theta + \tau_{pq} \qquad \ldots (6.18)$$

and $$\sigma_q + \tau_{pq} \tan\theta + \tau_{xy} \tan\theta = \sigma_y \qquad \ldots (6.19)$$

respectively.

Solving equations (6.16) to (6.19) for σ_p, σ_q and τ_{pq} yields:

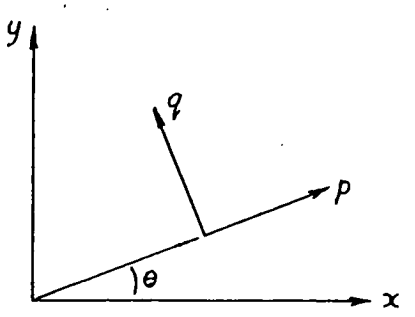

$$\sigma_p = \sigma_x \cos^2\theta + \sigma_y \sin^2\theta + \tau_{xy} \sin(2\theta),$$

$$\sigma_q = \sigma_x \sin^2\theta + \sigma_y \cos^2\theta - \tau_{xy} \sin(2\theta),$$

and $$\tau_{pq} = -\left[\frac{\sigma_x - \sigma_y}{2}\right] . \sin 2\theta + \tau_{xy} \cos(2\theta)$$

...(6.20)

6.3 Analysis of two-dimensional stress and strain conditions.

For a body in a condition of plane strain, it has been shown that the solution for stresses reduces to the determination of σ_x, σ_y and τ_{xy} only (section 6.2.5). There are a number of methods which may be used to solve for stress distributions, the more common ones being use of stress functions, solution for displacements and use of energy methods. The first two methods were used during this investigation.

In general, the solution to a plane strain problem must satisfy the equations of static equilibrium (equation 6.11) and geometric compatibility (equation 6.9) at every point within the body and the solution at the boundary must be compatible with the external forces.

6.3.1 Solving for stresses using "Airy" stress functions.

For simplicity, consider a material in which no body forces are present. The equations of equilibrium are therefore

$$\frac{\partial \sigma_x}{\partial x} + \frac{\partial \tau_{xy}}{\partial y} = 0$$

and

$$\frac{\partial \sigma_y}{\partial y} + \frac{\partial \tau_{xy}}{\partial x} = 0 \qquad \ldots (6.21)$$

Under the plane strain approximation, the load-deformation equations (6.5 and 6.6) become

$$\varepsilon_x = \frac{\sigma_x}{E_x}\left[1 - \mu_{zx}\cdot\mu_{xz}\right] - \frac{\sigma_y}{E_y}\left[\mu_{yx} + \mu_{zx}\cdot\mu_{yz}\right]$$

$$\varepsilon_y = -\frac{\sigma_x}{E_x}\left[\mu_{xy} + \mu_{zy}\cdot\mu_{xz}\right] + \frac{\sigma_y}{E_y}\left[1 - \mu_{zy}\cdot\mu_{yz}\right]$$

$$\gamma_{xy} = \frac{1}{G_{xy}}\,\tau_{xy}. \qquad \ldots (6.22)$$

In order to solve for the three stress components, a third equation in σ_x, σ_y and τ_{xy} is required. This is obtained directly from the compatibility equation

$$\frac{\partial^2 \varepsilon_x}{\partial y^2} + \frac{\partial^2 \varepsilon_y}{\partial x^2} = \frac{\partial^2 \gamma_{xy}}{\partial x \partial y} \qquad \ldots (6.9)$$

by substituting for the strain components from equations (6.22).

If the material is isotropic with

$$E_x = E_y = E, \quad \mu = \text{constant and} \quad G = \frac{E}{2(1+\mu)}$$

the substitution into equation (6.9) yields

$$\frac{\partial^2 \sigma_y}{\partial x^2} - \left[\frac{1}{1-\mu} \right] \left[\mu \frac{\partial^2 \sigma_y}{\partial y^2} + \mu \frac{\partial^2 \sigma_x}{\partial x^2} + 2 \frac{\partial^2 \tau_{xy}}{\partial x \partial y} \right] + \frac{\partial^2 \sigma_x}{\partial y^2} = 0 \qquad \ldots (6.23)$$

The three equations in σ_x, σ_y and τ_{xy} are therefore equations (6.21) and (6.23). In 1862, G.B. Airy proposed the use of a stress function, ϕ, defined by

$$\sigma_x = \frac{\partial^2 \phi}{\partial y^2} \quad , \quad \sigma_y = \frac{\partial^2 \phi}{\partial x^2} \quad \text{and} \quad \tau_{xy} = - \frac{\partial^2 \phi}{\partial x \partial y} \qquad \ldots (6.24)$$

A quick inspection shows that the function ϕ (as defined) satisfies equations (6.21). Substitution of the stresses in equation (6.23) gives, after re-arrangement,

$$\frac{\partial^4 \phi}{\partial x^4} + 2 \frac{\partial^4 \phi}{\partial x^2 \partial y^2} + \frac{\partial^4 \phi}{\partial y^4} = 0 \qquad \ldots (6.25)$$

Therefore, the solution for stresses in an isotropic body in a condition of plane strain reduces to the solution of equation (6.25) subject to the stresses on the boundary. Where differential thermal strains produce stresses in an isotropic body, the load-deformation relations for plane strain take the form

$$\varepsilon_x = \frac{\sigma_x}{E} (1 - \mu^2) - \frac{\sigma_y}{E} \cdot \mu (1 + \mu) + (1 + \mu) \alpha T$$

$$\varepsilon_y = - \frac{\sigma_x}{E} \mu (1 + \mu) + \frac{\sigma_y}{E} (1 - \mu^2) + (1 + \mu) \alpha T$$

$$\gamma_{xy} = \frac{1}{G_{xy}} \tau_{xy}$$

where α = co-efficient of thermal expansion

and T = temperature change.

Following the same steps as previously, equation (6.25) becomes

$$\frac{\partial^4\phi}{\partial x^4} + 2\frac{\partial^4\phi}{\partial x^2\partial y^2} + \frac{\partial^4\phi}{\partial y^4} = -\left[\frac{\alpha E}{1-\mu}\right]\left[\frac{\partial^2 T}{\partial x^2} + \frac{\partial^2 T}{\partial y^2}\right] \quad \ldots (6.26)$$

If the heated body is not acted upon by external forces, the boundary conditions are as shown in figure (6.8).

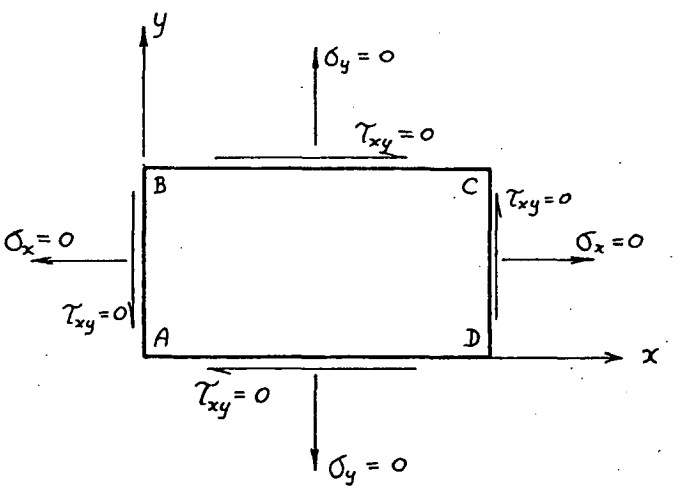

Figure 6.8

Along the y axis between A and B , $\sigma_x = 0$ and $\tau_{xy} = 0$, or, from equations (6.24),

$$\frac{\partial^2\phi}{\partial y^2} = 0 \quad \ldots (a)$$

and

$$\frac{\partial^2\phi}{\partial x\partial y} = 0 \quad \ldots (b)$$

Integrating along the boundary we find that equation (a) gives

$\frac{\partial \phi}{\partial y} = A$, $\phi = Ay + B$ and equation (b) gives $\frac{\partial \phi}{\partial x} = C$.

Since the stress components are represented by the second derivatives of ϕ, the linear functions containing the constants A, B and C will not affect the stress distribution and can therefore be chosen arbitrarily. If $A = B = C = 0$, then ϕ is zero along all unloaded sections of the boundary. Equation (6.26) need then be used only to calculate ϕ at points inside the boundary.

7.3.2 Solving for displacements.

Another method of solution of problems of elasticity is to eliminate the stress components from the equations of equilibrium (equations 6.7) using the generalised Hooke's Law equations (equations 6.5 and 6.6) and to express the strain components in terms of displacements using equations (6.1). For simplicity, consider an isotropic body in a condition of plane strain.

Under these circumstances,

$$E_x = E_y = E \text{ , } \mu = \text{constant, } G = \frac{E}{2(1+\mu)}$$

and equations (6.22) may be re-arranged to give the stress components in terms of strains, as in equations (6.27).

$$\sigma_x = E\left[\frac{1-\mu}{(1+\mu)(1-2\mu)}\cdot\varepsilon_x + \frac{\mu}{(1+\mu)(1-2\mu)}\cdot\varepsilon_y\right]$$

$$\sigma_y = E\left[\frac{\mu}{(1+\mu)(1-2\mu)}\,\varepsilon_x + \frac{1-\mu}{(1+\mu)(1-2\mu)}\cdot\varepsilon_y\right]$$

$$\tau_{xy} = G\,\gamma_{xy} \qquad \ldots (6.27)$$

Substitution of equations (6.27) and (6.1) into the equations of equilibrium, (6.21), yields, after re-arrangement,

$$\frac{\partial^2 u}{\partial x^2} + \frac{1-2\mu}{2(1-\mu)}\,\frac{\partial^2 u}{\partial y^2} + \frac{1}{2(1-\mu)}\,\frac{\partial^2 v}{\partial x\partial y} = 0$$

and $$\frac{\partial^2 v}{\partial y^2} + \frac{1-2\mu}{2(1-\mu)}\,\frac{\partial^2 v}{\partial x^2} + \frac{1}{2(1-\mu)}\,\frac{\partial^2 u}{\partial x\partial y} = 0 \qquad \ldots (6.28)$$

Equations (6.28) are the equations of equilibrium expressed in terms of the displacements u and v only.*

---

* Differentiating the first of equations (7.28) by x and the second by y and adding gives

$$\frac{\partial^2}{\partial x^2}(\varepsilon_x + \varepsilon_y) + \frac{\partial^2}{\partial y^2}(\varepsilon_x + \varepsilon_y) = 0 \qquad \ldots (a)$$

That is, the volume expansion of a body in a condition of plane strain satisfies the differential equation (a). Timoshenko and Goodier (1970,p.241) show that

$$\frac{\partial^2 e}{\partial x^2} + \frac{\partial^2 e}{\partial y^2} + \frac{\partial^2 e}{\partial z^2} = 0 \quad \text{where} \quad e = \varepsilon_x + \varepsilon_y + \varepsilon_z$$

holds in isotropic materials in states of three-dimensional strain.

These equations, along with the boundary conditions (expressed in terms of displacements) completely define the functions u and v. The components of strain are obtained from equations (6.1) and the components of stress from equations (6.27).

In the case where stresses arise from differential thermal strains only, equations (6.28) become

$$\frac{\partial^2 u}{\partial x^2} + \frac{(1-2\mu)}{2(1-\mu)}\frac{\partial^2 u}{\partial y^2} + \frac{1}{2(1-\mu)}\frac{\partial^2 v}{\partial x \partial y} = \frac{\alpha(1+\mu)}{(1-\mu)}\frac{\partial T}{\partial x}$$

and $$\frac{\partial^2 v}{\partial y^2} + \frac{(1-2\mu)}{2(1-\mu)}\frac{\partial^2 v}{\partial x^2} + \frac{1}{2(1-\mu)}\frac{\partial^2 u}{\partial x \partial y} = \frac{\alpha(1+\mu)}{(1-\mu)}\frac{\partial T}{\partial x}. \quad \ldots (6.29)$$

The boundary conditions are the same as those described in figure (6.8). However, in this case,

$\sigma_x = 0$ implies that $\left(\frac{1-\mu}{1+\mu}\right)\frac{\partial u}{\partial x} + \left(\frac{\mu}{1+\mu}\right)\frac{\partial v}{\partial y} = \alpha T \ldots (a)$

$\sigma_y = 0$ implies that $\left(\frac{\mu}{1+\mu}\right)\frac{\partial u}{\partial x} + \left(\frac{1-\mu}{1+\mu}\right)\frac{\partial v}{\partial y} = \alpha T, \ldots (b)$

and $\tau_{xy} = 0$ implies that $\frac{\partial v}{\partial x} + \frac{\partial u}{\partial y} = 0 \quad \ldots (c)$

Therefore, at the relevant points on the boundaries, equations (a), (b) and (c) must be satisfied as well as equations (6.29). Furthermore, throughout this chapter, it has been assumed that (sections 6.2.1 and 6.2.6.1) the body under consideration is subject to enough restraint to ensure that it cannot be displaced as a rigid

body. Hence, it is necessary to apply certain restrictions on the displacements at various points in order to prevent translation and rotation of the body as a whole. This may be affected by introducing body forces which are proportional to the displacement of relevant points, that is

$$\text{Body force} = K \times (\text{displacement})$$

where K may be thought of as similar to a stiffness.

The movement of the body may be controlled as shown in figure (6.9).

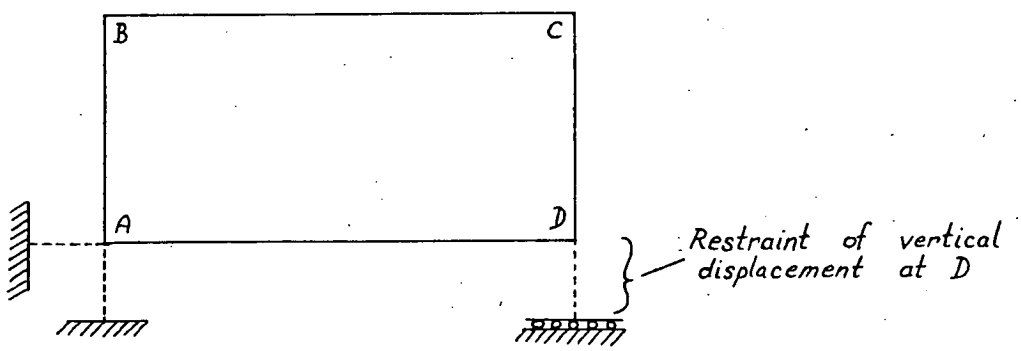

Figure 6.9

At point A, we replace the first of equations (6.29) by

$$\frac{\partial^2 u}{\partial x^2} + \frac{1-2\mu}{2(1-\mu)}\frac{\partial^2 u}{\partial y^2} + \frac{1}{2(1-\mu)}\frac{\partial^2 v}{\partial x \partial y} + Ku = \frac{\alpha(1+\mu)}{(1-\mu)}\frac{\partial T}{\partial x}$$

and at points A and D , we replace the second of equations (6.29) by

$$\frac{\partial^2 v}{\partial y^2} + \frac{1-2\mu}{2(1-\mu)}\frac{\partial^2 v}{\partial x^2} + \frac{1}{2(1-\mu)}\frac{\partial^2 u}{\partial x \partial y} + Kv = \frac{\alpha(1+\mu)}{(1-\mu)}\frac{\partial T}{\partial x} \quad .$$

"K" will have units of $\left(1/\text{unit length}\right)$ and may be made suitably large.*

The unknowns at every point in the material (including the boundary points) are u and v and therefore, if numerical solution methods are used, twice the number of equations as there are grid points must be handled. The boundary conditions are difficult to introduce and singularities difficult to avoid. For this reason, and the fact that the boundary conditions can be handled more easily, the stress function method is more often employed during elastic analysis.

6.4 Shrinkage and Thermal Stresses in Orthotropic Materials.

6.4.1 Introduction - The anisotropy of timber.

Timber is an anisotropic material; that is, its elastic properties vary with direction. The principal material property directions coincide with the longitudinal, radial and tangential directions with respect to a log. To meet the best length and longitudinal strength specifications possible, boards are sawn from logs so that their length lies in the longitudinal direction. Cross-sections cut

* $\left[\begin{array}{l} \text{If } K = 0 \text{ we have no restraint} \\ \text{If } K = \infty \text{ redundancies are introduced} \end{array}\right]$

perpendicular to the length of a board therefore fall in the *R-T* (radial-tangential) plane. Drying takes place mainly through the faces of boards (drying from the ends is insignificant in a long board - Chapter 3). If the drying is uniform, the shrinkage conditions at all cross-sections are the same. Thus, it is appropriate to analyse the drying stress conditions under the plane-strain simplification. The variation of elastic parameters over the cross-section is therefore of primary importance.

When analysing the conditions of stress and strain in a rectangular prismatic body, it is usual to orient the body in an orthogonal reference frame in such a way that the edges of the body run parallel to the axes of the frame. In this way, the boundary conditions are simplified. However, in anisotropic materials, the face planes of a body may not be cut parallel to the planes of elastic symmetry (for example, figures 6.10 and 6.11). To cope with this eventuality, the equations of elasticity must include terms relating the directions of the principal material property axes to the x, y, z reference frame.

A typical sawn timber board is shown in cross-section in figure (6.10)

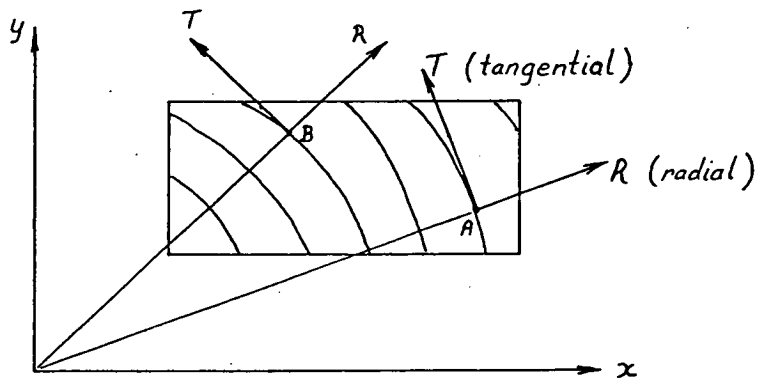

Figure 6.10

The orientation of the R-T axes with respect to the x-y axes varies markedly from point A to point B. The conditions of anisotropy in a board may be simplified if the radius from the center of the tree at which it is cut is large in comparison to its cross-sectional dimensions. Under these conditions, the "seasonal" rings are essentially linear over the cross-section. To a first approximation, then, there are three orthogonal planes of elastic symmetry; that is, the material can be considered as orthotropic.

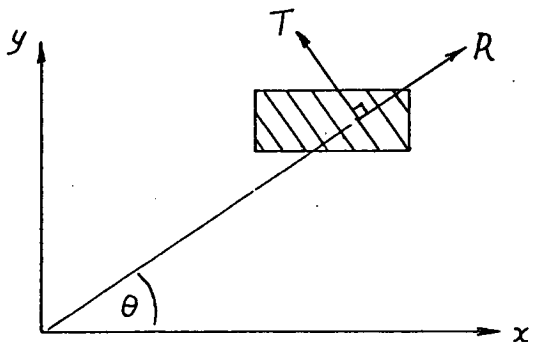

Figure 6.11

This simplification is illustrated in figure (6.11). Here, the R and T axes have a constant orientation with respect to the x-y co-ordinate system. The R-axis is rotated by the angle θ relative to the x-axis.

In the case of perfectly quarter-sawn or back-sawn timber (see figure 3.6), $\theta = 0^0$ or 90^0 and the R-T co-ordinate system coincides with the x-y system, providing further simplifications.

6.4.2 The Theory of Elasticity in Orthotropic Materials.

The derivation of the equations describing the state of stress and strain in orthotropic materials is based on the stress function approach outlined in section 6.3.1. The method of solving for displacements is equally applicable but is not as efficient in terms of computation time. Particular reference is made to the properties of wood throughout this section, but the resulting equations may be applied to any orthotropic material in a condition of plane strain.

The primary effect to be studied during this analysis is the development of stress due to differential shrinkage in wood during drying. In chapter 4 (section 4.2), it was stated that the tangential shrinkage in "Tasmanian Oak" is approximately twice that in the radial direction. Consider two small blocks of wood, as shown in figure (6.12)

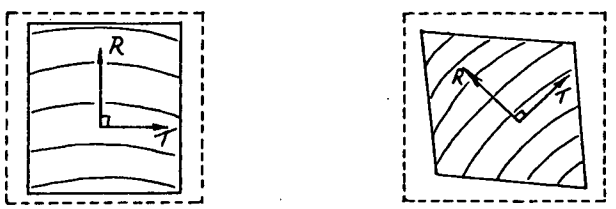

The seasonal rings may be considered as linear over the cross-sections of small blocks.

Figure 6.12

Block (a) is cut with its faces parallel to the principal axes of shrinkage and block (b) is cut obliquely. Block (a) remains rectangular during shrinkage but block (b) does not. Therefore, in the case where the face planes of

an element of orthotropic material are not parallel to the axes of principal shrinkage, a shearing component of shrinkage strain must be included.

Thus, it is easiest to introduce shrinkage terms in a system of axes coincident with the principal directions of shrinkage. On the other hand, if the faces of an orthotropic body are rotated with respect to the co-ordinate system in which the stress function has been defined, the introduction of boundary conditions becomes tedious. Hence, it is easiest to analyse the stress and strain conditions in a body in terms of components either parallel or perpendicular to its faces.

Consider the cross-section of a typical piece of sawn timber (figure 6.13).

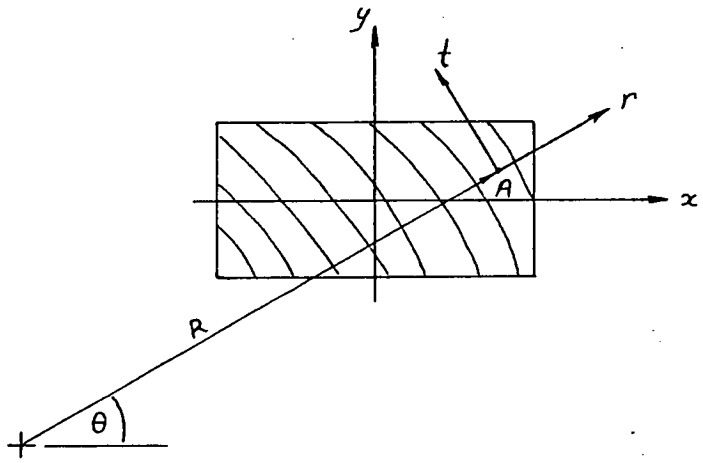

Figure 6.13

The r and t axes represent the principal material property directions at A. At A, the r-axis makes an angle, θ, with the x-axis.

As indicated, the boundary conditions are introduced in terms of σ_x, σ_y and τ_{xy} for simplicity. Therefore, it is convenient to define the stress function, ϕ, such that

$$\sigma_x = \frac{\partial^2 \phi}{\partial y^2} \quad , \quad \sigma_y = \frac{\partial^2 \phi}{\partial x^2} \quad \text{and} \quad \tau_{xy} = - \frac{\partial^2 \phi}{\partial x \partial y} \qquad \ldots (6.30)$$

In terms of stress and strain components in the x-y system, the three equations that must be satisfied at each point over the cross-section are

$$\frac{\partial \sigma_x}{\partial x} + \frac{\partial \tau_{xy}}{\partial y} = 0 \, , \qquad \ldots (6.31,a)$$

$$\frac{\partial \sigma_y}{\partial y} + \frac{\partial \tau_{xy}}{\partial x} = 0 \, , \qquad \ldots (6.31,b)$$

and

$$\frac{\partial^2 \varepsilon_x}{\partial y^2} + \frac{\partial^2 \varepsilon_y}{\partial x^2} = \frac{\partial^2 \gamma_{xy}}{\partial x \partial y} \qquad \ldots (6.31,c)$$

Equations (6.31,a and b) are satisfied by the stress function, ϕ (equations 6.30). By converting the strain components in equation (6.31,c) to stresses and introducing swelling and thermal effects, a differential equation in terms of ϕ is obtained. The solution to this equation defines the state of swelling or thermal stress in a body, subject to boundary conditions.

Thermal and swelling stresses are most easily introduced in terms of components in the principal material property directions. Thus, at A, the stress-strain relations for plane strain (equations 6.22) are:

$$\varepsilon_r = A_1\sigma_r - A_2\sigma_t + \alpha_r T + \beta_r c + \mu_{zr}(\alpha_z T + \beta_z c),$$

$$\varepsilon_t = -A_3\sigma_r + A_4\sigma_t + \alpha_t T + \beta_t c + \mu_{zt}(\alpha_z T + \beta_z c),$$

and $$\gamma_{rt} = \frac{1}{G_{rt}}\tau_{rt} \qquad \ldots (6.32)$$

where $\alpha_i T$ = the thermal strain in the "i" direction (α_i = co-efficient of thermal expansion in the "i" direction),

$\beta_i c$ = the swelling strain in the "i" direction,

β_i = the swelling co-efficients,

c = change of moisture (mass) concentration,

$$A_1 = \frac{1-\mu_{zr}\mu_{rz}}{E_r}, \qquad A_2 = \frac{\mu_{tr}+\mu_{zr}\mu_{tz}}{E_t},$$

$$A_3 = \frac{\mu_{rt}+\mu_{zt}\mu_{rz}}{E_r}, \qquad A_4 = \frac{1-\mu_{zt}\mu_{tz}}{E_t}.$$

Equations (6.20) give

$$\sigma_r = \sigma_x \cos^2\theta + \sigma_y \sin^2\theta + \tau_{xy} \sin 2\theta,$$

$$\sigma_t = \sigma_x \sin^2\theta + \sigma_y \cos^2\theta - \tau_{xy} \sin 2\theta,$$

and $$\tau_{rt} = -\left(\frac{\sigma_x-\sigma_y}{2}\right)\sin 2\theta + \tau_{xy}\cos 2\theta \qquad \ldots (6.33)$$

Substitution of equations (6.33) and (6.30) into equations (6.32) gives, after re-arrangement,

$$\varepsilon_r = \frac{\partial^2\phi}{\partial y^2}\left[A_1\cos^2\theta - A_2\sin^2\theta\right] + \frac{\partial^2\phi}{\partial x^2}\left[A_1\sin^2\theta - A_2\cos^2\theta\right]$$
$$- \frac{\partial^2\phi}{\partial x\partial y}\left[2A_1 + 2A_2\right]\sin\theta\cos\theta$$
$$+ \alpha_r T + \beta_r c + \mu_{zr}\left[\alpha_z T + \beta_z c\right] ,$$

$$\varepsilon_t = \frac{\partial^2\phi}{\partial y^2}\left[A_4\sin^2\theta - A_3\cos^2\theta\right] + \frac{\partial^2\phi}{\partial x^2}\left[A_4\cos^2\theta - A_3\sin^2\theta\right]$$
$$+ \frac{\partial^2\phi}{\partial x\partial y}\left[2A_4 + 2A_3\right]\sin\theta\cos\theta$$
$$+ \alpha_t T + \beta_t c + \mu_{zt}\left[\alpha_z T + \beta_z c\right] ,$$

and

$$\gamma_{rt} = -\frac{\partial^2\phi}{\partial y^2}\left[\frac{\sin\theta\cos\theta}{G_{rt}}\right] + \frac{\partial^2\phi}{\partial x^2}\left[\frac{\sin\theta\cos\theta}{G_{rt}}\right] + \frac{\partial^2\phi}{\partial x\partial y}\left[\frac{\sin^2\theta - \cos^2\theta}{G_{rt}}\right]$$

....(6.34)

Equations (6.34) represent the stress-strain relations in the principal material property directions at A (figure 6.13) in terms of the stress function, ϕ.

Converting the strain components ε_r, ε_t and γ_{rt} into components in the x and y directions (using equations 6.15), it is found that

$$\varepsilon_x = B_1 \frac{\partial^2\phi}{\partial y^2} + B_2 \frac{\partial^2\phi}{\partial x^2} + B_3 \frac{\partial^2\phi}{\partial x \partial y} + \left(\alpha_r T + \beta_r c\right)\cos^2\theta + \left(\alpha_t T + \beta_t c\right)\sin^2\theta$$

$$+ \mu_{zr}\left(\alpha_z T + \beta_z c\right)\cos^2\theta + \mu_{zt}\left(\alpha_z T + \beta_z c\right)\sin^2\theta ,$$

$$\varepsilon_y = B_4 \frac{\partial^2\phi}{\partial y^2} + B_5 \frac{\partial^2\phi}{\partial x^2} + B_6 \frac{\partial^2\phi}{\partial x \partial y} + \left(\alpha_r T + \beta_r c\right)\sin^2\theta + \left(\alpha_t T + \beta_t c\right)\cos^2\theta$$

$$+ \mu_{zr}\left(\alpha_z T + \beta_z c\right)\sin^2\theta + \mu_{zt}\left(\alpha_z T + \beta_z c\right)\cos^2\theta ,$$

and $$\gamma_{xy} = B_7 \frac{\partial^2\phi}{\partial y^2} + B_8 \frac{\partial^2\phi}{\partial x^2} + B_9 \frac{\partial^2\phi}{\partial x \partial y}$$

$$+ 2\sin\theta\cos\theta\left[T(\alpha_r - \alpha_t) + c(\beta_r - \beta_t) + \mu_{zr}(\alpha_z T + \beta_z c) - \mu_{zt}(\alpha_z T + \beta_z c)\right]$$

...(6.35)

The co-efficients $B_1 \ldots\ldots B_9$ of equations (6.35) are defined in the addendum to this chapter.

Swelling and thermal components of shear strain appear in the last of equations (6.35). Note that these components disappear when $\theta = 0^0$ or 90^0 in orthotropic materials and when α, β and μ are the same in all directions (isotropic materials).

Equations (6.35) are substituted directly into equation (6.31,c) to give the differential equation defining

the stress function, ϕ. Figure (6.13) indicates that in wood θ is a function of x and y; that is, θ varies over the cross-section of a piece of sawn timber. The derivatives of the strain components will therefore include terms such as $\partial\theta/\partial x$ and so on.

However, these terms may be neglected if the board being analysed is cut from a log at a sufficient distance from the center (Section 6.4.1, figure 6.11). Thus, for orthotropic materials, substitution of equations (6.35) into equation (6.31,c) gives

$$B_5\frac{\partial^4\phi}{\partial x^4} + (B_6-B_8)\frac{\partial^4\phi}{\partial x^3\,\partial y} + (B_2+B_4-B_9)\frac{\partial^4\phi}{\partial x^2\partial y^2} + (B_3-B_7)\frac{\partial^4\phi}{\partial x\partial y^3} + B_1\frac{\partial^4\phi}{\partial y^4}$$

$$= 2\sin\theta\cos\theta\frac{\partial^2}{\partial x\partial y}\left[(\alpha_r-\alpha_t)T+(\beta_r-\beta_t)c+\mu_{zr}(\alpha_z T+\beta_z c)-\mu_{zt}(\alpha_z T+\beta_z c)\right]$$

$$-\cos^2\theta\left[\frac{\partial^2}{\partial x^2}\left[\alpha_t T+\beta_t c+\mu_{zt}(\alpha_z T+\beta_z c)\right]+\frac{\partial^2}{\partial y^2}\left[\alpha_r T+\beta_r c+\mu_{zr}(\alpha_z T+\beta_z c)\right]\right]$$

$$-\sin^2\theta\left[\frac{\partial^2}{\partial x^2}\left[\alpha_r T+\beta_r c+\mu_{zr}(\alpha_z T+\beta_z c)\right]+\frac{\partial^2}{\partial y^2}\left[\alpha_t T+\beta_t c+\mu_{zt}(\alpha_z T+\beta_z c)\right]\right]$$

... (6.36)

where θ = angle between the x and r axes

and $B_1 \ldots\ldots B_9$ are defined in the addendum to chapter 6. Equation (6.36) replaces equation (6.26) in orthotropic material in a condition of plane strain.

6.4.3 Particular Cases in the Theory of Orthotropic Elasticity

(Applications of equations 6.36)

6.4.3.1 Quarter-sawn Timber.

The principal material property directions in wood are radial (r) and tangential (t). In quarter-sawn timber, the angle between the x and r axes (see figure 6.13) is zero. That is:

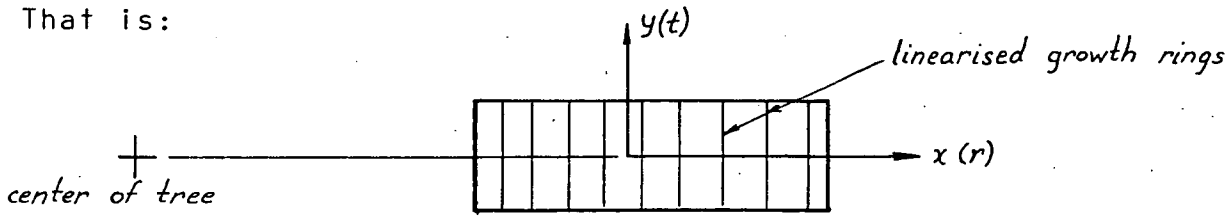

When $\theta = 0$, $\sin\theta = 0$ and $\cos\theta = 1$. Therefore, the co-efficients of equation (6.36) are

$$B_1 = A_1 \;, \quad B_2 = -A_2 \;, \quad B_3 = 0 \;,$$

$$B_4 = -A_3 \;, \quad B_5 = A_4 \;, \quad B_6 = 0 \;.$$

$$B_7 = 0 \;, \quad B_8 = 0 \quad \text{and} \quad B_9 = -\frac{1}{G_{rt}}$$

Where $A_1 \ldots\ldots A_4$ are defined in equations (6.32).

Thus, the fourth-order differential equation defining the stresses function, ϕ, (equation 6.36) reduces to

$$A_4\frac{\partial^4\phi}{\partial x^4} + \left(\frac{1}{G_{rt}} - A_2 - A_3\right)\frac{\partial^4\phi}{\partial x^2\partial y^2} + A_1\frac{\partial^4\phi}{\partial y^4}$$

$$= -\frac{\partial^2}{\partial x^2}\left[\alpha_t T + \beta_t c + \mu_{zt}(\alpha_z T + \beta_z c)\right] - \frac{\partial^2}{\partial y^2}\left[\alpha_r T + \beta_r c + \mu_{zr}(\alpha_z T + \beta_z c)\right] . \quad \ldots (6.37)$$

6.4.3.2 Back-sawn Timber.

In back-sawn timber, the angle between the x and r axes (figure 6.13) is 90^{o}. That is,

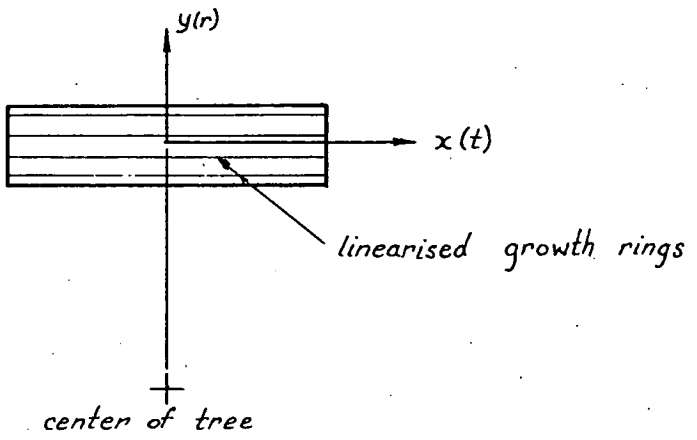

When $\theta = 90^{0}$, $\sin\theta = 1, \cos\theta = 0$ and the co-efficients of equation (6.36) become

$$B_1 = A_4 \;, \quad B_2 = -A_3 \;, \quad B_3 = 0 \;,$$

$$B_4 = -A_2 \;, \quad B_5 = A_1 \;, \quad B_6 = 0 \;,$$

$$B_7 = 0 \;, \quad B_8 = 0 \quad \text{and} \quad B_9 = -\frac{1}{G_{rt}}$$

where $A_1 \ldots\ldots A_4$ are defined in equations (6.32)!

Thus, equation (6.36) reduces to

$$A_1\frac{\partial^4\phi}{\partial x^4} + \left[\frac{1}{G_{rt}} - A_2 - A_3\right]\frac{\partial^4\phi}{\partial x^2\partial y^2} + A_4\frac{\partial^4\phi}{\partial y^4}$$

$$= -\frac{\partial^2}{\partial x^2}\left[\alpha_r T + \beta_r c + \mu_{zr}(\alpha_z T + \beta_z c)\right] - \frac{\partial^2}{\partial y^2}\left[\alpha_t T + \beta_t c + \mu_{zt}(\alpha_z T + \beta_z c)\right]$$

... (6.38)

6.4.3.3 Isotropic Materials.

In isotropic materials, α, β, μ, E and G are constants with $G = \frac{E}{2(1+\mu)}$. Therefore, from the definition of co-efficients $A_1 \ldots\ldots A_4$ (equations 6.32),

$$A_1 = A_4 = \frac{1-\mu^2}{E} \quad \text{and} \quad A_2 = A_3 = \frac{\mu(1+\mu)}{E} \quad .$$

Because the material properties are the same in all directions, the angle θ (figure 6.13) may be chosen arbitrarily. Taking $\theta = 0^0$ (as in section 6.4.3.1), equation (6.36) becomes

$$\frac{1-\mu^2}{E}\frac{\partial^4\phi}{\partial x^4} + \left(\frac{1}{G} - \frac{2\mu(1+\mu)}{E}\right)\frac{\partial^4\phi}{\partial x^2 \partial y^2} + \frac{1-\mu^2}{E}\frac{\partial^4\phi}{\partial y^4} = -(1+\mu)\nabla^2(\alpha T + \beta c)$$

where $\nabla^2 = \frac{\partial^2}{\partial x^2} + \frac{\partial^2}{\partial y^2}$.

Further manipulation of the above equation gives

$$\frac{\partial^4\phi}{\partial x^4} + 2\frac{\partial^4\phi}{\partial x^2 \partial y^2} + \frac{\partial^4\phi}{\partial y^4} = -\frac{E}{(1-\mu)}\nabla^2(\alpha T + \beta c). \qquad \ldots (6.39)$$

Omitting the swelling strain term (βc) from equation (6.39), we find that equation (6.39) is identical to the relationship derived by Timoshenko and Goodier (1970, p.469) for thermal stress in isotropic materials in a condition of plane strain. (See also equation 6.26).

6.5 Methods of Solving for Drying Stresses in Timber.

6.5.1.

The state of stress in isotropic materials has been studied extensively by many authors [Timoshenko and Goodier(1970), Southwell (1941), Love (1944)]. The most common form of solution to problems of elasticity in two dimensions are those based on Airy stress functions. The authors mentioned give the solutions to many simple problems and show that in most cases, the stress function can be expressed in the form of a polynomial or another basic function.

Thermal stresses developed in isotropic bodies during unsteady state heat conduction are analysed in terms of displacements by Timoshenko and Goodier. In order to obtain a particular solution to the differential equations (6.29), they introduce a potential thermo-elastic displacement function, Ψ, and show that for various types of bar in conditions of plane-strain, Ψ may be described analytically by a logarithmic function which includes time as a variable. The boundary conditions are satisfied by superimposing other loading conditions on the body.

Lekhnitskii (1963) makes use of the theory of analytic functions of several complex variables when solving for stress functions in anisotropic bodies

subjected to various externally-applied loadings. In the preface to his book, "Theory of Elasticity of an Anisotropic Elastic Body",* Lekhnitskii says:

> "The theory of elasticity of an isotropic body has been thoroughly investigated. This is not the case, however, for the theory of elasticity of anisotropic bodies; .....many problems of anisotropic bodies still have not been systematically examined."

Analytical solutions to the thermal (or swelling) stress problem in anisotropic bodies are not given by Lekhnitskii.

The elastic and diffusion parameters of timber are non-linear functions of moisture concentration. Therefore, even if analytical solutions to thermal stress problems in anisotropic bodies were readily available, they would have only limited application in the study of drying stresses in wood. However, numerical solutions can easily be adapted to handle variations in governing parameters and therefore offer a method of solution. The systems used in this investigation were the finite difference method and the method of collocation. Solutions by the

---

* This book summarises the state of the development of the theory of elasticity in anisotropic bodies up to 1950.

method of collocation give the stress function, ϕ, in terms of a continuous function in x and y over the cross-section of a body. On the other hand, solutions by the finite difference technique give the values of the stress function at a number of discrete points over a cross-section. This method was found to be the easiest and most reliable way of determining the state of stress in timber during drying.

6.5.2 The method of collocation applied to problems of elasticity in two dimensions.

The two-dimensional Airy stress function, ϕ, may be defined as the product of two functions, continuous over the cross-section of a body. That is,

$$\phi = f(x,y),\ g(x,y) \qquad \ldots (6.40)$$

where $f(x,y)$ is a function of x and y containing the boundary conditions and $g(x,y)$ is a continuous function of x and y containing n variable co-efficients. The equation (6.40) is fitted to the requirements of a particular problem in the following way.

The appropriate derivatives of equation (6.40) may be substituted directly into the differential equation describing the state of stress over the cross-section of a body (for example, equation 6.36). The differential equation is thus converted to an equation in x and y including

n unknown co-efficients. This equation is then evaluated at n arbitrarily-chosen points over the cross-section, giving n equations in n unknowns. The resulting group of equations may be solved directly to give the required values of the co-efficients of the function, g, subject to the conditions of the particular problem. The stresses at any point (x,y) in the cross-section of the body are then given by the second derivatives of the function, ϕ, evaluated at (x,y).

The uniqueness theorem associated with the theory of elasticity (Timoshenko and Goodier, 1970; Southwell, 1941) states that there can be only one exact solution to the state of stress or strain in a body under a particular set of loading conditions. As stated previously, the equation resulting from the substitution of the relevant derivatives of ϕ (defined by equation 6.40) into the governing fourth-order differential equation may be evaluated at arbitrarily-chosen points within the material. Therefore, a sufficient number, n, of well-chosen points ("characteristic points") must be used to ensure that any particular solution is truely representative of the state of stress in the body. Uniqueness may be checked by comparing two solutions to a particular problem based on different sets of "characteristic points".

Consider the state of stress in a piece of back-sawn timber during drying. Assuming for the moment

that the thermal and longitudinal shrinkage strains are small compared to the transverse shrinkage terms, the governing equation (equation 6.38) becomes

$$A_1 \frac{\partial^4 \phi}{\partial x^4} + \left(\frac{1}{G_{rt}} - A_2 - A_3 \right) \frac{\partial^4 \phi}{\partial x^2 \partial y^2} + A_4 \frac{\partial^4 \phi}{\partial y^4} = - \frac{\partial^2}{\partial x^2} (\beta_r c) - \frac{\partial^2}{\partial y^2} (\beta_t c) \quad \ldots (6.41)$$

As there are no externally-applied loads, the state of stress in the wood depends completely upon the terms on the right-hand side of equation (6.41); that is, upon the curvature of the shrinkage-strain distribution. From the discussion in chapter 4, section 4.3, the zones of highest curvature of shrinkage strain are very close to the surfaces of a board, particularly at the start of drying. The "characteristic points" should be concentrated in these areas.

When analysing the particular case of stress in a body of rectangular cross-section, subject to no externally-applied loads, it is convenient to introduce the boundary conditions (section 6.3.1) by putting

$$f(x,y) = (x^2-a^2)^2 (y^2- b^2)^2$$

Equation (7.40) therefore becomes

$$\phi = (x^2-a^2)^2 (y^2-b^2)^2 . g$$

where $g = g(x,y)$.

Note that $\phi = 0$ when $x = \pm a$

and when $y = \pm b$.

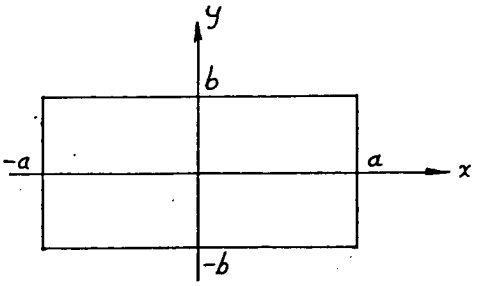

All stresses on the boundaries are zero.

Assuming the function g to be differentiable over the range

$$-a \leqslant x \leqslant +a \qquad \text{and} \qquad -b \leqslant y \leqslant +b$$

and denoting the derivates of g by

$$\frac{\partial g}{\partial x} = g_x, \qquad \frac{\partial g}{\partial y} = g_y, \qquad \frac{\partial^2 g}{\partial x^2} = g_{xx} \qquad \text{etc.,}$$

it is found that

$$\sigma_x = \frac{\partial^2 \phi}{\partial y^2} = (x^2-a^2)^2 \left[4g\,(3y^2-b^2) + 8yg_y(y^2-b^2) + (y^2-b^2)^2 g_{yy} \right]$$

$$= 0 \qquad \text{when} \qquad x = \pm a \ ,$$

$$\sigma_y = \frac{\partial^2 \phi}{\partial x^2} = (y^2-b^2)^2 \left[4g(3x^2-a^2) + 8xg_x(x^2-a^2) + (x^2-a^2)^2 g_{xx} \right]$$

$$= 0 \qquad \text{when} \qquad y = \pm b \ ,$$

and $$\tau_{xy} = -\frac{\partial^2 \phi}{\partial x \partial y} = -\left[\begin{array}{l} 16xy(x^2-a^2)(y^2-b^2)g + 4y(x^2-a^2)^2(y^2-b^2)g_x \\ +4x(x^2-a^2)(y^2-b^2)^2 g_y + (x^2-a^2)^2(y^2-b^2)^2 g_{xy} \end{array} \right]$$

$$= 0 \qquad \text{when} \qquad x = \pm a \qquad \text{and when} \qquad y = \pm b.$$

Hence, the boundary conditions are satisfied.

Consider the case where the function g is chosen to be the polynomial

$$g(x,y) = a_0 + a_1x + a_2y + a_3x^2 + a_4xy + \ldots\ldots\ldots$$

where the co-efficients a_0, a_1, a_2,..... are initially unknown. The number of characteristic points available for the fitting procedure is increased by simply truncating the polynomial after a larger number of terms. Unfortunately, this also has the effect of increasing the likelyhood of producing overshooting or oscillation in the solution due to the inclusion of x and y terms raised to higher powers. This problem is illustrated diagramatically in figure (6.14). "Oscillating" solutions are easily identified by checking the uniqueness requirement.

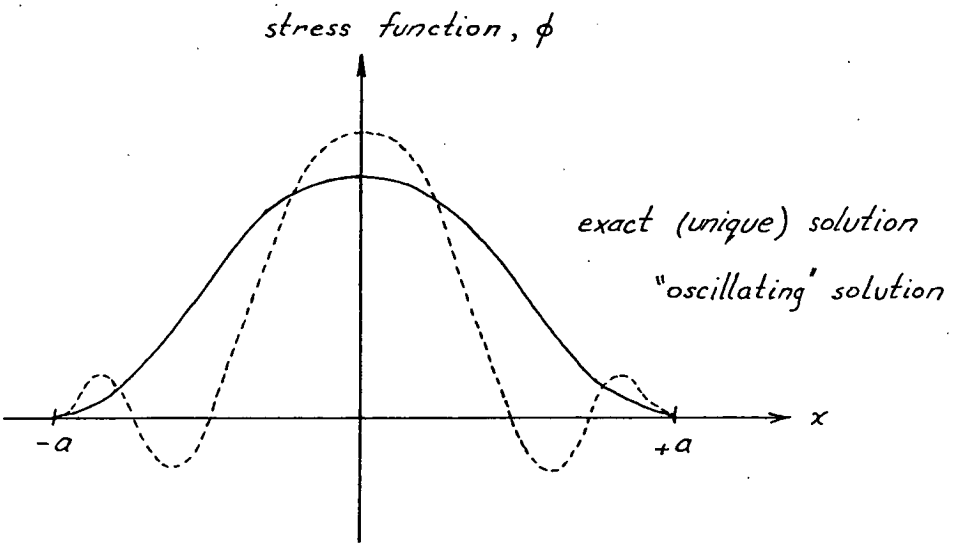

Figure 6.14

The author found that unique solutions to drying stress problems in timber were difficult to obtain by the method of collocation using polynomials. Other

functions such as Fourier series present problems of a similar nature.

6.5.3 Finite difference methods applied to problems of elasticity in two dimensions.

The analysis of the conditions of stress in a body using finite difference methods is based on the approximation of derivatives appearing in the governing equations by appropriate finite difference formulations. This is done by dividing the cross-section of a body into a discrete number of points, usually uniformly spaced for convenience. The derivatives of a function at any one point can then be expressed in terms of the value of the function at that and neighbouring points. In chapter 3, section 3.5.2 it was shown that the second derivatives of a function, ϕ at the point "0" of figure (6.15) could be approximated by:

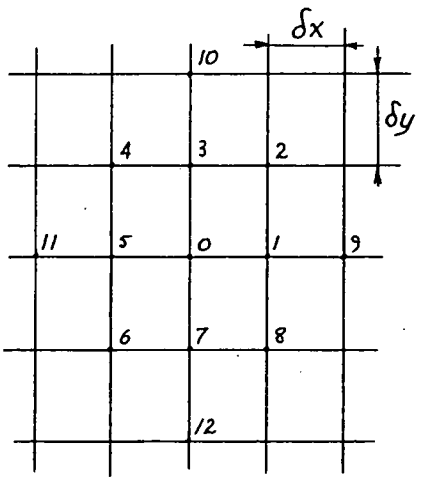

$$\frac{\partial^2 \phi}{\partial x^2} \simeq \frac{\phi_1 + \phi_5 - 2\phi_0}{\delta x^2}$$

$$\text{and } \frac{\partial^2 \phi}{\partial y^2} \simeq \frac{\phi_3 + \phi_7 - 2\phi_0}{\delta y^2} .$$

$$\text{Further, } \frac{\partial^2 \phi}{\partial x \partial y} \simeq \frac{\phi_2 + \phi_6 - \phi_4 - \phi_8}{4\delta x \delta y} \quad \ldots (6.42)$$

Figure 6.15

The derivatives of the stress function, ϕ, that appear in the governing equations for the cases of fully back-sawn or quarter-sawn timber are [refer to sections 6.4.3.1 and 6.4.3.2, equations (6.37) and (6.38)]:

$$\frac{\partial^4\phi}{\partial x^4} \quad , \quad \frac{\partial^4\phi}{\partial x^2 \partial y^2} \quad \text{and} \quad \frac{\partial^4\phi}{\partial y^4} \quad .$$

These may be approximated in the following manner:

$$\frac{\partial^4\phi}{\partial x^4} = \frac{\partial^2}{\partial x^2}\left(\frac{\partial^2\phi}{\partial x^2}\right) \simeq \frac{\left.\frac{\partial^2\phi}{\partial x^2}\right|_1 + \left.\frac{\partial^2\phi}{\partial x^2}\right|_5 - 2\left.\frac{\partial^2\phi}{\partial x^2}\right|_0}{\delta x^2} = \frac{\phi_{11} - 4\phi_5 + 6\phi_0 - 4\phi_1 + \phi_9}{\delta x^4}$$

Similarly, $$\frac{\partial^4\phi}{\partial y^4} = \frac{\phi_{10} - 4\phi_3 + 6\phi_0 - 4\phi_7 + \phi_{12}}{\delta x^4}$$

and $$\frac{\partial^4\phi}{\partial x^2 \partial y^2} = \frac{1}{\delta x^2 \delta y^2}\{\phi_2 + \phi_4 + \phi_6 + \phi_8 - 2(\phi_1 + \phi_3 + \phi_5 + \phi_7) + 4\phi_0\} \quad \ldots (6.43)$$

[The subscripts appearing in equations (6.43) refer to the numbered points of figure (6.15).]

Hence, the differential terms appearing on the left-hand side of equations (6.37), (6.38) and (6.39) can be expressed in terms of the value of the function ϕ at point "0" of figure (6.15) and the twelve points surrounding it. The right-hand sides of the equations

include second-order derivatives which may be approximated by equations (6.42).

When no external loads are present on a boundary, the stress function there may be given an arbitrary value (refer to section 6.3.1). It is convenient to put $\phi = 0$ on all boundaries. Thus, it is necessary to calculate the value of the stress function only at points inside the boundary.

Consider the application of the fourth-order finite difference equations at points on a grid over a rectangular cross-section.

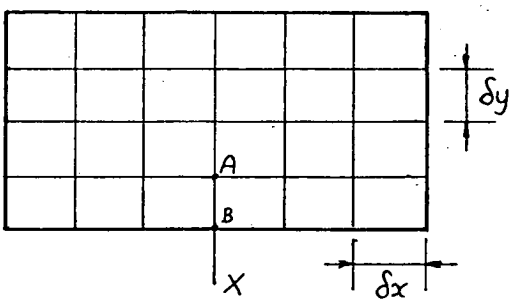

The stress function, ϕ, is zero at all grid points on the boundaries and is unknown at all grid points inside the boundaries.

Figure 6.16

When the finite difference equations (6.43) are applied at point A of figure (6.16), it is found that one point used by the difference scheme falls outside the boundary (point "X" of figure 6.16). The function ϕ is a potential function and can exist outside the cross-section although its derivatives outside the boundaries are

meaningless. The conditions that must be satisfied at point B on the boundary are

$$\sigma_y = 0 \quad \text{and} \quad \tau_{xy} = 0 \quad .$$

Zero shear stress on the boundary implies that

$$\frac{\partial^2 \phi}{\partial x \partial y} = 0$$

Integration along the boundary gives $\frac{\partial \phi}{\partial y} = \text{constant}.$

This constant may be chosen arbitrarily (as in section 6.3.1) and it is convenient to put it equal to zero.

Approximation of the derivative by a central difference gives

$$\left.\frac{\partial \phi}{\partial x}\right|_B \simeq \frac{\phi_A - \phi_X}{2\delta y} = 0$$

and therefore $\phi_X = \phi_A$.

A more detailed derivation of this result appears in Timoshenko and Goodier (1970). A generalised statement of the result is that the stress function, ϕ, is symmetrical about a plane of zero shear stress.

Thus, the problem of determining stresses at the nodal points of a 25-point finite difference grid may

be formulated in the following way:

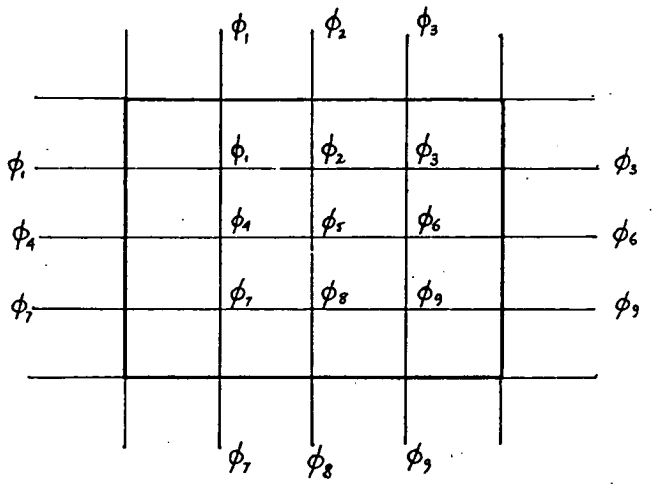

$\phi = 0$ on all boundaries. The unknown values of the stress function are $\phi_1 \ldots\ldots \phi_9$ The values of ϕ at the "imaginary" points outside the cross-section are the same as those opposite them across the boundary.

The governing equation must be satisfied at points *1.....9*. At each of these points, it can be expressed in terms of the unknowns $\phi_1 \ldots\ldots\ldots \phi_9$ by using equations (6.43) and (6.42). Note that different elastic parameters may be used at each of points *1.....9*; thus, the dependence of Youngs modulus of wood upon moisture concentration may be accommodated. The overall problem is therefore reduced to the solution of 9 equations in 9 unknowns. Once $\phi_1 \ldots\ldots\ldots \phi_9$ have been determined, the stresses in the material may be calculated using the equations

$$\sigma_x = \frac{\partial^2 \phi}{\partial y^2} \quad , \quad \sigma_y = \frac{\partial^2 \phi}{\partial x^2} \quad \text{and} \quad \tau_{xy} = -\frac{\partial^2 \phi}{\partial x \partial y}$$

and the finite difference approximations, equations (6.42).

6.6 Solving for Stresses in Non-linearly Elastic Material.

In the introduction to this chapter, it was assumed that the materials to be analysed were linearly elastic and homogeneous. However, timber is not linearly elastic and the relationship between stress and strain is dependent also on moisture concentration, c. Figure (6.17) demonstrates the form of this relationship, the measurement of which is discussed in chapter 7.

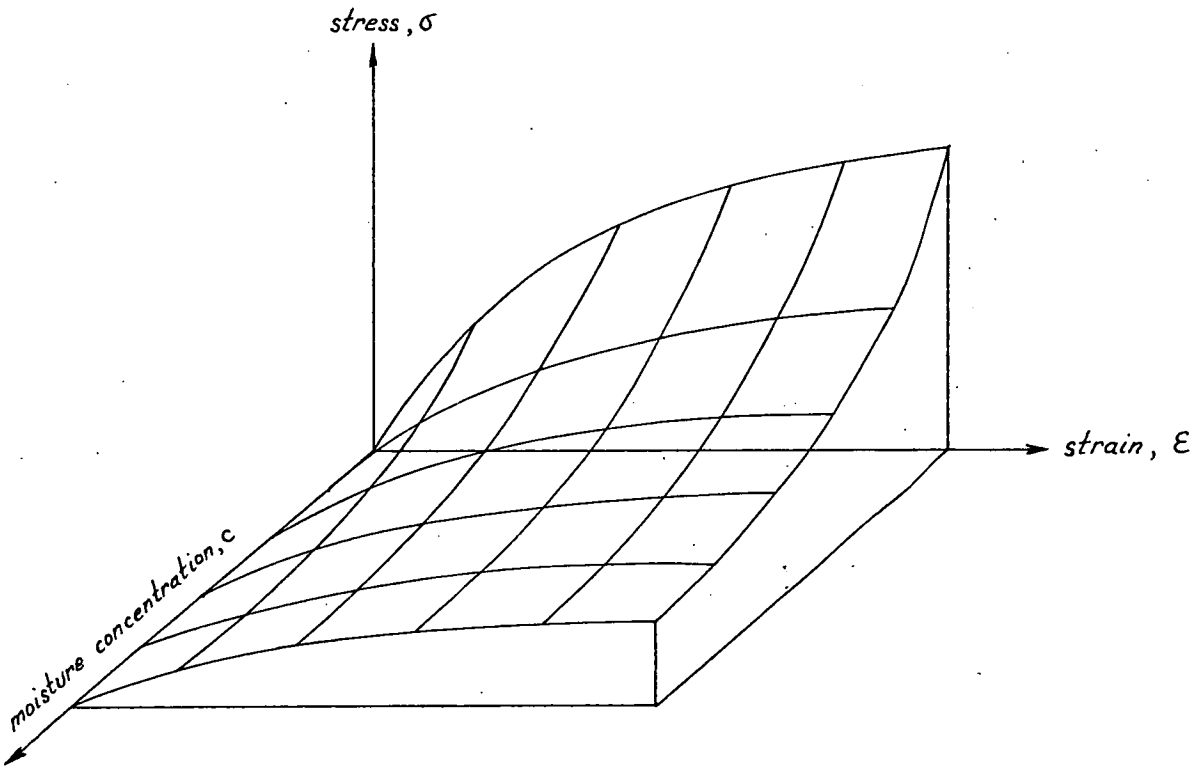

Figure 6.17

The equation to the surface takes the form

$$\sigma = A\left(1 - \frac{1}{B\varepsilon+1}\right) . \qquad \ldots (6.44)$$

A and B depend upon moisture concentration, c, such that

$$A = A_0 e^{-ac} + b$$

and $$B = B_0 e^{-dc} + f$$

where a, b, A_0, B_0, d and f are directionally dependent constants.

The slope of the surface in the stress-strain plane is

$$\frac{\partial\sigma}{\partial\varepsilon} = \frac{AB}{(B\varepsilon+1)^2} \qquad \ldots (6.45)$$

In wood, equation (7.44) replaces the simple relationship $\sigma = E\varepsilon$ for linearly elastic materials.

During drying, the moisture concentration and, therefore, the shrinkage strain at a point vary. Thus, the state of stress over the cross-section of a board changes with time. Stress waves within solids travel at the speed of sound. Therefore, drying stresses at a particular time are dependent only upon the states of differential shrinkage strain at that time and initial stress within the material and not the rate of change of stress (if the effects of creep are neglected). It is

therefore possible to approximate the drying of timber by a model which is piece-wise linear in time. The following discussion outlines a numerical method of determining the state of stress at a point in a body with elastic properties similar to those described in figure (6.17) while using the equations of orthotropic elasticity (equation 6.36) derived for linearly elastic materials.

Assume that at a point in a wooden body, the values of stress (σ), strain (ε), moisture concentration (c) and shrinkage strains (S) at time = t are known. Furthermore, assume that the values of stress and strain at the same point at the earlier time, $t-\delta t$, are known. That is, at time = t, the knowns are

$$\sigma_t,\ \varepsilon_t,\ c_t,\ S_t \quad \text{and} \quad \varepsilon_{t-\delta t}$$

where the subscripts indicate the time at which the variable has been determined.

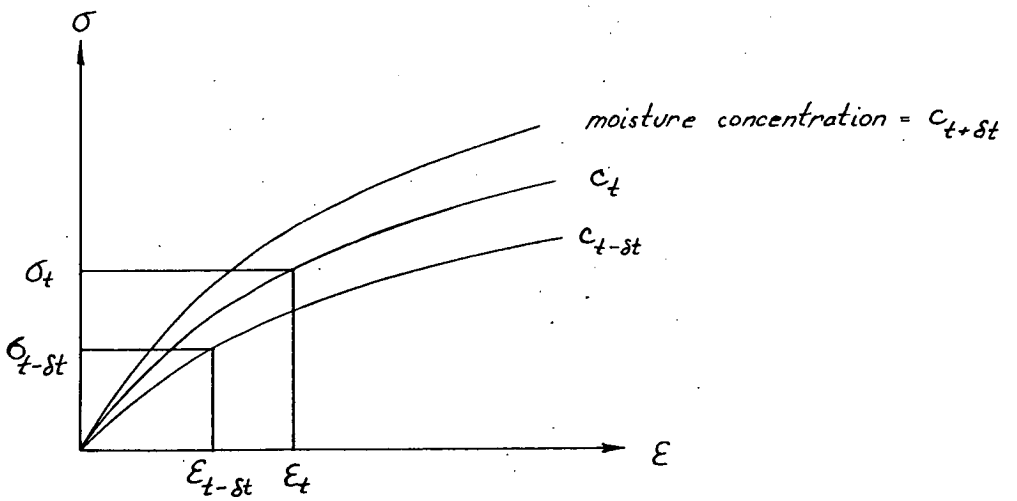

Figure 6.18

After the passage of time δt, the moisture concentration at the point is $c_{t+\delta t}$ (mass transfer theory, chapter 3) and the shrinkage strain $S_{t+\delta t}$ may be obtained directly from known material properties. The new stress condition in the wood must be described by a point on the graph of stress against strain (figure 6.18) corresponding to the moisture concentration $c_{t+\delta t}$. A predictor-corrector type method may be used to determine the change in stress, $\Delta\sigma$, due to the change in shrinkage strain, $S_{t+\delta t} - S_t$. The change in stress may be added to the known total stress at the previous time (σ_t), to give the new total stress $\sigma_{t+\delta t}$. The new elastic strain $\varepsilon_{t+\delta t}$ is then determined directly from the σ-ε relationship at moisture concentration = $c_{t+\delta t}$.

The change in stress, $\Delta\sigma$, is calculated from the equations of elasticity using the approximate mean slope of the stress-strain relationship (that is, the equivalent to Young's Modulus) over the associated change in total strain. An approximate mean slope can be obtained from the known rate of change of strain over the previous time interval.

By putting $\varepsilon^*_{t+\delta t} = \varepsilon_t + \frac{1}{2}(\varepsilon_t - \varepsilon_{t-\delta t})$,

the predicted value of the mean slope,

$$E^* = \frac{\partial\sigma}{\partial\varepsilon}\left(c_{t+\delta t}, \varepsilon^*_{t+\delta t}\right)$$

is obtained from equation (6.45).

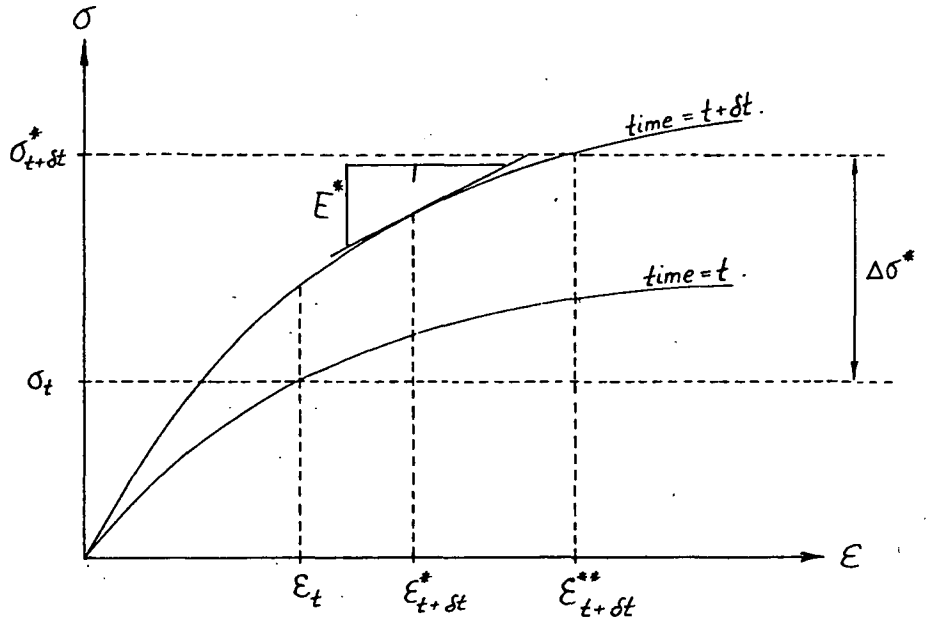

Figure 6.19

The predicted stress change $\Delta\sigma^*$ based on E^* and the change in shrinkage strain $(S_{t+\delta t} - S_t)$ is calculated using the theory of elasticity (hence the piece-wise linear model).

That is,

$$\Delta\sigma^* = fcn\left[E^*, (S_{t+\delta t} - S_t)\right] .$$

Thus, the predicted new total stress,

$$\sigma^*_{t+\delta t} = \sigma_t + \Delta\sigma^* ,$$

and the associated total strain is $\varepsilon^{**}_{t+\delta t}$ (see figure 6.19).

$(\varepsilon^{**}_{t+\delta t},\ \sigma^*_{t+\delta t})$ is the first approximation to the conditions in the wood at time = $t + \delta t$ and is based on the predicted

mean slope, E^*, over the interval ε_t to $\varepsilon^{**}_{t+\delta t}$. The corrected value of the mean slope,

$$E^{**} = \frac{\partial \sigma}{\partial \varepsilon}\left[c_{t+\delta t}, \tfrac{1}{2}(\varepsilon_t + \varepsilon^{**}_{t+\delta t})\right] ,$$

$$\Delta\sigma^{**} = \delta c n\left[E^{**}, (S_{t+\delta t} - S_t)\right]$$

and the corrected new total stress at time $(t + \delta t)$,

$$\sigma_{t+\delta t} = \sigma_t + \Delta\sigma^{**} .$$

The associated new total strain at the point, $\varepsilon_{t+\delta t}$, follows directly from the stress-strain relationship for $c_{t+\delta t}$.

In this manner, it is possible to calculate the drying stresses in a piece of timber as a function of time. Note that this method may be extended to include hysteresis effects associated with the stress-strain relationship and other non-ideal characteristics of timber.

Addendum - Chapter 6

The coefficients $B_1 \ldots\ldots\ldots B_9$ of equations (6.35) are

$$B_1 = (A_1\cos^2\theta - A_2\sin^2\theta)\cos^2\theta + (A_4\sin^2\theta - A_3\cos^2\theta)\sin^2\theta + \left(\frac{\sin^2\theta\cos^2\theta}{G_{rt}}\right)$$

$$B_2 = (A_1\sin^2\theta - A_2\cos^2\theta)\cos^2\theta + (A_4\cos^2\theta - A_3\sin^2\theta)\sin^2\theta - \left(\frac{\sin^2\theta\cos^2\theta}{G_{rt}}\right)$$

$$B_3 = -(A_1+A_2)2\sin\theta\cos^3\theta + (A_3+A_4)2\sin^3\theta\cos\theta - \left(\frac{\sin\theta\cos\theta(\sin^2\theta-\cos^2\theta)}{G_{rt}}\right)$$

$$B_4 = (A_1\cos^2\theta - A_2\sin^2\theta)\sin^2\theta + (A_4\sin^2\theta - A_3\cos^2\theta)\cos^2\theta - \left(\frac{\sin^2\theta\cos^2\theta}{G_{rt}}\right)$$

$$B_5 = (A_1\sin^2\theta - A_2\cos^2\theta)\sin^2\theta + (A_4\cos^2\theta - A_3\sin^2\theta)\cos^2\theta + \left(\frac{\sin^2\theta\cos^2\theta}{G_{rt}}\right)$$

$$B_6 = -(A_1+A_2)2\sin^3\theta\cos\theta + (A_3+A_4)2\sin\theta\cos^3\theta + \left(\frac{\sin\theta\cos\theta(\sin^2\theta-\cos^2\theta)}{G_{rt}}\right)$$

$$B_7 = (A_1\cos^2\theta - A_2\sin^2\theta + A_3\cos^2\theta - A_4\sin^2\theta)2\sin\theta\cos\theta - \left(\frac{\cos^2\theta-\sin^2\theta}{G_{rt}}\right)\sin\theta\cos\theta$$

$$B_8 = (A_1\sin^2\theta - A_2\cos^2\theta + A_3\sin^2\theta - A_4\cos^2\theta)2\sin\theta\cos\theta + \left(\frac{\cos^2\theta-\sin^2\theta}{G_{rt}}\right)\sin\theta\cos\theta$$

$$B_9 = -(A_1+A_2+A_3+A_4)4\sin^2\theta\cos^2\theta + \left(\frac{2\sin^2\theta\cos^2\theta - \sin^4\theta - \cos^4\theta}{G_{rt}}\right)$$

REFERENCES.

LEKHNITSKII, S.G. (1963): Theory of Elasticity of an Anisotropic Elastic Body.
Holden-Day, San Francisco, California, U.S.A.

LOVE, A.E.H. (1944): A Treatise on the Mathematical Theory of Elasticity.
Dover, England.

SOUTHWELL, R.V. (1941): Theory of Elasticity.
Oxford University Press, England.

TIMOSHENKO, S.P. and GOODIER, J.N. (1970): Theory of Elasticity.
McGraw Hill Kogakusha Ltd., Japan.

CHAPTER 7

CHAPTER 7

THE ELASTIC PROPERTIES AND SHRINKAGE BEHAVIOUR OF "TASMANIAN OAK"

7.1 Introduction

Wood is an anisotropic material; that is, its properties vary with direction. Twelve parameters are required to describe its elastic behaviour in terms of a linear model; three moduli of elasticity (E), three moduli of rigidity (G), and six Poisson's ratios (μ). A further six parameters, three thermal expansion and three rheological swelling co-efficients, are needed to describe the effects of temperature or moisture content changes on the material.

Various simplifications to the linear model are justified when studying the development of drying stresses in long boards. If drying is uniform, the plane-

strain condition prevails and one modulus of elasticity and two moduli of rigidity are no longer required. When drying takes place at low (atmospheric) temperatures, thermal strains are approximately 1/20 of shrinkage strains and may therefore be ignored. Furthermore, the shrinkage of most timbers in the longitudinal direction is about 1/20 of that in the transverse plane and can also be neglected. Therefore, the calculation of drying stresses using a simplified linear model requires definition of two elastic moduli, one modulus of rigidity, six Poisson's ratios and two swelling co-efficients.

However, timber is not linearly elastic and the properties required for the simplified drying stress model all depend upon moisture content and temperature. Numerical methods of analysis enable the calculation of drying stresses in timber using a piece-wise linear model based on actual wood properties (section 6.6). It is therefore necessary to fully define the governing parameters over the range of conditions occuring in the timber as it dries.

Wood behaves in a similar way to many high polymers. When loaded, it exhibits both immediate and delayed deformation (creep) and, upon removal of the load, partial strain recovery occurs. Further-more, studies have shown that load coupled with a change in moisture content may produce deformations far in excess of any produced by time-dependent creep under conditions of constant moisture content.

In his summary of research on wood rheology, Grossman (1969) concludes that:

> "..... the rheological behaviour of wood in practice is almost always accompanied and sometimes swamped by the interaction of load with moisture content change."

The assumption that responses are additive (Boltzmann's superposition principle) has been shown to be justified for wood over a wide range of loading conditions (Grossman, 1969). Thus, deformations may be expressed as the product of two factors; one being an elastic modulus whose variation and dependence upon external factors (such as moisture content, temperature, density, ...) is known from tests and the other describing the time-dependence (not strongly affected by moisture content, density or species, nor variable within species).

For the sake of simplicity, the effects of creep and visco-elastic deformation were not included in the model describing drying stresses although it was recognised that these factors have a major bearing on the behaviour of timber while seasoning. Few data are available concerning the magnitude of delayed and visco-elastic deformations in wood across the grain. Further work is necessary in this field.

An approximate description of the elastic properties of "Tasmanian Oak" and their dependence upon moisture content was built up from published data and a

small number of tests. The relationship between shrinkage in the principle transverse directions and moisture content was measured and found to agree well with published data. The variability of the elastic and shrinkage properties was not of major importance to this study. The primary aim was to establish the pattern of behaviour of "Tasmanian Oak" and to demonstrate the effect on stress levels of drying through a semi-permeable coating.

7.2 The Elastic Properties of "Tasmanian Oak".

7.2.1 Introduction

The strength and stiffness of wood are functions of both moisture content and temperature (U.S. F.P.L., 1974). Examination of published data leads to the conclusion that the variation of stiffness within a wooden board due to moisture content changes is much larger than that due to thermal effects when drying takes place under constant conditions. Hence, it is reasonable to ignore thermal effects when studying the development of drying stresses in "Tasmanian Oak".

Grossman (1969) summarises the difficulty of measuring the elastic behaviour of wood in the following way:

"To find all the mechanical responses of wood from a

> comprehensive testing programme would be an unmanagable task. Even for simpler materials, the number of tests would be prohibitive ..... For wood, the programme would become many times larger again. Various grain directions must be explored; the effects of moisture content must be taken into account and numerous replications are necessary because wood as a natural product is highly variable and requires the use of statistical methods for sampling and calculation."

Extensive research of literature failed to uncover a complete record of the elastic properties of "Tasmanian Oak". Data published for a number of North American timbers was examined. Tests showed that the elastic behaviour of "Tasmanian Oak" followed a similar pattern to those of the more dense North American hardwoods. The properties of these timbers were averaged for use in the drying stress model.

Preliminary work on the determination of the unpublished elastic parameters of "Tasmanian Oak" was conducted as part of this investigation. Techniques for measuring the relationships between direct stress and strain and for measuring moduli of rigidity were developed and tests conducted to determine:

1) The adequacy and performance of the equipment constructed.

2) External factors affecting tests (variation in atmospheric humidity, timber density, ...)

3) Variability of results and approximate trends.

The mathematical function producing the "closest" and most consistent fit to measured stress-strain curves was deduced by trial and error.

7.2.2 Published Data.

According to the U.S. F.P.L. * (1974), the longitudinal modulus of elasticity of wood with an average moisture content of 12% reduces by about 0.33% of its value at 20°C for every 1°C rise in temperature. During the drying of timber under conditions of constant temperature and humidity, the average wood temperature varys from the wet-bulb temperature of the atmosphere (early in drying) to the dry-bulb temperature (when the wood reaches equilibrium with the atmosphere). Typically, the change in average temperature would be 6°C giving a 2% reduction in stiffness. The temperature gradients within "Tasmanian Oak" during drying are small (of the order of 0.2°C, Chapter 5) and therefore differential effects are insignificant.

---

* U.S. F.P.L. - United States Forest Products Laboratory, Madison, Wisconsin.

On the other hand, the elastic modulus of wood in the longitudinal direction increases by about 2% for every 1% decrease in moisture content at moisture contents between 5% and 20%. The longitudinal modulus of elasticity at a moisture content of 12% is 16% greater than the value at moisture contents above the fibre saturation point (green). During drying in air, board surfaces reach a moisture content of approximately 12% while the bulk of the inner fibres have moisture contents greater than the fibre saturation point. Therefore, the variation of stiffness within sawn timbers due to moisture content changes is much larger than that due to thermal effects when drying takes place under constant, mild conditions (25°C, 50% *r.h.*).

Little information is available concerning the effects of thermal and moisture content changes on the elastic properties of wood in the transverse plane but it is reasonable to assume that they follow a similar pattern to those in the longitudinal direction (U.S. F.P.L. "Wood Handbook", 1974).

In Australia, over 80 species of timber are milled in large quantities. Because of limited budgets, research into elastic properties has been limited to those parameters required for structural design. Therefore, little information has been published regarding Poisson's ratios and the moduli of elasticity and rigidity in the transverse plane.

The U.S. F.P.L. "Wood Handbook" (1974) gives

a complete list of the elastic properties of 7 North American timbers at moisture contents of about 12%. The properties of the three most dense hardwoods covered, expressed as ratios with the elastic modulus in the longitudinal direction, are quoted in table 7.1.

SPECIES	Approx. specific gravity.	$\frac{E_t}{E_z}$	$\frac{E_r}{E_z}$	$\frac{G_{rz}}{E_z}$	$\frac{G_{tz}}{E_z}$	$\frac{G_{rt}}{E_z}$	μ_{zr}	μ_{rz}	μ_{tr}	μ_{rt}	μ_{zt}	μ_{tz}
Birch (yellow)	·64	·050	·078	·074	·068	·017	·426	·033	·447	·697	·457	·023
Sweet-gum	·53	·050	·115	·089	·061	·021	·325	·037	·297	·682	·403	·020
Walnut (black)	·59	·056	·106	·085	·062	·021	·495	·052	·379	·718	·632	·035
AVERAGES.		·052	·100	·083	·064	·020		·041		·700		·026

(Subscripts r, t and z refer to the radial, tangential and longitudinal directions respectively.)

TABLE 7.1

The elastic properties of 3 North American hardwoods.

The Poisson's ratios and elastic moduli are related by the expression

$$\frac{\mu_{ij}}{\mu_{ji}} = \frac{E_i}{E_j} \qquad (\text{where } i, j = r, t, z.)$$

derived from strain energy considerations (U.S. F.P.L. 1974: CSIRO, 1975). The elastic moduli, E_i, E_j,... and the ratios $\frac{E_i}{E_j}$ vary with moisture content. The moduli of rigidity also vary with moisture content but the Poisson's ratios change only slightly between the oven-dry and green conditions.

The elastic modulus in the longitudinal direction, E_z, varies according to the relationship shown in figure (7.1).

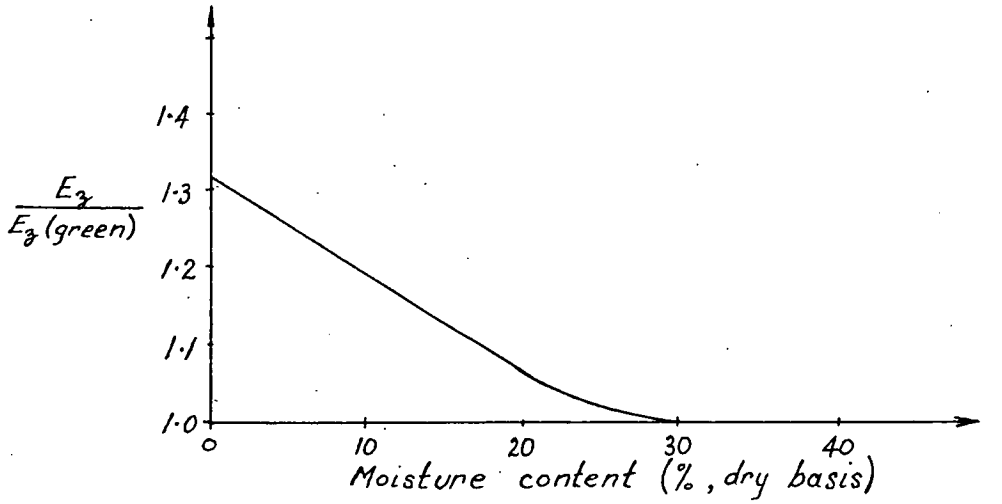

Figure 7.1

The variation of E_z with moisture content.

Tests on 23 trees of E. regnans reported by C.S.I.R.O. (1975) showed that

$$E_z \text{ (M = 12\%)} \simeq 20{,}000 \text{ MPa (mean)}$$

and $$E_z \text{ (green)} \simeq 17{,}400 \text{ MPa (mean)}.$$

These results are for compression tests on samples measuring 60 x 20 x 20 mm with an average density of 675 kg/m^3 at a moisture content of 12%.

7.2.3 Materials and Methods.

A small number of tests were conducted to

determine the approximate pattern of elastic behaviour of "Tasmanian Oak". The relationships between stress and strain were measured using small, clear samples having densities of about 700 kg/m^3 at a moisture content of 14%. A straining rate of approximately $250_{10}{}^{-6}$ per minute was used in most tests. The ultimate strength of samples tested in tension was recorded and used as an indication of the stress-strain condition at which checks might develop during drying. Tests were also conducted to determine G_{rz} and G_{tz} (the shear moduli in the radial-longitudinal and tangential-longitudinal planes).

7.2.3.1 Measurement of Strain

Tensile and compressive strains of up to $20_{10}{}^{-3}$ were measured on samples with moisture contents of 14% and 120%. Most adhesives will not bond to wood fibre with a moisture content greater than the fibre saturation point, thus reducing the range of suitable strain measuring techniques.

The strain gauges shown in figure 7.2(a) were used to measure strains in timber at all moisture contents. The gauges were used in pairs, as indicated by figure 7.2(b).

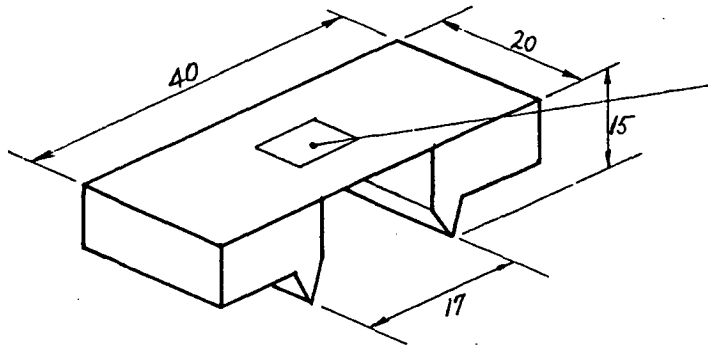

ERS gauges (electrical resistance strain gauges) top and bottom of 0.60 mm thick spring steel plate.

ERS gauges : MICRO-MEASUREMENTS
EA - 06 - 125 BT - 120

Figure 7.2(a)

De-mountable strain gauge for use on timber.

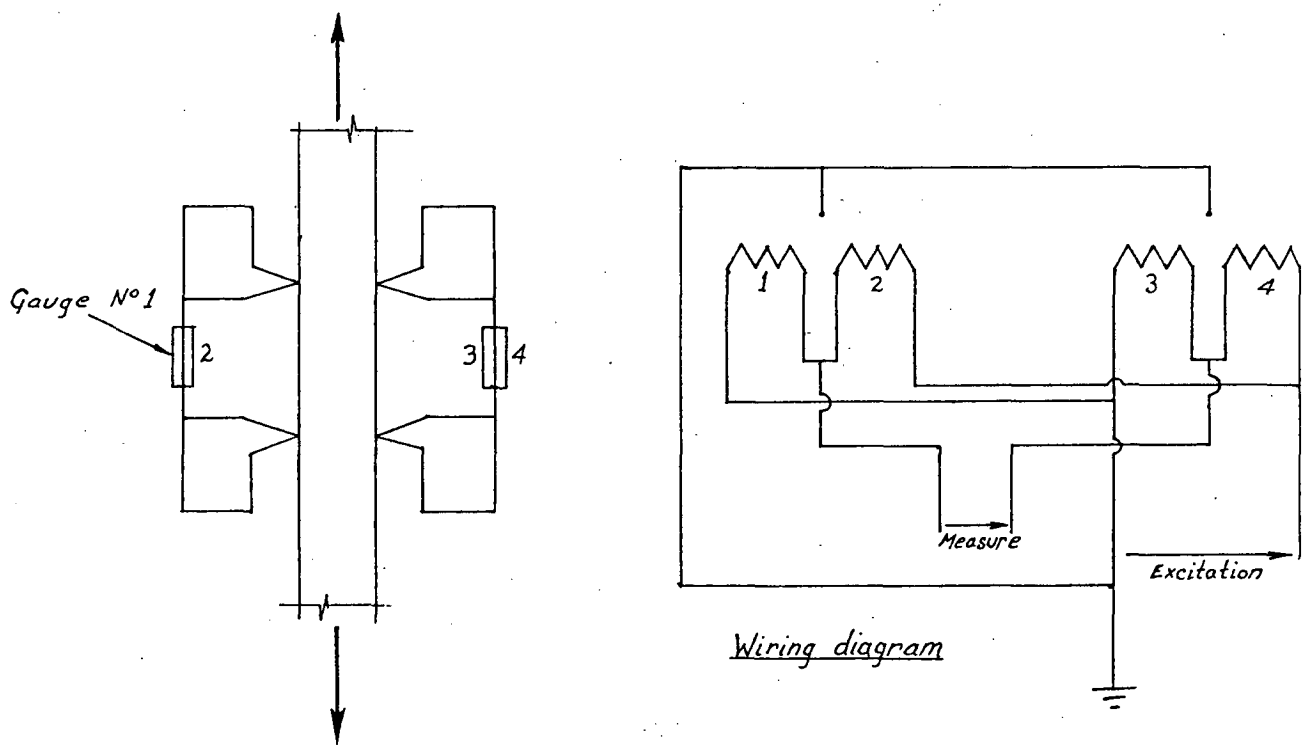

Figure 7.2(b)

The use of de-mountable strain gauges in pairs.

A force of approximately 7*N* acting between the knife edges was required at a strain of $20_{10}-^{3}$. Therefore, it was essential that the knife-edges were embedded in the surface fibres of the wood samples to avoid slip or creep due to crushing of the fibre in the zones of contact. Excessively deep embedment caused notching of the samples and subsequent failure at the knife-edges.

The gauges were wired in a Wheatstone bridge configuration and connected to a Bruel-Kjäer strain indicator. The sensitivity of the measurement system was $\pm 38_{10}-^{6}$ strain. The cable connecting the gauges to the strain indicator was shielded to minimise the effects of electro-magnetic interference.

7.2.3.2 Measurement of (direct) stress-strain relationships.

Tension tests in the radial and tangential directions were conducted in the apparatus shown in figure (7.3,a). The jaws holding the test specimens (figure 7.3,b) were designed to minimise bending and twisting effects and to make the alignment of the samples with the test bed as easy as possible. The samples were deformed via a manually-operated screw-thread system.

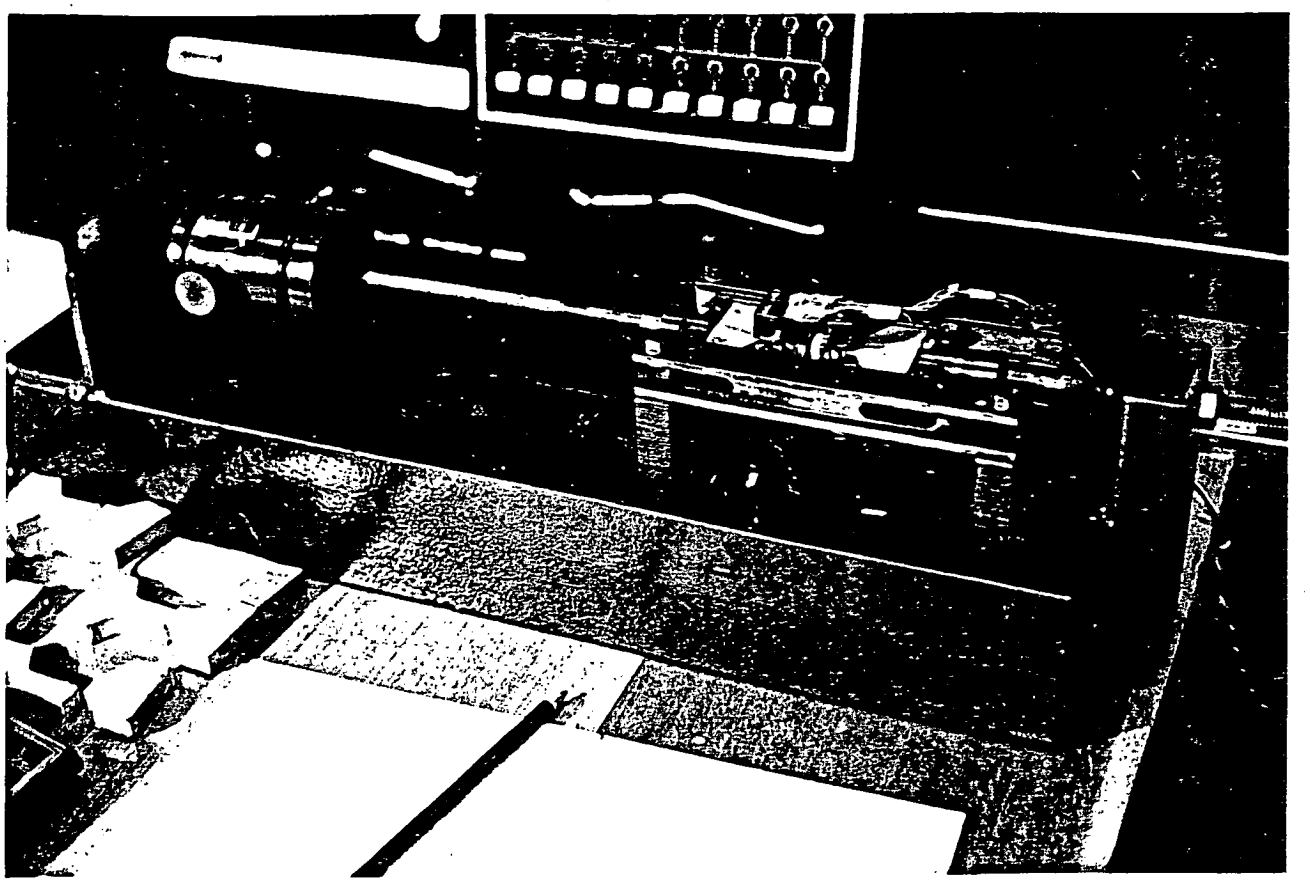

Figure 7.3(a)

Measurement of the relationship between tensile stress and strain.

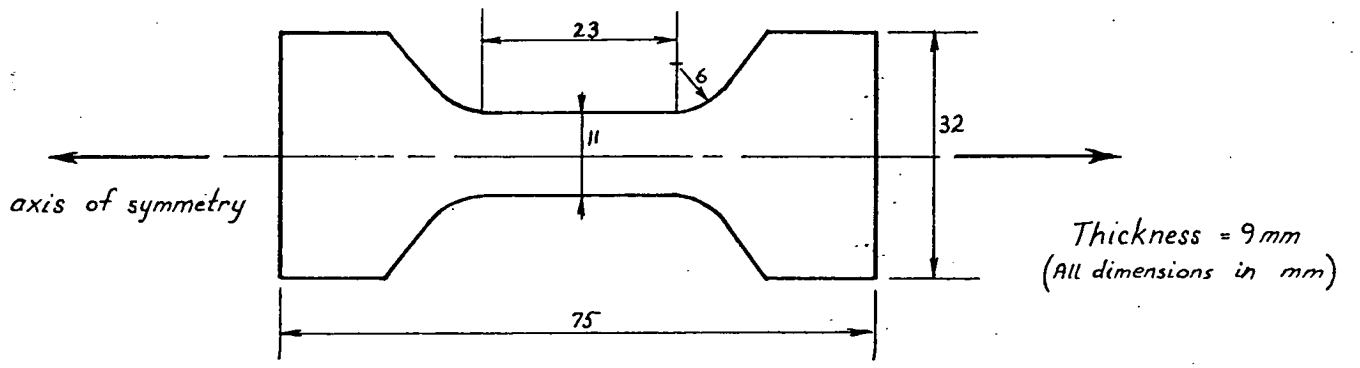

Figure 7.3(b)

Typical sample for tension tests across the grain.

The magnitude of the force transmitted through the sample was measured using an Ormond Load Cell (-10 *kN* to +10 *kN*) connected to a Dorric type D5-300-T2 indicator. The sensitivity of force measurement was ±1 *N*.

The strain gauges (section 7.2.3.1) were mounted on opposite faces of the test sample (figure 7.3,a) prior to the commencement of tests. Care was taken to ensure that the gauges were aligned with the axis of symmetry of the test sample and that the knife-edges were properly embedded in the surface fibres of the wood.

Compression tests were conducted in a Shimadzu testing machine operating on the 5 *kN* load range (sensitivity ± 5 *N*). A typical test sample is shown in figure (7.4).

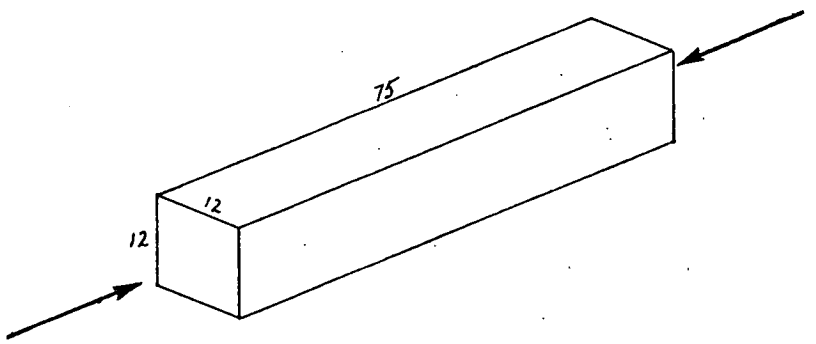

Figure 7.4

Typical sample for compression tests across the grain.

Tension and compression tests were conducted at a straining rate of approximately $250_{10}{}^{-6}$/ minute, the strain being increased in increments of roughly $750_{10}{}^{-6}$ every three

minutes. The standard (continuous) straining rates proposed for the testing of wood in compression perpendicular to the grain are 6000_{10}^{-6} /minute (A.S.T.M) and 12000_{10}^{-6} /minute (British Standard). Mack (1979) reports that tests on the Australian species have been conducted accordingly to the A.S.T.M. standards in the main. Therefore, direct comparison of measured and published data is not justified due to the effects of creep.

Samples which were to be tested at moisture contents significantly different from the equilibrium moisture content of wood fibre under normal atmospheric conditions were first conditioned to the required moisture content and then completely covered with a thin coat of paraffin wax in order to prevent adsorption or desorption of moisture while testing. In this way, the effects of swelling (shrinkage) due to changes in moisture content were eliminated.

7.2.3.3 Measurement of Moduli of Rigidity.

The approximate moduli of rigidity of "Tasmanian Oak" in the radial-longitudinal and tangential-longitudinal planes were determined from measurements of torsional stiffness. Long, thin strips of wood were twisted in apparatus similar to that shown in figure 7.5.

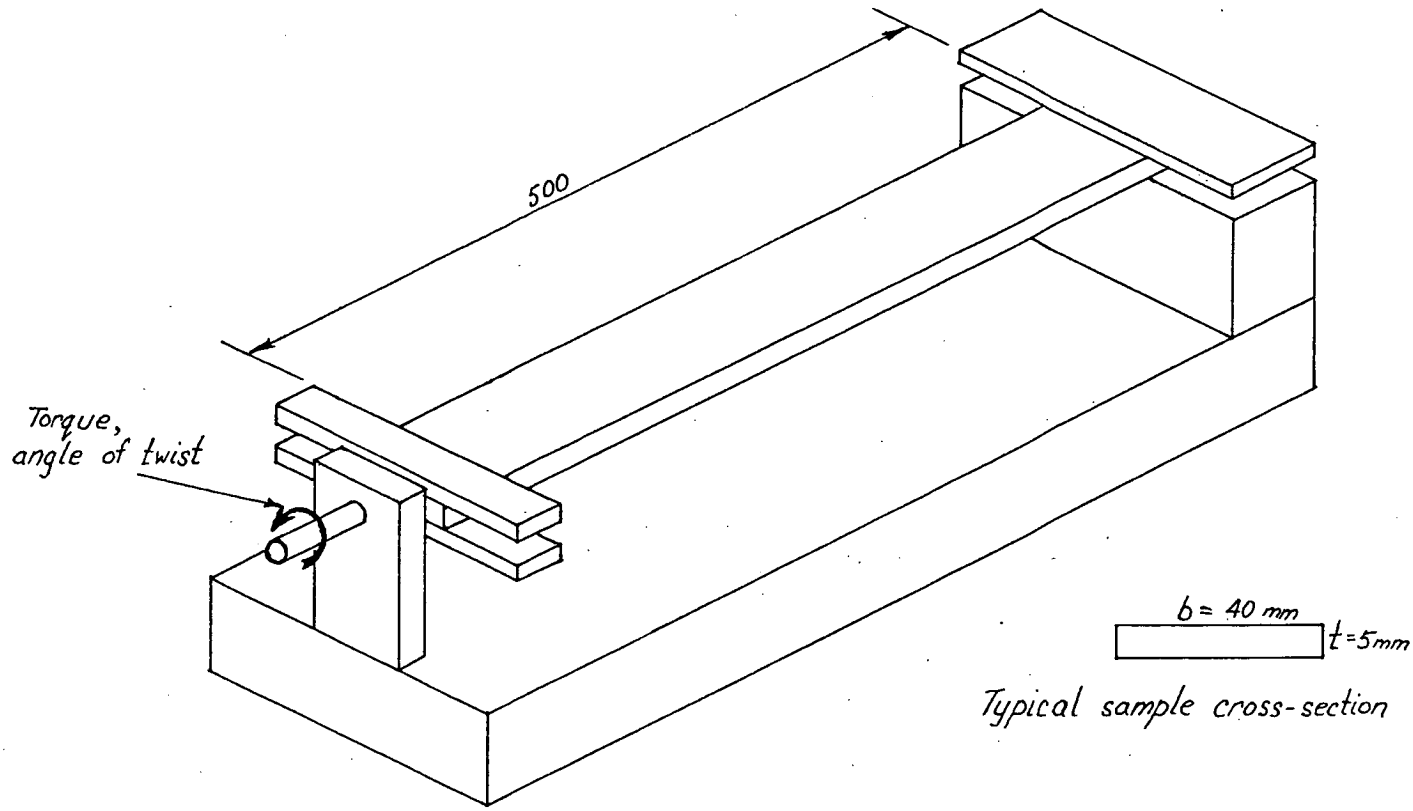

Figure 7.5

Measurement of torsional stiffness.

The relationship between applied torque and angle of twist was recorded.

Torque,

$$T = GJ\,\frac{\theta}{L}$$

where G = modulus of rigidity,

GJ = torsional stiffness ($J = \frac{1}{3}\,bt^3$),

θ = angle of twist of one end relative to the other,

and L = length of sample.

Tests were conducted at a twisting rate of 0.25 radians per minute. The moduli of rigidity were determined from the slopes of graphs of $J\frac{\theta}{L}$ plotted against applied torque, T.

7.2.4 Measured Material Properties.

7.2.4.1 The relationships between stress and strain in the principle transverse directions.

Samples of "Tasmanian Oak" (predominantly E. delegatensis and E. regnans) having densities between 690 and 750 kg/m^3 at 14% moisture content (dry basis) were selected randomly. Specimens for testing in tension were machined from blanks (figure 7.6) in such a way that their axes of symmetry coincided with either the radial or tangential directions. The blanks were conditioned to the required moisture content prior to final machining. Immediately after machining, the test samples were coated with paraffin wax to prevent moisture content changes. Sealed samples were usually left for 24 hours before testing to ensure uniformity of moisture content. Tension tests were conducted in both the radial and tangential directions according to table (7.2). The results of tests are given in detail in Appendix E .

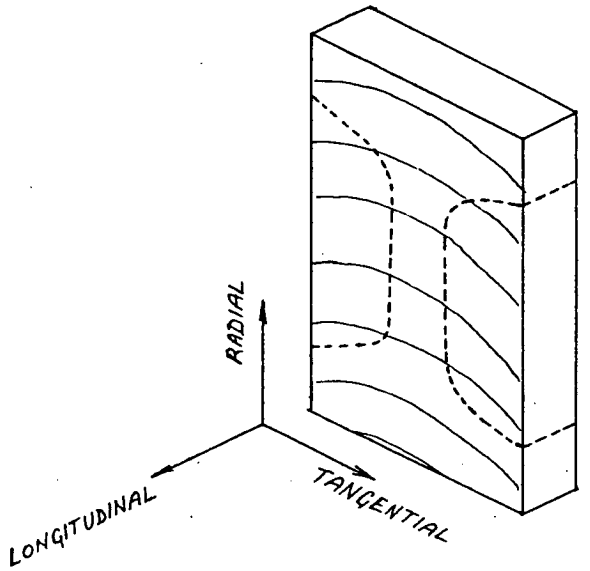

Figure 7.6

Sample blanks.

DIRECTION	MOISTURE CONTENT / NUMBER OF TESTS	MOISTURE CONTENT / NUMBER OF TESTS	MOISTURE CONTENT / NUMBER OF TESTS
RADIAL	14% / 5	56% / 1	120% / 3
TANGENTIAL	14% / 4	56% / 1	120% / 3

TABLE 7.2

Summary of tension tests conducted.

Tests were conducted to failure by increasing the strain in increments of about $750_{10}{}^{-6}$ and allowing a

"settling" period of 3 minutes before recording load and strain. Curves of the type

$$\sigma = A\left(1 - \frac{1}{B\varepsilon + 1}\right)$$

where σ = stress,

ε = strain,

A, B = constants,

were found to fit the measured stress-strain relationships well. Two typical results are shown in figure (7.7).

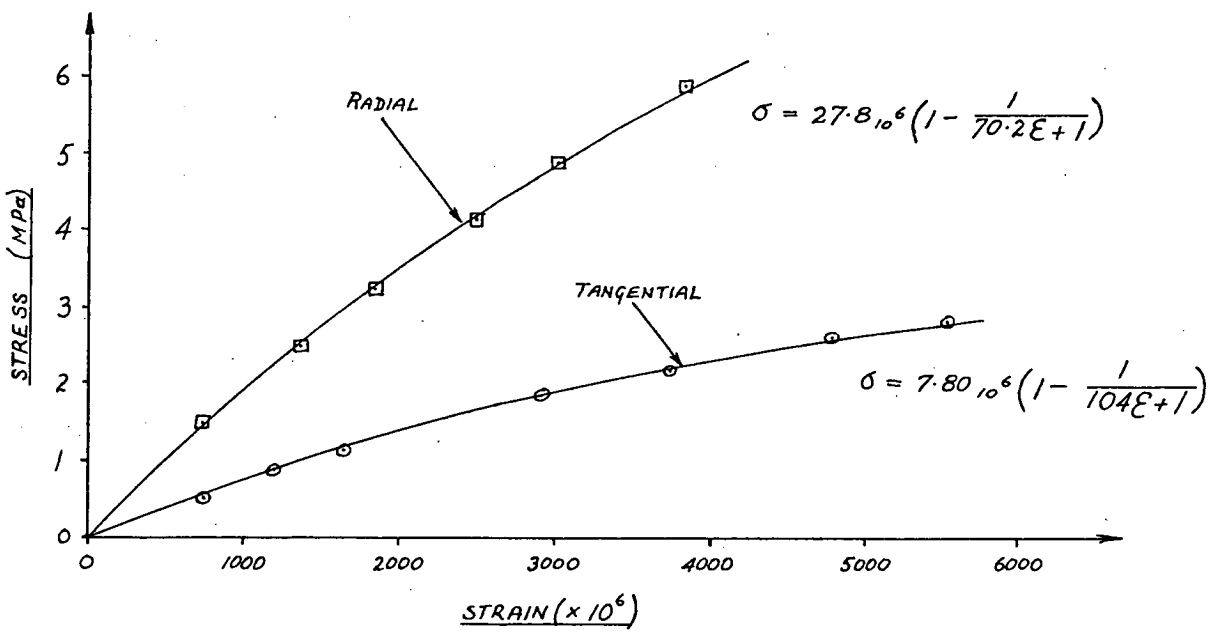

Figure 7.7

Mathematical functions fitted to measured stress-strain relationships - tension across the grain.

(moisture content = 14%)

Tension tests on samples cut from the same piece of wood produced variable results. The measurements graphed in figure 7.8 resulted from tests on samples with moisture contents of 120 ± 4%, all cut from a piece of green "Tasmanian Oak" measuring 125 x 125 x 250 mm.

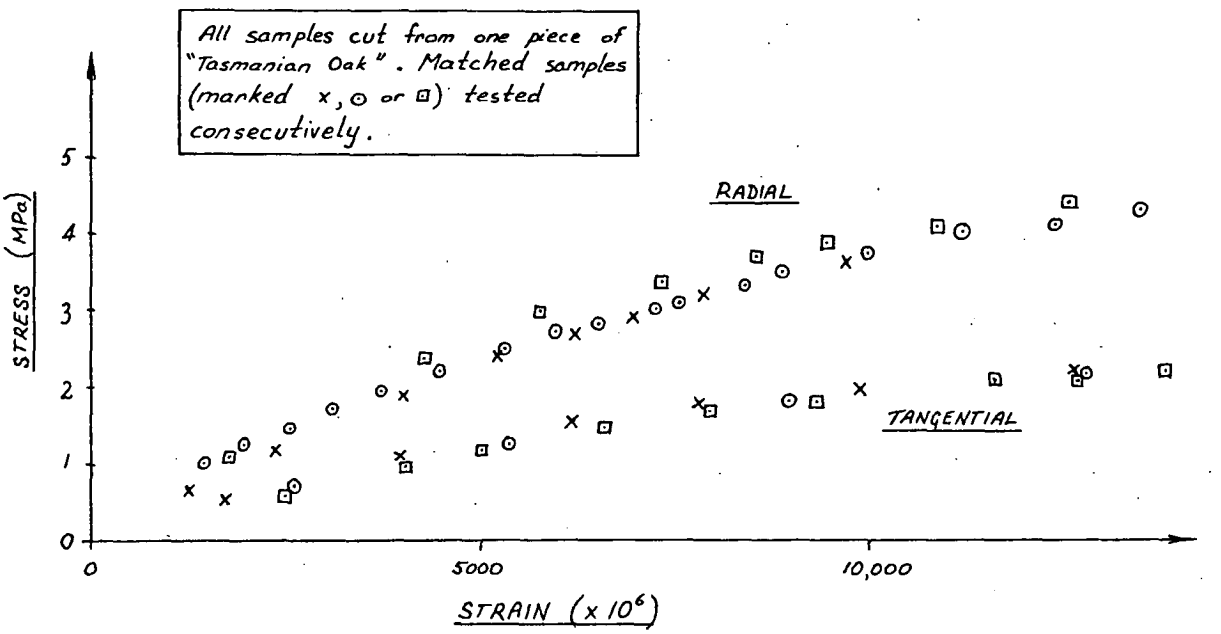

Figure 7.8

Variability of tension tests across the grain for one sample (moisture content = 120%)

From figure (7.8), the approximate mean moduli of elasticity over the range $0 - 5000_{10}{}^{-6}$ strain are

$$E_r \simeq 500 \text{ MPa} \pm 10\% \quad (\text{at } M = 120\%)$$

and $$E_t \simeq 250 \text{ MPa} \pm 10\% \quad (\text{at } M = 120\%)$$

Tension tests in the radial direction conducted on dry samples (moisture content ≃ 14%) cut from five

different pieces of wood (see Appendix E .) gave the modulus of elasticity in the radial direction as

$$E_r \simeq 1300 \text{ MPa} \pm 20\% \quad (\text{at } M \simeq 14\%)$$

The strain at failure was $5000_{10}{}^{-6}$ ± 15%.

A similar number of tension tests on tangentially-loaded samples produced highly variable results. Here, the elastic moduli over the range 0 to $5000_{10}{}^{-6}$ strain ranged from 320 MPa to 1250 MPa; the strain at failure ranged from $2500_{10}{}^{-6}$ to more than $20{,}000_{10}{}^{-6}$.

Compression tests on six samples at a moisture content of 14% gave

$$E_r \simeq 1100 \text{ MPa} \pm 30\% \quad (\text{at } M = 14\%)$$

and $$E_t \simeq 800 \text{ MPa} \pm 25\% \quad (\text{at } M = 14\%)$$

(results are summarised in Appendix E .)

It is impossible to draw quantitative conclusions from the results presented although it appears that, for green timber,

$$\frac{E_r}{E_t} \simeq 2$$

and that $$\frac{E_r \ (M = 14\%)}{E_r \ (M > \text{f.s.p.})} \simeq 2$$

where f.s.p. = fibre saturation point.

Extensive testing based on suitable sampling techniques (C.S.I.R.O., 1969) is necessary to fully define the relationships between stress, strain, moisture content and temperature in the principle transverse directions for each species making up the "Tasmanian Oak" group. Further work is necessary to determine the effects of creep and moisture content changes on deformations in timber during drying.

7.2.4.2 Measured moduli of rigidity.

The approximate values of the moduli of rigidity, G, in the radial-longitudinal (r-z) and tangential-longitudinal (t-z) planes were determined from measurements made in the apparatus described in section 7.2.3.3. Strips of wood, cut as shown in figure 7.9, were placed in the test rig and twisted at a rate of approximately 0.25 radians per minute.

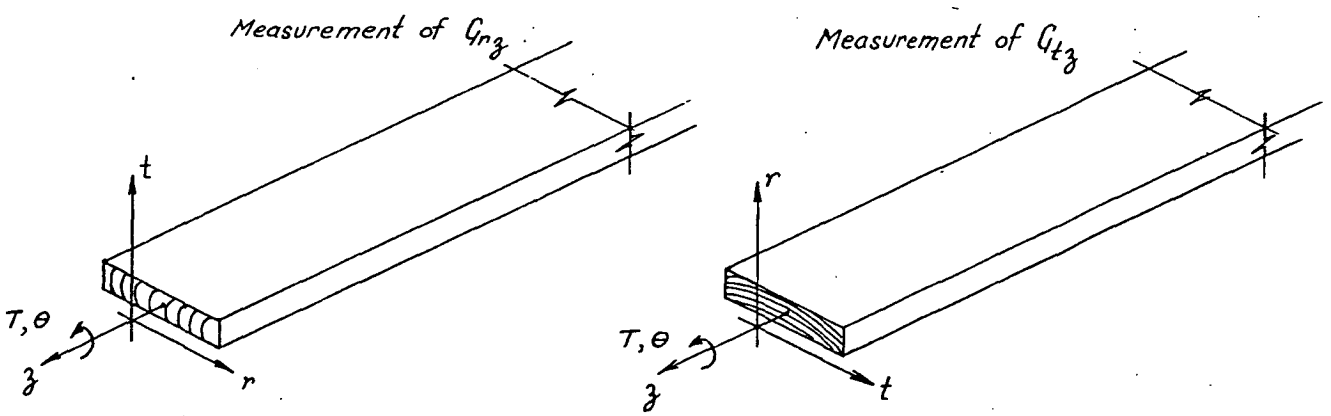

Figure 7.9

Tests for torsional stiffness.

Tests were restricted to samples at 14% moisture content with a density (at M = 14%) of between 690 and 760 kg/m^3. The relationship between applied torque and angle of twist was recorded. Both G_{rz} and G_{tz} were determined for each of 14 different dry boards. (Individual test results are given in Appendix E). The distribution of results is shown in figure (7.10).

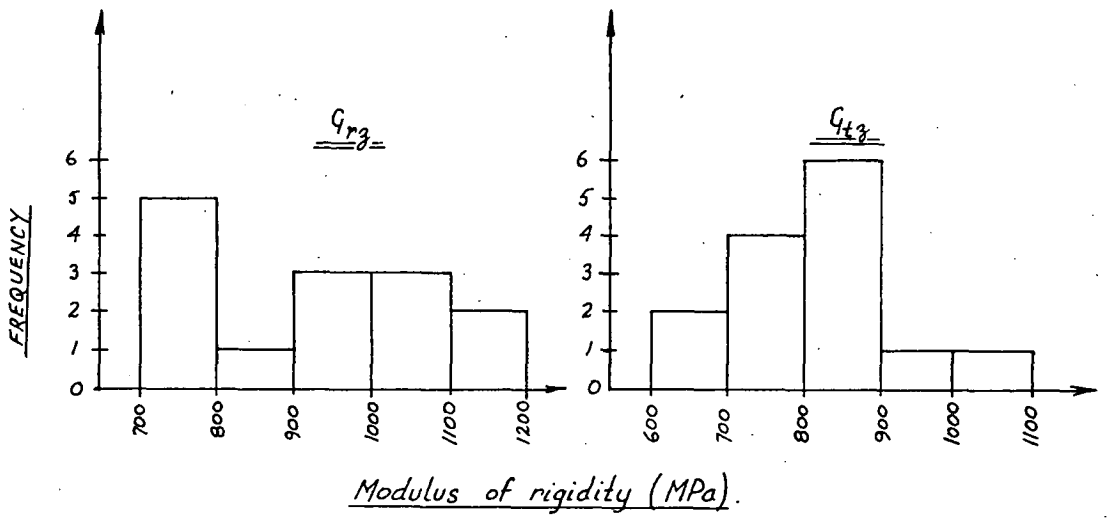

Figure 7.10

Distributions of moduli of rigidity measured in 28 tests.

Very much larger sample populations are required before a meaningfull statistical analysis of the results can be made. The average moduli of rigidity were found to be

G_{rz} (average) = 930 MPa

G_{tz} (average) = 820 MPa

Indiviaual results varied by up to 25% of the averages quoted.

The effects of prolonged loading on twist were not studied.

7.2.4.3 The approximate elastic properties of "Tasmanian Oak".

The primary objective of the analysis of drying stresses in timber was to demonstrate the effects of drying through semi-permeable surface coatings rather than to accurately determine the magnitudes of the drying stresses. Therefore, it was necessary to establish whether or not the elastic properties of"Tasmanian Oak" were similar to those of other timbers and, if so, to define the "average" pattern of elastic behaviour of hardwoods. It was also necessary to describe approximately the effect of moisture concentration upon the elastic parameters.

The approximate relationships between the four elastic parameters of "Tasmanian Oak" measured on small sample populations (at a moisture content of 14%) were found to be

$$\frac{E_t}{E_r} \simeq 0.7 \ (0.5, \text{green}), \frac{G_{rz}}{E_r} \simeq 0.8 \text{ and } \frac{G_{tz}}{E_r} \simeq 0.7 \quad \ldots(7.1)$$

The same (average) ratios for the 3 North American hardwoods quoted in table (7.1) are

$$\frac{E_t}{E_r} \simeq 0.52, \quad \frac{G_{rz}}{E_r} \simeq 0.83 \text{ and } \frac{G_{tz}}{E_r} \simeq 0.64 \quad ..(7.2)$$

The ratios (7.2) are derived from tests conducted according to the ASTM standards which are characterised by very much faster straining rates than those used during tests resulting in ratios (7.1) (see section 7.2.3.2). Nevertheless, the similarity in material property ratios is encouraging and preliminary indications are that the "Tasmanian Oak" group of species behave (elastically) in a similar manner to other hardwoods.

The average material property ratios given in table (7.1) were used in the mathematical model describing the development of drying stresses in "Tasmanian Oak". A summary of these values appears in table (7.3).

$\frac{E_t}{E_z}$	$\frac{E_r}{E_z}$	$\frac{G_{rz}}{E_z}$	$\frac{G_{tz}}{E_z}$	$\frac{G_{rt}}{E_z}$	μ_{zr}	μ_{rz}	μ_{tr}	μ_{rt}	μ_{zt}	μ_{tz}
·052	·100	·083	·064	·020	·410	·041	·364	·700	·500	·026

TABLE 7.3

Adopted elastic parameters of "Tasmanian Oak"
(moisture content = 12%)

The longitudinal modulus of elasticity of E. regnans at 12% moisture content (C.S.I.R.O., 1975), $E_z \simeq 20{,}000$ MPa. The value of E_z varies with moisture content according to the relationship described in figure 7.1.

Tests showed that $\dfrac{E_r \ (m.c. = 14\%)}{E_r \ (green)} \simeq 2$.

The parameters required for a linear, plane-strain model of drying stresses are E_r, E_t, G_{rt} and the six Poisson's ratios. It was assumed that the values of E_t and G_{rt} (like E_r) doubled as the moisture content fell from above the fibre saturation point to 14%. The variation of E_r, E_t and G_{rt} with moisture content was assumed to have a form similar to that describing the variation of E_z and was expressed as

$$P\ (\text{at m. concentration} = c) = P(\text{green})(1+2.72\ e^{-c/90}) \quad \text{where } P = E_r,\ E_t \text{ or } G_{rt}. \qquad \ldots.(7.3)$$

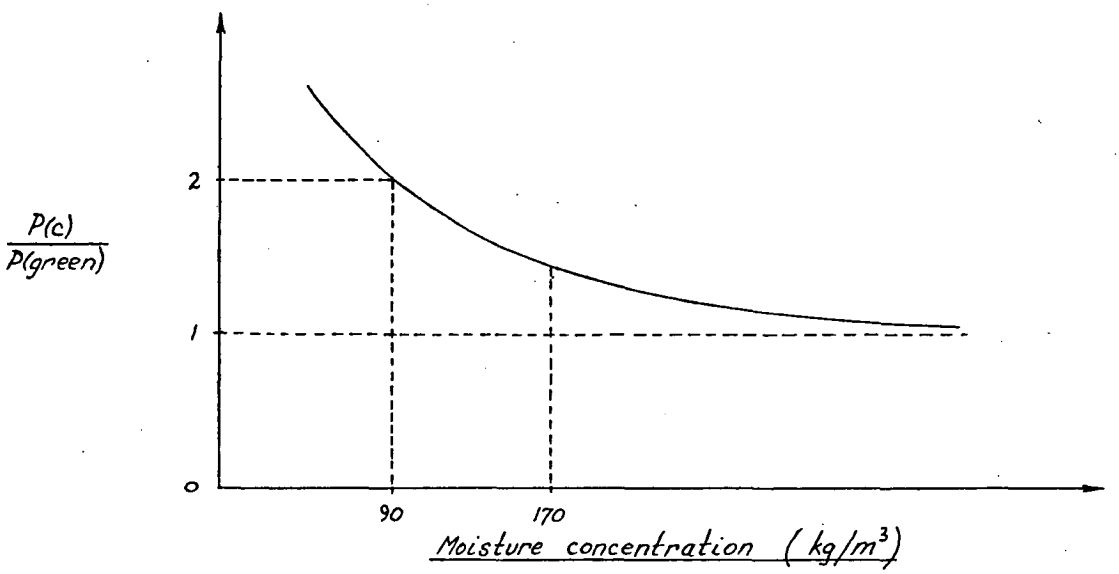

Figure 7.11

The variation of elastic moduli with moisture concentration.

Thus, $E_r \simeq 1000_{10}{}^6\ (1 + 2.72\ e^{-c/90})$,

$E_t \simeq 500_{10}{}^6\ (1 + 2.72\ e^{-c/90})$

and $G_{rt} \simeq 200_{10}{}^6\ (1 + 2.72\ e^{-c/90})$

The Poisson's ratios were assumed to be independent of moisture content. (U.S. F.P.L., 1974).

7.3 The Shrinkage of "Tasmanian Oak"

7.3.1 Introduction

Wood exhibits anisotropic shrinkage characteristics. It shrinks most in the direction of the annual growth rings (tangentially), about half this amount across the rings (radially) and very little along the grain (longitudinally). The combined effects of radial and tangential shrinkage can distort the cross-section of boards because of the difference in shrinkage and the curvature of the seasonal rings.

Wood-fibre is dimensionally stable when its moisture content is above the fibre saturation point but its dimensions change as it gains or loses moisture below this point. Shrinkage occurs when water is lost from the wood cell walls.

The moisture content-shrinkage relationships in the radial and tangential directions are required for the calculation of drying stresses as differential shrinkage strains are the major contributing factor. The shrinkage of most timbers milled on a large scale is well researched and a large amount of data has been published (Kingston and von Steigler, 1966: U.S. F.P.L., 1974).

Tests were conducted to verify published data and to determine the exact shape of the moisture content-shrinkage

relationships. The measured relationships were used in a mathematical model (based on linear elastic properties) to demonstrate the effectiveness of proposed stress-control methods (see chapter 8).

7.3.2 Published Data

The shrinkage characteristics of many Australian timbers are summarised by Kingston and von Steigler (1966). In this summary, shrinkage is expressed as a percentage of green dimensions. Values of shrinkage from green to a moisture content of 12% both before and after reconditioning are given. The difference between these values gives an estimate of the incidence of collapse. The values given "after reconditioning" correspond to the "normal" (unrestrained) shrinkage of the fibre.

The unit shrinkage is also tabulated by Kingston and von Steigler. This is the shrinkage (%) for a 1% change in moisture content and applies only between about 5% and 25% moisture content.

For E. delegatensis, the "normal" shrinkage from green to 12% moisture content is 3.5% in the radial direction and 6.3% in the tangential direction. The unit shrinkages in the radial and tangential directions are 0.22% and 0.35% respectively. From this information, the relationships shown in figure (7.12) may be deduced.

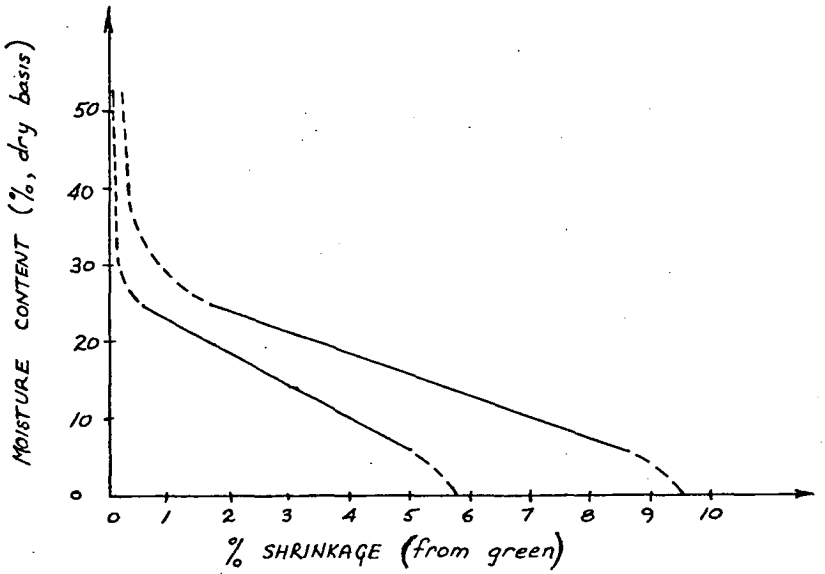

Figure 7.12

Published shrinkage data for E. delegatensis.

The published shrinkage data for the three species making up the "Tasmanian Oak" group are summarised in table (7.4).

SPECIES	Green to M=12% (dry basis)		Unit shrinkage	
	RADIAL	TANGENTIAL	RADIAL	TANGENTIAL
E. delegatensis	3·5	6·3	0·22	0·35
E. regnans	3·7	7·1	0·23	0·36
E. obliqua	3·3	6·3	0·23	0·36

TABLE 7.4

Shrinkage properties of "Tasmanian Oak"

7.3.3 Materials and Methods.

Slabs of green "Tasmanian Oak" were selected at random from off-cuts available at sawmills. The wood was placed in oxygen-proof polythene bags and taken directly to the laboratory for testing. Test samples (figure 7.13) were cut from green slabs using a band-saw. Care was taken to avoid any reaction wood, sapwood and that close to the center of the tree. Thin slices of "Tasmanian Oak" were cut from slabs of green timber, as shown in figure (7.13).

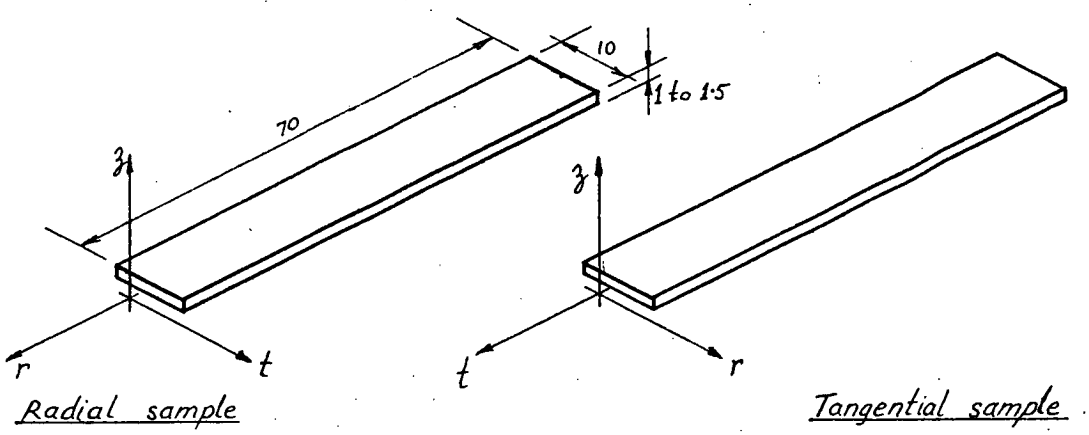

Figure 7.13

Typical samples used in shrinkage tests.

The upper limit to the thickness of samples used in shrinkage tests was 1.5 mm in order to minimise the effects of drying stresses on deformations. The samples were restrained from deforming out of the plane but were not restrained against shrinkage within the plane (see figure 7.14). Two small markers (brass filings) were

embedded in the faces of each green sample, one near each end, and the distance between them measured using a travelling microscope.

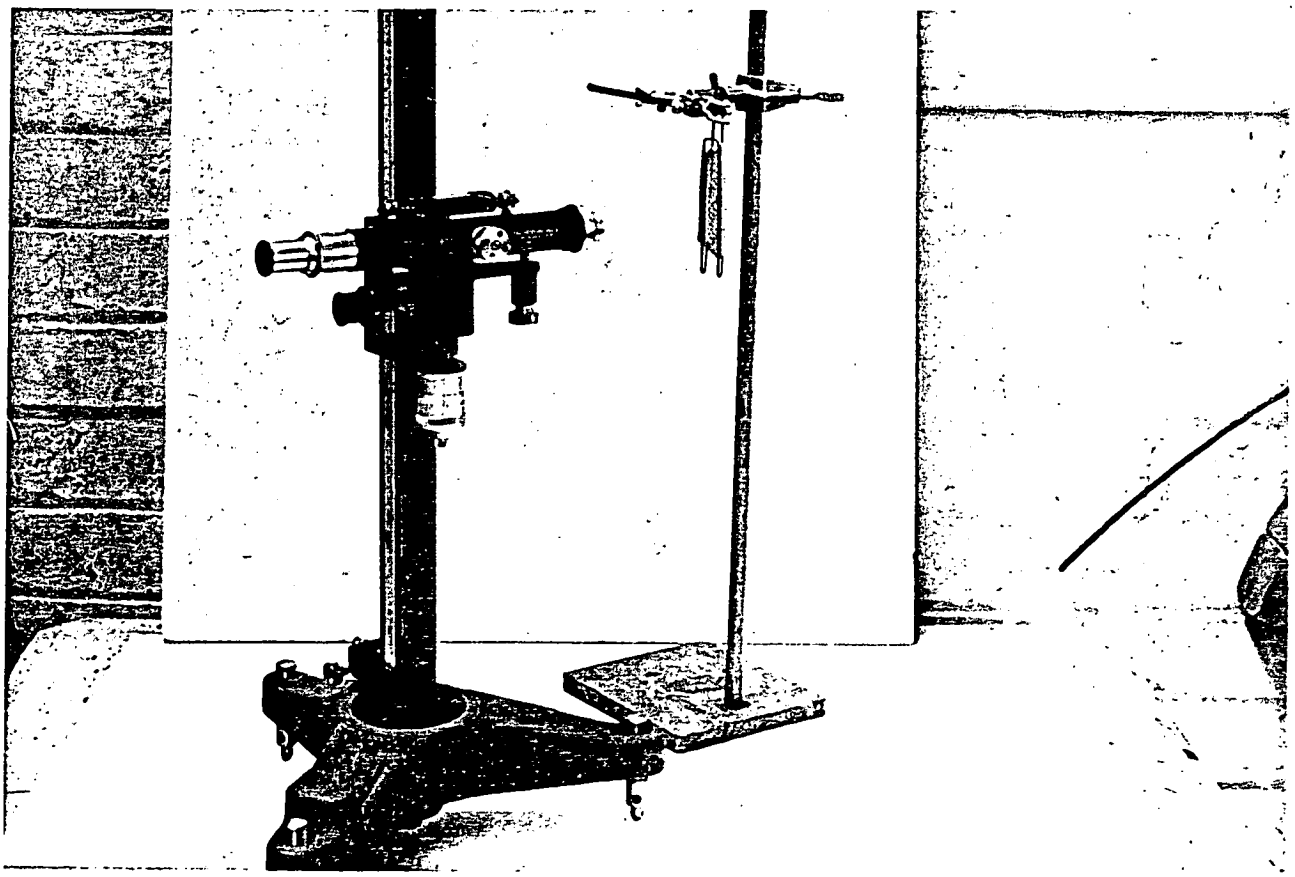

Figure 7.14

Shrinkage test in progress.

The samples were allowed to dry in air. The distance between the markers was measured every 15 minutes and the sample

(plus restraining frame) weighed on a Projecta balance (sensitivity ± 0.0001 g). It was essential that the weighing was conducted within about 30 seconds of the length measurement as the sample dried at a rate of approximately 0.008 grams of water per minute in the early stages (initial sample weight ≃ 3 g.). The drying rate reduced as the samples approached equilibrium under the atmospheric conditions in the laboratory. The samples were conditioned to moisture contents below the equilibrium value in the laboratory and finally oven dried.

7.3.4 Measured shrinkage-moisture content relationships.

In all, nine radial and eight tangential shrinkage tests were conducted according to the procedure described in section 7.3.3. A detailed summary of the results appears in Appendix E .

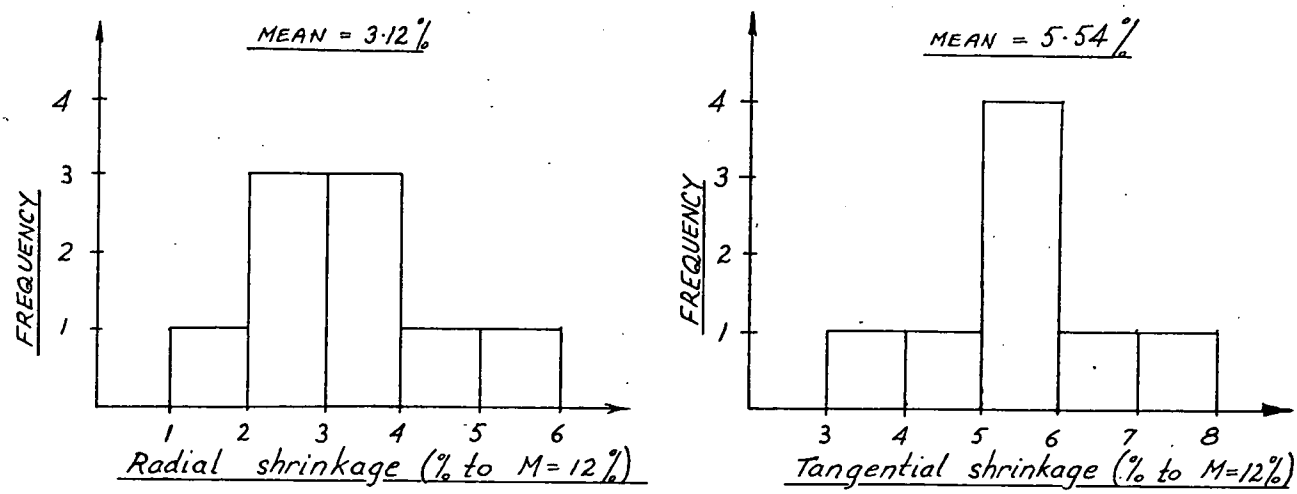

Figure 7.15

Distributions of shrinkage to 12% moisture content from 17 tests.

The measured mean shrinkage to 12% moisture content compare favourably with those given in table (7.4). The mean shrinkage in the radial and tangential directions at moisture contents of 0, 5, 10, 15.....(%) were determined from measurements (Appendix *E*) and the average shrinkage-moisture content relationships plotted (figure 7.16).

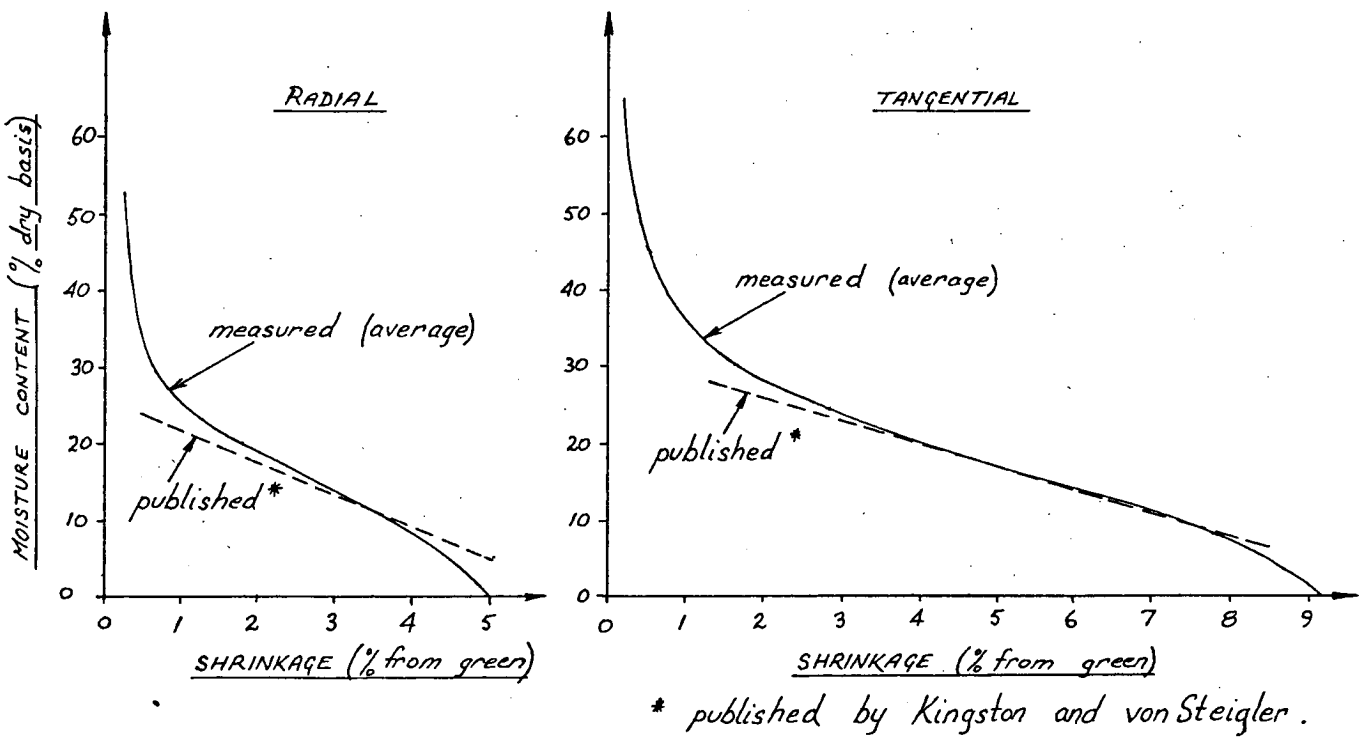

Figure 7.16

Average relationships between shrinkage and moisture content.

The measured relationships of figure (7.16) were approximated mathematically and used in the calculation of drying stresses (chapter 8).

In terms of moisture concentration, the measured relationships may be approximated by the following relationships:

Radial shrinkage strain,

$$\varepsilon_{s_r} = 0.03 + \frac{0.06}{\pi} \arctan\left(\frac{82-c}{41}\right)$$

Tangential shrinkage strain,

$$\varepsilon_{s_t} = 0.055 + \frac{0.110}{\pi} \arctan\left(\frac{90-c}{53}\right) \quad \ldots\ldots(7.4)$$

REFERENCES

C.S.I.R.O. (1969): Sampling of Timber for Evaluation of Species Properties.
Forest Products Technical Note - No.5
Division of Forest Products, C.S.I.R.O., Melbourne, Aust.

C.S.I.R.O. (1975): Fundamentals of Timber Engineering.
Lectures (publ.) by Leicester, Armstrong and Kloot.
Division of Building Research, C.S.I.R.O., Melbourne, Aust.

GROSSMAN, P.U.A.; L.D. ARMSTRONG and R.S.T. KINGSTON (1969):
An Assessment of Research in Wood Rheology.
Wood Sci. and Tech. 3 (4) : 324 - 328.

KINGSTON, R.S.T.; A.E. von STIEGLER (1966):
Shrinkage and Density of Australian and other woods.
C.S.I.R.O. Forest Products Newsletters Nos. 332-6.

MACK, J.J. (1979): Australian Methods for Mechanically Testing Small Clear Specimens of Timber.
C.S.I.R.O. Division of Building Research - Tech. paper No. 31. (second series).

U.S. F.P.L. (1974): Wood Handbook: Wood as an Engineering Material.
Agriculture Handbook No. 72.
Forest Products Laboratory, Forest Service,
U.S. Dpt. of Agric.
U.S. Govt. Printing Office,
Washington, D.C.

CHAPTER 8

CHAPTER 8

DRYING STRESSES

8.1 Introduction

A number of factors contribute to the magnitude of drying stresses in sawn timbers, the more important ones being:

1) The particular permeability, shrinkage and elastic properties of any given piece of timber.
2) Whether the board is quarter-sawn or back-sawn.
3) Board thickness.
4) The initial moisture content.
5) The drying conditions.
6) Surface coating thickness and permeability.

The method of determining the state of stress in a piece of wood in a condition of plane strain (chapter 6), together with the "short-term", linear elastic behaviour and shrinkage properties of "Tasmanian Oak" (chapter 7), were used to calculate drying stresses in boards dried under conditions similar to those used in the Tasmanian timber industry. In the model, no allowance was made for the time-dependence of elastic deformations, the effects of hysteresis or the development of checks. The purpose of the analysis reported in this chapter is to demonstrate the relative stress levels in back-sawn "Tasmanian Oak" dried with and without permeable surface coatings. The mathematical model may be made more realistic by including the effects of non-linear elasticity, creep and hysteresis via the introduction of piece-wise linear approximations to the measured behaviour of timber (for example, section 6.6).

A one-dimensional model of drying and stress-development based on a finite difference approximation to the governing differential equations was formulated. Typical properties of "Tasmanian Oak" (from chapters 5 and 7) were used in the calculation of drying stresses in coated and uncoated boards with various thicknesses dried under the same conditions. The approximate conditions under which checking becomes a problem were deduced from a comparison of calculated and observed behaviour . The results of calculations clearly demonstrate that the maximum drying stresses in coated timber are lower than those in uncoated timber dried under the same conditions.

The use of combined moisture transfer and stress analysis in the design and optimisation of drying schedules is discussed.

8.2 A mathematical model for the determination of drying rates and stresses.

When timber is stacked for drying under industrial conditions, individual boards are stacked edge to edge in layers approximately 1.8 m wide. Therefore, drying takes place almost entirely through the faces of a board and moisture transfer through the wood fibre can be analysed using a one-dimensional model. In one dimension, the mass diffusion equation (equation 3.18) becomes:

$$\frac{\partial c}{\partial t} = D \frac{\partial^2 c}{\partial x^2} \qquad \ldots\ldots(8.1)$$

where c = mass concentration (kg/m^3),

t = time(s),

D = diffusion co-efficient or "diffusivity" (m^2/s)

and x = space increment (m).

Uni-directional drying gives rise to a condition in which the lines of constant moisture concentration are parallel to the board faces and therefore shrinkage strains vary only in the direction perpendicular to the board faces (i.e. the direction of moisture transfer).

The diffusion co-efficients in both the radial and tangential directions were assumed to be constant (independent of moisture concentration, see chapter 5).

The boundary conditions used in the calculation of moisture distributions in coated timber were based upon curves fitted to measured surface fibre moisture concentration - time relationships. Surface fibre moisture concentrations were inferred from moisture distributions measured using the microtoming technique described in chapter 5. Three typical curves are illustrated in figure (8.1).

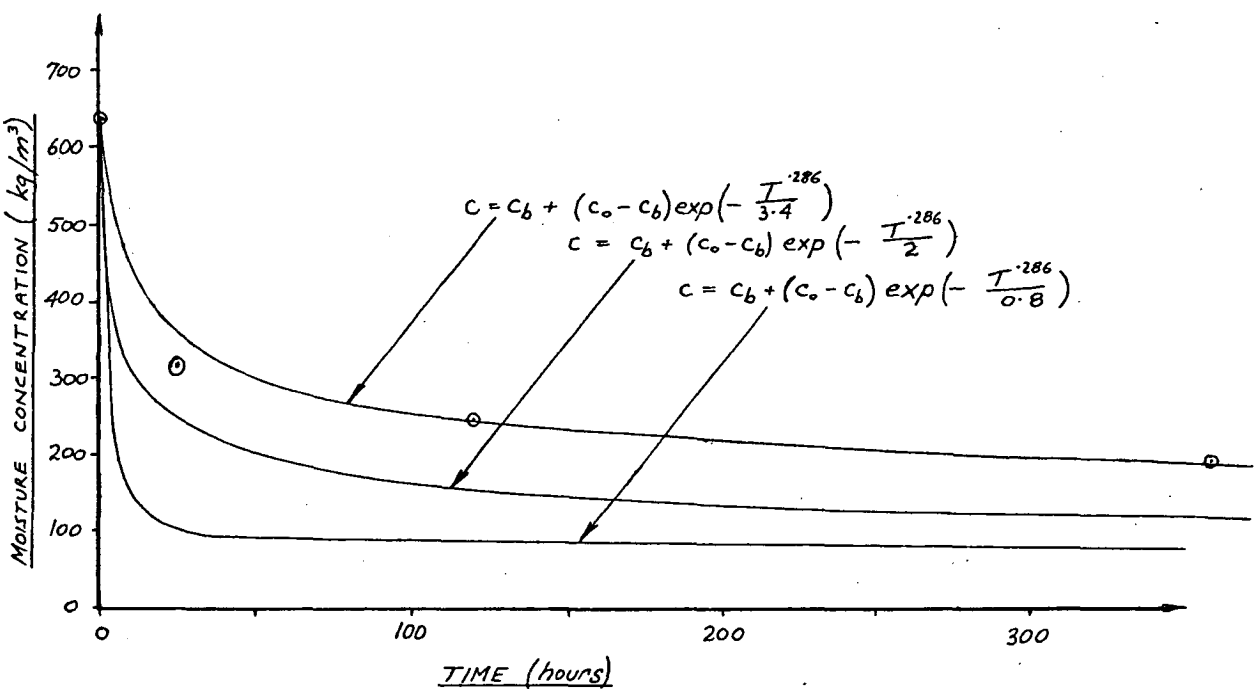

Figure 8.1

Surface fibre moisture concentration variation with time.

The points marked ⊙ correspond to surface fibre moisture concentrations measured on a 27.4 mm thick back-sawn board

with an initial moisture concentration of approximately 640 kg/m^3 dried at 25^{0}C and 50% relative humidity with a 0.7 mm thick animal glue-talcum powder coating (chapter 5). The board has a radial diffusivity of approximately $2.1_{10}{}^{-7}$ m^2/hr based on a model using a constant diffusion co-efficient. The lowest of the curves in figure (8.1) corresponds to the boundary condition of an uncoated board and the middle curve approximates the surface fibre moisture concentration variation of a thinly coated board (thickness of between 0.3 and 0.5 mm animal glue-talcum powder).

To simplify the mathematics, the analysis of drying stresses in "Tasmanian Oak" was restricted to either purely back-sawn or purely quarter-sawn boards (sections 6.4.3.2 and 6.4.3.1 respectively). Furthermore, the boards were assumed to be very wide compared to their thickness. Under this condition, the stresses acting in the direction perpendicular to the board faces are small at every point on the cross-section (away from the edges) and may be neglected. This leads to the deduction that the Airy stress function, ϕ (section 6.3.1), has a constant value along lines parallel to the faces of a wide board (at a sufficient distance from the edges).

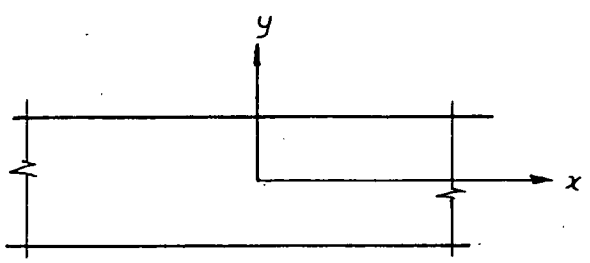

Hence,

$$\frac{\partial^4\phi}{\partial x^4} = \frac{\partial^2\phi}{\partial x^2} = 0 ; \left[\sigma_y = \frac{\partial^2\phi}{\partial x^2} \right]$$

and,

$$\frac{\partial^4\phi}{\partial x^2 \partial y^2} = \frac{\partial^2\phi}{\partial x \partial y} = 0 ; \left[\tau_{xy} = -\frac{\partial^2\phi}{\partial x \partial y} \right.$$

For back-sawn timber, the differential equation describing the state of stress takes the form

$$K_1\frac{\partial^4\phi}{\partial x^4} + K_2\frac{\partial^4\phi}{\partial x^2\partial y^2} + K_3\frac{\partial^4\phi}{\partial y^4} = -\frac{\partial^2}{\partial x^2}\begin{bmatrix}\text{radial}\\ \text{shrinkage}\end{bmatrix} - \frac{\partial^2}{\partial y^2}\begin{bmatrix}\text{tangential}\\ \text{shrinkage}\end{bmatrix} \qquad \text{.....(8.2)}$$

(see equation 6.38) where K_1, K_2 and K_3 are (elastic) constants.

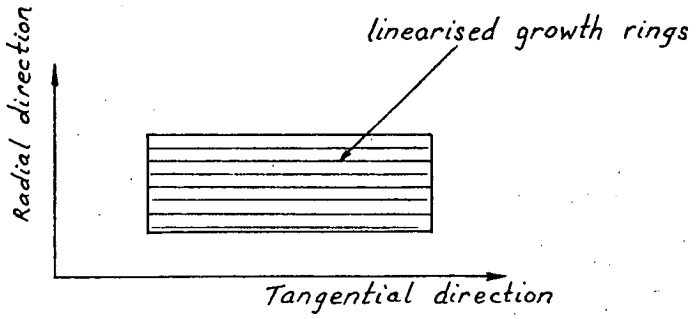

Back-sawn board (in cross-section)

Under the simplifications outlined, equation (8.2) reduces to

$$K_3\frac{\partial^4\phi}{\partial y^4} = -\frac{\partial^2}{\partial y^2}(\text{tangential shrinkage})$$

or

$$\left[\frac{1-\mu_{zt}\mu_{tz}}{E_t}\right]\frac{\partial^4\phi}{\partial y^4} = -\frac{\partial^2}{\partial y^2}(\beta_t c) \qquad \text{.....(8.3,a)}$$

Similarly, for quarter-sawn boards, it is found that

$$\left[\frac{1-\mu_{zr}\mu_{rz}}{E}\right]\frac{\partial^4\phi}{\partial y^4} = -\frac{\partial^2}{\partial y^2}(\beta_r c) \qquad \text{.....(8.3,b)}$$

(The variables used in equations (8.3,a and b) are defined in chapter 6).

The calculations were simplified further by ignoring the effects of creep and hysteresis and the development of checks. The material was assumed to be linearly elastic and the results of material property tests of short duration (approximately 1 minute, see chapter 7) were used in all calculations. Assumptions regarding the variation of the elastic properties of timber with moisture concentration are detailed in section 7.2.4.3.

The approximate mean shrinkage strain-moisture content (concentration) relationships of equation (7.4) were used in conjunction with calculated moisture distributions to determine the right-hand sides of equations (8.3, a & b).

Stresses were calculated subject to the boundary conditions of zero shear stress and zero direct stress (acting perpendicular to the board face) at the free surfaces (see section 6.3.1).

A computer program using finite difference approximations to equations (8.1) and (8.3) was used to calculate moisture and stress distributions (the "PASCAL" program is detailed in Appendix *F*).

8.3 Assessment of the one-dimensional moisture transfer model.

In the large-scale drying tests conducted on stacks made up of 2.3 m long coated and uncoated back-sawn boards reported in Chapter 5, drying was essentially one-dimensional (section 8.2). The stacks were dried under normal atmospheric conditions (17^{0}C and 60% relative humidity). Most of the uncoated material checked. The coated boards dried without checking. A 0.7 mm coating of the animal glue-talcum powder mix described in chapter 5 was used.

The one-dimensional moisture transfer model described in section 8.2 was used to analyse the mean drying curves for the uncoated and coated material in each stack (see figure 5.20). The results for stack number 3 are given in figure (8.2).

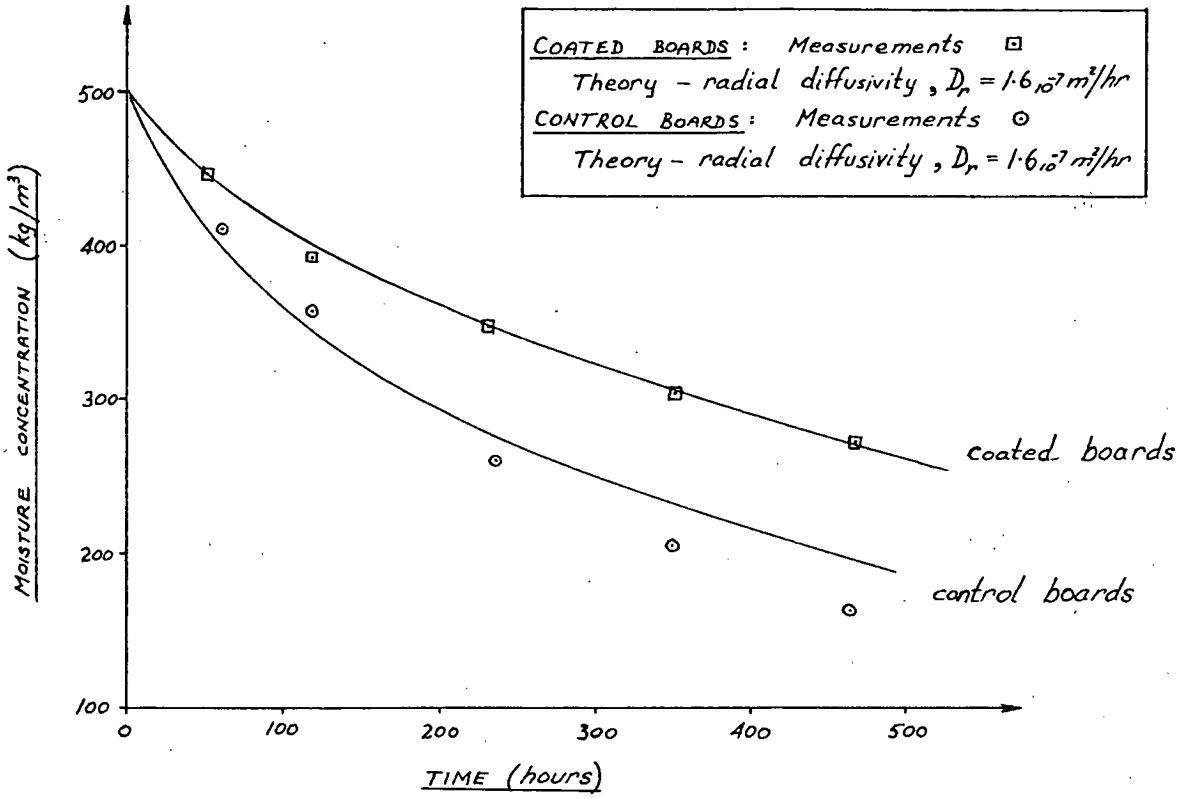

Figure 8.2

Typical drying curves for coated and uncoated boards.

The calculated curves are based on the actual board thickness of 27.0 mm (green) and a diffusion coefficient in the wood (in the radial direction),

$$D_r = 1.6_{10}{}^{-7} \quad m^2/hr.$$

Comparison of the measured and calculated drying curves for the control (uncoated) boards is not valid as the theoretical model makes no allowance for the acceleration of drying due to checking. The surface fibre moisture concentration-time relationship used in the calculations was

$$c = c_b + (c_o - c_b) \exp\left(-\frac{T^{.286}}{A}\right)$$

where $A = 0.8$ (for uncoated boards)

or $A = 3.4$ (for coated boards),

c_o = original moisture concentration,

c_b = equilibrium moisture concentration of wood fibre in the atmosphere,

and T = time (hours).

This function fits the measurements quoted in figure (8.1). The calculated drying curve (figure 8.2) for the coated material agrees well with the measured drying curve.

In order to determine the validity of the one-dimensional model as a means for calculating drying curves for uncoated boards, a 150 x 25 mm (nominal cross-section) green, quarter-sawn "Tasmanian Oak" board, 2.4 m long, was obtained and cut into 3 lengths, each of 0.7 m. These boards were sealed on the ends and edges with paraffin wax and dried under constant conditions of 37°C and 50% relative humidity. The boards did not check. The measurements are compared to the calculated drying curves in figure (8.3).

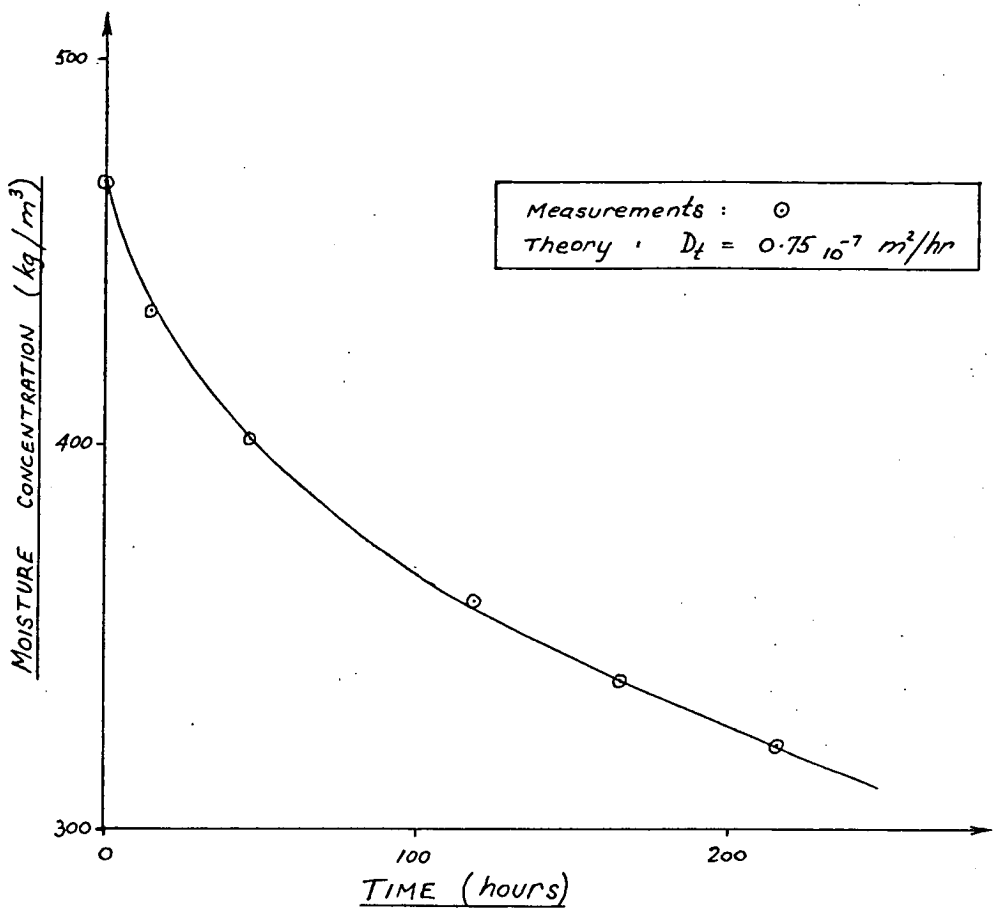

Figure 8.3

One-dimensional drying of a quarter-sawn board.

The calculated drying curves are based on the original (green) thickness of 25.0 mm and a constant diffusion co-efficient in the wood (tangential direction) of $D_t = 0.75_{10}{}^{-7}$ m²/hr. The surface fibre moisture concentration—time relationship used was

$$c = c_b + (c_o - c_b) \exp\left(-\frac{T^{\cdot 286}}{0.8}\right)$$

(see figure 8.1)

The agreement between measurements and calculations based upon the one-dimensional moisture transfer model using a constant diffusion co-efficient is remarkably good.

8.4 Calculated Drying Stresses.

8.4.1 Introduction

The drying of boards with different thicknesses but with the same material properties was analysed in order to study the changes in stress levels in timber brought about by drying through permeable coatings. A DIGITAL PDP 11/10 computer and a PASCAL program (listed in Appendix F) based on the theory and assumptions listed in section (8.2) were used for this purpose. The effects of thickness, sawing pattern (whether quarter-sawn or back-sawn) and coating properties (performance) on the maximum tensile stresses generated at the board surfaces were investigated. The theoretical drying conditions used in all calculations were identical. The following data were used and the results graphed in figures (8.4, a, b, c, d & e).

Material Properties:

Tangential diffusivity, $\mathcal{D}_t = 1.2_{10}{}^{-7}$ $m^2/hr.$

Radial diffusivity, $\mathcal{D}_r = 1.7_{10}{}^{-7}$ $m^2/hr.$

(values assumed constant: temperature = 20^0C).

Tangential shrinkage strain, $\varepsilon_{s_t} = 0.055 + \frac{0.11}{\pi}\arctan\left[\frac{90-c}{53}\right]$.

Radial shrinkage strain, $\varepsilon_{s_r} = 0.03 + \frac{0.06}{\pi}\arctan\left[\frac{82-c}{41}\right]$.

Tangential modulus of elasticity,

$$E_t = 500_{10}{}^6(1+2.72\ exp(-\frac{c}{90}))\ Pa.$$

Radial modulus of elasticity,

$$E_r = 1000_{10}{}^6\ (1 + 2.72\ exp\ (-\frac{c}{90}))\ Pa.$$

Modulus of rigidity in the radial-tangential plane,

$$G_{rt} = 200_{10}{}^6\ (1 + 2.72\ exp\ (-\frac{c}{90}))\ Pa.$$

Poisson's ratios (assumed independent of moisture concentration),

$$\mu_{zt} = 0.50\ , \qquad \mu_{tz} = 0.026\ ;$$

$$\mu_{zr} = 0.41\ , \qquad \mu_{rz} = 0.041.$$

Initial moisture concentration, $c_o = 500\ kg/m^3$

Constant drying conditions of 20°C and 60% relative humidity giving a wood fibre equilibrium moisture concentration = 70 kg/m^3 (roughly equivalent to a moisture content of 11% on a dry basis).

Boundary moisture concentration conditions:

General expression $$c = c_b + (c_o - c_b)\ exp\ (-\frac{T^{\cdot 286}}{A})$$

(see figure 8.1)

The following values of the constant A are strictly applicable to 28 mm boards dried under conditions of 25°C and 50% relative

humidity only, although, when used on boards of a different thickness, they give an indication of the performance of the various coatings.

Uncoated boards, $A = 0.8$

Coated boards: - (animal glue-talcum powder mix, Chapter 5)

- thickness = 0.7 mm, $A \simeq 3.4$
- thickness = 0.3 - 0.5 mm, $A \simeq 2.$

From calculated stress distributions, the maximum tensile stresses in sawn boards (during the early stages of drying) were found to act at the free surfaces.

Figures (8.4) give the calculated drying curves and the variation of the surface stresses with time for boards with original (green) thicknesses of 12, 19, 23, 28 and 45 mm. Each figure compares the drying of uncoated quarter-sawn and back-sawn boards with coated back-sawn boards of the same thickness.

12 mm THICK BOARD — DRYING CURVES AND TENSILE STRESS SURFACE

KEY: 1 - Quarter-sawn , uncoated.
2 - Backsawn , uncoated.
3 - Backsawn , coated , TF = 3·43
4 - Backsawn , coated , TF = 2·0

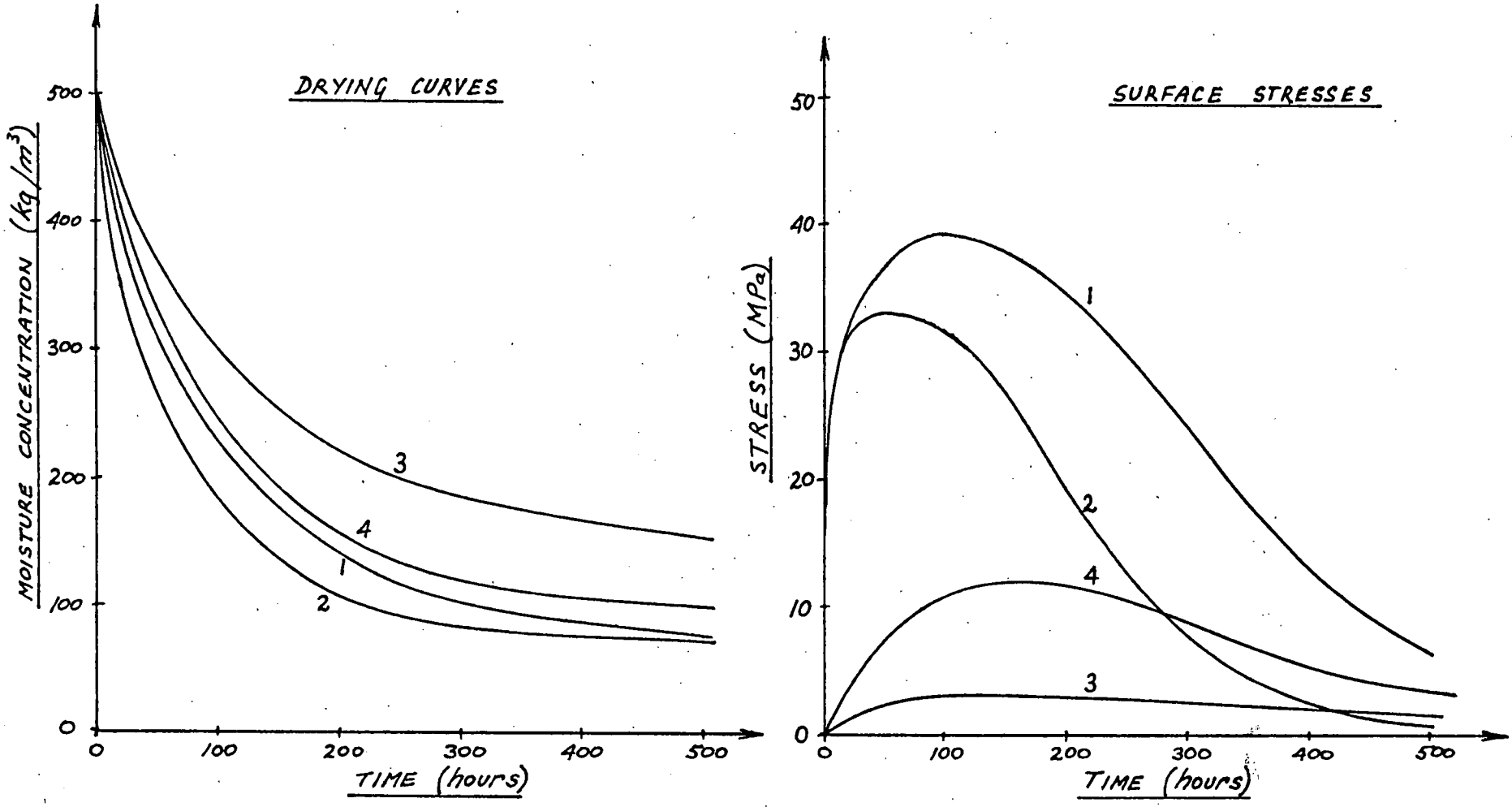

FIGURE (8·4, a)

19 mm THICK BOARD — DRYING CURVES AND TENSILE STRESS AT SURFACE

KEY: 1 – Quarter-sawn, uncoated.
2 – Back-sawn, uncoated.
3 – Back-sawn, coated, TF = 3·43
4 – Back-sawn, coated, TF = 2·0

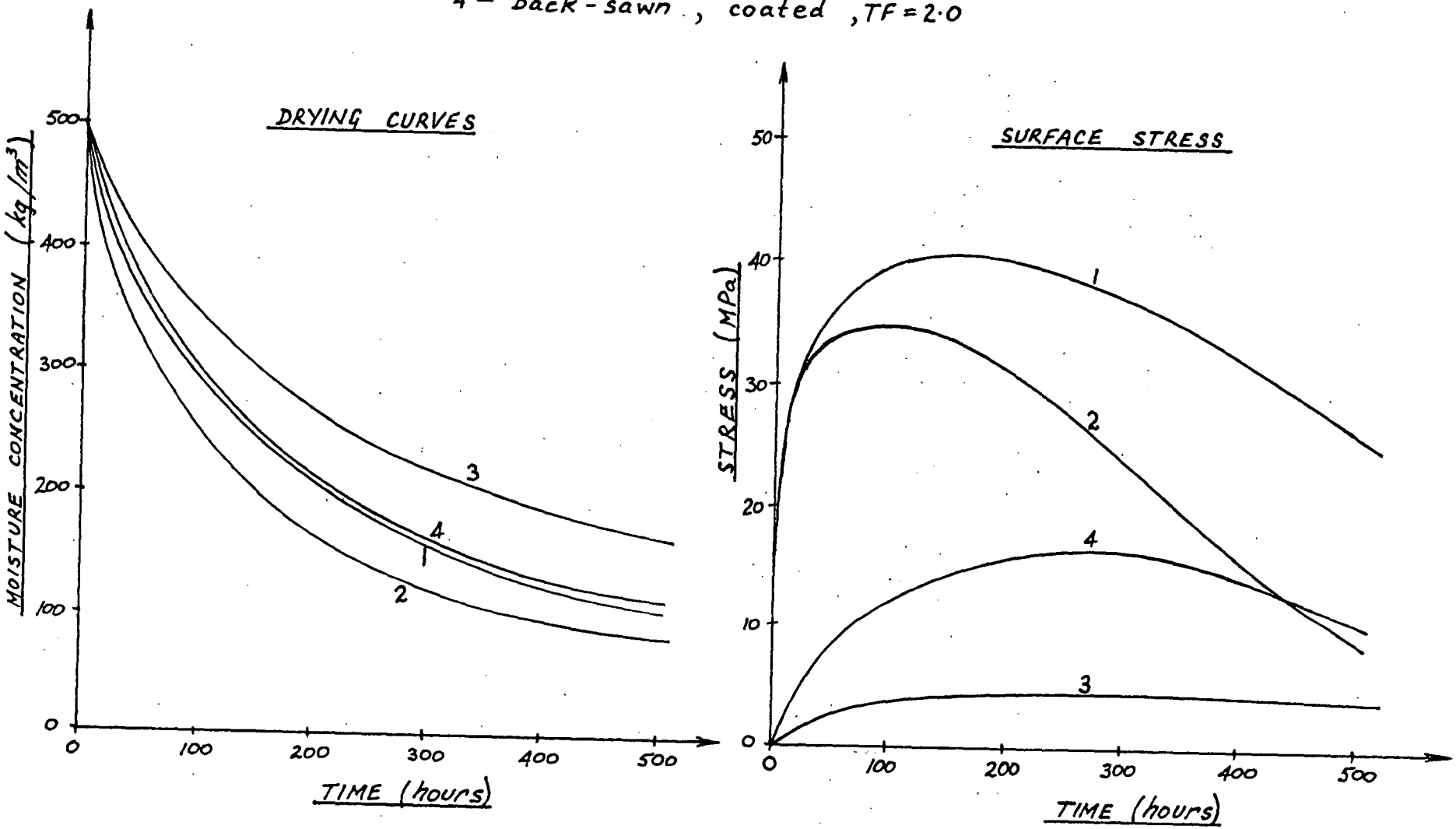

FIGURE (8·4, 6)

23 mm THICK BOARD — DRYING CURVES AND TENSILE STRESS AT SURFACE

KEY: 1 - Quarter-sawn, uncoated.
2 - Back-sawn, uncoated.
3 - Back-sawn, coated, TF = 3·43
4 - Back-sawn, coated, TF = 2·0

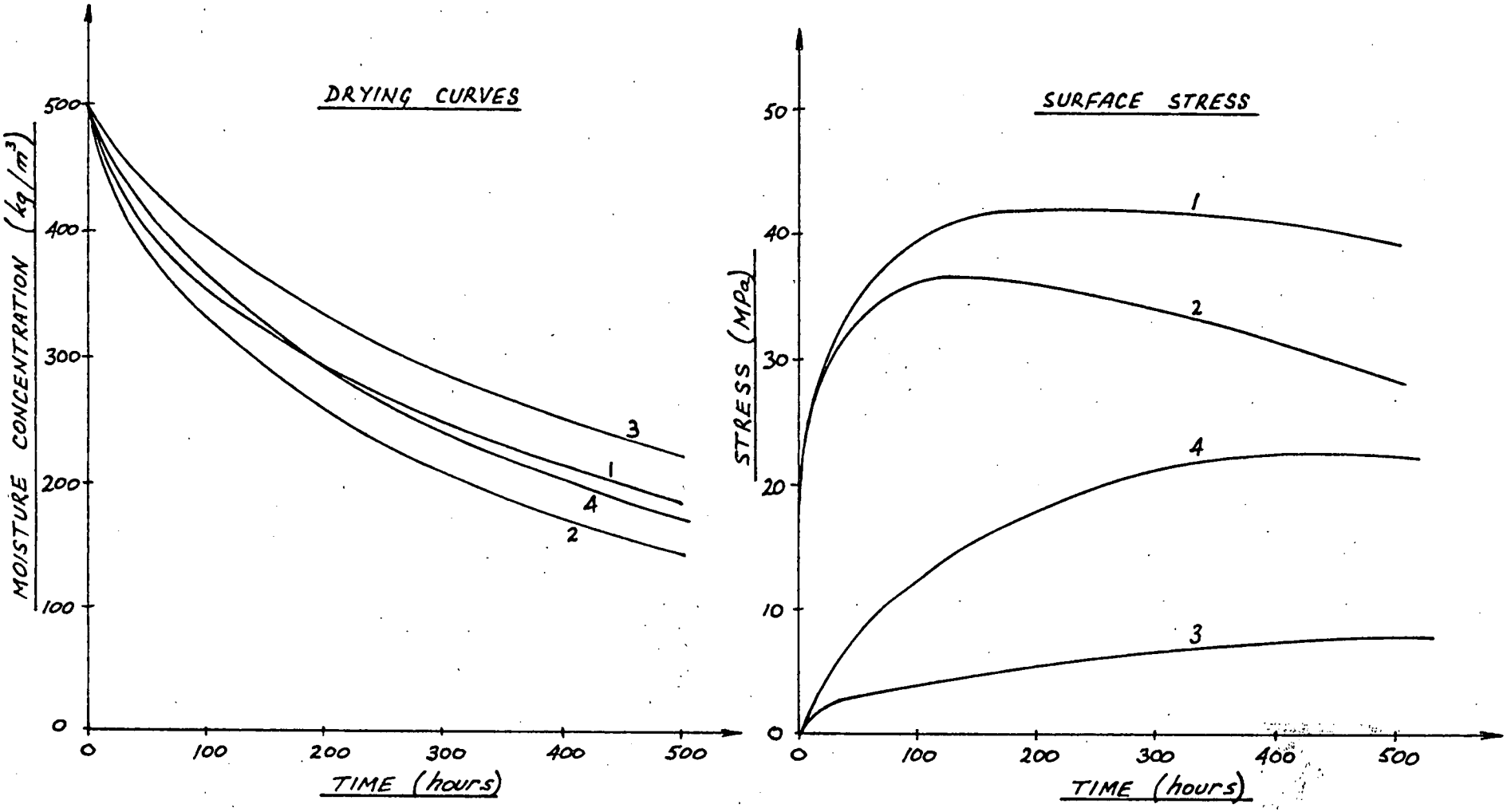

FIGURE (8·4, c)

28 mm THICK BOARD — DRYING CURVES AND TENSILE STRESS AT SURFACE

KEY: 1 – Quarter-sawn, uncoated.
2 – Back-sawn, uncoated.
3 – Back-sawn, coated, TF = 3·43.
4 – Back-sawn, coated, TF = 2·0.

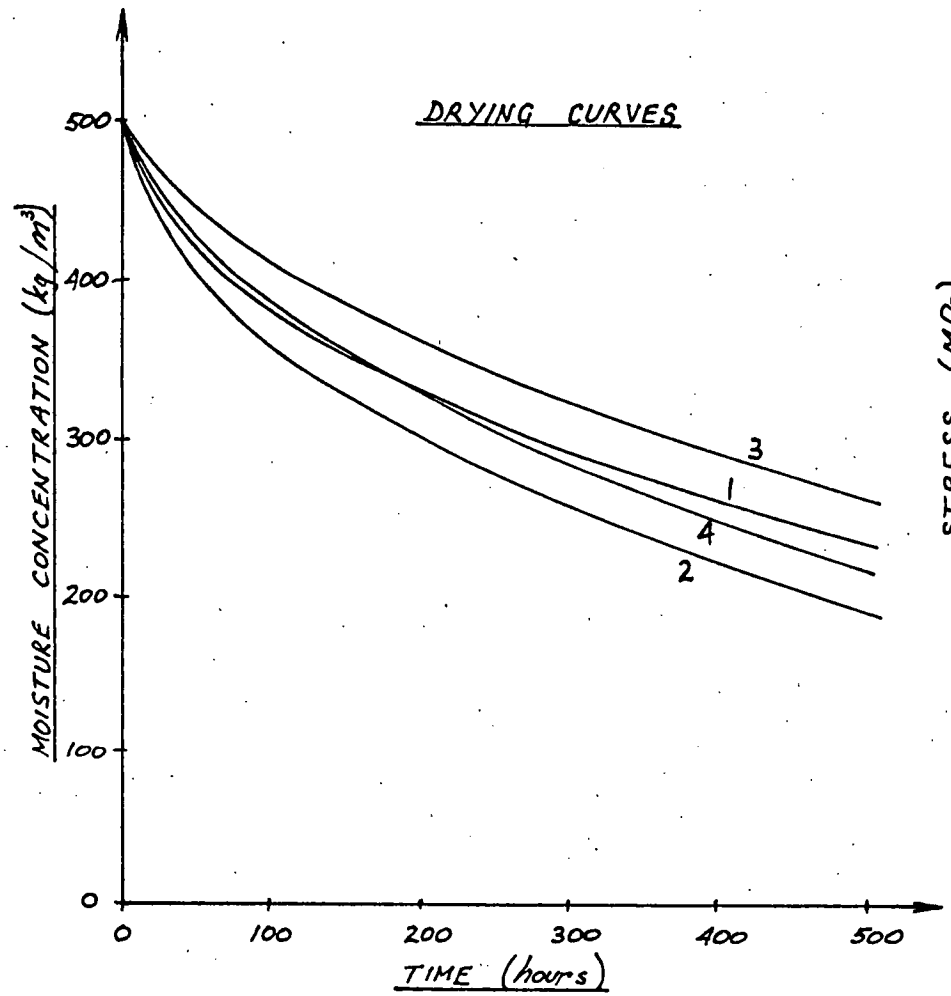

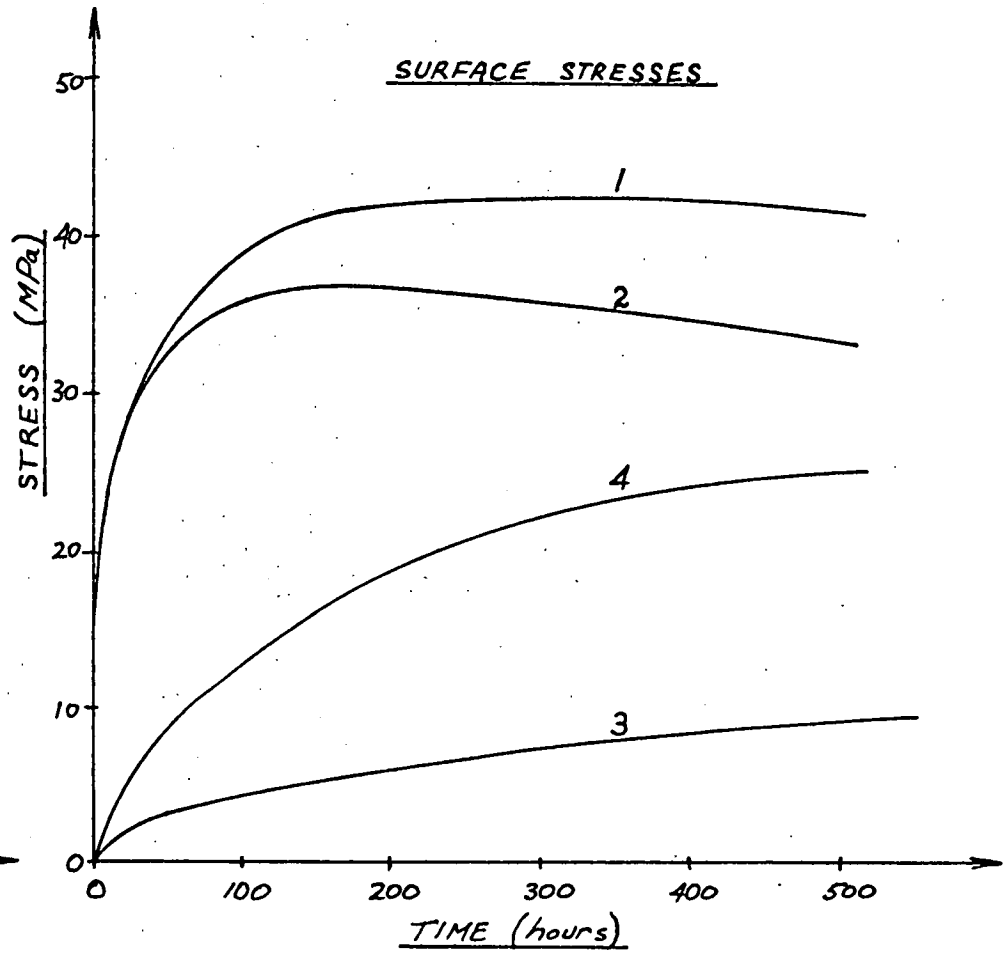

FIGURE (8·4.d)

45 mm THICK BOARD — DRYING CURVES AND TENSILE STRESS AT SURFACE

KEY: 1 - Quarter-sawn, uncoated.
2 - Back-sawn, uncoated.
3 - Back-sawn, coated, TF=3·43
4 - Back-sawn, coated, TF=2·0

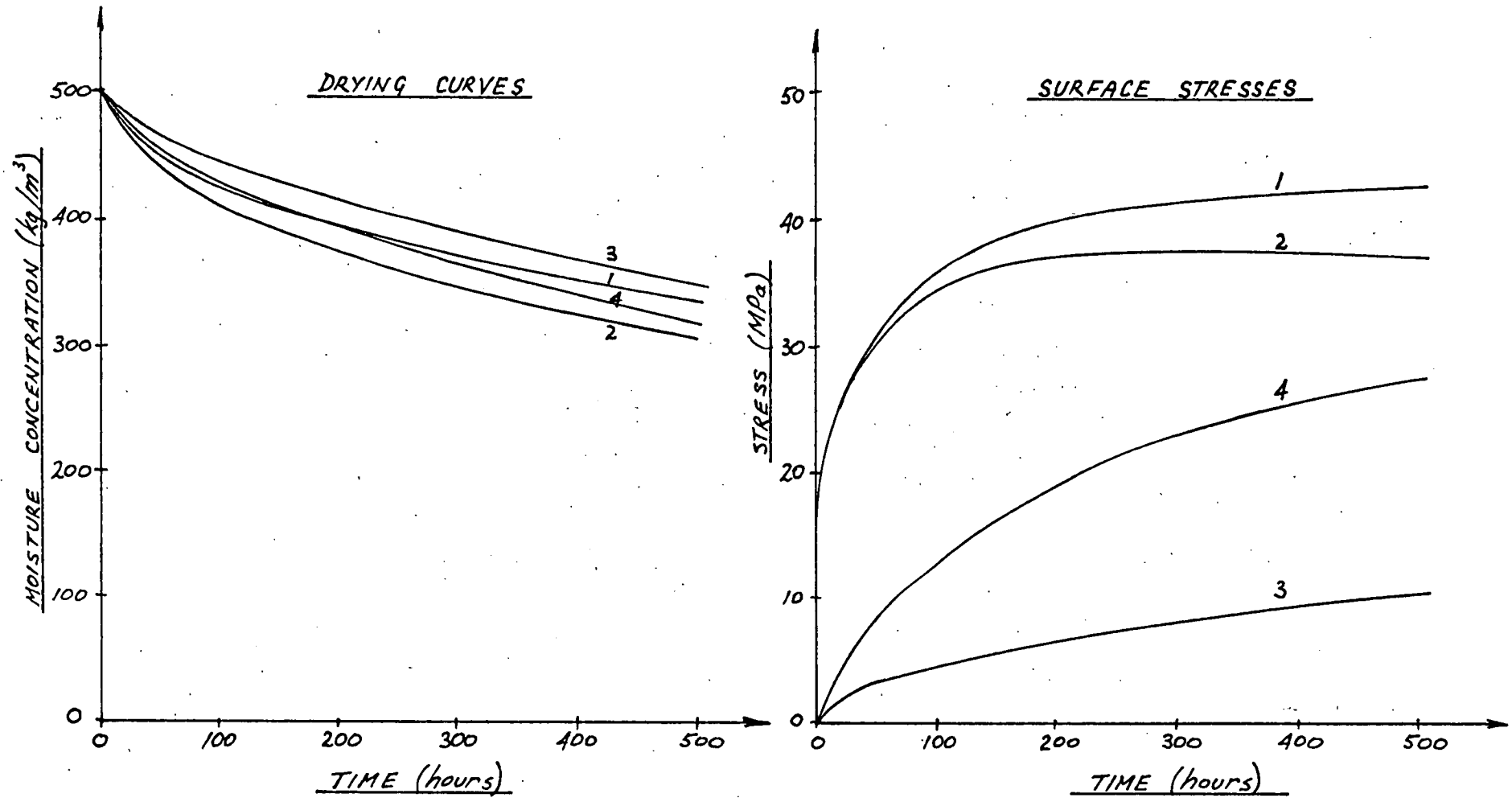

FIGURE (8·4, e)

8.4.2 General Trends.

A number of deductions can be made from a comparison of the results presented in figures (8.4).

Firstly, and most importantly, the drying stresses in coated boards are considerably less than those in uncoated boards of the same thickness, dried under the same conditions. However, coated material dries at a slower rate than uncoated material.

The maximum tensile drying stresses at the surface of uncoated quarter-sawn boards are approximately 15% larger than those in uncoated back-sawn boards over the range of thicknesses analysed. The incidence of face-checking in quarter-sawn "Tasmanian Oak" is very low (unlike back-sawn "Tasmanian Oak"), indicating that the ultimate tensile strength in the tangential direction is significantly less than that in the radial direction. Tests reported in chapter 7 and Appendix E indicate that

$$\frac{\text{Ultimate radial tensile strength}}{\text{Ultimate tangential tensile strength}} \simeq 1.6$$

The calculated maximum stress levels in uncoated back-sawn boards vary by only 10% between 12 and 45 mm thick material. However, the thicker the board, the longer the duration of "high stress levels"

("high stress levels" : stresses less than, say, 20% below the maximum) and the thicker the coating required to limit the surface stresses to a given level.

In practice, it has been observed that the percentage of 12 mm back-sawn (uncoated) "Tasmanian Oak" boards drying without face checks is very much greater than that for 25 mm back-sawn stock (approximately 50% compared to 15%). The indication (from figures 8.4, a and c) is that the duration of the period of "high stress" is extremely important.

8.4.3 Drying stresses in 25 mm (nominal thickness) "Tasmanian Oak" Boards. Refer to figure (8.4,d).

After 500 hours (3 weeks) of drying from their original moisture concentrations of 500 kg/m^3, the average moisture concentration in the back-sawn board with the 0.7 mm coating (figure 8.4,d, curve"3") is 260 kg/m^3 compared with 235 kg/m^3 for the uncoated quarter-sawn board and 190 kg/m^3 for the uncoated back-sawn board (according to the mathematical model). The maximum tensile stress in the surface fibres of the uncoated back-sawn board is 3 times that in the back-sawn board with the 0.7 mm coating. The maximum stress in the uncoated back-sawn board is reached only after 170 hours (7 days) drying but the stresses in the coated board reach a maximum some time after 500 hours drying.

The large-scale drying tests described in chapter 5 indicated that drying 25 mm (nominal thickness) back-sawn "Tasmanian Oak" boards using the 0.7 mm animal glue-talcum powder coating resulted in the elimination of face checks from a large proportion of material. Furthermore, the 0.4 mm coating applied to stack 1 (section 5.5.5) was found only to delay the onset of face-checking by three to four days. From these observations and an examination of the calculated surface stress-time relationship of figure (8.4,d), it was deduced that prolonged action of tensile stresses greater than approximately 15 MPa at the board surface (according to the model used) is likely to result in face-checking in 25 mm back-sawn "Tasmanian Oak" boards.

CHAPTER 9

CHAPTER 9

CONCLUSION

INTRODUCTION

The primary aim of this investigation was to develop a means of consistently and economically seasoning back-sawn "Tasmanian Oak" without degradation due to face-checking. The method of controlling checking by coating back-sawn boards with permeable materials, "green off saw", was thoroughly investigated. Emphasis was placed on developing the theory and mathematics related to the behaviour of coated timber and to demonstrate the effectiveness of one particular coating material in controlling face-checking in 25 mm (nominal thickness) back-sawn "Tasmanian Oak" boards. In proving the coating technique suitable for controlling checking in back-sawn "Tasmanian Oak", the economic and some of the practical (production) requirements of industry were not of

primary importance. However, as a result of the establishment of a reliable method of controlling checking, the way has been cleared for the development of an economic industrial process.

During this investigation, theory and measurements have been developed in parallel. Accurate modelling of the processes occuring in individual boards enables prediction of the behaviour of large populations to be made. Mathematical models were used to analyse data collected from tests on small sample populations. Any refinements to the models indicated by the results of such an analysis were checked by subsequent testing. Following the development of the models to the required degree, the effects of various surface coatings on the seasoning of back-sawn "Tasmanian Oak" were examined quantitatively.

It is intended that the simple mathematical models developed during this investigation be refined further and used extensively during the development and optimisation of an economic process for seasoning back-sawn "Tasmanian Oak" on an industrial scale, thus limiting the need for large-scale, time-consuming and expensive testing programs.

FURTHER WORK

The ultimate conclusion to research into the seasoning of back-sawn "Tasmanian Oak" is the introduction of an economic process to industry. It is the intention

of the Tasmanian Timber Promotion Board to actively pursue this end.

There are a number of related fields in which further work is required if the coating (or pre-surfacing) technique of seasoning is to be developed for use in the Tasmanian hardwood milling industry. These areas may be summarised under four general headings, none of which should be considered independently of the others:

1) Coating materials - physical properties, practical requirements. Economics.

2) Refinement of the mass transfer model - effects at wood/coating interface (eg. moisture concentration discontinuities, chemical effects etc.).

3) Refinement of the drying stress model - inclusion of the effects of curvature of growth rings, non-linear material properties, creep, etc.

4) Wood property determination and correlation.

Work is proceeding in the area of item 1) and an extensive study under the heading of item 4) is scheduled for commencement in the near future. It is the author's intention to investigate topics related to items 2) and 3) as the needs arise during the development of the coating/seasoning process in industry.

The requirments of the coatings are many fold:

1) They must have the correct combination of thickness and diffusivity.

2) They must adhere to the surfaces of "green" timber and air must be excluded from the interface.

3) They must remain pliable for long periods - that is, they must shrink as the board shrinks (or deforms) without affecting the wood/coating bond.

4) They must be economic in terms of material cost, capital investment and drying time.

5) They must be relatively tough - suitable for handling within a short time after application (of the order of 1 minute).

6) They must be applied quickly and uniformly.

7) They must be easily (economically) removable.

The animal glue/talcum powder coating mix used during this investigation was found to satisfy requirements 1, 2, 3, 5 and 6. However, it was difficult to remove on completion of drying, due mainly to its abrasive nature. Furthermore, at current (1981) bulk prices, the material cost of coating a total volume of 1 m^3 of 25 mm (nominal thickness) boards with the animal glue/talcum powder mix is roughly $A180. The current market value of 1 m^3 of premium grade 25 mm quarter-sawn timber is between $A350 and $A400. It is estimated that if the material cost of the coating were reduced to $A40/$m^3$ or less, a large percentage of the total volume of hardwood produced annually in Tasmania for

decorative end uses could be economically back-sawn.

The work presently being conducted on coatings is centred on a number of readily available materials. Particular attention is being paid to economics.

It is proposed that the mathematical model be refined by making a number of modifications. The effects of creep (semi-permanent deformation), hysteresis (permanent deformation) and the time-dependence of fracture stresses should be introduced. This would ensure that the behaviour of "Tasmanian Oak" during drying predicted by the model would more closely match that observed.

Further refinement is possible by catering for the non-linear elastic properties of timber and the addition of the full expression describing the state of stress in orthotropic bodies, including allowance for the curvature of growth rings. Upon reaching this stage, it might be worth while including the effects of changing mass diffusivity and shrinkage separately and to work with the changing dimensions of the board.

According to foresters and timber-millers, the properties of timber vary markedly within species as a result of growing conditions (soil type, rainfall, altitude, slope.....). Hence, the average properties and the variability of the raw material (logs) available at each mill is different.

The simple model used during this investigation would provide an adequate means of predicting the bahaviour of back-sawn boards for an initial feasibility study, providing that the mean (linearised) properties of the available material were known. A more refined model would have to be used to maximise profitability at any particular mill and, in keeping with this, a more detailed picture of the properties of the available resource would be needed.

The profitability of production of back-sawn "Tasmanian Oak" using the coating method depends upon the balance between the rate of degradation, drying time and coating cost per unit thickness.

Associated with the determination of the mean wood properties and their variation is the possibility of correlating particular properties such as density, permeability, shrinkage and strength. If relatively simple tests could be devised to identify material, the behaviour of which deviated greatly from the mean, profitability could be increased further by grouping the logs (before sawing) into:

1) Those requiring thick coatings and long drying times if back-sawn. For economic reasons, these would most probably be quarter-sawn;

2) Those that would dry at an economic rate if back-sawn and coated: and

3) Those that would dry with minimal degrade if back-sawn and not coated.

Experimental work in the immediate future will be conducted in the related fields of coating property measurement (and economic analysis etc.) and statistical wood property determination and correlation.

APPENDICES

APPENDIX A

NOMENCLATURE

Except where otherwise specified, the symbols used in the text of this thesis have the meanings specified in the following tables. Where the "occurence" is not given the meaning quoted applies throughout the text.

UPPER-CASE LETTERS

Symbol	Occurence	Description	Units
A	Ch. 5	Area	m^2
A	Ch. 7	Constant	
$A_1,...A_4$.	Ch. 6	Elastic coefficients (see equation 6.32, page 186)	m^2/N
$B_1,...B_9$.	Ch. 6	Elastic coefficients (see Addendum, Ch. 6, page 211)	m^2/N
C	———	Specific heat	kJ/kgK
D	———	Mass diffusion coefficient (or diffusivity)	m^2/s or m^2/hr
D	Eq. 3.3	Mass diffusion coefficient	m^2s
E	Ch. 3	Activation energy of diffusion	kJ/kg
E	———	Young's modulus	Pa
F	Ch. 3	Mass flux per unit area	kg/m^2s
G	———	Modulus of rigidity (sheer)	Pa
J	Ch. 7	Polar moment of inertia	m^4
K	Ch. 3	Constant	
K	Ch. 6	"Stiffness" of a restraint on a body	1/m
M	———	Moisture content	kg/kg
P	Ch. 3	Vapour pressure (of water)	Pa
Q	Ch. 3	Heat flux per unit area	W/m^2
R	———	Universal gas constant (R=8.317)	kJ/moleK

Symbol	Occurence	Description	Units
T	———	Temperature	^{o}C
T	Ch. 7	Torque (applied)	Nm
T	Ch. 8	Time	s
X	Ch. 6	Body force per unit volume acting in the x-direction	N/m^3
y	Ch. 6	Body force per unit volume acting in the y-direction	N/m^3
Z	Ch. 6	Body force per unit volume acting in the z-direction.	N/m^3

LOWER-CASE LETTERS

a	Ch. 3	constant	
c	———	Moisture concentration	kg/m^3
d	Eq. 3.21	Interface mass transfer coefficient	m/s
d	Eq. 3.22	Coating thickness	m
d	Ch. 5	Coating thickness	m
e	———	Mass flux per unit area	kg/m^2s
f	Ch. 3	Mass flux per unit area	kg/m^2s
f	Ch. 6	A function of x and y.	
g	Ch. 6	A function of x and y.	
i	———	Finite difference mesh coordinate	
j	———	Finite difference mesh coordinate	
k	Ch. 3	Thermal conductivity	$W/m^{o}C$
p, q	Ch. 6	Direction coordinates	
	Ch. 6, 7	Radial direction (w.r.t. a log of wood)	
t	Ch. 3, 5	Time	s
t	Ch. 6, 7	Tangential direction (w.r.t a log of wood)	

Symbol	Occurence	Description	Units
u	Ch. 3	Direction coordinate	m
u	Ch. 6	Displacement in the x-direction	m
v	Ch. 3	Direction coordinate	m
v	Ch. 6	Displacement in the y-direction	m
w	Ch. 6	Displacement in the z-direction	m
x, y	———	Direction coordinates	m
z	Ch. 6, 7	Direction coordinate Longitudinal direction (w.r.t. a log of wood)	m

GREEK LETTERS

α	Ch. 3	Angle	rad.
α	Ch. 6	Coefficient of thermal expansion	$1/^{o}C$
α_{dry}	Ch. 3	Thermal diffusion coefficient (diffusivity)	m^2/s
β	———	Material swelling coefficient	m^3/kg
γ	———	Shear strain	m/m
ε	———	Direct strain	m/m
ε_s	———	Shrinkage strain	m/m
ζ	Ch. 3	Direction coordinate	
η	Ch. 3	Direction coordinate	
θ	Ch. 6	Angle or rotation of one frame of reference relative to another.	rad.
θ	Ch. 7	Angle of twist	rad.
μ	———	Poisson's ratios (material constants)	
ξ	Ch. 3	Direction coordinate	

Symbol	Occurence	Description	Units
ρ	———	Density	kg/m^3
σ	———	Direct stress	Pa
τ	———	Shear stress	Pa
ϕ	———	Airy stress function	

APPENDIX B

2-DIMENSIONAL MOISTURE TRANSFER PROGRAM - "TIMBER"

COMPUTER LANGUAGE - BASIC

MACHINE - DIGITAL PDP 11/10

GENERAL DESCRIPTION:

This program was originally written to enable the analysis of drying tests on small samples of "Tasmanian Oak". It solves the equation (3.18),

$$\frac{\partial c}{\partial t} = \frac{\partial}{\partial x}\left(D_{xx}\frac{\partial c}{\partial x}\right) + \frac{\partial}{\partial y}\left(D_{yy}\frac{\partial c}{\partial y}\right)$$

using the implicit finite difference method described in section 3.5.2. The above equation is applicable only to perfectly quarter-sawn or perfectly back-sawn timber under the assumption that the principal directions of diffusion are invariant over the cross-section of a board (section 3.3). Furthermore, as drying tests were conducted at low temperatures (dry bulb temperature < $40^{o}C$), and reasonably high humidities (typically 60% relative humidity), the thermal effects on diffusion coefficients have been ignored (section 5.3.2). The program listing included in this appendix contains some of the modifications necessary to solve the more general two-dimensional diffusion equation, equation (3.10).

DETAILS:

Grid points have been concentrated near the boundaries of the cross-section where the highest curvature of the moisture distribution occurs. The spacing of grid lines takes the form of a geometric progression with the geometric ratio ("distortion ratio"), R2. The grid covers only one quarter of the cross-section as the simplifications made in section 3.3 guarantee the symmetry of the

solution.

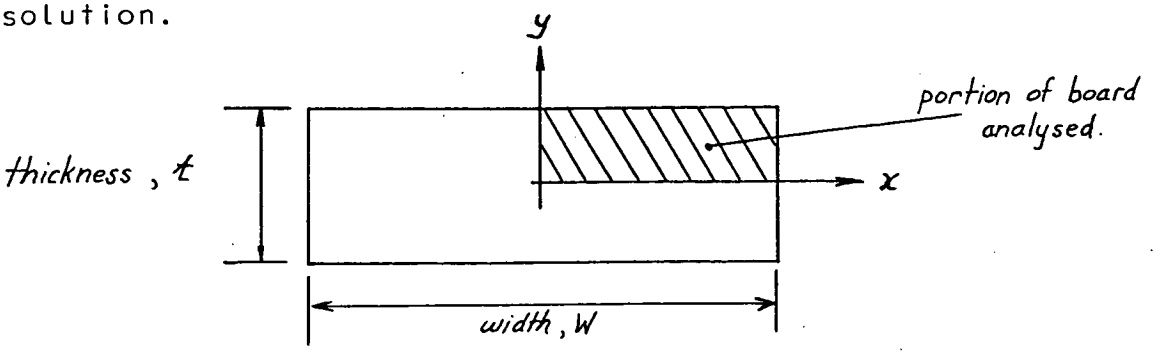

Consider the spacing of grid-lines in the y - direction.

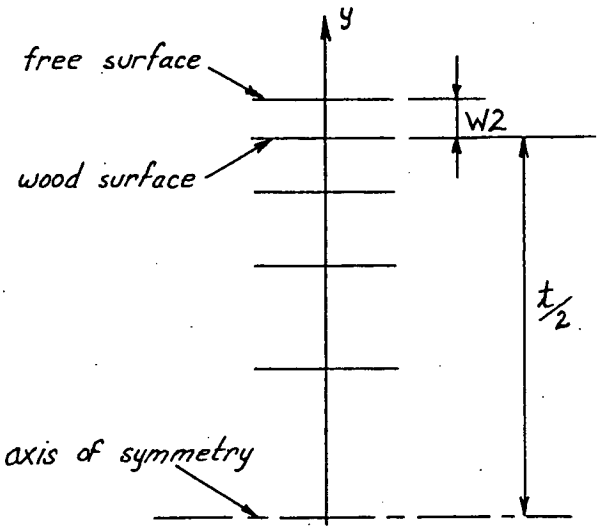

Provision has been made in the program for coatings on the wide face of the boards. Assume the first grid interval lies outside the timber.

W2 = the base y - increment size

M = the number of intervals in the y - direction ($M \leqslant 7$)

R2 = the distortion ratio of the grid.

Thus,

$$\frac{t}{2} = W2 \left[\frac{(R2)^{M} - 1}{R2 - 1} - 1 \right]$$

For given t, R2, M,

$$W2 = \frac{t}{2 \left[\frac{(R2)^{M} - 1}{R2 - 1} - 1 \right]}$$

Similarly, in the x - direction,

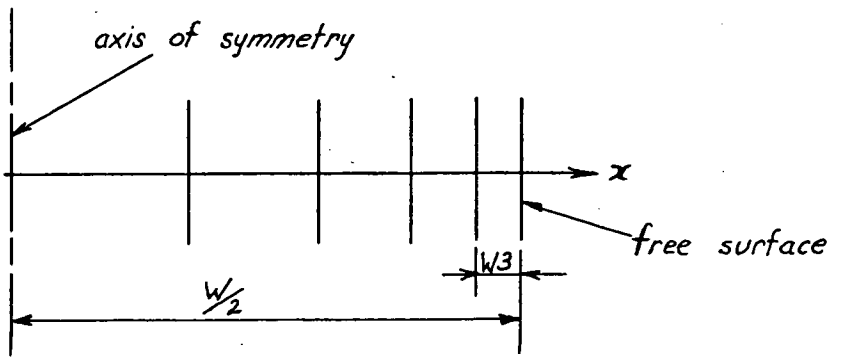

W3 = base x - increment size

N = number of intervals in the x - direction ($N \leqslant 12$)

R2 = grid distortion ratio (same in x & y direction).

For given W, R2, N,

$$W3 = \frac{W(R2 - 1)}{2\left[(R2)^{N} - 1\right]}$$

As previously mentioned, this program is suitable for analysis of moisture transfer through either perfectly quarter-sawn or back-sawn timber. The angle, A, between the linearised growth rings and the edge-planes of a board specify the type of board, viz:

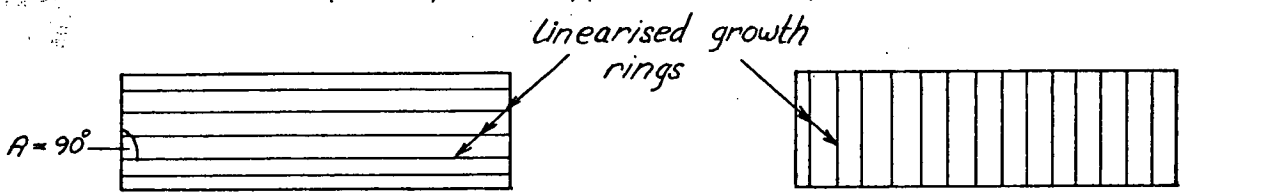

Back-sawn board, A = 90° Quarter-sawn board, A = 0°

The diffusion coefficients have been assumed to be constatnt (no variation with moisture concentration). Experiments show that

$$\frac{\text{Tangential diffusion coefficient}}{\text{Radial diffusion coefficient}} \simeq 0.7$$

at all concentrations.

For the purpose of easily handling the variation of diffusion coefficients found in Tas. Oak,

value of the radial diffusion coefficient, G1, has been left as a variable. Typically, G1 = $1.7_{10}{}^{-7}$ m^2/hr.

The required time step for the differencing system, T1, is quoted in hours.

The initial (uniform) average moisture concentration of a board, C7, is quoted in the units of mass concentration (kg/m^3), as is the equilibrium moisture concentration of the timber, C6, under the conditions of drying.

The distortion ratio of the grid, R2, should be less than 1.5 to ensure a stable solution. A typical value of R2 used was 1.4.

The number of intervals within a coating, I1, and the diffusivity of the coating, D5, have been included in the program for future analysis of coated timber. These parameters are not applicable to the drying of uncoated timber and for convenience may be given the following values:

I1 = 1

D5 = 1

INPUT/OUTPUT

Consider the analysis of the board shown below

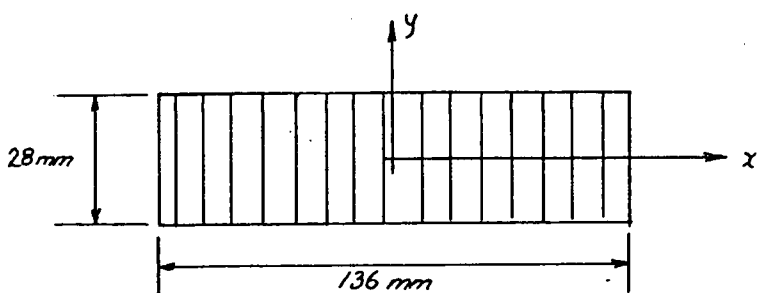

Quarter-sawn board

The initial moisture concentration in the board is 600 kg/m^3 and its dry density is approximately 700 kg/m^3. Drying takes place at 34°C and 72% relative humidity which gives an equilibrium moisture concentration in wood fibre

of approximately 85 kg/m^3 (from sorption isotherm and/or equilibrium tests).

Choose the number of grid intervals in both the x and y directions to be 7 and adopt a distortion ratio of 1.4. Therefore, the base y - increment size,

$$W2 = \frac{0.028}{2\left[\frac{(1.4)^7 - 1}{1.4 - 1} - 1\right]} = 613_{10}{}^{-6} \text{ m.}$$

Similarly, the base x - increment size,

$$W3 = \frac{0.136\ (1.4 - 1)}{2\left[(1.4)^7 - 1\right]} = 2.85_{10}{}^{-3} \text{ m.}$$

The board is quarter-sawn; thus, $A = 0^{o}$.
An initial estimate of the radial diffusion coefficient is $1.7_{10}{}^{-7}$ m^2/hr.

The data is entered into the program in the following way:

```
NO. OF INTERVALS WITHIN COATING =? 1
BASE X-INC. SIZE =? 2.85E-03
NO. OF INTERVALS IN X-DIRN.=? 7
BASE Y-INC. SIZE=? 6.13E-04
NO. OF INTERVALS IN Y-DIRN.=? 7
TIME STEP (HRS.)=? 2
ANGLE OF G.R. TO EDGE PLANES =? 0
MAX. RADIAL DIFF.COEFF.=? 1.7E-07
INITIAL M/C OF TIMBER =? 600
E.M.C. OF TIMBER IN AMBIENT AIR =? 85
DISTORTION RATIO OF GRID=? 1.4
DIFFUSIVITY OF COATING =? 0.01
```

Data output takes the following form:

```
 TIME(HRS.)= 10 AV.M.C.= 516.925
 TIME(HRS.)= 20 AV.M.C.= 496.538
 TIME(HRS.)= 30 AV.M.C.= 480.683
 TIME(HRS.)= 40 AV.M.C.= 467.315
 TIME(HRS.)= 50 AV.M.C.= 455.589
 TIME(HRS.)= 60 AV.M.C.= 445.056
 TIME(HRS.)= 70 AV.M.C.= 435.439
 TIME(HRS.)= 80 AV.M.C.= 426.554
 TIME(HRS.)= 90 AV.M.C.= 418.271
 TIME(HRS.)= 100 AV.M.C.= 410.497
 TIME(HRS.)= 110 AV.M.C.= 403.158
 TIME(HRS.)= 120 AV.M.C.= 396.198
 TIME(HRS.)= 130 AV.M.C.= 389.57
 TIME(HRS.)= 140 AV.M.C.= 383.239
 TIME(HRS.)= 150 AV.M.C.= 377.173
 TIME(HRS.)= 160 AV.M.C.= 371.346
```

```
1 REM:NAME "TIMBER"   DISTORTED GRID   PARTIALLY MODIFIED FOR COATINGS
2 DIM C(9,8),B(72,20),D(72,10),E(72,10),K(81),M(72),R(9)
4 PRINT "NO. OF INTERVALS WITHIN COATING ="; \ INPUT I1
5 PRINT "BASE X-INC. SIZE ="; \ INPUT W3
6 PRINT "NO. OF INTERVALS IN X-DIRN.="; \ INPUT N
7 PRINT "BASE Y-INC. SIZE="; \ INPUT W2
8 PRINT "NO. OF INTERVALS IN Y-DIRN.="; \ INPUT M
9 PRINT "TIME STEP (HRS.)="; \ INPUT T1                                    DATA
10 PRINT "ANGLE OF G.R. TO EDGE PLANES ="; \ INPUT A \ A=(A/180)*3.14159   INPUT
11 PRINT "MAX. RADIAL DIFF.COEFF.="; \ INPUT G1
12 PRINT "INITIAL M/C OF TIMBER ="; \ INPUT C7
13 PRINT "E.M.C. OF TIMBER IN AMBIENT AIR ="; \ INPUT C6
14 PRINT "DISTORTION RATIO OF GRID="; \ INPUT R2
15 PRINT "DIFFUSIVITY OF COATING ="; \ INPUT D5 \ PRINT  \ PRINT
16 FOR I=1 TO M \ FOR J=1 TO N \ C(I,J)=C7 \ NEXT J \ NEXT I
23 G=1 \ FOR Z=1 TO 80 \ T=Z*T1 \ C9=C6
24 FOR I=0 TO M \ C(I,0)=C9 \ NEXT I                                  INITIALISING
25 FOR J=0 TO N \ C(0,J)=C9 \ NEXT J \ GOSUB 100
26 IF G=5 GO TO 27 \ GO TO 43
27 PRINT "TIME(HRS.)="; \ PRINT T; \ PRINT "AV.M.C.="; \ PRINT C8   DATA OUTPUT
28 G=0
43 G=G+1 \ NEXT Z
44 G1=G1-2.50000E-08
45 PRINT  \ PRINT                                                  CONTROL STATEMENTS
46 GO TO 16
50 STOP
100 REM:SET UP AND SOLVE
102 J=1 \ FOR I=1 TO M \ K=I \ GOSUB 200
106 B(K,M+1)=1 \ B(K,2*M+1)=-X4 \ IF K=1 GO TO 110 \ IF K=M GO TO 112
108 B(K,M)=-Y4 \ B(K,M+2)=-Y3 \ B(K,2*M+2)=W1+X3*C(I,J-1) \ GO TO 114
110 B(K,M+2)=-Y3 \ B(K,2*M+2)=W1+X3*C(I,J-1)+Y4*C(I-1,J) \ GO TO 114
112 B(K,M)=-2*Y4 \ B(K,2*M+2)=W1+X3*C(I,J-1)
114 NEXT I
116 FOR J=2 TO N-1 \ FOR I=1 TO M \ K=M*(J-1)+I \ GOSUB 200
120 B(K,M+1)=1 \ B(K,2*M+1)=-X4 \ B(K,1)=-X3 \ IF I=1 GO TO 124 \ IF I=M GO TO 126
122 B(K,M)=-Y4 \ B(K,M+2)=-Y3 \ B(K,2*M+2)=W1 \ GO TO 128
124 B(K,M+2)=-Y3 \ B(K,2*M+2)=W1+Y4*C(I-1,J) \ GO TO 128          SETTING UP
126 B(K,M)=-2*Y4 \ B(K,2*M+2)=W1                                    MATRIX
128 NEXT I \ NEXT J
130 J=N \ FOR I=1 TO M \ K=M*(J-1)+I \ GOSUB 200
134 B(K,M+1)=1 \ B(K,1)=-2*X3 \ IF I=1 GO TO 138 \ IF I=M GO TO 140
136 B(K,M)=-Y4 \ B(K,M+2)=-Y3 \ B(K,2*M+2)=W1 \ GO TO 142
138 B(K,M+2)=-Y3 \ B(K,2*M+2)=W1+Y4*C(I-1,J) \ GO TO 142
140 B(K,M)=-2*Y4 \ B(K,2*M+2)=W1
142 NEXT I
```

```
144 FOR L=M+1 TO 2*M+2 \ D(1,L-M-1)=B(1,L) \ NEXT L
150 FOR Q=1 TO M*N-1 \ FOR L=M+1 TO 2*M+2 \ E(Q,L-M-1)=B(Q,L) \ NEXT L
152 FOR K=Q TO Q+M \ IF K>M*N GO TO 164 \ M(K)=-B(K,M-K+Q+1)/E(Q,0)
153 IF ABS(M(K))>1.00000E-10 GO TO 154 \ M(K)=0
154 FOR L=1 TO 2*M+1 \ IF L+K-Q-M-1<0 GO TO 158 \ IF L+K-Q-M-1>M GO TO 160
156 B(K,L)=M(K)*E(Q,L+K-Q-M-1)+B(K,L)
158 NEXT L                                          GAUSSIAN ELIMINATION
160 B(K,2*M+2)=M(K)*E(Q,M+1)+B(K,2*M+2)
162 NEXT K
164 FOR L=M+1 TO 2*M+2 \ D(Q+1,L-M-1)=B(Q+1,L) \ NEXT L \ NEXT Q
170 FOR K=M*N TO 1 STEP -1 \ R=0
172 FOR P=1 TO M \ R(P)=K(K+P)*D(K,P) \ R=R+R(P) \ NEXT P
174 K(K)=(1/D(K,0))*(D(K,M+1)-R) \ NEXT K          BACK-SUBSTITUTION
176 FOR I=1 TO M \ FOR J=1 TO N \ K=M*(J-1)+I
178 C(I,J)=K(K) \ NEXT J \ NEXT I
180 U8=0 \ FOR I=I1+1 TO M \ FOR J=1 TO N
181 U8=U8+((1/4)*(C(I,J)+C(I-1,J)+C(I,J-1)+C(I-1,J-1))*W2*W3*(R2^(I+J-2)))
182 NEXT J \ NEXT I                                 AVERAGE MOISTURE CONCENTRATION
184 U7=W2*W3*(1-R2^N)*(1-R2^M)/((1-R2)*(1-R2)) \ C8=U8/U7
186 RETURN
200 REM: MATRIX CO-EFFICIENTS
202 X5=(2*T1)/(W3*W3*(R2+1)*(R2^(2*J-1)))
204 Y5=(2*T1)/(W2*W2*(R2+1)*(R2^(2*I-1)))
                                    MATRIX CO-EFFICIENTS FOR DISTORTED GRID
206 IF I<I1 GO TO 252
208 M1=I \ N1=J-1 \ GOSUB 220 \ X3=D3*R2*X5
210 M1=I \ N1=J+1 \ IF N1>N GO TO 211 \ GOSUB 220 \ X4=D3*X5 \ GO TO 214
211 X4=X3
214 IF I=I1 GO TO 215 \ GO TO 216
215 Y4=D5*R2*Y5 \ GO TO 217
216 M1=I-1 \ N1=J \ GOSUB 220 \ Y4=D4*R2*Y5
217 M1=I+1 \ N1=J \ IF M1>M GO TO 218 \ GOSUB 220 \ Y3=D4*Y5 \ GO TO 219
218 Y3=Y4
219 GOSUB 260 \ RETURN
220 IF C(M1,N1)>71.26 GO TO 222 \ GO TO 224
222 D1=G1 \ D2=.7*G1 \ GO TO 230                    DIFFUSION
224 D1=.3*G1*(C(M1,N1)*C(M1,N1)/(71.26*71.26)) \ D2=.72*D1   CO-EFFICIENTS
230 D3=2*SQR(1/((2*COS(A)/D1)^2+(2*SIN(A)/D2)^2))
232 A1=(3.14159/2)-A
234 D4=2*SQR(1/((2*COS(A1)/D1)^2+(2*SIN(A1)/D2)^2))
235 RETURN
252 X3=D5*R2*X5 \ X4=D5*X5 \ Y3=D5*Y5 \ Y4=D5*R2*Y5
255 GO TO 219
260 R1=X3+X4+Y3+Y4+1                               MATRIX CO-EFFICIENTS (cld.)
262 X3=X3/R1 \ Y3=Y3/R1 \ X4=X4/R1 \ Y4=Y4/R1
264 W1=C(I,J)/R1
266 RETURN
270 IF T<20 GO TO 273 \ GO TO 277
273 C9=80+.8*T \ GO TO 290
277 IF T<40 GO TO 280 \ GO TO 283                  BOUNDARY CONDITIONS FOR
280 C9=96 \ GO TO 290                              PARTICULAR TEST
283 IF T<61 GO TO 285 \ GO TO 287
285 C9=134.8-.882*T \ GO TO 290
287 C9=85.23-.0693*T
290 RETURN
```

APPENDIX C

RESULTS OF DRYING TESTS

RUN 1 Samples from Geeveston area (S. Tas)
- probably E. delegatensis
- 4 fully quarter-sawn boards were used.

Samples 1 & 2 (136 x 28mm) - from same board: light in colour
Samples 3 & 4 (136 x 28mm) - from same board: dark in colour
Samples 5 & 6 (81 x 28mm) - from same board: dark in colour
Sample 7 (136 x 28mm) - light in colour.

All samples cut to a length of 360mm (approx)
- ends coated with a silicone-based sealant.

Drying was conducted in kiln A (section 5.2.2).
Approximate conditions 34°C (D.B.) and 30°C (W.B.)
corresponding to a relative humidity of about 75%.
The air-speed over the board faces was approx. 7.2 m/s.

The actual measured drying conditions are summarized below:

TIME (hours)	0	16	20	24	40	44	136	161.5
D.B. (°C)	34.1	33.8	33.8	35.9	34.0	34.0	34.2	33.9
W.B. (°C)	28.6	29.4	29.8	29.9	30.0	30.0	28.2	27.9

Notes:

1) After 16 hours drying, marked edge-checking on samples 3, 4, 5 and 6; face-checking on sample 7.
2) After 40 hours, little change in appearance of samples.
3) The moisture concentrations quoted in the results table are approximate only (see figure 5.1).

RUN 1

SAMPLE NUMBER	1		2		3		4		5		6		7	
Initial Mass (g)	1072.8		980.1		789.5		845.5		377.2		350.0		595.4	
Initial average moisture content	1.118		1.111		.914		.943		1.036		1.048		.843	
Initial average moist. concentration (kg/m^3)	674		669		552		569		625		632		509	
Mass after 16 hours	977.8	.930	883.3	.913	723.0	.753	774.3	.779	341.9	.845	317.4	.857	546.1	.690
Average m. content / Average m. concentration		561		551		455		471		510		517		418
20 hours	965.5	.906	877.8	.891	715.3	.734	766.4	.761	337.6	.822	313.2	.833	540.0	.672
		547		538		444		460		497		503		407
24 hours	953.9	.883	867.9	.869	708.0	.716	758.9	.744	333.8	.802	309.7	.812	534.3	.654
		533		525		433		450		485		491		396
40 hours	916.6	.810	834.2	.797	684.9	.660	734.4	.688	321.4	.735	298.0	.744	516.8	.600
		489		482		400		404		445		450		364
44 hours	909.0	.795	827.2	.782	679.9	.648	729.0	.675	318.8	.721	295.5	.729	512.7	.587
		480		473		393		409		436		441		356
48.5 hours	900.5	.778	819.8	.766	674.6	.635	723.0	.661	316.1	.706	292.7	.713	508.6	.574
		470		463		385		400		427		431		348
136 hours	789.9	.559	718.5	.548	604.3	.465	646.5	.486	280.0	.511	258.7	.514	453.8	.405
		339		333		283		296		311		312		247
161.5 hours	763.6	.508	693.5	.494	587.3	.424	628.3	.444	271.6	.466	250.8	.468	440.0	.362
		309		300		259		271		284		285		221

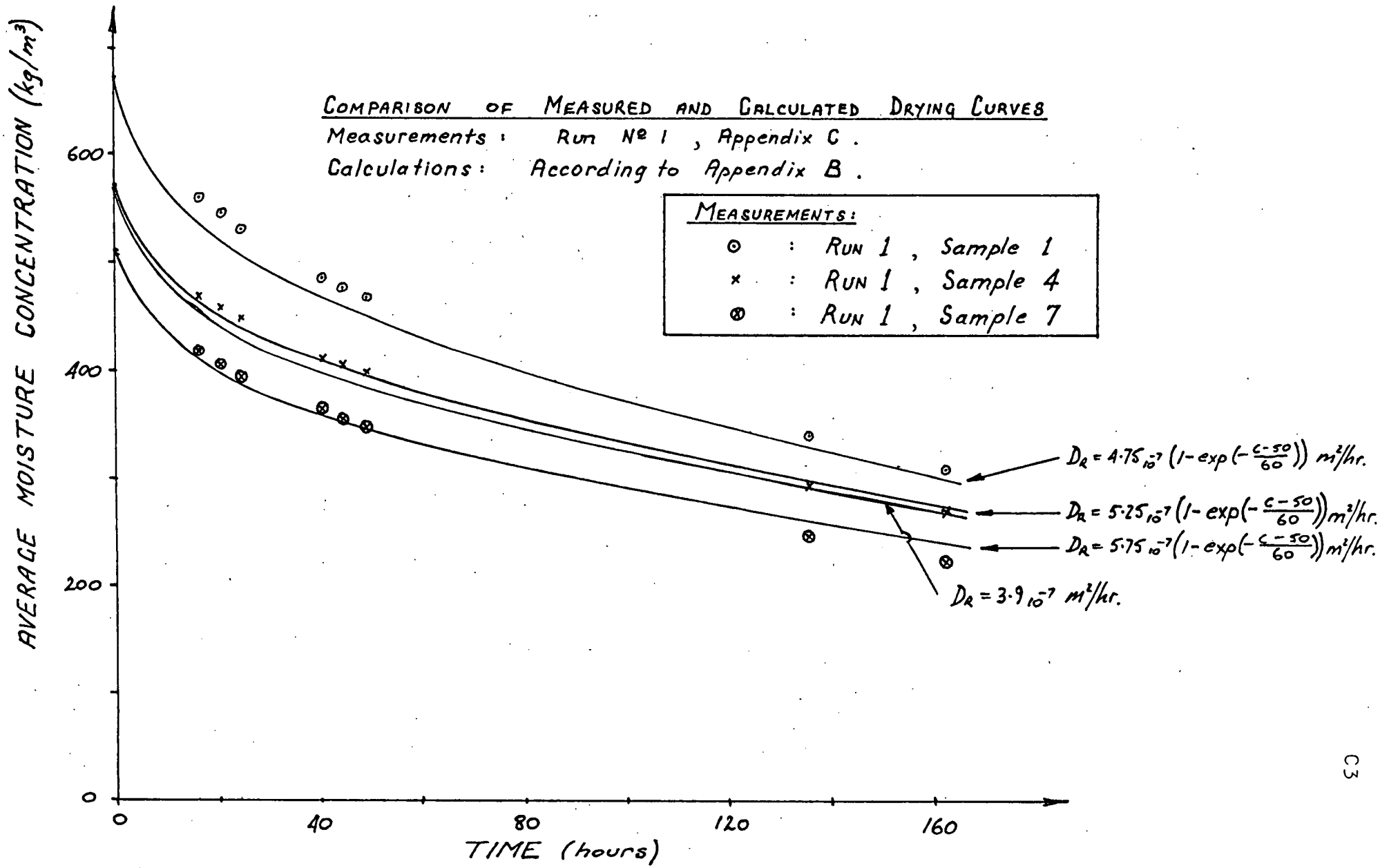
COMPARISON OF MEASURED AND CALCULATED DRYING CURVES
Measurements : Run Nº 1 , Appendix C .
Calculations : According to Appendix B .
MEASUREMENTS:
⊙ : RUN 1 , Sample 1
× : RUN 1 , Sample 4
⊗ : RUN 1 , Sample 7
AVERAGE MOISTURE CONCENTRATION (kg/m³)
600
400
200
0
0
40
80
120
160
TIME (hours)
$D_R = 4.75\,10^{-7}\,(1-\exp(-\frac{c-50}{60}))$ m²/hr.
$D_R = 5.25\,10^{-7}\,(1-\exp(-\frac{c-50}{60}))$ m²/hr.
$D_R = 5.75\,10^{-7}\,(1-\exp(-\frac{c-50}{60}))$ m²/hr.
$D_R = 3.9\,10^{-7}$ m²/hr.

RUN 2 Samples from Geeveston area (S. Tas.)
- probably E. delegatensis.
- 2 quarter-sawn boards were used.

Samples 1, 2, 3 and 4 were cut from one board (136 x 28mm) and samples 5, 6, 7 and 8 were from the other (136 x 28mm).

All samples cut to a length of 360mm (approx.)
- ends coated with a silicone-based sealant.

Drying was conducted in kiln A (section 5.2.2). Approximate conditions 37°C (D.B.) and 32°C (W.B.) for the first 145 hours, then 41°C (D.B.) and 33°C (W.B.). The air-speed over the board faces was approx. 3.6 m/s.

Notes:

1) After 4.7 hours drying, minor face checking was first noted.
2) 21 hours:- edge-checking apparent in 7 & 8
3) 45 hours:- slight face-checking 3, 5 & 6; edge-checking 7 & 8.
4) 285 hours:- collapse and/or dimensional distortion apparent in all samples.
5) 309 hours:- samples 3 & 4 in best condition.
6) The moisture concentrations quoted in the table of results are approximate only (figure 5.1).

RUN 2

SAMPLE NUMBER	1		2		3		4		5		6		7		8	
Initial Mass (g)	1109·5		1099·6		1107·1		1183·7		1050·5		1057·7		1020·4		1010·8	
Initial average moisture content	·963		·963		·994		·994		·962		·962		·922		·922	
Initial average moisture concentration (kg/m^3)	581		581		599		599		580		580		556		556	
Mass after 4·7 hours	1085·8		1082·6		1091·7		1171·7		1025·7		1038·5		1002·7		985·1	
Average m. content	·917		·931		·970		·974		·914		·926		·888		·871	
Average m. concentration	553		562		585		587		552		559		536		526	
21 hours	1030·8		1016·1		1030·0		1107·2		958·1		966·5		932·2		928·5	
	·820		·813		·859		·865		·788		·793		·755		·763	
	495		491		519		522		476		479		456		461	
45 hours	977·4		966·5		987·1		1055·5		897·9		903·6		882·9		876·6	
	·725		·724		·781		·778		·676		·676		·662		·665	
	439		438		472		470		409		409		401		403	
117 hours	890·3		877·1		907·2		968·7		810·1		810·9		796·5		794·8	
	·572		·565		·637		·632		·512		·504		·499		·509	
	347		343		386		383		311		306		303		309	
145·5 hours	866·0		851·6		886·2		944·4		784·6		785·7		774·2		772·4	
	·529		·519		·599		·591		·464		·457		·457		·467	
	321		315		363		358		282		278		278		284	
165.2 hours	844·0		829·6		866·2		922·3		763·1		764·1		753·9		752·2	
	·490		·480		·563		·554		·424		·417		·419		·428	
	298		292		342		336		259		254		256		261	
213·5 hours	806·1		793·9		833·6		885·4		727·9		728·7		720·9		717·6	
	·423		·416		·504		·492		·359		·352		·357		·363	
	258		254		306		299		220		215		218		222	
285 hours	769·6		759·3		802·8		849·5		690·5		693·3		688·2		685·7	
	·359		·355		·449		·431		·289		·286		·296		·302	
	220		217		274		263		178		176		182		186	
309 hours	757·7		746·7		791·0		835·8		680·4		682·4		676·5		673·7	
	·338		·332		·425		·408		·271		·266		·274		·281	
	207		204		259		249		167		164		169		173	
381 hours	721·7		711·3		757·2		798·8		651·5		652·5		647·6		644·3	
	·274		·269		·364		·346		·217		·210		·220		·225	
	169		166		223		212		135		131		137		140	
453 hours	686·4		677·1		721·6		761·7		625·7		626·1		620·7		617·6	
	·212		·208		·302		·283		·168		·161		·169		·173	
	132		129		186		174		105		101		106		108	

RUN 3 Samples from Geeveston area (S. Tas.)
- probably E. delegatensis
- 5 different boards were used.

Sample 1 (110 x 56mm) - quarter-sawn
Sample 2 (136 x 28mm) - quarter-sawn
Sample 3 (136 x 28mm) - back-sawn
Sample 4 (136 x 28mm) - back-sawn
Sample 5 (136 x 28mm) - back-sawn.

All samples were cut to a length of approx. 360mm
- ends coated with a silicone-based sealant.

Drying was conducted in kiln A (section 5.2.2)
Approximate conditions 41°C (D.B.) and 37°C (W.B.).
Air-speed over the board faces was approx. 2.5 m/s.

The actual measured drying conditions are summarised below:

TIME (hours)	0	5	21	25	45	52.2	117.5
D.B.(°C)	40.5	42.5	40.5	40.5	40.5	41.0	40.5
W.B.(°C)	35.5	37.5	36.5	36.3	35.5	36.0	35.5

Notes:

1) 3 hours: face-checking apparent in 2, 3 & 4
edge-checking in 3
2) 21 hours: severe face-checking in 2, 3 & 4
minor face-checks in 7.
3) Moisture concentrations quoted in the table of results are only approximate (figure 5.1).

RUN 3

SAMPLE NUMBER		1		2		3		4		5	
Initial Mass (g)		977.2		873.0		892.4		822.2		878.9	
Initial average moisture content		1.220		1.294		.939		1.079		1.128	
Initial average moisture concentration		735		779		567		650		680	
Mass after 3 hours	Average m. content	957.4	1.175	850.3	1.234	869.4	.889	799.5	1.022	859.1	1.080
	Average m. concentration	708		743		537		616		651	
5 hours		948.4	1.155	838.9	1.204	858.9	.866	790.7	.999	850.0	1.058
		696		725		523		602		638	
21 hours		904.7	1.055	789.2	1.074	820.7	.783	746.8	.888	801.1	.940
		636		647		473		536		567	
25 hours		897.1	1.038	779.5	1.048	812.9	.766	740.3	.872	791.0	.915
		626		632		463		526		552	
45 hours		861.3	.957	733.2	.927	776.2	.687	701.7	.774	744.4	.802
		577		559		416		468		485	
52.2 hours		850.0	.931	721.5	.896	765.0	.662	690.7	.746	731.3	.771
		562		541		401		451		466	
117.5 hours		771.8	.753	632.3	.662	687.7	.494	614.8	.555	643.0	.557
		455		401		300		337		338	
141.5 hours		756.5	.719	616.8	.621	676.3	.469	600.4	.518	626.2	.516
		435		376		285		315		314	
165 hours		741.7	.685	601.4	.580	664.9	.445	581.5	.470	611.7	.481
		415		352		271		286		293	

RUN 4 Samples from Geeveston area (S. Tas.)
- probable E. delegatensis
- 1 fully back-sawn board used (109 x 60mm).

All samples were cut to a length of approximately 360mm. Ends of samples 1, 2 & 3 coated with silicone-based sealant - ends of sample 4 not sealed.

Samples 1 & 2 were dried in kiln A (section 5.2.2). Approximate conditions 34.5°C (D.B.) and 33.7°C (W.B.). Air-speed over the board faces was approx. 2.3 m/s.

Samples 3 & 4 were dried outside, under cover in ordinary atmospheric air.

Day 1: Mild, sunny day. 9°C, 55%r.h., light wind.
Day 2: Overcast and drizzling. 9°C & light wind.
Day 3: Clear, mild and still; changing to very windy and cold.
Day 4: Windy, overcast, cool.
Day 5: Overcast, cool, still.

Notes:

1) 22.6 hours: Bad face-checking on all samples - appears to be worse on one face than the other
2) 100 hours: Checks closing on 1 & 2? Checks on 3 & 4 more severe than those on 1 & 2.
3) Moisture concentrations only approximate (figure 5.1).

RUN 4

SAMPLE NUMBER		1		2		3		4	
Initial Mass (g)		2435.4		2405.3		2578.7		2605.7	
Initial average moisture content		1.035		1.035		1.035		1.035	
Initial average moisture concentration		624		624		624		624	
Mass after 3 hours	average content	2451.8	1.049	2421.0	1.048				
	average concentration		632		632				
4.5 hours		2446.4	1.044	2418.8	1.046				
			629		631				
22.6 hours		2410.2	1.014	2365.0	1.001	2538.2	1.003	2588.6	1.022
			611		604		605		616
28 hours		2402.7	1.008	2361.0	.998				
			608		602				
95 hours		2332.5	.949	2326.0	.968	2357.1	.860	2377.8	.857
			573		584		519		517
100 hours		2330.0	.947	2324.7	.967				
			571		583				
103.3 hours		2328.6	.946	2320.6	.963				
			571		581				
118.8 hours		2300.5	.922	2302.4	.948				
			556		572				
124.0 hours		2295.9	.918	2294.5	.941	2340.4	.847	2348.2	.834
			554		568		512		504
146 hours		2271.4	.898	2278.2	.927	2314.2	.826	2316.7	.809
			542		559		499		489
167.8 hours		2269.5	.896	2259.7	.921	2291.5	.808	2285.3	.785
			541		556		488		474
191 hours		2264.3	.892	2245.8	.900				
			538		543				
263 hours		2227.5	.861	2223.0	.881	2228.6	.759	2199.5	.718
			520		532		459		434

COMPARISON OF MEASURED AND CALCULATED DRYING CURVES (ONE - DIMENSIONAL DRYING)

MEASUREMENTS:

25·0 mm thick back-sawn board, sealed on edges and ends; dried in an atmosphere at 37 °C and 50 % relative humidity. No checking occured.

CALCULATIONS:

Computer program of Appendix F with radial diffusivity of wood, $D_R = 0{\cdot}75_{10}{}^{-7}$ m²/hr.

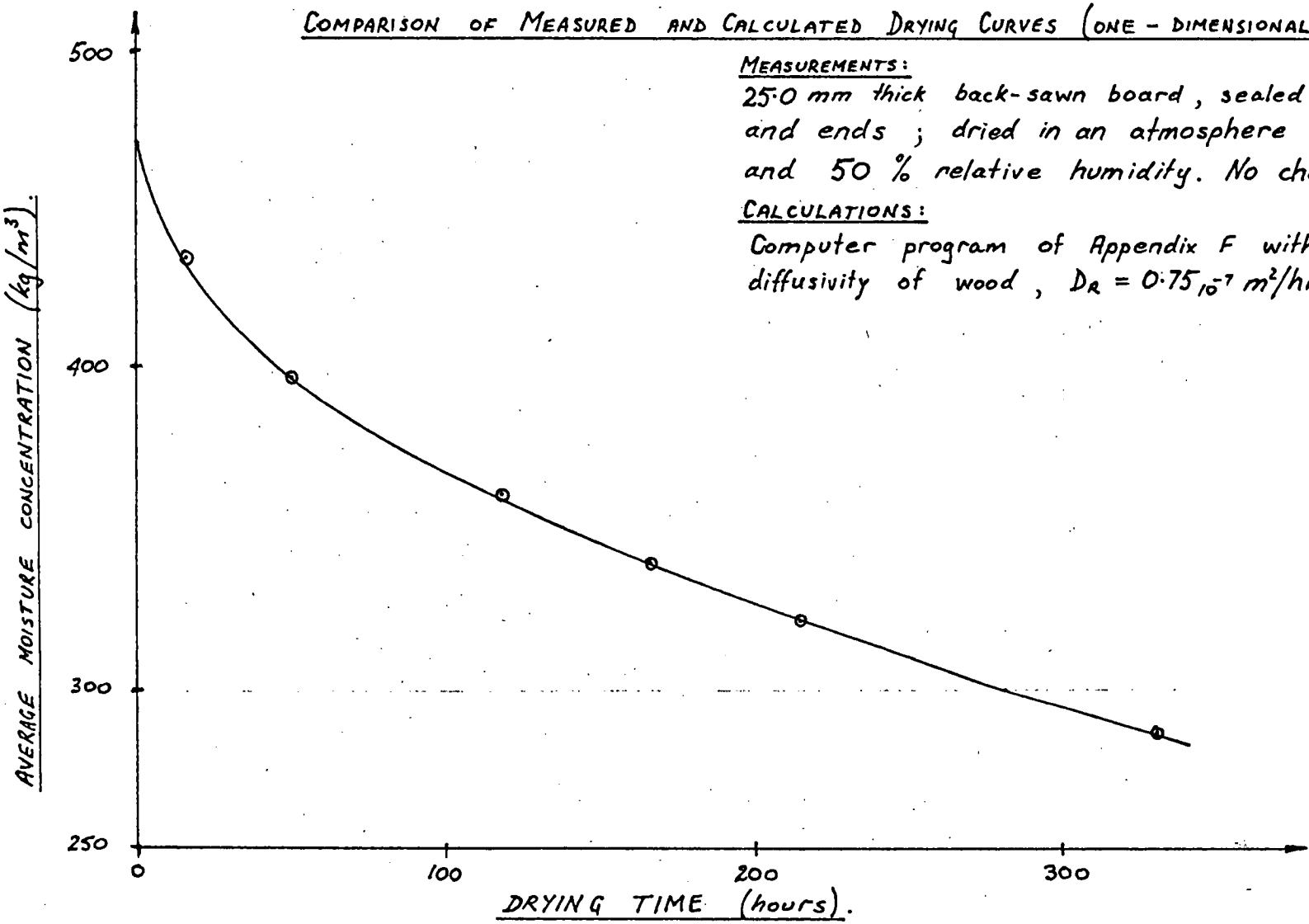

APPENDIX D

Selection of coating materials

Doe (1973,a) found that the mass diffusivity of gelatine was approximately $0.78_{10}{}^{-10}$ m^2/s. The thickness of gelatine required to hold the surface fibres of "Tasmanian Oak" above the fibre saturation point for 5 days (from equation 3.28) is in the range of 3.45 to 4.85 mm (see section 5.4.2). It was proposed that gelatine be used as a bonding agent for a coating based on wood-pulp as both materials were readily available. With proper compaction, it was estimated that the wood-pulp coating would have a diffusivity similar to that of wood fibre in sawn timber. Based on this assumption, the thickness of coating required was calculated to be between 1.73 and 2.45 mm.

Coatings made from dry saw-dust, gelatine and water mixed in the proportions

1 water : 0.10 to 0.18 saw-dust : 0 to 0.08 gelatine (by weight) were prepared in a high-speed mixer and applied to the faces of back-sawn "Tasmanian Oak" boards. The large amount of water present in the mix was found necessary to produce a workable paste. After application to the surfaces of boards, the coating was rolled in an attempt to eliminate air bubbles. However, the rolling process resulted in the loss of a large amount of the liquid and hence the dissolved bonding agent. The thickness of the wet coating was roughly 2.5mm. Drying was conducted at 25°C and 50% relative humidity.

The uncoated control boards all checked during the first 5 hours of the test. Checks also appeared in all of the coated boards but in these, checking was delayed

for approximately 1 day. The delay in the onset of checking indicated that the surface fibre moisture concentrations had been held above the fibre saturation point for about 20 hours.

Close examination of the coating revealed that the gelatinous material had shrunk by an excessive amount and had created voids amongst the randomly-orientated wood fibres of the coating. Therefore, moisture transfer pathways of low resistance were numerous. It was proposed that the observed delay in checking was primarily due to the long drying time required by the coating rather than the desired moisture transfer effect.

Further tests were conducted on mixtures of wood flour, gelatine and water. These were more successful; however, the shrinkage of the coating upon drying was excessive and its cohesion and adhesion remained generally poor. A better bonding agent was required.

Animal glue (cologen) was mixed with water and wood flour in the proportions

1 water : 0 to 0.30 wood flour : 0.04 to 0.60 animal glue (dry crystals)

by weight. The mixture was prepared at a temperature of approximately 50°C (cologen undergoes an irreversible chemical change when heated above 60°C) and was found to "set" (form a jelly) at a definite, reproducable temperature, depending upon the ratio of animal glue to water (by weight) in the mix.

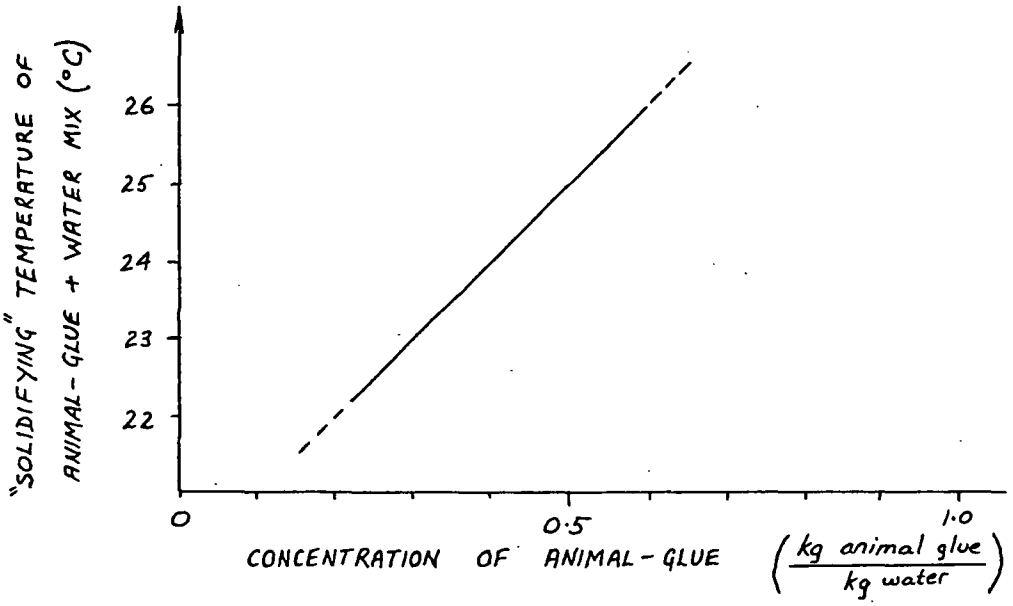

Following the set, the coating adhered strongly to the surfaces of green timber. Early tests on slabs of animal glue indicated that its diffusivity at moisture concentrations of approximately 10% (dry basis) was about $0.7_{10}{}^{-7}$ m^2/hr (determined by the method of inference, section 5.2.6.3. From equation 3.28, the required thickness of animal glue (at M = 10%) was 1.04 ± 0.18 mm. The inclusion of wood flour in the coating (even in small proportions was found to increase its diffusivity markedly; this practice was therefore discontinued.

Shrinkage of the gel was related directly to the ratio of water to animal glue in the mix (by weight); the larger the ratio, the greater the shrinkage. It was found necessary to use a minimum of 2 kg of water to 1kg animal glue to maintain workability. Impermeable fillers were added to an animal glue/water base in an attempt to reduce firstly, the shrinkage of the coating, and secondly, the amount of animal glue required to cover a unit area. This had the added advantage of slightly reducing the diffusivity of the coating.

A mixture of 1 kg water, 0.4 kg animal glue and 0.75 kg talcum powder was found to produce a tough

coating with a diffusivity of approximately $0.7_{10}{}^{-7}$ m^2/hr (at M = 5%). The shrinkage of this coating was approximately 60% of its original thickness meaning that the required wet thickness was 2.1± 0.35 mm. Initially, the coating mix (at 50°C) was brushed onto test samples. It was therefore difficult to control the thickness and uniformity of coverage and test results were rather inconsistent. A technique for spraying the hot mixture was developed (figure 5.18) but it was found necessary to increase the water content by 40% in order to maintain a reasonable rate of application.

APPENDIX E

THE ELASTIC PROPERTIES AND SHRINKAGE BEHAVIOUR OF "TASMANIAN OAK".

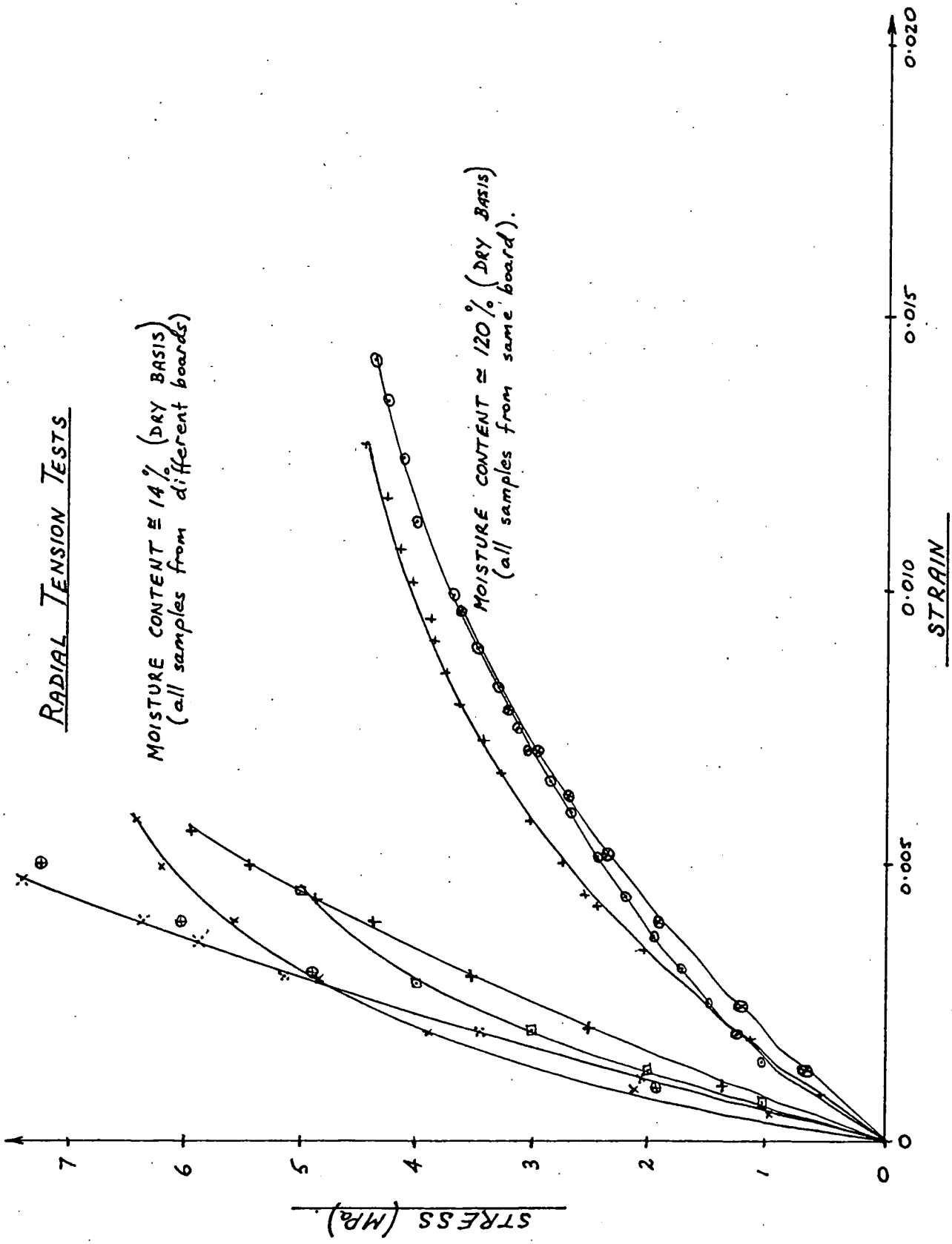

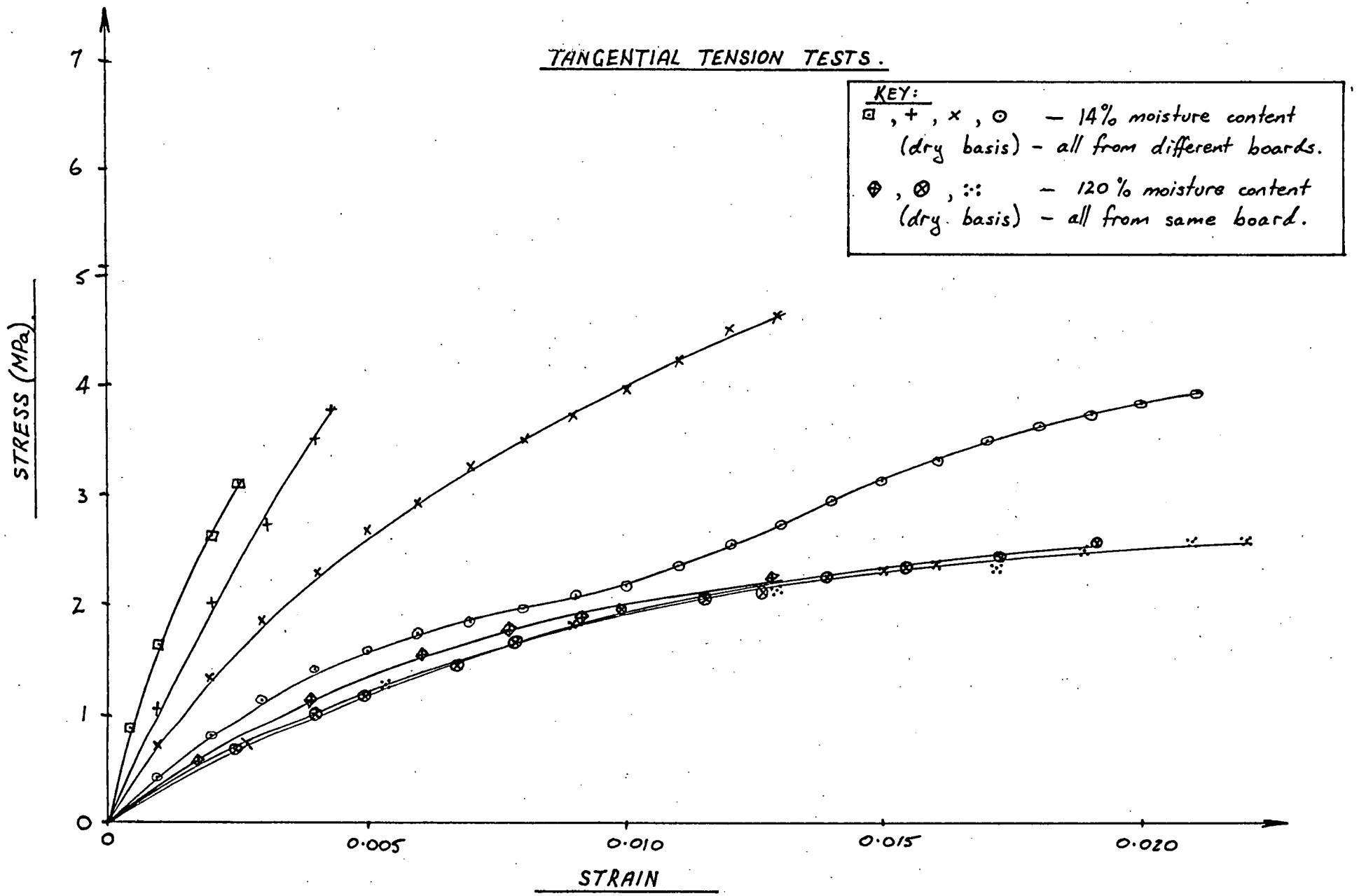
TANGENTIAL TENSION TESTS.
KEY:
⊡ , + , × , ⊙ — 14% moisture content (dry basis) - all from different boards.
⊕ , ⊗ , :: — 120% moisture content (dry basis) - all from same board.
STRESS (MPa).
0
1
2
3
4
5
6
7
0
0·005
0·010
0·015
0·020
STRAIN

RADIAL COMPRESSION TESTS

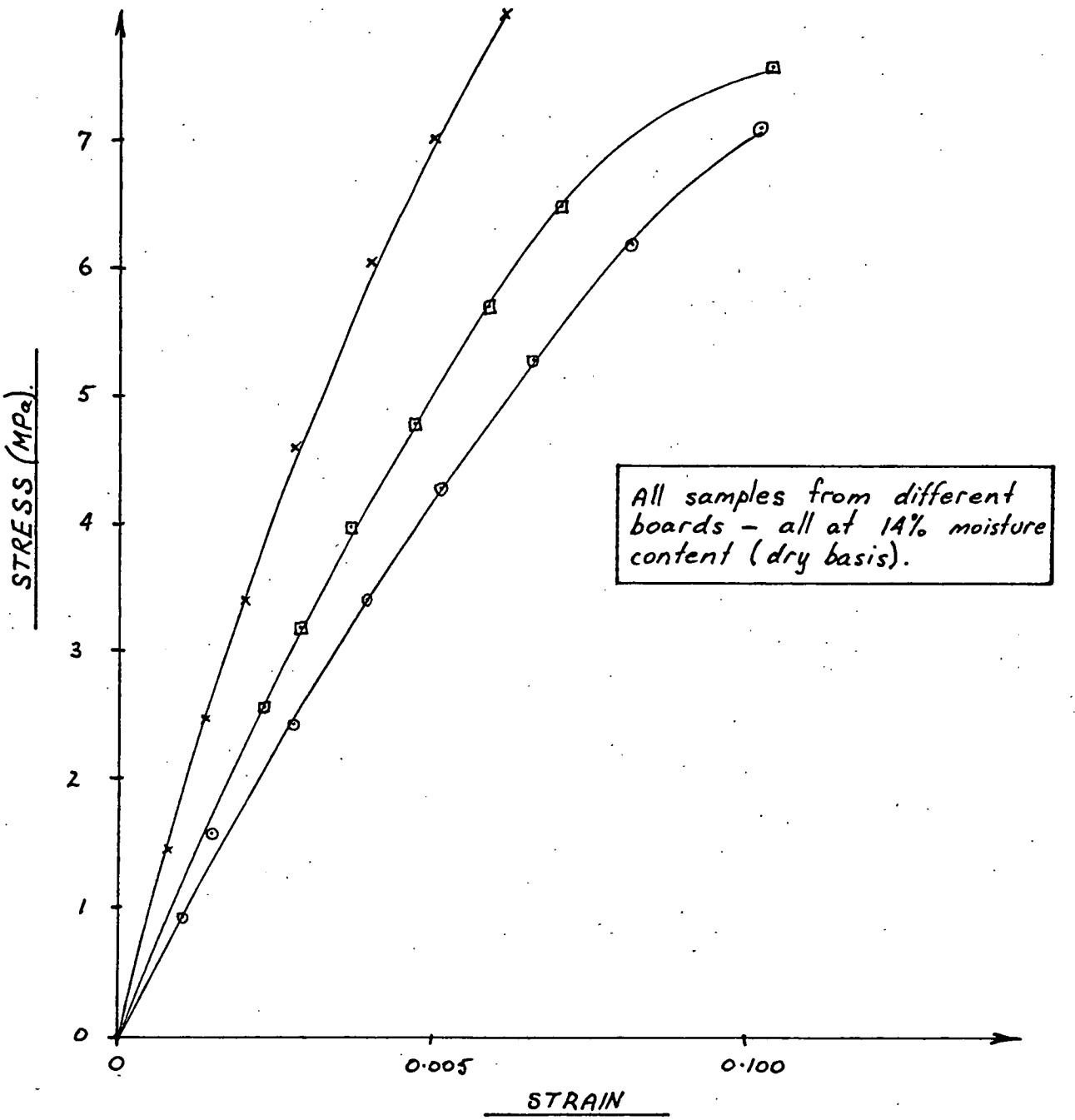

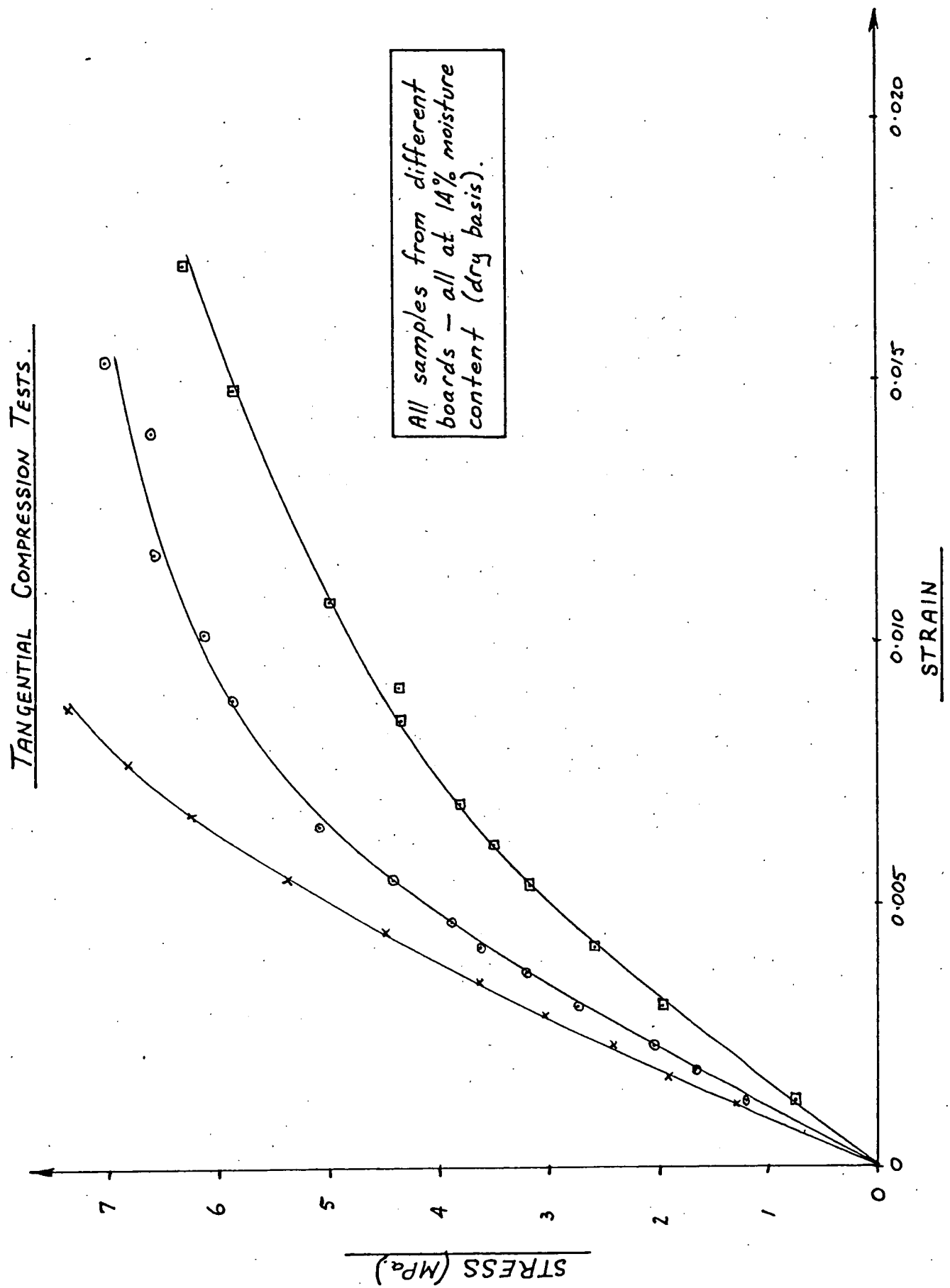
TANGENTIAL COMPRESSION TESTS.
All samples from different boards - all at 14% moisture content (dry basis).
STRESS (MPa.)
STRAIN
0
1
2
3
4
5
6
7
0
0·005
0·010
0·015
0·020

TESTS FOR SHEAR MODULI

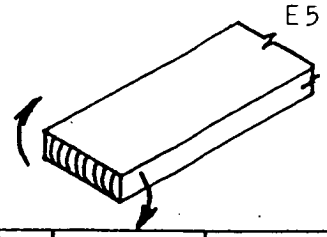

Torsion tests for G_{rz}

Torque (Nm)	$J\frac{\theta}{L}$ ($\times 10^{10}$)	Torque (Nm)	$J\frac{\theta}{L}$ ($\times 10^{10}$ m^3)	$J\frac{\theta}{L}$	$J\frac{\theta}{L}$	$J\frac{\theta}{L}$	$J\frac{\theta}{L}$
0	0	0	0	0	0	0	0
·196	1·64	·39	4·35	4·63	5·07	3·64	4·53
·588	4·98	·78	9·57	10·5	10·9	8·23	10·2
·981	8·31	1·18	14·8	15·6	15·6	12·5	15·4
		1·57	19·1	20·3	19·9	16·4	20·6
G_{rz} (MPa) →	1190	G_{rz} (MPa) →	789	797	770	1050	739

Torque (Nm)	$J\frac{\theta}{L}$ ($\times 10^{10}$ m^3)	$J\frac{\theta}{L}$	$J\frac{\theta}{L}$	$J\frac{\theta}{L}$	$J\frac{\theta}{L}$	$J\frac{\theta}{L}$	$J\frac{\theta}{L}$
0	0	0	0	0	0	0	0
·39	4·04	5·05	3·80	3·87	4·51	4·28	3·30
·78	7·41	10·1	7·60	8·07	9·32	9·41	7·70
1·18	10·9	15·2	11·2	12·3	13·2	14·2	12·3
1·57	13·7	19·4	14·2	16·1	16·8	17·8	16·1
G_{rz} (MPa) →	1110	781	1080	1050	969	842	920

$G_{rz} = 930$ MPa ± 25%.

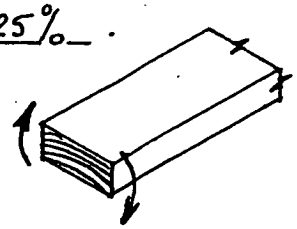

Torsion tests for G_{tz}

Torque (Nm)	$J\frac{\theta}{L}$ ($\times 10^{10}$ m^3)	Torque (Nm)	$J\frac{\theta}{L}$ ($\times 10^{10}$ m^3)	$J\frac{\theta}{L}$	$J\frac{\theta}{L}$	$J\frac{\theta}{L}$	$J\frac{\theta}{L}$
0	0	0	0	0	0	0	0
·196	2·08	·39	4·06	4·67	5·55	4·12	5·25
·588	6·23	·78	9·07	9·53	12·6	8·83	11·7
·981	9·86	1·18	14·4	14·9	19·0	13·5	17·7
		1·57	19·0	19·6	24·7	17·4	22·6
G_{tz} →	1010	G_{tz} →	796	783	631	871	686

Torque (Nm)	$J\frac{\theta}{L}$ ($\times 10^{10}$ m^3)	$J\frac{\theta}{L}$	$J\frac{\theta}{L}$	$J\frac{\theta}{L}$	$J\frac{\theta}{L}$	$J\frac{\theta}{L}$	$J\frac{\theta}{L}$
0	0	0	0	0	0	0	0
·39	4·78	4·83	5·36	6·75	4·88	5·91	3·%
·78	9·75	10·1	10·7	13·0	10·5	11·5	8·91
1·18	14·0	14·9	15·5	17·4	15·5	16·6	13·3
1·57	17·6	19·3	19·7	20·5	18·7	19·8	17·3
G_{tz} →	908	840	858	867	766	724	871

$G_{tz} = 815$ MPa ± 25%

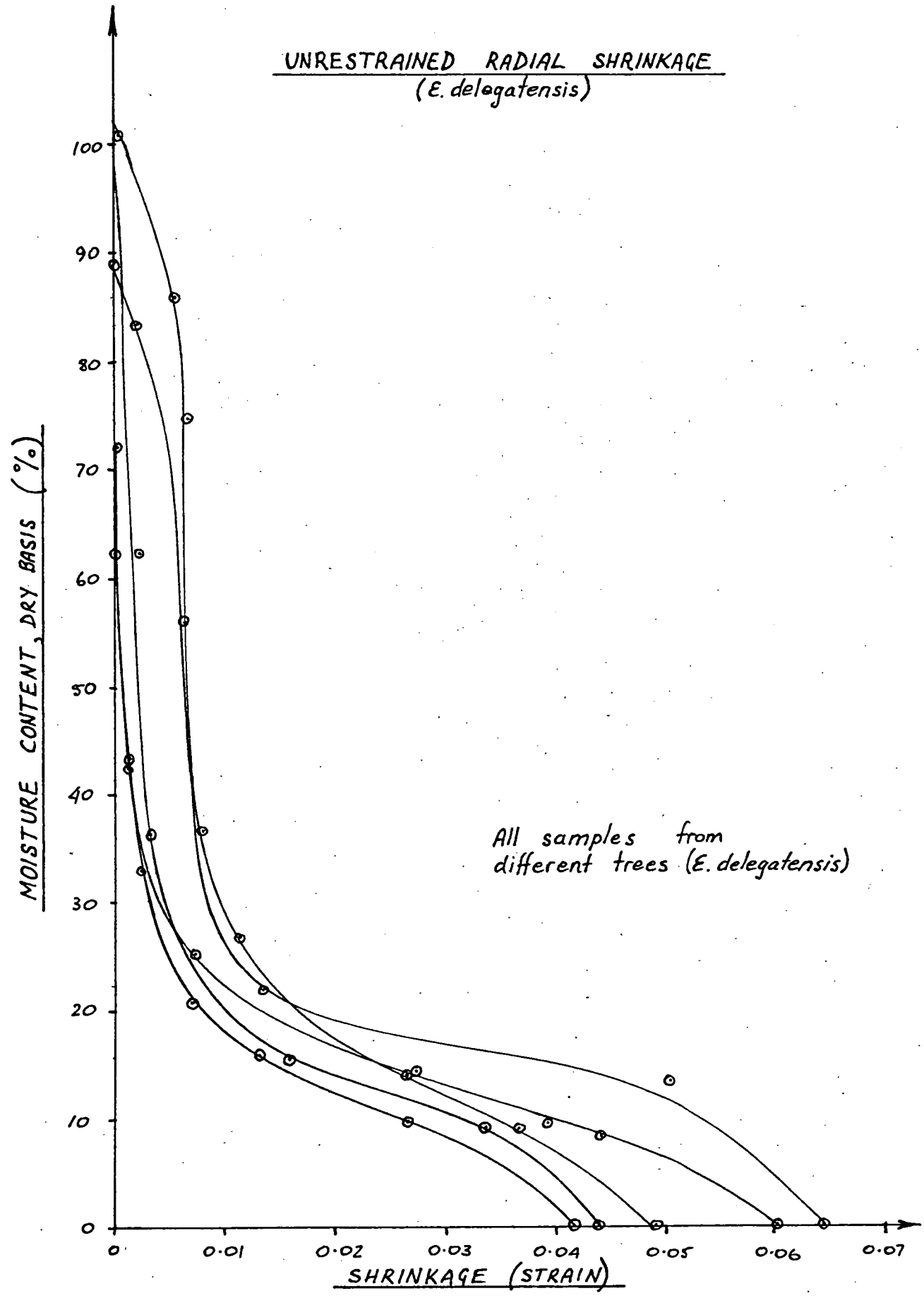
UNRESTRAINED RADIAL SHRINKAGE
(E. delegatensis)
MOISTURE CONTENT, DRY BASIS (%)
100
90
80
70
60
50
40
30
20
10
0
0
0·01
0·02
0·03
0·04
0·05
0·06
0·07
SHRINKAGE (STRAIN)
All samples from
different trees (E. delegatensis)

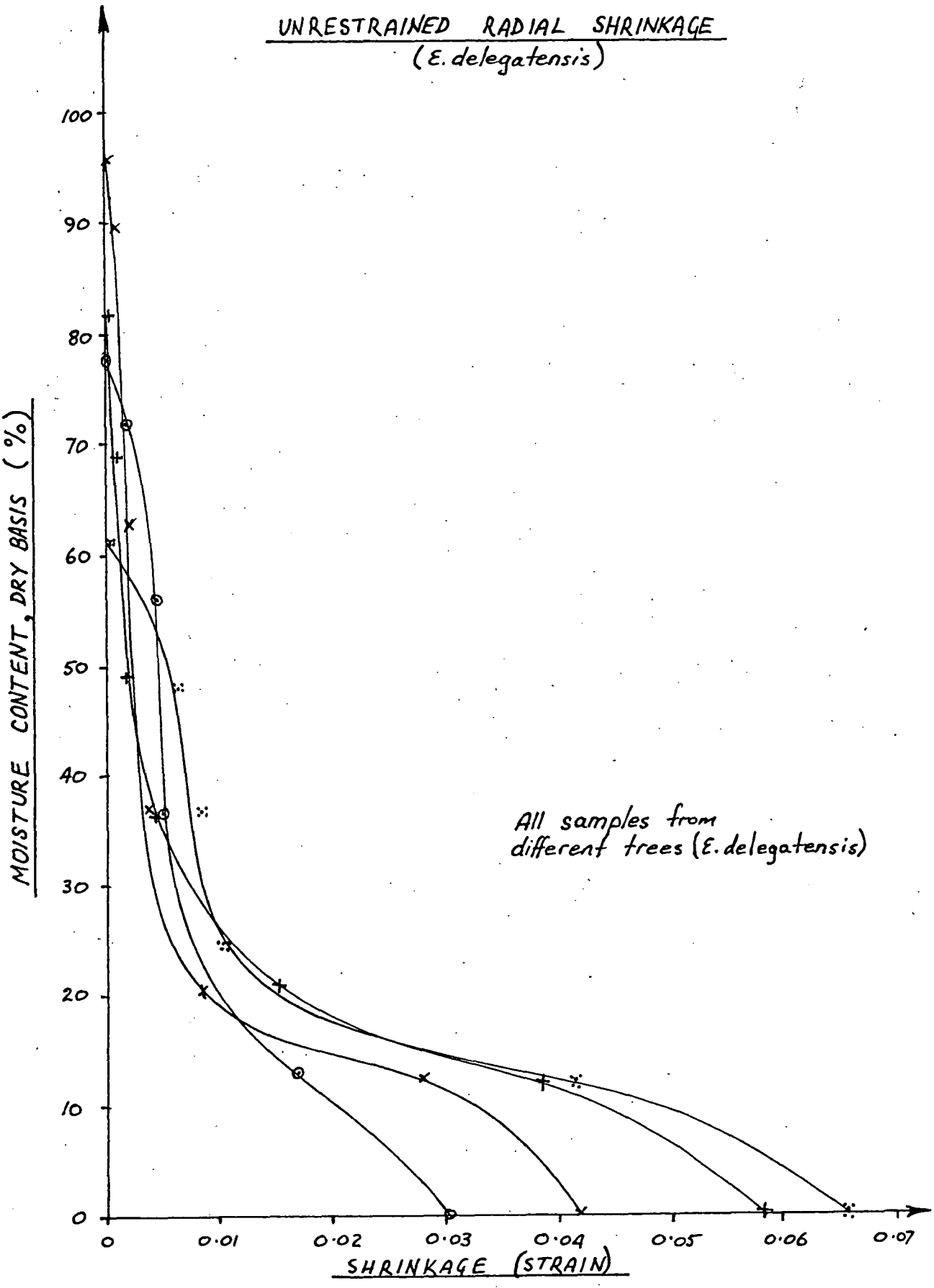
UNRESTRAINED RADIAL SHRINKAGE
(E. delegatensis)
MOISTURE CONTENT, DRY BASIS (%)
100
90
80
70
60
50
40
30
20
10
0
0
0·01
0·02
0·03
0·04
0·05
0·06
0·07
SHRINKAGE (STRAIN)
All samples from
different trees (E. delegatensis)

TasTimber NEWS

March, 1982

NEWSLETTER OF THE TASMANIAN TIMBER PROMOTION BOARD

Vital meeting for industry

A seminar critical to the future prosperity of our industry is to be held at Shearwater on March 16 and 17.

It is a live-in seminar for key management personnel, and has been organised on the recommendation of PA Consultants, the Board's marketing consultants.

As you will be aware, PA consultants were engaged to assess the market for Tasmanian Oak in other States, and to recommend ways in which sales can be lifted.

The firm said it would be necessary to hold the seminar to:

- develop promotional and marketing plans and strategies for the Tasmanian Timber Promotion Board to undertake on behalf of its members,
- identify and agree on action plans which will support the strategies, and
- obtain industry support and commitment to these plans and strategies.

It is essential that key people from throughout the State attend — in fact, this extremely important exercise could be in jeopardy if they do not.

It is a very important meeting. Whether or not individual companies or groups gain a bigger share of the interstate market could well depend on representation at Shearwater.

There will be a follow-up meeting, probably of one day, to be held in April, to put the final seal of approval on the plan of attack.

John Kirwan,
Chairman.

"Restoration" TV series now showing on ABC

The Australian Broadcasting Commission has already begun screening of the series of programmes on restoration of a colonial cottage in Hobart.

The project is being supported by the Tasmanian Timber Promotion Board, through donations of timber and help with expert advice.

Screening of the first series began on February 12, and finishes the week before Easter.

One segment is shown each week — on Fridays at 6.40 p.m. with a repeat on Sundays at 12.40 p.m.

The executive producer of "Restoration", Mike Swinson, of the ABC's rural department, says the first series deals with replacing a ceiling, restoring walls and cedar skirting boards, doors, wallpapering, building an archway and repairing and renovating a floor and fireplace.

The second series, to be filmed later in the year, is where Tasmanian native timbers will be required.

Mike Swinson says it will cover building a bathroom and kitchen using timber, wall panelling and cupboards, and renovating a staircase and an upstairs bedroom.

The programmes afford an excellent opportunity to demonstrate the many uses of native timbers in general home restoration.

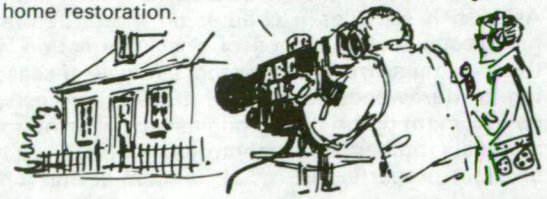

Thesis: Tasmanian Oak i

Richard Schaffner submitted his thesis for the degree of Master of Engineering Science early in November. Those people unfamiliar with the workings of a University and the training of engineers would probably question the relevance of higher degree studies being funded by the Timber Promotion Board. Perhaps the explanation should begin by listing what is required by the University before awarding a master's degree.

The degree of Master of Engineering Science, or any higher degree for that matter, follows on from a 4-year bachelors degree of an approved standard. The student is required to undertake a research project over a period of one to three years and submit for examination a bound thesis. Richard began his work for the degree early in '79 when the TTPB decided to fund the Backsawn Tasmanian Oak Project. Much of what has happened since has been described in Board Annual Reports, newspaper articles and Tas. Timber News. The project has enjoyed dollar-for-dollar funding from the Tasmanian Government. What is less well known is that as well as getting the coating method to work and solving the practical problems of producing check-free backsawn oak Richard had to satisfy the academics at the University.

Why is the University involved? The answer to that question lies partly in the facilities that the University has to offer. The Civil & Mechanical Engineering Department has a well equipped workshop and laboratories containing equipment necessary for the project such as drying kilns and microscopes. Also the staff of the Department can fairly claim to have expertise in some aspects of timber engineering.

The thesis itself is a rather impressive document; it runs to 280 pages not counting the appendices. Richard's aim was to make the thesis a complete record of the work on the Backsawn Timber Project. As such it includes a chapter on the structure of hardwoods and the sites of check formation, the theory of mass transfer in wood, a review of seasoning of hardwoods, details of the drying tests, a development of the theory of elasticity of orthotropic materials (timber is an orthotropic material — it has different properties in radial, tangential and longitudinal directions), the elastic properties and shrinkages behaviour of "Tasmanian Oak", and a chapter in which drying stresses in wood are described and computed. The thesis abstract reads as follows:

Richard Schaffner, with the new kiln

The aim of this investigation was to develop an economically viable method of seasoning back-sawn native Tasmanian eucalypts and to reduce the seasoning time required for these timbers.

The theory of unsteady state mass transfer based upon Fick's law of diffusion was used to study the drying process. The diffusion coefficients were measured directly by the diffusion cell method or deduced from a comparison of measured and calculated drying curves. The relationship between shrinkage of wood fibre and moisture concentration was obtained by slowly drying thin strips of wood and regularly measuring deformations. The effects of

close-up

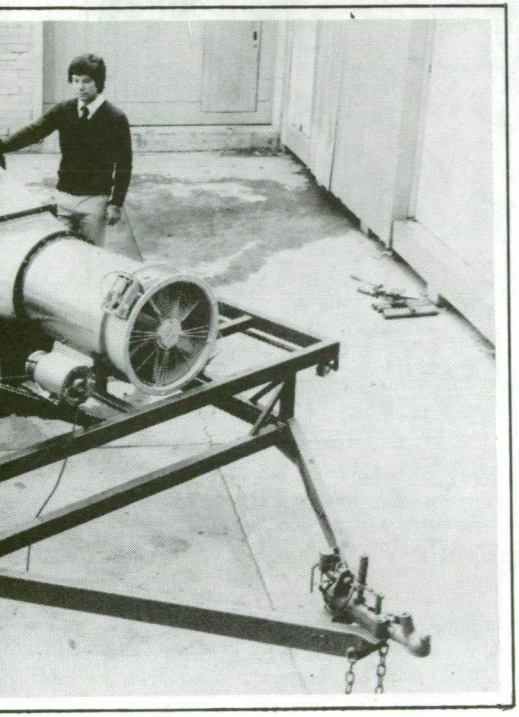

falling diffusivity and shrinkage with reducing moisture concentration were found to effectively cancel one-another in the case of the timbers tested during this investigation.

Drying stresses in wood were studied using the theory of elasticity in anisotropic bodies. Airy stress functions were used when solving for stresses. For simplicity, sawn boards were approximated to orthotropic bodies and only boards cut with face-planes parallel/perpendicular to the principle material property directions were studied. Some elastic properties of native Tasmanian eucalypt timbers were measured on small sample populations and found to be similar to those of various North American hardwoods (with similar densities) reported by other authors. The approximate elastic properties of Tasmanian eucalypts were deduced from this comparison.

The theories of mass transfer and stress analysis were combined to form a model describing the development of drying stresses. The wood was assumed to be linearly elastic and to free from the effects of hysteresis and creep. The governing differential equations were solved by numerical methods.

The model was used to assess the effectiveness of semi- permeable surface coatings in reducing drying stresses in timber. Tests on timber coated with animal glue (cologen) showed that checking (cracking) in Tasmanian eucalpyts brought about by high drying stresses was reduced in severity or completely eliminated, depending upon the thickness of the coating.

As can be seen from the above, the thesis is not likely to get into the best-seller list. But despite its apparent weighty nature it is well written and readable — even to the members of the timber industry with no background in timber engineering. Copies of the thesis will be available for timber industry people to borrow in December. Parts of the study will be written up for technical journals such as Wood Science. In this way the Research and Development Group will build up a reputation for its research ability which may attract work (and financial support) for the Group from interstate and overseas.

Meanwhile, the Group has more than enough work ahead of it to keep it busy for the next twelve months and beyond. Apart from the work expected in timber coating plant from pilot-plant to industrial scale there is a planned study of the anatomy and strength properties of check-prone material also work on developing improved structured timber joints. Other areas of activity are concerned with the proposed Australian uniform building regulations and the structural design manual.

Perhaps one of the readers of Tas. Timber News can help with a problem that has the R & D Group bluffed. How can the Group positively distinguish (after sawing) between the three eucalypt species which comprise "Tasmanian Oak?"

If anyone can help, please contact the R & D Group on 20 2130 or 20 2142.

Meet the team

The Tasmanian Timber Promotion Board's research team members are pictured in the "Faces" series this month.

From the left: Dr. Peter Doe. Steve Weeden, Richard Schaffner, Scott Goodwin and John Morrisby (absent are Leigh Oates & Tod Jillett)

Richard Schaffner
Richard has been the driving force behind the backsawn timber project. Appointed as the Board's engineer in 1978, he convinced the Board to support the research programme at the University. Besides his work on the Backsawn Project, Richard contributes to national technical committees and is in the final stages of writing a structural timber design manual. A keen sailor, Richard and his brother-in-law are the current Tasmanian Fireball champions.

Scott Goodwin:
Scott is the Group's Technical Officer. He served his time as a fitter and turner before joining the Group in August 1979. Scott built the 200 super ft. kiln at the University and much of the test equipment used in the research. He also has been the Group's lab assistant, machinist, welder and general 'fixit' man. Scotts extra-curricular interest is boat building.

Stephen Weeden:
Stephen was appointed with an honours degree in Botany with a Chemistry major in April, 1980. Stephen's qualifications and expertise complement those of the engineers in the team. His responsibilities include the assessment of coating materials, timber testing and the scientific aspects of the project. Stephen is active in political circles and is Secretary of the Hobart Hoo-Hoo Club.

John Morrisby:
John was appointed early in 1981 as a mechanical design engineer. Together with Scott Goodwin, John designed the pilot coating plant. John is rapidly gaining experience in timber engineering and will be closely involved in the commercial development of the backsawn process. Formerly a first grade football player, John is now more interested in skin diving.

Leigh Oates:
Leigh, formerly a technician with the University, joined the R & D Group at the beginning of the year to assist with the construction of the pilot plant. Leigh runs a small farm in the Huon in his spare time.

Dr. Peter Doe:
Formerly supervisor of Richard Schaffner's postgraduate studies and now Leader of the R & D Group, Peter's field of research is drying. A Senior Lecturer in Mechanical Engineering at the University, Peter has been a consultant for the United Nations on several occasions advising on fish drying in developing countries. Interests include musical instrument playing and sailing.

Tod Jillett:
A retired construction engineer, has given valuable assistance to the research and development group, particularly with the structural timber design manual. Tod also advises the other engineers during the design of unusual structures when his busy lifestyle permits.

Tasmanian Timber Promotion Board
68 York Street, Launceston, Tel. (003) 31 5006

TasTimber NEWS

NEWSLETTER OF THE TASMANIAN TIMBER PROMOTION BOARD

OCTOBER 1981

New Man Joins Team

The Tasmanian Timber Promotion Board has a new Director.

He is Mr Barry Lumley of Launceston, who replaces Mr John Clark, now working with private industry.

Mr Lumley, who has a wide experience in marketing and promotion, officially began duties with the Board on August 3.

Mr Lumley was previously Tasmanian manager of a national company.

He has spent the first few weeks in his new post travelling around Tasmania meeting people in the industry, and talking with people at the helm of the Board's research programme at the University of Tasmania.

He is anxious to hear from members wanting to discuss the various areas of the Board's activities. He can be contacted by telephone at the Board's headquarters on (003) 31 5006 or by mail at 68 York Street, Launceston.

WELCOME . . .

- *This is the first newsletter to be published under the name of the Board's new Director, Mr. Barry Lumley*

The Chairman of the TTPB, Mr John Kirwan, welcomes Mr Lumley to the Board, and wishes him the best in his new position.

This is also the first of a new-look newsletter.

The change in format is aimed at making the newsletter a "better read" with more content, yet easier to absorb for the business man with little time.

We hope it is useful to you.

THE Research and Development Group has commenced its third year of operation with the end of the development phase of the backsawn Tasmanian Oak project clearly in sight. The project has as its aim a commercially viable method of seasoning backsawn eucalypts.

The small quantity of seasoned backsawn timber already produced has created considerable interest both within the industry and with members of the public in general. A display of seasoned backsawn oak at the University's open day in May prompted many enquiries as to when the timber would be available for sale.

When the project was initiated by the Timber Promotion Board, in mid 1979, mainly through the foresight of Jim Hammond and John Clark, there were some doubts expressed as to whether it would be possible even to season some of the more difficult timbers cut on the back let alone come up with a commercially viable technique.

Where our approach differed from previous attempts was in laying down a sound theoretical basis for the experimental work.

This was one of the reasons why the University became involved. Richard Schaffner, the TTPB engineer, enrolled for postgraduate study in the Civil and Mechanical Engineering Department.

Richard developed a method of computing the stresses in timber during drying and hit on the idea of applying a semi-permeable coating to the backsawn surface of boards so that the surface of the board remains above the fibre saturation point.

The theory was tested in the 0.5 cubic metre capacity kiln at the University built by the Research and Development Group's technician, Scott Goodwin.

The results were impressive — in three stacks of backsawn timber from different parts of the State (including some highly refractory material from the Central Highlands) the recovery of essentially check free material was between 70 to 95%.

Unfortunately the cost of the coating used for these trials, based on animal glue and talc, was high (about $180/cubic metre of timber coated) and animal glue is not being produced in quantities sufficient to meet the anticipated demand.

Recent research effort has concentrated on finding an alternative coating material which is both readily available and cheap.

The group's chemist, Stephen Weeden has completed a study of possible coatings, including a lignin-based coating and various synthetic adhesives, and has selected a commercially available poly vinyl acetate (PVA).

Tests on half-metre long boards have shown that the same behaviour as achieved with the animal-glue based coating can be achieved with the PVA coating but with much thinner applications.

Uni' resear

***The** first pilot coating plant for dryir*
to industry from February 1 next

After trials, a second plant will be c
modifications.

The Senior Lecturer in Mechanica
Dr Peter Doe, who has been clos
progress made by the Board's Res

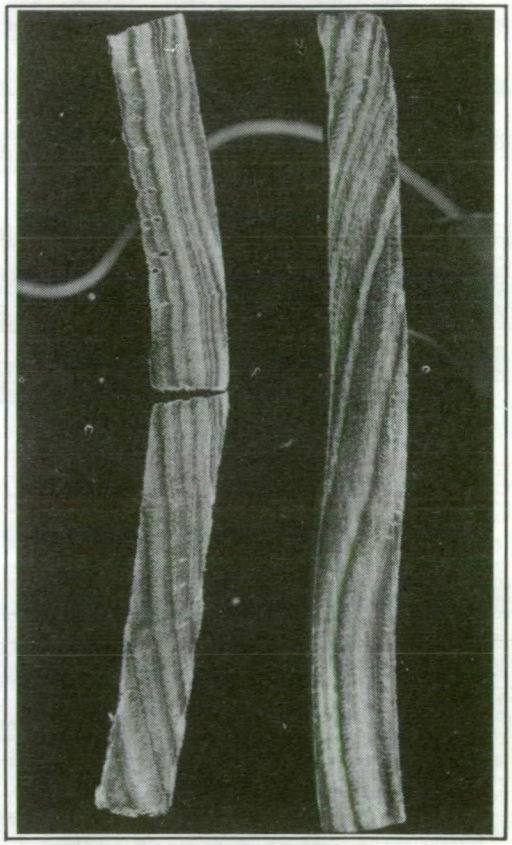

● SAMPLES from the same board dried at the same time under constant conditions. The sample on the le has had heavy checking; the sample on the right was coated and has only minor checks.

ı report

ksawn Tasmanian Oak will be available

ssioned and will include any necessary

neering at the University of Tasmania, volved with the project reports on the and Development team.

ıe preliminary cost estimates are $40/cubic metre coated ut a firm cost and recovery figure will not be available ntil the end of October when a kiln load of PVA coated oards has been seasoned.

eanwhile the group has decided on the basis of eliminary results to proceed with the design and onstruction of a mobile coating plant which will be made vailable to mills together with a trained operator early in e New Year.

ıere is another possibility which, if proven effective, has e potential to reduce the coating costs to as low as $15 a ubic metre.

ıe idea is to shrink-wrap a plastic film onto the boards. achinery for doing this for a different purpose, that is to otect and package already seasoned timber, is available in urope. The problem is to obtain a shrink-wrap that has the quired permeability.

manufacturer of plastic sheeting is to provide samples for to test; the results should be available by the end of the ar.

ıere are a number of other projects in which the group is volved.

ıe is the publication of a structural timber design manual. ıe manual will be distributed in draft form later in the year ith publication scheduled for mid 1982 at a promotional nction to be attended by engineers and architects involved timber design from the mainland and New Zealand.

sociated with the use of timber in structures there is a oposal to design and test moment resisting joints in ue-laminated frames.

ıother project will be to identify refractory material at the ll skids. Stephen Weeden, working with the Botany partment at the University is to measure growth aracteristics of trees and attempt to relate these to the bsequent milling and seasoning behaviour of the timber. is an ambitious project, but one with considerable mmercial implications — particularly if it can be used as a eans of pre-selecting sawlogs for back or quarter sawing.

However, the group's first priority is to get production of backsawn oak going.

The Research and Development Group has offices within Engineering Building of the University of Tasmania and welcomes enquiries and visits from people in the timber industry. Any enquiries should be directed to Dr Peter Doe, phone: 20 2130.

Colour guide will be ready soon

THE full-colour multi-lingual edition of the Tasmanian Oak Buyers' Guide is now in the final stages of preparation.

The final version should be available before the end of the year.

The black and white edition has generated a number of enquiries and interest is already being shown in the colour edition, before it is off the presses.

The colour edition will be a prestige publication for the industry, and will be circulated on both the domestic and international markets.

Seeking experts

THE Tasmanian Timber Promotion Board plans to take more advantage of the expertise available within the industry.

The Chairman, Mr. John Kirwan, says there are many people in the industry who are recognised authorities within given areas.

Increased emphasis will be placed on ensuring that these people have the opportunity to take part in Board activities.

Mr Kirwan says that in some cases, industry representatives will be invited to attend Board meetings to discuss common areas of concern.

This approach will have two main benefits:

- It will give the Board the chance to tap available expertise to help solve problems; and
- Create a channel for feedback between the Board and industry

Structural design manual gets first critical test

ARCHITECTS and specifiers from the State Department of Housing and Construction have been among the first to have the chance to assess the Timber promotion Board's new manual on structural timber design.

The manual is the result of eighteen months of painstaking work by the Research and Development team.

The manual is still in draft form, and will be circulated both in Tasmania and interstate for comment before it is published. A final draft should be ready by mid-March next year, with the publication to be launched about June.

It is expected the manual will become perhaps the most authoritative publication of its kind in Australia in relation to the use of structural timbers.

The architects and specifiers from the department of Housing and Construction attended a seminar in Hobart, titled "Why Use Wood", at which the manual was discussed The importance placed on the Seminar by the Department was evidenced by the attendance — thirty eight departmental officers.

The Timber Promotion Board hopes that the seminar will result in feedback from the department about the new manual.

Apart from the manual, the seminar also covered areas such as forest practices, milling processes, domestic structural uses, durability and preservation, decorative uses, heavy timber structures and properties of timber, fire rating, manufacture and applications of glue-laminated timber.

Films were shown, and a panel discussion was held to allow departmental officers the chance to question the speakers, who included Mr Richard Schaffner, Mr Fred Frampton, Mr Tony Leitch, Mr Chris Ward, Mr John Beasley, Mr John Clark and Mr Ed Vincent.

Market Survey

A COMPREHENSIVE survey is being planned to give the industry direction for further marketing activities.

Constant changes in the market places make it necessary for the industry to be kept fully informed.
Details of the survey are now being finalised, and further details will be advised as they come to hand.

Reactions sought

THE Board would like to draw to your attention an article in the June edition of the Australian Forest Industries Journal.

It is written by Peter Koch, called "Some thoughts on wood utilisation research", and is on page four.

The Board would be pleased to receive your reactions and comments.

Restoration project to be televised

THE Timber Promotion Board has taken the opportunity to help the Australian Broadcasting Commission restore an historic residence next to its Hobart studios.

The Board agreed with an ABC request to supply timber and technical advice.

The restoration project will be the subject of ten to twelve programmes on ABC television.

The Board believes participation in the restoration of the residence, which is classified by the National Trust, will be an excellent means of highlighting the use of Tasmanian timber in the growing home renovation and do-it-yourself market.

The industry will be kept advised about when the series of programmes will go to air.

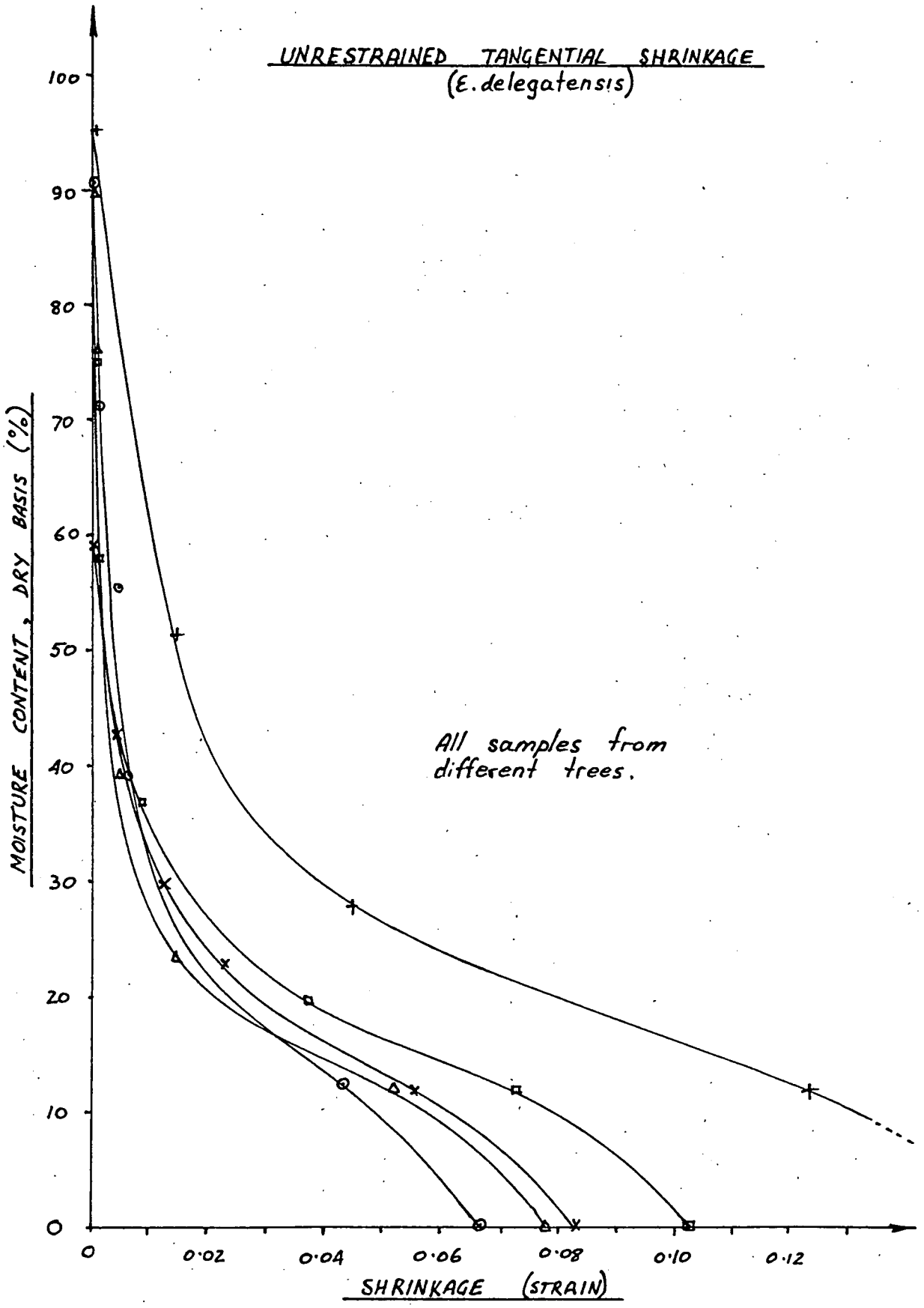
UNRESTRAINED TANGENTIAL SHRINKAGE
(E. delegatensis)
MOISTURE CONTENT, DRY BASIS (%)
100
90
80
70
60
50
40
30
20
10
0
0
0·02
0·04
0·06
0·08
0·10
0·12
SHRINKAGE (STRAIN)
All samples from different trees.

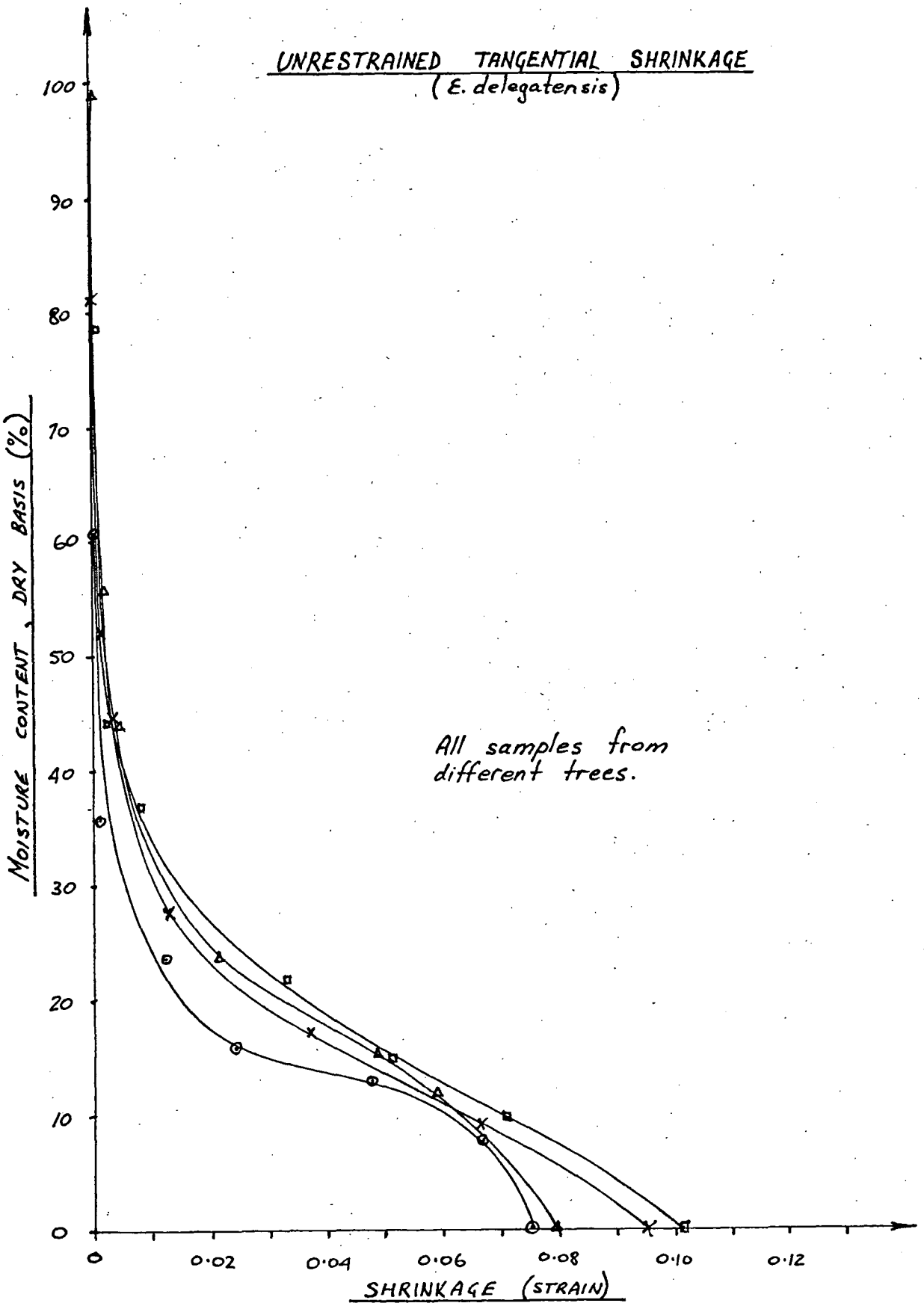
UNRESTRAINED TANGENTIAL SHRINKAGE
(E. delegatensis)
MOISTURE CONTENT, DRY BASIS (%)
100
90
80
70
60
50
40
30
20
10
0
0
0·02
0·04
0·06
0·08
0·10
0·12
SHRINKAGE (STRAIN)
All samples from different trees.

APPENDIX F

1-DIMENSIONAL MOISTURE TRANSFER AND STRESS ANALYSIS PROGRAM - "BKSAW2"

COMPUTER LANGUAGE - PASCAL

MACHINE - DIGITAL PDP 11/10

General Description:

This program is based on an implicit finite difference approximation to the simplified governing equations describing moisture transfer in one direction and the state of stress in a long, wide board. For back-sawn material, these are:

$$\frac{\partial c}{\partial t} = \mathcal{D}_t \frac{\partial^2 c}{\partial x^2} \qquad \text{(see section 3.2.1)}$$

and

$$A_1 \frac{\partial^4 \phi}{\partial x^4} + \left(\frac{1}{G_{rt}} - A_2 - A_3 \right) \frac{\partial^4 \phi}{\partial x^2 \partial y^2} + A_4 \frac{\partial^4 \phi}{\partial y^4} = -\frac{\partial^2}{\partial x^2}(\beta_t c)$$

(see equation 6.38).

These equations are applicable only to perfectly back-sawn material but may be altered easily for perfectly quarter-sawn boards.

The simplifications made when writing this program are described in detail in Chapter 8, sections 8.2, 8.3 and 8.4.1.

The one dimensional finite difference grid used as a basis for calculations takes the form shown below:

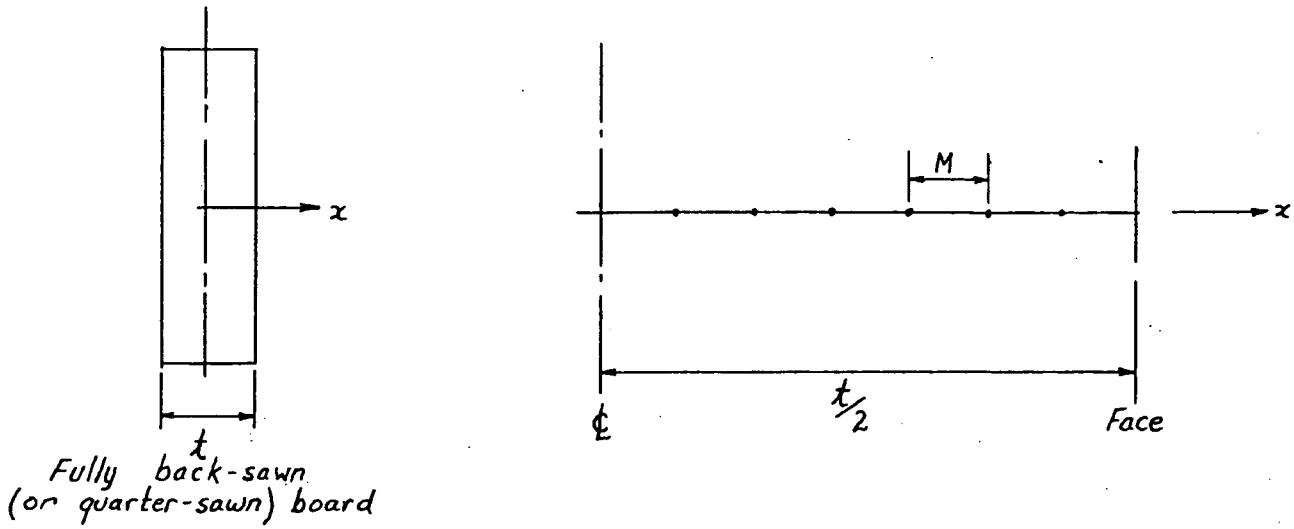

M = grid interval or "space-interval" in meters

N = number of grid intervals (must be even).
(The number of grid points = N + 1)

Thus, $\frac{t}{2}$ = MN where t is in meters

1) The diffusion coefficient of the timber in the x-direction, D, must be specified in units of (m^2/hr)
2) The equilibrium moisture concentration of wood fibre in the atmosphere in which drying takes place, C, and the original moisture concentration of the board, OMC, must be specified in units of (kg/m^3).
3) The time increment, or time step, used in the finite difference calculations, DT, and the total time of drying to be simulated, TLIM, must be specified in units of hours.
4) The variable, BQ, gives the option of analysing either back-sawn or quarter-sawn boards.
   For back-sawn boards, put BQ = 1
   and for quarter-sawn boards, put BQ = 0.
5) The moisture concentration in the wood at the wood/coating interface is expressed as a function of time in the following manner:

$$c = c_b + (c_o - c_b)\ exp\left(-\frac{T^{.286}}{TF}\right)$$

The variables in the above equation are defined in section 8.3 with the exception that TF is replaced by the variable A in section 8.3. TF is dimensionless and varies

between approximately 0.8 for uncoated boards and up to approximately 3.4 for coated boards.

There are two variables which control the amount and format of the output.

6). The "Print Factor", PF, defines the number of time increments (DT) between output of data. For example, if PF = 10, print-out will occur after every 10th step in time during calculations.

7) The variable PF1 controls the format of the output.
If PF1 = 0, only the surface moisture concentration and surface stress (along with average moisture concentration) are printed.
If PF1 = 1, the complete moisture concentration and stress distributions are printed.

Example

A 27mm thick, uncoated, back-sawn board with radial diffusivity of $1.75_{10}-7$ m^2/hr (at 25^oC) and with an initial (uniform) moisture concentration of 580 kg/m^3 is dried in an atmosphere at 25^oC and 65% relative humidity. Under these conditions, the equilibrium moisture concentration of wood fibre is approximately 80 kg/m^3. 10 grid intervals are to be used over the half-thickness of the board. A one hour time increment will be used in the calculations and results will be printed at 50 hour intervals over the first 500 hours of drying simulated. Only the drying stresses at the wood surface and the average moisture concentration of the board are required as output.

Data Input

```
DIFFUSION COEFF.(SQ.M/HR)=1.75e-07
E.M.C. IN ATMOS.(KG/CU.M)=80
SPACE INCREMENT (M) =.00135
NO. OF GRID INTERVALS (EVEN) =10
TIME INCREMENT (HRS) =1
TIME LIMIT (HRS) =500
ORIGINAL M/C (KG/C.M) =580
B-SAWN OR Q-SAWN (B=1,Q=0):1
BOUNDARY M.C. FACTOR=0.8
PRINT FACTOR=50
M.C. & STRESS DISTN.(1 FOR DIST):0
```

Output

```
TIME = 50.000    AV. M/C = 462
  STRESS AT SURFACE=2.773550E+07
    M.C. AT SURFACE=  91

TIME =100.000    AV. M/C = 410
  STRESS AT SURFACE=3.129780E+07
    M.C. AT SURFACE=  85

TIME =150.000    AV. M/C = 370
  STRESS AT SURFACE=3.237120E+07
    M.C. AT SURFACE=  83

TIME =200.000    AV. M/C = 336
  STRESS AT SURFACE=3.265450E+07
    M.C. AT SURFACE=  82

TIME =250.000    AV. M/C = 307
  STRESS AT SURFACE=3.258680E+07
    M.C. AT SURFACE=  81

TIME =300.000    AV. M/C = 282
  STRESS AT SURFACE=3.231550E+07
    M.C. AT SURFACE=  81

TIME =350.000    AV. M/C = 259
  STRESS AT SURFACE=3.190090E+07
    M.C. AT SURFACE=  81

TIME =400.000    AV. M/C = 239
  STRESS AT SURFACE=3.137360E+07
    M.C. AT SURFACE=  80

TIME =450.000    AV. M/C = 222
  STRESS AT SURFACE=3.075120E+07
    M.C. AT SURFACE=  80

TIME =500.000    AV. M/C = 206
  STRESS AT SURFACE=3.004440E+07
    M.C. AT SURFACE=  80
```

The PASCAL program is listed on the following pages.

```
PROGRAM BKSAW2;
/*1-D MOISTURE TRANSFER-STRESS ANALYSIS*/
LABEL   1,2;
VAR     I,J,K,N,CTR,BQ,PF,PF1      :INTEGER;
        TIME,DT,OMC,C,D,R,DX,A1   :REAL;                    DECLARATIONS
        S,TLIM,AV,TF,MTZ,MZT       :  REAL;
        A  :ARRAY [0..20,1..4] OF REAL;
        B  :ARRAY [1..20,1..6] OF REAL;
        STRESS,YM,ESN  :ARRAY [0..20] OF REAL;
PROCEDURE TANGENT;
BEGIN                                                   WOOD PROPERTIES
YM[I]:=5.0E+08*(1+2.72*EXP(-A[I,4]/90));                       IN
ESN[I]:=-(0.055+0.035*ARCTAN((90-A[I,4])/53));          TANGENTIAL DIRECTION
MTZ:=0.026;MZT:=0.5;
END;
PROCEDURE RADIAL;
BEGIN                                                   WOOD PROPERTIES
YM[I]:=1.0E+09*(1+2.72*EXP(-A[I,4]/90));                       IN
ESN[I]:=-(0.03+0.0191*ARCTAN((82-A[I,4])/41));          RADIAL DIRECTION
MTZ:=0.041;MZT:=0.41;
END;
BEGIN
WRITE ('DIFFUSION COEFF.(SQ.M/HR)=':35);READ (D);
WRITE ('E.M.C. IN ATMOS.(KG/CU.M)=':35);READ (C);
WRITE ('SPACE INCREMENT (M) =':35);READ (DX);
WRITE ('NO. OF GRID INTERVALS (EVEN) =':35);READ (N);
WRITE ('TIME INCREMENT (HRS) =':35);READ (DT);                  DATA ENTRY
WRITE ('TIME LIMIT (HRS) =':35);READ (TLIM);
WRITE ('ORIGINAL M/C (KG/C.M) =':35);READ (OMC);
WRITE ('B-SAWN OR Q-SAWN (B=1,Q=0):':35);READ (BQ);
WRITE ('BOUNDARY M.C. FACTOR=':35);READ (TF);
WRITE ('PRINT FACTOR=':35);READ (PF);
WRITE ('M.C. & STRESS DISTN.(1 FOR DIST):':35);READ (PF1);
CTR:=0;
FOR I:=0 TO N DO STRESS[I]:=0;                                  INITIALISE
FOR I:=1 TO N DO A[I,4]:=OMC;TIME:=0;
1:  TIME:=TIME+DT;A[0,4]:=C+(OMC-C)*EXP(-EXP(LN(TIME)*0.286)/TF);
CTR:=CTR+1;
FOR I:=1 TO N DO
 BEGIN
 R:=D*DT/(DX*DX);A1:=1/(2*R+1);
 A[I,1]:=-R*A1;A[I,3]:=-R*A1;A[I,2]:=1;A[I,4]:=A[I,4]*A1;
IF I=1 THEN
BEGIN A[I,1]:=0;A[I,4]:=A[I,4]+R*A1*A[0,4];                 SET UP MASS
END;                                                        TRANSFER MATRIX
IF I=N THEN
BEGIN A[I,1]:=2*A[I,1];A[I,3]:=0;
END;
 END;
FOR I:=2 TO N DO
 BEGIN                                                  GAUSSIAN ELIMINATION
 A[I,2]:=A[I,2]-A[I,1]*A[I-1,3];
 A[I,4]:=(A[I,4]-A[I,1]*A[I-1,4])/A[I,2];
 A[I,3]:=A[I,3]/A[I,2];
 END;
```

```
FOR I:=(N-1) DOWNTO 1 DO A[I,4]:=A[I,4]-A[I,3]*A[I+1,4];
S:=A[0,4]+A[N,4];                                    BACK-SUBSTITUTION AND
K:=N DIV 2;FOR I:=1 TO K DO S:=S+4*A[2*I-1,4];       CALCULATION OF AVERAGE
K:=(N DIV 2)-1;FOR I:=1 TO K DO S:=S+2*A[2*I,4];     MOISTURE CONCENTRATION
AV:=S/(3*N);
```

```
IF CTR=PF THEN                                       CONTROL STATEMENT
```

```
BEGIN CTR:=0;
FOR I:=1 TO N DO                                     SET UP LEFT-HAND SIDE OF
 BEGIN                                               STRESS MATRIX
 B[I,1]:=1;B[I,2]:=-4;B[I,3]:=6;B[I,4]:=-4;B[I,5]:=1;
 END;
B[1,1]:=0;B[1,2]:=0;B[2,1]:=0;B[N-1,5]:=0;B[N,5]:=0;B[N,4]:=0;
B[1,3]:=7;B[N-1,3]:=7;B[N,2]:=-8;B[N,1]:=2;
```

```
FOR I:=0 TO N DO IF BQ=1 THEN TANGENT ELSE RADIAL;
FOR I:=1 TO (N-1) DO                                 R.H.S. OF STRESS MATRIX
B[I,6]:=-(ESN[I-1]+ESN[I+1]-2*ESN[I])*DX*DX*YM[I]/(1-MZT*MTZ);
B[N,6]:=-2*(ESN[N-1]-ESN[N])*DX*DX*YM[N]/(1-MZT*MTZ);
```

```
FOR I:=1 TO N DO
 BEGIN                                               PUT "1"'S ON LEADING DIAGONAL
 S:=B[I,3];FOR J:=1 TO 6 DO B[I,J]:=B[I,J]/S;
 END;
```

```
FOR K:=1 TO (N-2) DO
 BEGIN
 B[K+1,3]:=B[K+1,3]-B[K+1,2]*B[K,4];                 ELIMINATION
 B[K+1,4]:=B[K+1,4]-B[K+1,2]*B[K,5];                    BY
 B[K+1,6]:=B[K+1,6]-B[K+1,2]*B[K,6];                 "DOUBLE SWEEP"
 B[K+2,2]:=B[K+2,2]-B[K+2,1]*B[K,4];                   METHOD.
 B[K+2,3]:=B[K+2,3]-B[K+2,1]*B[K,5];
 B[K+2,6]:=B[K+2,6]-B[K+2,1]*B[K,6];
 FOR I:=1 TO 2 DO
  BEGIN
  S:=B[K+I,3];FOR J:=1 TO 6 DO B[K+I,J]:=B[K+I,J]/S;
  END;
 END;
B[N,3]:=B[N,3]-B[N-1,4]*B[N,2];
```

```
B[N,6]:=(B[N,6]-B[N-1,6]*B[N,2])/B[N,3];             BACK-SUBSTITUTION TO GET
B[N-1,6]:=B[N-1,6]-B[N-1,4]*B[N,6];                  STRESS FUNCTION, ϕ.
FOR K:=2 TO (N-1) DO
B[N-K,6]:=B[N-K,6]-B[N-K,4]*B[N-K+1,6]-B[N-K,5]*B[N-K+2,6];
```

```
FOR I:=2 TO (N-1) DO
STRESS[I]:=(B[I-1,6]+B[I+1,6]-2*B[I,6])/(DX*DX);
STRESS[0]:=2*(B[1,6])/(DX*DX);                       DETERMINATION OF
STRESS[1]:=(B[2,6]-2*B[1,6])/(DX*DX);                STRESS DISTRIBUTION.
STRESS[N]:=2*(B[N-1,6]-B[N,6])/(DX*DX);
```

```
WRITELN ('TIME =':6,TIME:7:3,'   ':3,'AV. M/C =':9,AV:4:0);
WRITELN ('STRESS AT SURFACE=':20,STRESS[0]:3);
WRITELN ('M.C. AT SURFACE=':20,A[0,4]:4:0);
WRITELN;
IF PF1=1 THEN                                        OUTPUT
BEGIN
WRITELN ('  M/C    STRESS':14);
FOR I:=0 TO N DO WRITELN (A[I,4]:4:0,'    ':3,STRESS[I]:3);
WRITELN;
END;
```

```
END;                                                 CONTROL STATEMENT.
IF TIME<TLIM THEN GOTO 1 ELSE GOTO 2;
2: END.
```